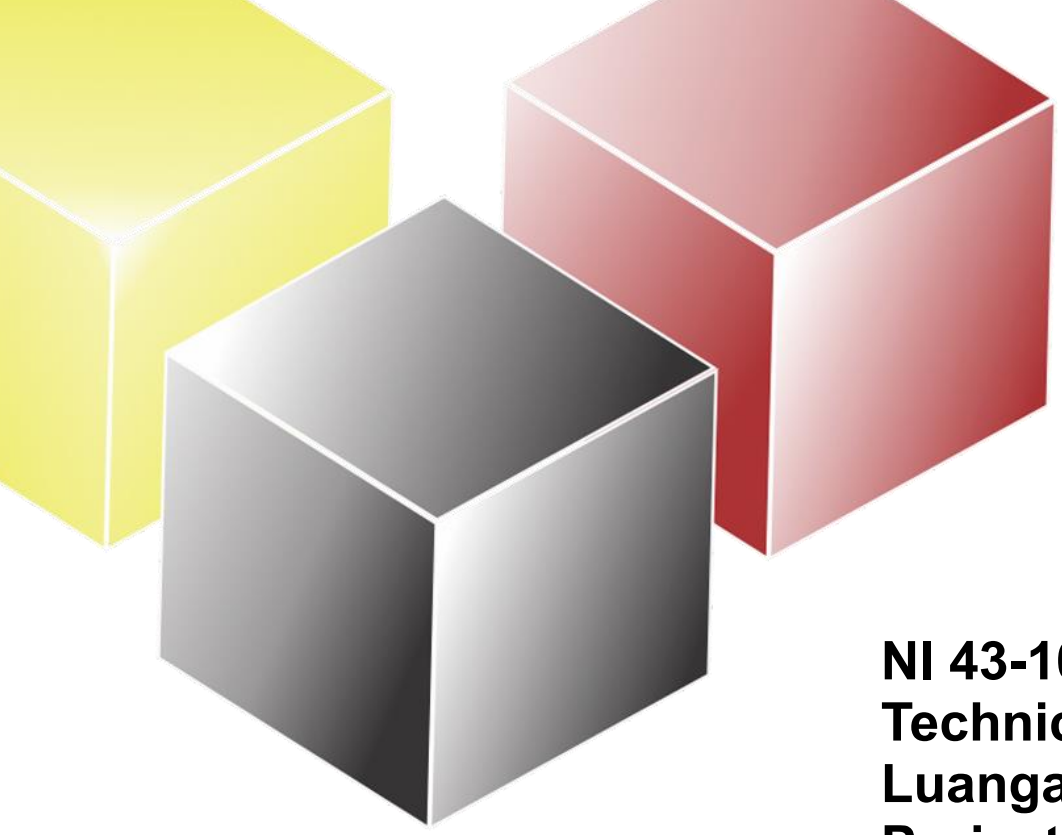

NI 43-101 Independent Technical Report Luanga PGM + Au + Ni Project Pará State, Brazil

Prepared by:

GE21 Consultoria Mineral Ltda.

Av. Afonso Pena, 3130, 9th floor, Belo Horizonte, MG, Brazil
30.130-910
portal@grupoge21.com

On behalf of:

Bravo Mining Corp.

Burrard Street, 505, Bentall 5, Suite 1008, Vancouver, British Columbia, Canada, V6C 2B5
info@bravomining.com

Project GE21 nº: 240908
Effective date: February 18, 2025

Qualified Persons:

Porfirio Cabaleiro Rodriguez, BSc Mining Engineering, FAIG

Bernardo Viana, BSc Geology, FAIG

Independent Technical Report on the Luanga PGM + Au + Ni Project, Pará State, Brazil

GE21 Project nº: 240908

Effective date: February 18, 2025

Issue date: April 2, 2025

Version: Initial Issue

Work directory: S:\Projetos\Bravo\20908-Luanga-MRE-Update

Copies: Bravo Mining Corp.
GE21 Consultoria Mineral Ltda.

Review	Description	Author(s)	Date

DATE AND SIGNATURE

This report, titled “NI 43-101 Independent Technical Report Luanga PGM + Au + Ni Project Pará State, Brazil”, having an effective date of February 18, 2025, was prepared by GE21 Consultoria Mineral Ltda. For Bravo Mining Corp. and signed.

Dated at Belo Horizonte, Brazil, on April 2, 2025.

<Signed and sealed in the original>

Porfirio Cabaleiro Rodriguez

<Signed and sealed in the original>

Bernardo Horta Cerqueira Viana

IMPORTANT NOTICE

This Report was prepared following the National Instrument 43-101 - Standards of Disclosure for Mineral Projects of the Canadian Securities Administrators (“NI 43-101”) requirements by GE21 Consultoria Mineral Ltda. (“GE21”) for Bravo Mining Corp. (Bravo).

This report is intended for use by Bravo, subject to the terms and conditions of its individual contracts with the report authors and to the relevant securities legislation.

Except for the purposes legislated under applicable securities law, any other uses of this report by any third party are at that party’s sole risk.

Currency is expressed in U.S. dollars, and metric units are used unless otherwise stated.

UNITS, SYMBOLS, AND ABBREVIATIONS

Ac/Ab	Definition/Term
A	
ACT	Survey Drilling Software
Ag	Silver
AIG	Australian Institute of Geoscientists
AIPL	Americas Investments e Participation Ltd.
ANM	National Mining Agency
Amp	Amphibole
AMSA	Amazonia Mining S.A
As	Arsenic
Act	Actinolite
Au	Gold
B	
B	Boron
BAIP	Brazil Americas Investments and Participation
BASF	Badische Anilin- und Soda-Fabrik
Be	Beryllium
BHEM	Borehole Electromagnetics
Bi	Bismuth
Bt	Biotite
BIF	Banded Iron Formation
BBWi	Bond Ball Work index
BNDES	Banco Nacional de Desenvolvimento Econômico e Social
Bravo	Bravo Mining Corp.
BSc	Bachelor of Science
BVI	British Virgin Islands
C	
Ca	Calcium
CDM	Mineral Development Center
Ccp	Chalcopyrite
Cd	Cadmium
Ce	Cerium
CEF	Caixa Econômica Federal
CEP	Código de Endereçamento Postal (Postal Code)
CETEM	Centro de Tecnologia Mineral
CFEM	Compensação Financeira pela Exploração de Recursos Minerais
Chl	Chlorite
Chr	Chromite
Chr-PGM	Chromite-associated Zone
CIM	Canadian Institute of Mining, Metallurgy and Petroleum
CIL	Carbon-in-Leach
CPRM	Companhia de Pesquisa de Recursos Minerais
CMP	Carajas Mineral Province
cm	centimetre(s)
cm³	cubic centimetre
CMM	Companhia Meridional de Mineração
CMC	Carboxymethyl Cellulose
CN	Sodium cyanide
Co	Cobalt
CODIM	Mineral Industries Development Company
Cl	Chlorite
Cpx	Clinopyroxene
Ccp	Chalcopyrite
Cr	Chromium
CRM	Certified Reference Materials

	C
CTSZ	Cinzento Transcurrent Shear Zone
Cu	Copper
Cu/Ni	Copper/Nickel ratio
CVRD	Companhia Vale do Rio Doce (now Vale S.A.)
CW	Central West
D	
DC	Direct Current
DD	Diamond Drilling
DEM	Digital Elevation Model
DDH	Diamond Drill Hole
DNPM	Departamento Nacional de Produção Mineral (now ANM)
DOCE GEO	Rio Doce Geologia e Mineração S.A. (subsidiary of CVRD) (Now Vale SA)
E	
E	East
e.g.	for example
Eh	Electrode potential
EIA	Environmental Impact Study
EOH	End of Hole
ESG	Environmental, Social and Governance
Et	Extraction rate
EM	Electromagnetic
ESE	East-Southeast
E-W	East-West
F	
F	Fluorine
FA/AAS	Fire Assay/Atomic Absorption Spectrometry
FAIG	Fellow Australian Institute of Geoscientists
Fe	Iron
FUNAI	National Indian Foundation
FFA	FFA Legal
FFAH	FFA Holding e Mineração Ltda
FLTEM	Fixed-Loop Transient Electromagnetics
FR	Fresh Rock
G	
g	gram(s)
Ga	Billion years
g/cm³	grams per cubic centimeter
g/L	grams per liter
GPS	Global Positioning System
Grt	Garnet
g/t	grams per ton
H	
ha	Hectares
HCDs	Hydrodynamic Cavitation Devices
HELITEM	Time Domain Electromagnetic and Magnetic
HG	High Grade
Hg	Mercury
hr	hour
HQ	96.4 mm diameter drill core
I	
IBGE	Instituto Brasileiro de Geografia e Estatística
IBAMA	Brazilian Institute of Environment and Renewable Natural Resources

I	
ICP-OES	Inductively Coupled Plasma Optical Emission Spectrometry
ICP-AES	Inductively Coupled Plasma – Atomic Emission Spectroscopy
ICP-MS	Inductively Coupled Plasma/Mass Spectrometry
ID	Identification
in	Indium
IOCG	Iron-Oxid Copper Gold
IP	Induced Polarization
Ir	Iridium
ISO/IEC	International Organization for Standardization/ International Electrotechnical Commission
K	
K	thousand
K	Potassium
KPa	Kilopascal
kg	kilogram(s)
Kg/h	kilograms per hour
km	kilometre(s)
km^2	square kilometre(s)
kg/t	kilograms per ton
kV	kilovolt
kVA	kilovolt-amperes
kWh/t	kilowatt-hour per ton
kWh/st	kilowatt-hours per short ton
L	
L	Liter
La	Lanthanum
TBS	Test Bulk Sample
LG	Low Grade
L/h	Liters per hour
LI	Installation License
LMIs	Layered Mafic Intrusions
Ltd.	Limited
Ltda.	Limited
LCT	Locked cycle test
LU	Luanga
LIP	Large Igneous Province(s)
LO	Operation License
LP	Preliminary License
LSZ	Low Sulphide Zone
M	
m	metre(s)
M	Million(s)
Ma	Million years
Mag	Magnetite
MASH	Melting-assimilation-storage-homogenization
MAIG	Member of Australian Institute of Geoscientists
MASU	Massive Sulphide Zone
MBs	Micro-bubbles
Mg	Mgnesium
MG	Minas Gerais State
mg	milligram
mg/L	milligrams per liter
min	minute
MIBC	Methyl Isobutyl Carbinol
mm	millimetre(s)
MF	mill-float
MME	Ministry of Minerals and Energy
Mn	Manganese

M	
Moz	million ounces
Mr.	Mister
MRE	Mineral Resource Estimate
MSZ	Main Sulphide Zone
Mt	Million tonnes
MUM	Mafic-Ultramafic
Mv	millivolts
MW	Megawatt
MZ	Mafic Zone
m^2/tpd	square meters per ton per day
N	
Nº	Number
N	North
NA	Not Applicable
NBR	Brazilian Technical Standard
NBs	Nanobubbles
n/d	Not Determined
NE	Northeast
Ni	Nickel
NI	National Instrument
Ni-Rh	Nickel/Rhodium Zone
NQ	76.2mm diameter core drilling
NOR	Norite
N-S	North-South
Ni/Cu	Nickel/Copper ratio
NSR	Net Smelter Return
NNW	North-Northwest
NNE	North-Northeast
NW	Northwest
NX	Cross polarized light
N//	Plane polarized light
O	
Ol	Olivine
OPY	Orthopyroxenite
Opx	Orthopyroxene
Os	Osmium
OX	Oxide
P	
P	Pressure
PA	Pará State
PAX	Potassium Amyl Xanthate
Pb	Lead
Pd	Palladium
PGC	Projeto Grande Carajás
PGE	Platinum Group Elements
PGM	Platinum Group Metals
PEA	Preliminary Economic Assessment
PFS	Pre-Feasibility Study
PI	Intercumulus plagioclase
pOPY	Plagioclase-orthopyroxenite
Pn	Pentlandite
Pd/Rh	Paladium/Rhodium ratio
Po	Pyrrhotite
ppb	parts per billion
Pt/Pd	Platinum/Paladium ratio
$PtAs_2$	Sperrylite
ppm	parts per million
Pt	Platinum

P	
PVC	Polyvinyl chloride
Py	Pyrite
Q	
QA/QC	Quality Assurance and Quality Control
QLS	Quality Level Sampling
QP	Qualified Person
Qp	Volumetric flow rate
Qz	Quartz
R	
rd	third
RIMA	Environmental Impact Report
RL	Reflected Light
Rh	Rhodium
rpm	Revolutions Per Minute
Rh/Pd	Rhodium/Palladium ratio
Rh/Pt	Rhodium/Platinum ratio
RTK	Real Time Kinematic
RQD	Rock Quality Designation
Ru	Ruthenium
S	
S	Sulphur
s	seconds
S.A.	Corporation
SAD69	South American Datum
SAG	Semi-Autogenous Grinding
Sb	Antimony
Sc	Scandium
SE	Southeast
SEMA	State Secretariat for the Environment
Sul	Sulphide
SUDAM	Superintendence for the Development of the Amazon
SEC	Securities and Exchange Commission
SGS	Société Générale de Surveillance
sol.	solids
SSE	South-southeast
SIRGAS	Sistema de Referência Geocêntrico para as Americas
Sn	Tin
SPDS	Serra Pelada Divergent Splay
SZ	Sulphide Zone
Sr	Strontium
Srp	Serpentine
Sul	Sulphide
T	
T	Tonnes
t	time
TB	Test Bulk
TC	Test Comparison
TD	Test Characterization
Te	Tellurium
TH	Test High-Grade
t/h.m²	tons per hour square meter
Tlc	Talc
TTG	Tonalite-Trondhjemite-Granodiorite

T	
t/m³	Tons per cubic meter
TEM	Transient Electromagnetic
Ti	Titanium
Tur	tourmaline
Th+U	Thorium plus uranium
TZ	Transition Zone
U	
U-Pb	Uranium-Lead
US$	United States dollar
U.S.	United States
USD	United States dollar
UTM	Universal Transverse Mercator (coordinate system)
UZ	Ultramafic Zone
V	
V	Vanadium
v	Vertex
Vale	Vale S.A. (ex-Companhia Vale do Rio Doce - CVRD)
vol%	volume percent
vs.	versus
W	
W	West
WNW	West-northwest
Wp	Flow of mineralization
wt.	Weight
W	Tungsten
Z	
Zn	Zinc
ZWF	192 mm diameter core drilling

Units and Symbols			
%	Percentage	Mt	Megaton
“	Inches	Mtpa	Million Tonnes per Annum
°C	Celsius	MW	Megawatt
Au	Gold	N	North
cm	Centimetre(s)	N.	Number
g/t	Grams per Tonne	NE	Northeast
Ga	Giga-annum	Ni	Nickel
h	hours	Ni	Nickel
Ha	Hectare(s)	NW	Northwest
k	Thousands	Oz	Troy Ounce
k$	Thousands of Dollars	Pd	Palladium
Kg	Kilogram	ppb	Parts per Billion
km	Kilometre(s)	ppm	Parts per Million
km²	Square Kilometre(s)	Pt	Platinum
kOz	Kilo-ounce	Rh	Rhodium
kPa	Kilopascal	S	South
kV	Kilovolt	s	Second
L	Litre	SSW	South-southwest
m	Metres	SW	South-West
M	Millions	t	Tonne
ml	Millilitre	USD	United States Dollars ($)
µµ	Micrometre	V	Volts

TABLE OF CONTENTS

LIST OF TABLES

LIST OF FIGURES

1 EXECUTIVE SUMMARY

1.1 Introduction

GE21 Consultoria Mineral Ltda. is an independent mineral consulting company based in Belo Horizonte, Brazil, specializing in Mineral Resource and Reserve declarations under NI 43-101 standards.

Bravo Mining Corp. is a Canadian and Brazil-based mineral exploration and development company focused on the Luanga Project in the Carajás Mineral Province. It has offices in Rio de Janeiro and Vancouver.

Bravo has commissioned GE21 to prepare a Mineral Resource Estimate (MRE) Technical Report for the Luanga Project in compliance with NI 43-101 guidelines.

1.2 Qualifications, Experience and Independence

The Qualified Persons (QPs) responsible for the independent Technical Report are Mr. Porfirio Cabaleiro Rodriguez and Mr. Bernardo Viana.

- Mr. Rodriguez, an engineer with over 30 years of experience, was responsible for multiple sections of the report and meets the NI 43-101 requirements for a QP. He conducted site visits in July 2023, October 2023, and January 2025, alongside Mr. Viana in the last two visits. During the visits, drill collars were located, coordinates validated, and core samples inspected.
- Mr. Viana, a geologist with over 20 years of experience, was responsible for key sections and meets the NI 43-101 requirements for a QP.

Neither GE21 nor the authors have any financial interest in Bravo Mining Corp., maintaining a strictly professional and independent consultant-client relationship. The report was prepared under a commercial agreement, with payment not contingent on its results.

Table 1-1 below relates each QP with their report items' responsibility.

Table 1-1: Report Items and assigned QP responsibilities

Company	QP	Section Responsibility	Site Visit	Responsibility
GE21	Porfirio Cabaleiro Rodriguez, FAIG	2, 3, 4, 5, 6, 13, 14, and 23, with co-responsibility for Sections 1, 11, 12, 25, 26 and 27	July 4 to 7, 2023; October 3 to 6, 2023; and January 27 to 31, 2025	Author
GE21	Bernardo Viana, FAIG	7,8,9, 10 and 20 with co-responsibility for 1, 11, 12, 25, 26 and 27	October 3 to 6, 2023; and January 27 to 31, 2025	Author

Source: GE21, 2025.

1.3 Reliance on Other Experts

The authors of this report are Qualified Persons (QPs) under NI 43-101, with expertise in mineral exploration, data validation, and resource estimation.

Information regarding tenure, status, and permitted work within Bravo's property is based on publicly available data from Brazil's National Mining Agency (ANM).

Bravo Mining Corp. engaged Linneu de Albuquerque Mello, a qualified lawyer in Brazil, to provide a title opinion on the Luanga Mineral Rights, confirming their validity and good standing as of January 31, 2025.

1.4 Property Description and Location

The Luanga Project is an advanced-stage mineral project located in Pará, Brazil, which contains platinum group metals (PGM), gold (Au), and nickel (Ni). It is held under Exploration License Nº.1961 (ANM.851.966/1992) and covers 7,810.02 hectares (Table 1-2).

The project is located on private farmland used for cattle ranching, with no indigenous claims or protected forests. Land access agreements with six key landowners cover 97% of the known mineralized area. The land access agreements are renewable every two years.

The initial exploration permit expired in 1998; however, due to bureaucratic delays at ANM, its renewal was granted only in 2005 for an additional three years. Vale submitted a Final Exploration Report in 2008, and a Mining License application was filed in 2013. The ANM has not yet approved the Final Exploration Report, and Bravo expects this delay to continue until a new feasibility study is submitted.

Table 1-2: Mineral tenement summary

ANM Process	Municipality	Stage	Mineral	Title Owner	Size (hectares)	License No.	Expiry Date
851.966/1992	Curionópolis	Application for Mining License	Au, Pd, Pt, Ni	Bravo Mineração Ltda	7,810.02	1961	
				TOTAL	**7,810.02**		

Notes:
Comments: Mining License pending
ANM = Mining National Agency
Source: ANM, February 2025.

The Luanga mineral property is centred approximately at coordinates -05º57'24.34" S/-49º32'51.00" W (Figure 1-1).

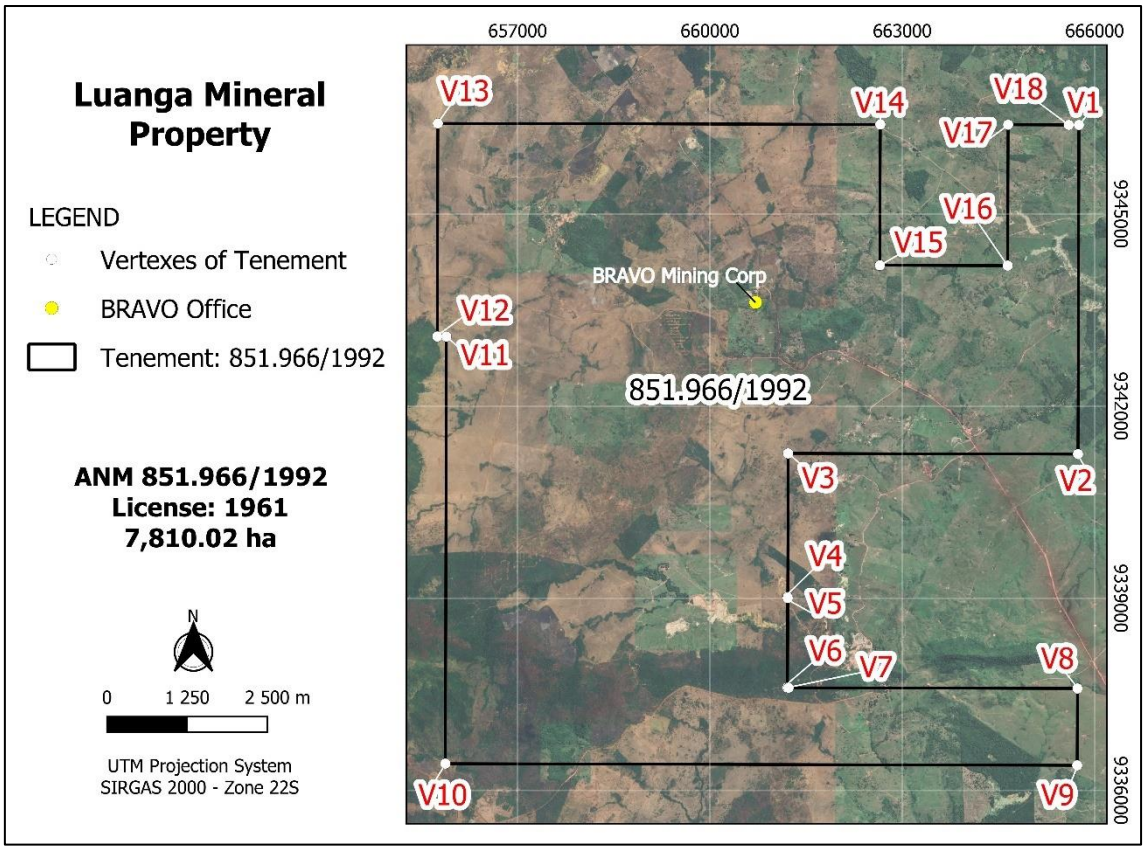

Figure 1-1: Luanga Project tenement map

Source: GE21, 2025.

1.5 Accessibility, Climate, Local Resources, Infrastructure, and Physiography

The Luanga Project is in Curionópolis, Pará, Brazil, about 500 km south of Belém. It is accessible via paved roads from Parauapebas and Marabá, both of which have commercial airports with multiple daily flights. The project is reached via a municipal paved road off Highway PA-275 (Figure 1-2).

The nearest towns are Curionópolis (17,846 people, 17 km south-southwest) and Serra Pelada (12 km west). Parauapebas, located 40 km away, is a key mining hub that provides labour, services, and infrastructure for the region.

The project is situated in the Carajás Mineral Province, within the South Pará Plateau (elevation 500-700m), near the Serra Seringue range. The Sereno River and its tributaries drain the area.

The climate is equatorial, with warm, dry winters and wet, humid summers. 75% of annual rainfall occurs from December to April, ensuring ample water availability for potential mining activities.

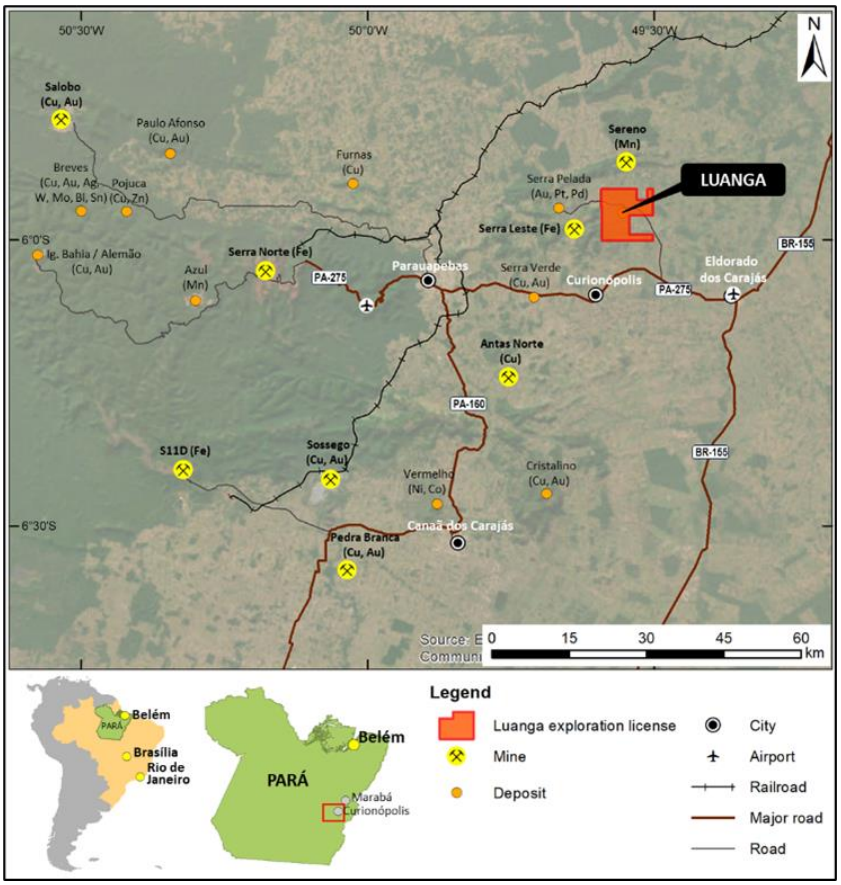

Figure 1-2: Access map for Luanga Project

Source: Bravo, 2025.

1.6 History

Due to access challenges, geographical studies in the Carajás region were limited until the 1960s. In 1966, CODIM, a subsidiary of Union Carbide, discovered the Serra do Sereno manganese deposit, sparking interest from US Steel. In 1967, a Brazilian team identified high-grade iron mineralization (66% Fe), though the government restricted foreign control.

In 1970, the Brazilian government established Amazônias Mineração SA (AMSA), with Vale (formerly Companhia Vale do Rio Doce, or CVRD) holding a 51% stake and CMM owning 49%. By 1974, AMSA secured exclusive rights to Carajás iron mineralization, and by 1977, Vale acquired the remaining 49% of CMM for US$55 million, gaining full control over the Carajás Mineral Province.

Vale began the construction of the Carajás Railroad in 1978, linking the mine to Ponta da Madeira, Maranhão. The Carajás Iron Mineralization Project (total cost: US$3 billion) included significant investments in infrastructure:

The Luanga Project exploration dates back to 1983 when DOCEGEO identified mafic-ultramafic rocks in the Luanga Complex, discovering chromitite mineralization and conducting initial geochemical surveys. By 1997, a joint venture between DOCEGEO and Barrick Gold had identified gold anomalies in stream sediments.

In 2000, Vale expanded its exploration with a soil geochemistry survey, revealing a 4 km Pt-Pd anomalous trend in the Luanga Complex. This led to further integration of geological, geophysical, and remote sensing data by Vale in 2001.

Between 1992 and 2003, Vale carried out comprehensive diamond drilling campaigns, totaling 256 drill holes (50,786.74m):

This extensive exploration established the Luanga Project as a key PGM-Au-Ni target within the Carajás Mineral Province, laying the foundation for continued resource evaluation and development.

In 2023, GE21 conducted a Mineral Resource Estimate (MRE) for Bravo, accompanied by a pit optimization study, to classify the Mineral Resources. The pit-constrained MRE had an effective date of October 22, 2023, and it was comprised of 73 Mt grading 1.75 g/t PdEq for a total of 4.1 Moz of PdEq in the Indicated category and 118 Mt grading 1.50 g/t PdEq for 5.7 Moz PdEq in the Inferred category. This 2023 MRE has been superseded by the current MRE.

1.7 Geological Setting and Mineralization

The Carajás Mineral Province (CMP), located on the southeastern margin of the Amazon Craton, is one of South America's most important mineral provinces. It hosts world-class Fe, Cu-Au, and Ni deposits, including the Serra Pelada, Salobo, and Igarapé Bahia Cu-Au deposits. The province is bounded by the Araguaia Neoproterozoic Belt to the east and south and overlain by Paleoproterozoic sequences to the west. The geological boundaries of the CMP are not precisely defined to the north, where Paleoproterozoic gneiss-migmatite-granulite terrains dominate.

Within the Carajás Domain, several mafic-ultramafic complexes intrude into both the Xingu Complex and the Archean volcano-sedimentary sequences. These intrusions are host to major Ni laterite deposits (e.g., Onça-Puma, Vermelho, Jacaré) and PGM deposits (e.g., Luanga, Lago Grande). The magmatic structure and evolution of these layered intrusions suggest that they belong to different Neoarchean magmatic suites, contrary to previous regional studies that ascribed them all to the Cateté Suite.

The Luanga Layered Mafic-Ultramafic Complex, commonly referred to as the Luanga Complex, is a significant geological feature situated within the Carajás Mineral Province. The complex spans approximately 6 km in length and up to 3.5 km in width, covering an area of around 18 km². It belongs to the Neoarchean Large Igneous Province (LIP) of the Carajás Mineral Province. The intrusion is characterized by abundant unweathered outcrops, massive blocks, and boulders, which are more prominent compared to the surrounding areas of the province.

The geomorphology of the complex features a smooth hill that is elongated in shape and arc-like, underlain primarily by ultramafic rocks. This hill is up to 60 meters higher than the surrounding flat areas, where gabbroic rocks prevail. The layering within the complex forms an arc-shaped structure that mirrors the overall morphology of the region

1.7.1 Stratigraphy and Geological Features

The central part of the Luanga Complex contains the thickest sequence of layered rocks. Moving toward the north and northeast, the layered sequence is truncated by granitic intrusions, while to the south, the sequence becomes progressively thinner. The complex and its host rocks are intersected by NNW-SSE dolerite dykes that are up to several meters wide.

Geological sections from drilling data reveal that the igneous layers in the central and southwestern portions of the complex exhibit steep dips to the southeast. These sections show that the Ultramafic Zone (UZ) overlies the Transition Zone (TZ), which in turn overlies the Mafic Zone (MZ), indicating that the layered sequence is tectonically overturned. Previous studies (Ferreira Filho et al., 2007; Teixeira et al., 2015) also described an overturned layered sequence in the Luanga and Lago Grande Complexes, suggesting that regional structural features led to the formation of large, overturned blocks in the Serra Leste region.

1.7.2 Mineralization at the Luanga Complex

The Luanga PGM + Au + Ni mineralized envelope follows the arc-shaped structure of the Mafic-Ultramafic Complex for approximately 8.1 km. The deposit is divided into three main mineralized sectors: North, Central, and Southwest. The mineralization is primarily found within the Transition Zone (TZ) of the Luanga Complex, which contains several PGM mineralized units.

The Main Sulphide Zone (MSZ) is the most significant mineralized zone, hosting the bulk of the PGM resources within the Luanga Complex. Additional mineralized layers are identified both within the Transition Zone (TZ) and the Ultramafic Zone (UZ).

In addition to the primary PGM mineralization, the Luanga Complex also contains thin chromitite layers or lenses. These are found either in the Transition Zone's upper or lower stratigraphic portions. The chromitite layers hosted in the lower portions of the TZ are associated with ultramafic cumulates, while the upper chromitite layers are located in immediate contact with the overlying Mafic Zone (MZ). These upper layers are hosted by plagioclase-bearing norite cumulates, indicating a complex stratigraphic relationship within the layered sequence of the complex.

1.8 Deposit Types

The majority of PGM resources come from mafic-ultramafic layered intrusions, particularly from stratiform mineralized layers near the transition from mafic to ultramafic cumulate rocks. The Bushveld Complex (South Africa) exemplifies this type of mineralization, known as reef-type deposits. These intrusions also host deposits of base metal sulphides (Ni-Cu-Co), chromite, and magnetite-ilmenite due to magmatic processes during the cooling and emplacement of mafic-ultramafic magmas.

Ni-Cu-PGM sulphides accumulate through the separation of sulphide liquid from silicate magma. In the Luanga Complex, textural features in the MSZ and other zones confirm the

magmatic origin of PGM, Au, and Ni mineralization. Sulphide blebs are found interstitial to olivine and pyroxene, with rounded faces supporting a magmatic origin.

The Luanga Complex exhibits several mineralized horizons with varying metal ratios, indicating multiple mineralizing events during its magmatic evolution, similar to the Bushveld and Stillwater (U.S.A.) deposits.

While widespread alteration has affected the Luanga Complex, the primary magmatic features of cumulate rocks and PGM zones are preserved, despite partial alteration of sulphides to magnetite and Fe-hydroxides. The alteration is heterogeneous, maintaining key textures throughout the intrusion.

1.9 Exploration

1.9.1 Topography

In 2023, RR Topografia & Engenharia of Brazil completed a new Orthophotography and Digital Elevation Model (DEM).

1.9.2 Geophysics

The first geophysical work for Bravo was completed in 2021 by Southern Geoscience Consultants of Australia (SGC) and Southernrock Geophysics of Chile (Southernrock). Southernrock reprocessed the historic Induced Polarization (IP) data, while SGC reprocessed the historic magnetic data.

Ground geophysical activities conducted during 2022, and January 2023 included borehole electromagnetics and surface electromagnetic surveys. Both surveys were conducted by Geomag S/A (Geomag).

Borehole electromagnetic surveys (BHEM) were carried out along five drill holes totalling 1,109 linear metres. The best BHEM response was associated with drill hole DDH22LU047, which intersected 11 metres of massive sulphides.

A Fixed-Loop Transient Electromagnetics (FLTEM) survey was concentrated on the Central and North Sectors along 34 survey transversal lines (total of 30.27km). Loop dimensions were 600 x 400 metres, and survey lines were spaced 100 metres apart.

In 2024, Bravo conducted a ground geophysics survey consisting of magnetometry and micro-gravity, using a 100 m line-spacing grid performed over an area of approximately 18.7 km^2, covering the ultramafic and transition zones of the Luanga Complex.

Also in 2024, a helicopter-based electromagnetic survey (HeliTEM) was carried out over an area of 99.72 km^2, covering the whole Luanga mineral property. The survey was conducted by Xcalibur Multiphysics (Xcalibur) and consisted of a total of 771.2 km of lines.

1.9.3 Trenching

The trenching program started in Q4/2022 and aims to provide detailed information about the mineralized zones at the surface level. Up to the Effective Date of this report, 45 trenches were opened, totalling 9,065.73 linear meters. All opened trenches were mapped and sampled, and their channel samples were precisely surveyed with an RTK. After the work was completed, all trenches were closed. A total of 9,521 channel samples, including Quality Assurance and Quality Control (QA/QC) samples, were collected and analyzed for 3PGM and Au at independent laboratories.

1.9.4 Petrography

To enhance the geological understanding of the deposit, a petrographic study was conducted between 2022 and 2024 using 117 selected from the drill core representing the lithological diversity and multiple mineralized styles, and polished thin sections were prepared for all of them.

1.9.5 Mapping

Bravo hired PRCZ Consultores Associados (PRCZ) to carry out detailed geological and structural mapping work at the Luanga Project. This work was performed from November 2022 to July 2023.

Geological units identified in the Project area included rocks from the basement of the Carajás Domain, consisting mainly of gneiss, migmatite, and granulite terrains of the Xingu Complex, as well as metavolcanic and metaplutonic rocks of the Grão Pará Group.

1.10 Drilling

Approximately 123,610 meters in 601 drill holes have been drilled on the Property since 1992. Of these, 256 (50,787 m) are diamond drill holes (DDH) executed by DOCEGEO (Vale) and include Luanga's North, Central, and Southwest geological targets. Bravo's drilling totals 72,823.45 m and 345 holes, representing 59% of the project's drilled length (Table 1-3).

Drilling by Bravo commenced in March 2022 and has continued since then. The program was designed primarily for infill drilling and resource definition at Luanga. Bravo also performed 8 drill holes for metallurgical sample collection purposes. In 2023/2024, Bravo´s drilling program also included some exploration drill holes over several geophysical targets located outside the Luanga PGM+Au+Ni deposit. The whole diamond drilling developed by Bravo was performed using a mixture of HQ and NQ2 diameters.

Table 1-3: Drilling summary for Luanga

Year	Drill Type	Drill Holes	Total Metres	Company	Contractor
1992	DD	4	643.69	DOCEGEO	DOCEGEO
2001	DD	86	14,584.35		Geosol
2002	DD	71	15,423.25		Geosol

Year	Drill Type	Drill Holes	Total Metres	Company	Contractor
2003	DD	95	20,135.45		Geosol / Rede
2022	DD	135	23,258.20	Bravo	Servdrill
2023	DD	116	30,296.60		Servdrill
2024	DD	94	19,268.65		Servdrill
TOTAL		**601**	**123,610.19**		

Source: Bravo, 2025.

1.11 Sample Preparation, Analyses and Security

Bravo's QA/QC Policy is designed to ensure the reliability of exploration data and laboratory analytical results, maintaining an accurate and secure database for the project. The procedures followed include detailed processes for the transportation, verification, and analysis of samples to guarantee data integrity.

Bravo's diamond drilling campaign includes the use of Field Duplicates, Certified Reference Materials (CRMs), Blank samples, and Umpire Assay samples. Control samples (blank, CRM, and duplicate) are inserted into the analytical batch at a 1:20 ratio of regular samples. Blank and CRM samples are sourced from reputable suppliers like OREAS, AMIS, and Brasil Minas.

Bravo's QA/QC program accounts for 14,159 control samples, including Certified Reference Materials, Blank Samples, Field Duplicates and Umpire Check Assays, representing 10.7 % of the total samples.

Bravo conducted a resampling and assay campaign to validate Vale's historical data and to establish a correlation between total Ni grades and potentially recoverable sulphide-hosted Ni. Results from this campaign were entered into the drilling database, replacing the original data.

Bravo's team produces regular QA/QC internal reports to monitor the quality of assay results, ensuring consistent data quality. These reports specify which batches should be reanalyzed based on any discrepancies detected.

Although Vale's historical database did not include CRM insertion, the correlation procedures applied by Bravo have validated the database for estimation work. Despite attempts, Bravo was unable to obtain internal QA/QC results from Vale's laboratory (SGS Geosol).

Overall, Bravo's QA/QC procedures meet the industry's best practices, and the Luanga Project database is considered suitable for Mineral Resource Estimation.

1.12 Data Verification

Since 2022, GE21 team members have conducted multiple field visits to the Luanga Project to assess Bravo's exploration procedures, infrastructure, and data collection processes, ensuring the adequacy and reliability of data for the Mineral Resource estimate. Key visits took place on July 4-7, 2023; October 3-6, 2023; and January 27-31, 2025. During the last two visits,

the GE21 Qualified Persons team included Geologist Bernardo Viana and Engineer Porfirio Rodriguez, an independent consultant assisting Bravo in developing the resource estimate.

Drill hole logging adheres to industry-standard practices, which Bravo has successfully established. GE21 reviewed procedures on a randomly selected set of drill cores and confirmed log completeness, with only minor omissions that were not considered significant.

Based on these observations, GE21 concludes that the exploration data at the Luanga Project is suitable for the Mineral Resource estimate, with data collection, quality control, and storage procedures meeting industry standards and no significant issues identified in Bravo's exploration activities.

1.13 Mineral Processing and Metallurgical Testing

Bravo developed metallurgical tests aimed at achieving results comparable to those of Vale's preliminary test work on PGM mineralization from the Luanga Project and recorded recommendations on metallurgical input parameters considered for the Mineral Resource Estimate (MRE). The scope of test work completed to date includes:

1. Extensive comminution and flotation test work was conducted from 2022 to 2025, including a review and validation of historical work conducted by the previous project owner between 2001 and 2004.
2. Several test programs were conducted on oxide material, including exploratory leaching and physical separation tests, as well as parameter optimization tests, between 2022 and 2025.
3. Preliminary pyrometallurgical tests to evaluate the treatability of Luanga concentrates.

The metallurgical tests have been conducted since 2002, including by Vale, using Mintek. Laboratories in South Africa, followed by tests in CDM Vale laboratory using the circuit developed by Mintek.

Bravo resumed the metallurgical test work, from 2022 to 2023, submitting approximately three tonnes of sulphide metallurgical samples and 150kg of oxide samples to CETEM and TESTWORK laboratories in Brazil.

1.13.1 Bravo 2024/2025 Program

Ultimately, Bravo prepared a global bulk composite from the north zone of the Luanga deposit, totalling approximately 3.6 tonnes, which was constituted from diamond drill core samples.

Global composites were also prepared for the Central and SW zones of the deposit. The Central and SW composite was used in conjunction with the North composite for detailed comminution test work, while only the North composite was used in further minerals processing tests thus far.

Similar to the 2022/2023 scope, the 2024/2025 test work program was developed in phases. Laboratories used in those phases are listed below:

- Comminution – Metso Brazil
- Flotation – CETEM
- Flotation test work, North Sector – Base Metal Laboratories
- Mini Plant Program – CIT SENAI Laboratory
- Concentrate Production Run – CIT SENAI Laboratory
- Parameter Circuit Run – CETEM

1.13.2 2025 MRE Metallurgical Assumption Recommendations

The current metallurgical model shows recoveries of ca. 75 – 84% across a feed grade of 0.9 – 7.0 g/t PGM+Au, generating concentrate grades above 80 g/t PGM+Au, which is than that assumed in the 2023 MRE of 76 – 85%.

Recent locked cycle test work performed by Bravo at Base Metal Labs demonstrated 62% Ni recovery in both sets of North Sector tests at feed grades of 0.21% Ni. Locked cycle testing on the Central Sector sample demonstrated a 44% recovery from a 0.3% feed grade while producing the highest Ni grade in concentrate yet seen at Luanga at 16% Ni in concentrate (202 g/t PGM+Au in concentrate) (Table 1-4).

Table 1-4: MRE recommendation fresh sulphide rock global recovery

MRE Recommendation Fresh Rock Material	4E PGM	Pt	Pd	Rh	Au	Ni
Global Recovery (2 g/t)	78 %	81 %	77 %	51 %	48 %	50 %
MRE Recommendation High-Talc Domain	**Pt**	**Pd**	**Rh**	**Au**	**Ni**	
Global Recovery (2 g/t)	51 %	56 %	27 %	27 %	0 %	

Source: Bravo, 2025.

It is important to note in the table below that the quantity of oxide material has decreased by almost 50% to around 5% – compared to the 10% oxide which made up the 2023 MRE. This reducing oxide tread is likely to continue as Luanga is expanded by further drilling. This reduces the significance of the oxide zone and the priority for further metallurgical study relating to the oxides.

Input assumptions for the 2025 MRE have relied on data from extensive follow-up parameter investigation test work, which has resulted in improved assumptions for Pd, similar assumptions for Au and more conservative assumptions for Pt and Rh as compared to those assumed in the 2023 MRE (Table 1-5).

Table 1-5: MRE recommendation oxide global recovery

MRE Recommendation Oxide Material	Au	Pd	Pt	Rh
Global Recovery (1-3 g/t)	90 %	81 %	23 %	54 %

Source: Bravo, 2025.

1.14 Mineral Resource

With the intention to simplify the Mineral Resource statement, an additional variable, based on the valuation of a calculation of palladium equivalent grade (PdEq), was created based on the following assumed metal prices and recoveries:

Metal price assumptions are based on 10-year trailing averages: Pd price of US$1,380/oz, Pt price of US$1,100/oz, Rh price of US$6,200/oz, Au price of US$1,500/oz, Ni price of US$7.10 USD/lb

Palladium Equivalent (PdEq) Calculation

- The PdEq equation is: PdEq = Pd g/t + F1 + F2 + F3 + F4

Where: *e:* $\boldsymbol{F1 = \frac{(Pt_p * Pt_R)}{(Pd_p * Pd_R)} Pt_t \; F2 = \frac{(Rh_p * Rh_R)}{(Pd_p * Pd_R)} Rh_t \; F3 = \frac{(Au_p * Au_R)}{(Pd_p * Pd_R)} Au_t \; F4 = \frac{(Ni_p * Ni_R)}{(Pd_p * Pd_R)} Ni_t}$

$_P$ = *Metal Price* $_R$ = *Recovery*

Several of these considerations (metallurgical recovery, metal price projections, for example) should be regarded as preliminary in nature, and therefore, PdEq calculations should be regarded as preliminary in nature.

Luanga Project's pit-constrained Mineral Resource Estimate (MRE) has an effective date of February 18, 2025, and is tabulated below (Table 1-6).

Table 1-6: MRE statement at a cut-off of 0.5g/t Pd Eq*

Resource	Classification	Domain	Mass	*Average Value*						*Material Content*					
			Mt	Pd eq ppm	Pd g/t	Pt g/t	Au g/t	Rh g/t	Ni %	Pd eq koz	Pd koz	Pt koz	Au koz	Rh koz	Ni klb
Open Pit	Measured	Ox	4	1.51	0.90	0.88	0.05	0.12	0.00	197	117	115	7	15	—
		High Talc	—	—	—	—	—	—	—	—	—	—	—	—	—
		Fresh	32	2.06	0.97	0.67	0.04	0.08	0.11	2,144	1,009	694	46	88	77,621
		Total	**36**	**2.00**	**0.96**	**0.69**	**0.04**	**0.09**	**0.10**	**2,340**	**1,126**	**809**	**53**	**104**	**77,621**
	Indicated	Ox	6	1.51	0.97	0.73	0.04	0.11	0.00	314	200	151	9	23	0
		High Talc	2	1.83	1.12	0.54	0.11	0.08	0.13	146	89	43	9	6	6,952
		Fresh	113	2.09	0.99	0.59	0.05	0.09	0.14	7,599	3,583	2,133	193	318	344,092
		Total	**122**	**2.06**	**0.99**	**0.59**	**0.05**	**0.09**	**0.13**	**8,058**	**3,872**	**2,326**	**210**	**348**	**351,044**
	Measured + Indicated	**Ox**	**10**	**1.51**	**0.94**	**0.79**	**0.04**	**0.11**	**0.00**	**510**	**317**	**266**	**15**	**38**	—
		High Talc	**2**	**1.83**	**1.12**	**0.54**	**0.11**	**0.08**	**0.13**	**146**	**89**	**43**	**9**	**6**	**6,952**
		Fresh	**145**	**2.08**	**0.98**	**0.60**	**0.05**	**0.09**	**0.13**	**9,743**	**4,592**	**2,827**	**239**	**407**	**421,713**
		Total	**158**	**2.04**	**0.98**	**0.62**	**0.05**	**0.09**	**0.12**	**10,399**	**4,998**	**3,135**	**262**	**451**	**428,665**
	Inferred	Ox	3	1.57	0.88	1.04	0.05	0.13	—	130	73	86	4	11	—
		High Talc	0	1.76	1.08	0.53	0.10	0.07	0.14	5	3	2	0	0	292
		Fresh	75	2.02	0.97	0.58	0.05	0.08	0.13	4,878	2,344	1,389	123	191	214,690
		Total	**78**	**2.01**	**0.97**	**0.59**	**0.05**	**0.08**	**0.13**	**5,013**	**2,421**	**1,476**	**128**	**202**	**214,981**

Notes:

1. The MRE has been prepared by Porfirio Cabaleiro Rodriguez, Mining Engineer, BSc (Mine Eng), MAIG, director of GE21 Consultoria Mineral Ltda., an independent Qualified Persons (QP) under NI43-101. The effective date of the MRE is February 18, 2025.
2. Mineral resources are reported using the 2014 CIM Definition Standards and were estimated in accordance with the CIM 2019 Best Practices Guidelines, as required by National Instrument 43-101 Standards of Disclosure for Mineral Projects (NI 43-101).
3. Mineral resources that are not Mineral Reserves do not have demonstrated economic viability. There is no certainty that all Mineral Resources will be converted into Mineral Reserves.
4. Chemical elements are estimated using different estimation methodologies according to the Weathering Model. Ordinary Kriging was applied to the Oxidized domain, while the Turning Bands Simulation was applied to fresh rock.
5. This MRE includes Inferred Mineral Resources, which have had insufficient work to classify them as Indicated Mineral Resources. It is uncertain but reasonably expected that inferred Mineral Resources could be upgraded to indicated Mineral Resources with continued exploration.
   - The Mineral Resource Estimate is reported/confined within an economic pit shell generated by Dassault Geovia Whittle software, using the following assumptions (Generated from work completed for Bravo and historical test work):
     - Metallurgical recovery in sulphide material of 77% Pd, 81% Pt, 51% Rh, 48% Au, 50% Ni to a saleable Ni-PGM concentrate.
     - Metallurgical recovery in oxide material of 81% Pd, 23% Pt, 54% Rh, 90% Au to a saleable PGM ash residue (Ni not applicable).
     - Metallurgical recovery in high-talc sulphide material of 51% Pd, 55% Pt, 27% Rh, 27% Au, 0% Ni to a saleable Ni-PGM concentrate.
     - Independent Geotechnical Testwork – Overall pit slopes of 40 degrees in oxide and 50 degrees in Fresh Rock.
     - Densities are based on 27,170 drill hole cores and 112 in situ sample density measurements. The Mineral Resources are reported on a dry density basis.
     - External downstream payability has not been included, as the base case MRE assumption considers internal downstream processing.

a. Payable royalties of 2%, (only considering CFEM, for reserves a complete set of royalties must be considered)

6. Metal Pricing
   a. Metal price assumptions are based on 10-year trailing averages (2014-2023): Pd price of US$1,380/oz, Pt price of US$1,100/oz, Rh price of US$6,200/oz, Au price of US$1,500/oz, Ni price of US$7,10/lb.
   b. Palladium Equivalent (PdEq) Calculation
   c. The PdEq equation is: PdEq = Pd g/t + F1 + F2 + F3 + F4

      Where: $\boldsymbol{F1} = \frac{(Pt_p * Pt_R)}{(Pd_p * Pd_R)} \boldsymbol{Pt_t}$ $\boldsymbol{F2} = \frac{(Rh_p * Rh_R)}{(Pd_p * Pd_R)} \boldsymbol{Rh_t}$ $\boldsymbol{F3} = \frac{(Au_p * Au_R)}{(Pd_p * Pd_R)} \boldsymbol{Au_t}$ $\boldsymbol{F4} = \frac{(Ni_p * Ni_R)}{(Pd_p * Pd_R)} \boldsymbol{Ni_t}$

      $_P$ = Metal Price

      $_R$ = Metallurgical Recovery

7. Costs are taken from comparable projects in GE21's extensive database of mining operations in Brazil, which includes not only operating mines, but recent actual costs from what could potentially be similarly sized operating mines in the Carajás. Costs considered a throughput rate of ca. 10Mtpa:
   a. Mining costs: US$2.00/t oxide, US$3.00/t Fresh Rock. Processing costs: US$9.00/t fresh rock, US$7.50/t oxide. US$1.50/t processed, for General & Administration. US$1.00/t processed for grade control. US$0.50/t processed for rehabilitation.
   b. Several of these considerations (metallurgical recovery, metal price projections, for example) should be regarded as preliminary in nature, and therefore, PdEq calculations should be regarded as preliminary in nature.

8. The current MRE supersedes and replaces the Previous Estimate (2023), which should no longer be relied upon.
9. The QP is not aware of political, environmental, or other risks that could materially affect the potential development of the Mineral Resources other than those typical for mining projects at this stage of development and as identified in this report.
10. Totals may not sum due to rounding.

Source: GE21, 2025.

1.15 Interpretation and Conclusions

1.15.1 Mineral Exploration and Geology

In general terms, the geological descriptions, sampling procedures and density tests that were evaluated were found to be of acceptable quality and in accordance with industry best practices.

It was noted that the data collection process was executed with the aim of maintaining data security. Data was stored in a standardized database, which was found to be secure and auditable.

GE21 reviewed the process through which density was determined and concluded that it was in conformity with industry best practices.

1.15.2 QA/QC

GE21 performed the evaluation of the QA/QC data, which includes Blanks, CRMs, Field Duplicates, Check Assays, and Umpire Check Assays.

QA/QC procedures, sampling methodology, and analytical methods applied by Bravo are within the industry's best practices standard. The QP responsible for this report, considering the data presented in Section 11, is of the opinion that the Luanga Project's Database is suited for Mineral Resource Estimation work.

1.15.3 Geological Model

The procedure that was adopted to produce the 3D geological models (wireframes), consisting of generating triangulations between interpreted geological cross sections, was executed properly and in accordance with the opinions of GE21 staff.

1.15.4 Grade Estimation

The heterogeneity of the geological model leads GE21 to select the Turning Bands Simulation method to estimate the grades for the Luanga Project.

The variograms that were used in the estimation method are satisfactory and consistent with respect to the grade estimation that was calculated via Simulation (E-Type), making use of search anisotropy determined in the variography study. A valid conditional simulation in geostatistics ensured that simulated values honour both spatial continuity and data distribution.

To classify Mineral Resources, a study of spatial continuity for Pd Equivalent was conducted using variography followed by ordinary kriging interpolation. This study established a continuity zone suitable for considering:

- The Measured Mineral Resource was classified according to a reference grid of approximately 45mx45m, with a minimum number of 3 holes in the section along the strike and dip directions, surrounded by the pit shell.

- The Indicated Mineral Resource classification had as a reference a drilling grid of approximately 75m x 75m, extending both along the strike and dip directions and requiring a minimum of two drill holes.
- Manual post-processing was undertaken to construct wireframes representing the volumes categorized as Measured and Indicated while considering the blocks within the resource pit shell.
- The Inferred Mineral Resource classification is all remaining estimated blocks within the resource pit shell.

GE21 considers the Mineral Resource classification model and the analysis of criteria for the classification of those Mineral Resources to be satisfactory, although some recommendations have been made for future improvements.

1.15.5 RPEEE

GE21 has not identified any mining, metallurgical, infrastructure, permitting, legal, political, environmental, technical, or other relevant factors that could materially affect the potential development of the Mineral Resources other than those typical for a project at this stage of development and as identified in this report.

GE21 performed a pit optimization study to classify the mine's Mineral Resources to ensure the RPEEE was met. The parameters in the benefit function are presented in Table 1-7.

Table 1-7: Pit parameters generated by RPEEE

Optimization Parameters - RPEEE				
Item				Unit
Lithotype	Fresh & Weathered & High Talc			-
Slope Angle	Weathered		40	°
	Fresh / High Talc		50	°
Mining	Density	Block Model		
	Mining Recovery		100	%
	Mining Dilution		0	%
	Cut-off grade (Whittle)	Fresh	-	-
		Weathered	-	-
Processing	Metallurgic Recovery - Weathered	Pd	81.0%	Mill
		Pt	23.0%	Mill
		Rh	54.0%	Mill
		Au	90.0%	Mill
		Ni	0.0%	Mill
	Metallurgic Recovery - Fresh	Pd	77.0%	Mill
		Pt	81.0%	Mill
		Rh	51.0%	Mill
		Au	48.0%	Mill
		Ni	50.0%	Mill
	Metallurgic Recovery - High Talc	Pd	51.0%	Mill
		Pt	55.5%	Mill
		Rh	27.3%	Mill
		Au	27.0%	Mill
		Ni	0.0%	Mill
Costs	Weathered	Mining Cost	2.00	USD/t mined
		Processing Cost	7.50	USD/t ROM
		Grade Control	1.00	
		Logistics	0.50	

Optimization Parameters - RPEEE				
Item				Unit
		Rehabilitation	1.00	
		G&A	1.50	
	Fresh / High Talc	Mining Cost	3.00	USD/t mined
		Processing Cost	9.00	USD/t ROM
		Grade Control	1.00	
		Logistics	0.50	
		Rehabilitation	1.00	
		G&A	1.50	
Selling	Price	Pd	1 380	USD/Oz
		Pt	1 100	USD/Oz
		Rh	6 200	USD/Oz
		Au	1 500	USD/Oz
		Ni	7.10	USD/lb
	Royalties	All	2.0	%

Source: GE21, 2025.

1.15.6 Mineral Resource Estimate

The Luanga Project's pit-constrained MRE has an effective date of February 18, 2025. In summary, It comprises 36 Mt at 2.00 g/t Pd Eq for a total of 2.3 Moz Pd Eq in the Measured category, 122 Mt at 2.06 g/t Pd Eq for 8.0 Moz Pd Eq in the Indicated category, 158 Mt at 2.04 g/t Pd Eq for a total of 10.4 Moz Pd Eq in the Measured + Indicated categories, and 78 Mt at 2.01 g/t Pd Eq for a total of 5.0 Moz Pd Eq in the Inferred category.

1.16 Recommendations

GE21 recommends completion of the outstanding metallurgical work that was not completed in 2024, including final assays, review, interpretation and reporting. This has the potential to unlock modest gains in metallurgical recoveries, which could be applied to subsequent updates to the current 2025 MRE. If a further MRE upgrade is deemed desirable, GE21 recommends:

- Drilling at depth in areas where the constraining pit constraints the reported Luanga MRE due to the absence of drill data at depth. Further refinement of the geological and mineralogical models may result in unlocking a modest gain in MRE metal grades.
- Completion of the outstanding metallurgical test work noted above.
- Resource estimation by the conditional simulation method defining the Selective Call Unit (SCU) to define the recoverable resource.

Collectively, the above work could deliver a further upgrade to the Luanga MRE, both in overall tonnage and, potentially, the average grades of the MRE.

Following on from the successful and significant upgrade to the Luanga MRE (as compared to the maiden 2023 MRE), the next significant stage for the Company would be the completion of either (a) a Preliminary Economic Assessment (PEA) and/or (b) a Pre-Feasibility Study (PFS) that would define Mineral Reserves (given that most of the MRE is now classified in the Measured and Indicated categories).

1.16.1 Luanga Exploration Potential

The results of Bravo's 2024 exploration drilling, based on the HeliTEM Electromagnetic (EM) survey covering the entire Luanga property, have generated intersections of massive sulphide mineralization, including:

- Ni/Cu/PGM and Ni/Cu massive sulphides are probably related to the emplacement of the Luanga deposit.
- More interestingly, compelling evidence of Carajás -style Iron Oxide Copper Gold (IOCG) mineralization, particularly in work reported from the T5 target, where high-grade copper-gold mineralization (see DDH2405T002 (in press release May 28, 2023) which intercepted 11.48m at 14.3% Cu, 3.3g/t Au including 2.9m at 22.9% Cu, 3.6g/t Au).

GE21 recommends that exploration work in 2025 should focus on continuing the exploration for mineralization outside of the Luanga PGM+Au+Ni deposit, particularly the potential for IOCG deposits, given the results from early exploration works in 2024.

1.16.2 Luanga Carbon Capture Potential

The Luanga deposit is hosted almost entirely in ultramafic rocks which early works indicated the potential for permanent carbon sequestration in tailings and/or waste rock. This is an opportunity that can be investigated further, subject to test results and economic assessment, and could be incorporated into future study phases with the potential to create a carbon-negative operation in combination with other mitigation efforts such as the use of hydroelectric power, mine electrification and reforestation.

1.16.3 Recommended Work Program

GE21 recommends completion of the outstanding metallurgical work that was not completed in 2024, including final assays, review, interpretation and reporting. This has potential to unlock modest gains in metallurgical recoveries, which could be applied to subsequent updates to the current 2025 MRE. If a further MRE upgrade is deemed desirable, GE21 recommends:

- Drilling at depth in areas where the constraining pit that constrains the reported Luanga MRE due to the absence of drill data at depth. Further refinement of the geological and mineralogical models may result in unlocking a modest gain in MRE metal grades.
- Completion of the outstanding metallurgical testwork noted above.
- Resource estimation by the conditional simulation method defining the Selective Call Unit (SCU) to define the recoverable resource.

Collectively, the above work could deliver a further upgrade to the Luanga MRE, both in overall tonnage and, potentially, the average grades of the MRE.

Following on from the successful and significant upgrade to the Luanga MRE (as compared to the maiden 2023 MRE), the next significant stage for the Company would be the completion of either (a) a Preliminary Economic Assessment (PEA) and/or (b) a Pre-Feasibility Study (PFS) that would define mineral reserves (given that most of the MRE is now classified in the Measured and Indicated categories).

1.16.3.1 Luanga Exploration Potential

The results of Bravo's 2024 exploration drilling, based on the HeliTEM Electromagnetic (EM) survey covering the entire Luanga property, has generated intersections of massive sulphide mineralization, including:

- Ni/Cu/PGM and Ni/Cu massive sulphides, probably related to the emplacement of the Luanga deposit.
- More interestingly, compelling evidence of Carajás-style Iron Oxide Copper Gold ("IOCG") mineralization, particularly in work reported from the T5 target, where high-grade copper-gold mineralization (see DDH2405T002 (in press release May 28, 2023) which intercepted 11.48m at 14.3% Cu, 3.3g/t Au including 2.9m at 22.9% Cu, 3.6g/t Au).

GE21 recommends that exploration work in 2025 should focus on continuing the exploration for mineralization outside of the Luanga PGM+Au+Ni deposit, and particularly the potential for IOCG deposits given the results from early exploration works in 2024.

1.16.3.2 Luanga Carbon Capture Potential

The Luanga deposit is hosted almost entirely in ultramafic rocks which early works indicated the potential for permanent carbon sequestration in tailings and/or waste rock. This is

an opportunity that can be investigated further, subject to test results and economic assessment, could be incorporated into future study phases with the potential to create a carbon negative operation in combination with other mitigation efforts such as use of hydroelectric power, mine electrification and reforestation.

1.16.3.3 Recommended Work Program

The recommended work program comprises two phases, with Phase 5 covering recommended work subsequent to the date of the Technical Report, and Phase 6. Phase 5 is subdivided into four subcategories (A-D) covering continuing metallurgical test work, a PEA, potential resource expansion drilling and regional exploration outside of the PGM+Au+Ni deposit. Phase 6 is contingent on the completion of Phase 5A and, in certain circumstances, Bravo could elect to proceed directly to completion of Phase 6, and not complete Phase 5B.

PHASE 5A – Metallurgical testwork at Luanga

Completion of outstanding 2024 metallurgical testwork:	
Estimate	US$0.20M
Continuation of carbon sequestration study:	
Estimate	US$0.05M
Continued Metallurgical testwork and optimization	
Estimate	US$0.20M
Updated MRE and technical report in accordance with NI 43-101:	
Estimate	US$0.10M
Sub-total – Phase 5A	***US$0.55M***

PHASE 5B – PEA

MRE Update implicit model:	
Estimate	US$0.3M
Completion of a PEA, including market studies:	
Estimate	US$0.3M
Sub-total – Phase 5B	***US$0.6M***

PHASE 5C – Deep Drilling below the Luanga PGM+Au+Ni deposit

Deep drilling at the Luanga PGM+Au+Ni deposit.	
8 holes @ ~500m = 4,000m @ US$450/m	
Estimate	US$1.8M
Sub-total – Phase 5C	***US$1.8M***

Phase 5D – Regional Exploration

Exploration of new (IOCG and/or massive sulphide Ni/Cu/ PGM targets):

Geological, geophysical and drilling programs to evaluate the potential for the discovery of additional zones of mineralization:

Geophysics	US$0.1M
Drilling: 35 holes x 200m for 7,000m @ US$400m (all inclusive)	US$2.8M

Sub-total – Phase 5D	***US$2.9M***
TOTAL – PHASE 5	***US$5.85M***

PHASE 6 – PFS following favorable results from a PEA

Completion of a PFS:

Estimate US$1.0M

Sub-total – Phase 6	***US$1.0M***
Sub-total – Phase 6	***US$1.0M***

2 INTRODUCTION

GE21 Consultoria Mineral Ltda. (GE21), headquartered in Belo Horizonte, Minas Gerais, Brazil, is an independent mineral consulting company composed of a team of professionals qualified to report Mineral Resources and Reserves in accordance with the guidelines of the Canadian Institute of Mining, Metallurgy and Petroleum (CIM) code, as required by "National Instrument 43-101 – Standards of Disclosure for Mineral Projects" (NI 43-101).

Bravo Mining Corp. (TSX.V: BRVO, OTCQX: BRVMF) is a Canadian and Brazil-based mineral exploration and development company focused on advancing its Luanga PGM+Au+Ni Project in the Carajás Mineral Province of Brazil. The Company's head office is located at Av. Jornalista Ricardo Marinho, nº. 360, room 247, Barra da Tijuca, Rio de Janeiro, RJ, Brazil, Zip code 22631-350 and its registered office is located at Bentall 5, 550 Burrard Street, Suite 2501, Vancouver, British Columbia, V6C 2B5.

Bravo has commissioned GE21 to prepare a Mineral Resource Estimate (MRE) Technical Report for the Luanga Project in Pará, Brazil, in accordance with the requirements of NI 43-101.

The Effective Date of February 18, 2025, is based on the receipt date for the Project database. Bravo indirectly owns 100% of the Luanga Project. The organizational structure of Bravo and ownership of the Luanga Project is shown in Figure 2-1.

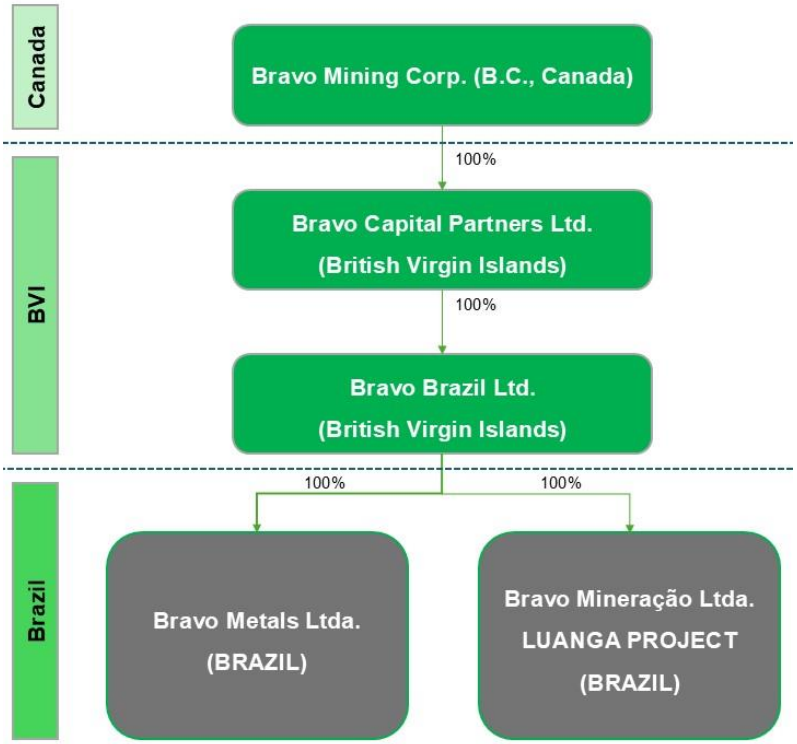

Figure 2-1: Bravo organization chart

Source: Bravo, 2025.

2.1 Qualifications, Experience and Independence

GE21 is a specialized, independent mineral consulting company. The geological reconnaissance and due diligence evaluation have been conducted by GE21 staff members, who are members of the Australian Institute of Geoscientists (AIG) and meet the requirements of independent QPs as defined in NI 43-101.

2.2 Qualified Persons

The QPs responsible for this independent Technical Report are Mr. Porfirio Cabaleiro Rodriguez and Mr. Bernardo Viana.

Mr. Porfirio Cabaleiro Rodriguez is one of the QPs regarding the objectives of this report. Mr. Porfirio was responsible for sections 2, 3, 4, 5, 6, 13, 14, and 23 and co-responsible for Sections 1, 11, 12, 25 and 26 with Mr. Viana. Mr. Rodriguez is an engineer and a FAIG and has sufficient experience relevant to the style of mineralization and type of deposit under consideration. Mr. Rodriguez has more than 30 years of experience working with exploration and mining projects. Mr. Rodriguez is considered as an independent QP, as defined in NI 43-101

Mr. Rodriguez visited the property from July 4 to 7, 2023, October 3 to 6, 2023, and January 27 to January 31, 2025. On the last two visits, GE21's qualified persons team was composed of Mr. Rodrigues and Mr. Viana. During the site visit, some diamond drill collars were located, their recorded coordinates were validated with a handheld GPS, and the core was inspected in the onsite core storage facility.

Mr. Bernardo Viana is the other QP responsible for this Report; Mr. Viana was responsible for sections 7,8,9 and 10 and co-responsible for Sections 1, 11, 12, 25 and 26. Mr. Viana is a geologist and a FAIG and has sufficient experience relevant to the style of mineralization and type of deposit under consideration for being considered an independent QP, as defined in NI 43-101. Mr. Viana has more than 20 years of experience working with exploration and mining projects.

Neither GE21 nor the Authors of this Technical Report have had any material interest invested in Bravo or any of its related entities. GE21's and the Author's relationship with Bravo is strictly professional, consistent with that held between a client and an independent consultant. This report was prepared in exchange for payment based on fees that were stipulated in a commercial agreement. Payment of these fees is not dependent on the results of this report. Table 2-1 below relates each QP with their report items' responsibility.

Table 2-1: Report Items and assigned QP responsibilities

Company	QP	Section Responsibility	Site Visit	Responsibility
GE21	Porfirio Cabaleiro Rodriguez, FAIG	2, 3, 4, 5, 6, 13, 14, and 23, with co-responsibility for Sections 1, 11, 12, 25, 26 and 27	July 4 to 7, 2023; October 3 to 6, 2023; and January 27 to 31, 2025	Author
GE21	Bernardo Viana, FAIG	7,8,9, 10 and 20 co-with responsibility for 1, 11, 12, 25, 26 and 27	October 3 to 6, 2023; and January 27 to 31, 2025	Author

Source: GE21, 2025.

The Effective Date of this report is February 18, 2025. The Authors have relied on information provided by Bravo, which was provided in a database with full access given to the QPs.

3 RELIANCE ON OTHER EXPERTS

The authors of this Report are Qualified Persons, as defined under NI 43-101, with relevant experience in mineral exploration, data validation, and Mineral Resource estimation.

The information presented regarding the tenure, status and work permitted by permit type within the Bravo property in Section 4 – Property Description and Location, is based on information published by the National Mining Agency of Brazil (Agência Nacional de Mineração, ANM) and is available to the public.

Bravo retained Linneu de Albuquerque Mello, whose lawyers are qualified to practice law in the Federative Republic of Brazil. According to a title opinion by Linneu de Albuquerque Mello dated January 31, 2025, the Luanga Mineral Rights were valid and in good standing at that time.

The environmental licensing status information and work plans related to community and social outreach included in Section 20 – Environmental Studies, Permitting and Social or Community Impact, were prepared by Bravo and reviewed by GE21. GE21 determined that the economic factors used in the determination of specific technical parameters of this Report, including gold, PGM, nickel and the USD: BRL assumptions used, were in line with industry norms and broader market consensus and are acceptable for use in the current Mineral Resource estimate.

The authors of this Report have not identified any significant risks in the underlying assumptions as, in addition to the above, the underlying assumptions are in line with spot market conditions as of the date of this Report.

4 PROPERTY DESCRIPTION AND LOCATION

4.1 Project Description & Ownership

Luanga is an advanced-stage mineral project comprising the Luanga deposit in Pará State, Brazil, which contains PGM+Au+Ni. as shown in (Figure 4-1). It is held under the Exploration Licence Nº.1961 and designated ANM.851.966/1992, comprising an area of 7,810.02 hectares in extent.

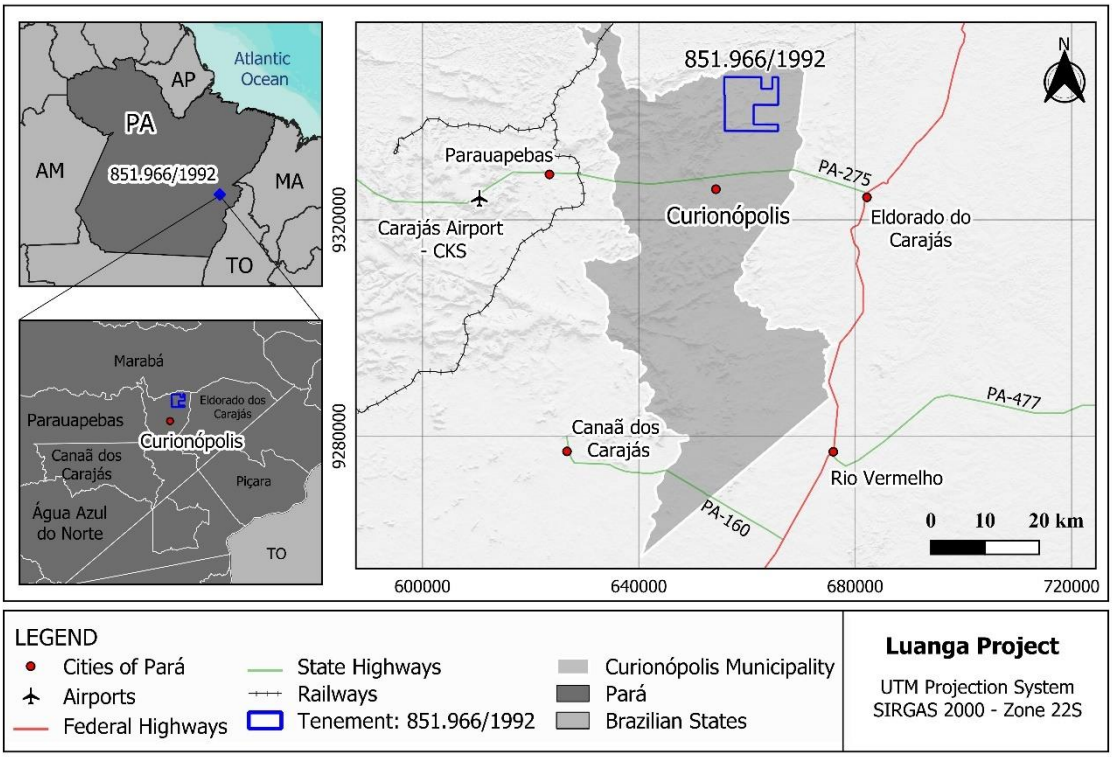

Figure 4-1: Luanga Project location map

Source: GE21, 2025.

4.2 Land Access

The Luanga Project is located on private farmland generally used for cattle farming. There are no indigenous claims or protected forests in the area. To carry out exploration/feasibility works, such as drilling, an access agreement is required with the surface rights owner (landowner).

Land access agreements (Figure 4-2) are currently in place with six key landowners, covering 97% of the known mineralized envelope of the Luanga deposit. These agreements have recently been renewed and are valid for two years each time. There is no reason to believe that the land access contracts will not be renewed again in the future. See Section 4.3 for a discussion on Bravo's rights in respect of non-owned surface rights.

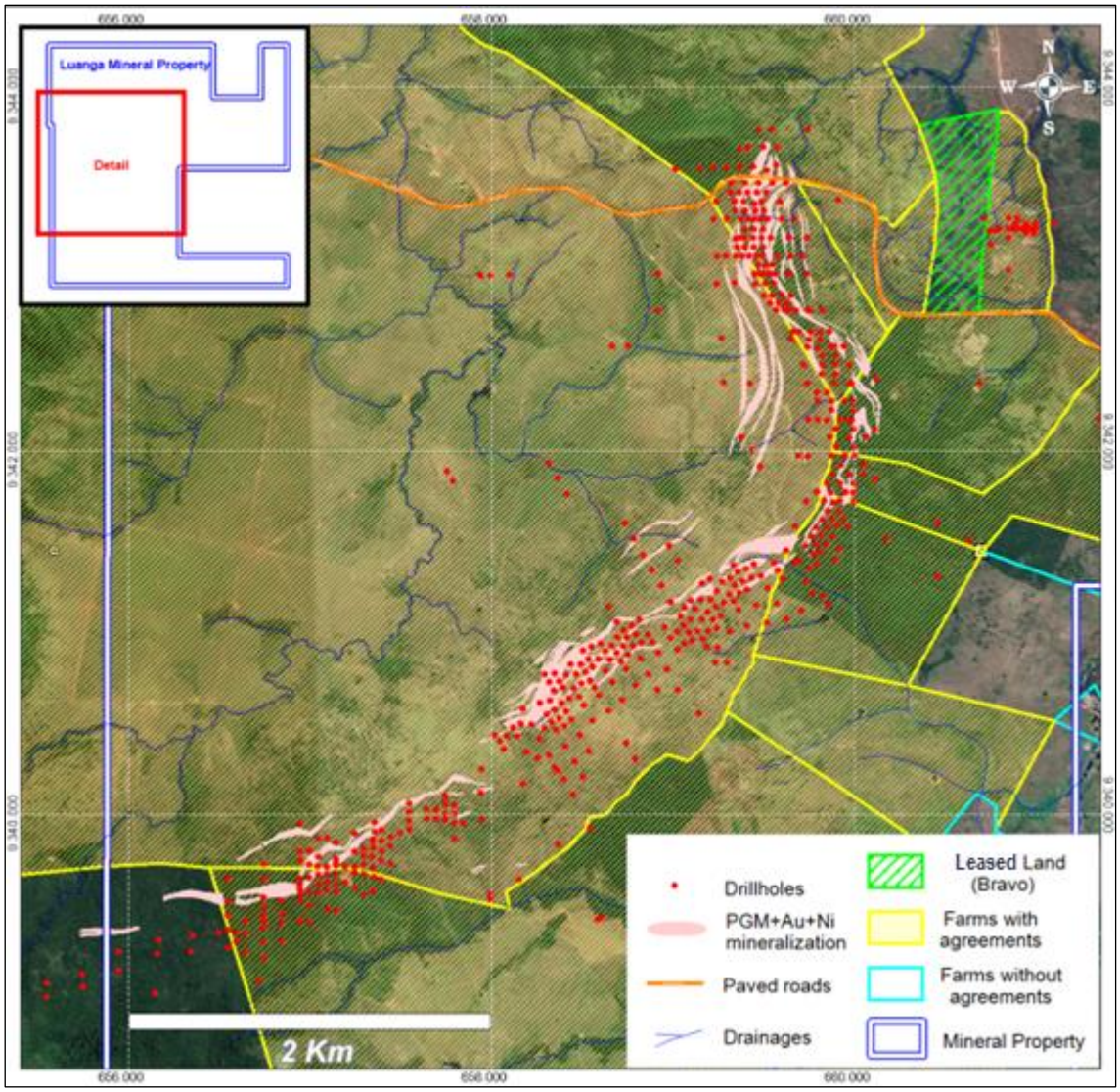

Figure 4-2: Luanga land access agreements map

Source: Bravo, 2025.

Under Brazilian mining law, exploration and study work (including all works in the recommendations of this report) do not require any permits, as the land is privately owned, and permission to conduct work is incorporated under the land access agreements with various owners.

As far as the authors are aware, there are no other significant factors or risks that may impede access or the ability to perform the proposed work on the property; the information contained in this report is current and complete as of the report's Effective Date and complies with Section 4.2(8) of NI 43-101.

4.3 Mining Legislation, Administration and Rights

Brazilian Mining Legislation, Administration and Rights are governed by the Brazil Mining Code (Federal Law Decree No. 227/1967), which regulates the exploration and development of Mineral Resources and mining projects in Brazil.

Mineral tenements in Brazil generally comprise Prospecting Licenses, Exploration Licenses and Mining Licenses. These are granted subject to various conditions, including an annual fee per hectare payment and reporting requirements. Each tenement is granted subject to standard conditions that regulate the holder's activities and regulations that are designed to protect the environment.

The holder of a granted Prospecting License, Exploration License or Mining License is not required to spend a set annual amount per hectare in each tenement on exploration or mining activities. There is no statutory or other minimum expenditure requirement in Brazil. However, annual rental payments are made to the Brazilian National Department of Mineral Production (Mining National Agency, ANM), and the holder of an Exploration License must pay rates and taxes ranging, based on the current exchange rate, from US$0.69 to US$1.03 per hectare to the Government.

If a mineral tenement is located on private land, then the holder must arrange or agree with the landowners to access the property; however, in the absence of an agreement, the company can request access in court and by depositing a compensation value that is established and estimated by the court.

4.3.1 Prospecting Licenses

A Prospecting License entitles the holder, to the exclusion of all others, to explore for minerals in the License but not to conduct commercial mining. A Prospecting License may cover a maximum area of 50 hectares and remain in force for up to 5 years. The holder may apply for a renewal of the Prospecting License, which is subject to approval by ANM. The period of renewal may be up to a further five years.

4.3.2 Exploration Licenses

The federal department responsible for issuing Exploration Licences is ANM. Exploration licenses are typically granted for three years and can be extended for a further three years maximum, subject to ANM approval. An exploration license allows the holder to explore for minerals in the granted concession but not to conduct commercial mining.

License applications must include applicant details, the elements or metals to be explored, and the application license area. They must also be accompanied by stipulated technical documents prepared under the responsibility of a qualified geologist or mining engineer. Such documents typically include:

- Budget forecasts for the planned exploration program.
- Maps of the intended area.
- Payment of governmental fees and taxes.
- Proof of sufficient funds or financing for the investment forecast set forth in the proposed exploration plan.

Licenses are deemed granted when they are published in the National Official Gazette.

In order to renew the exploration license, the ANM shall take into consideration the development of the work performed. The request for renewal of the exploration license must be presented 60 days before the expiration date of the original license. As to the renewal request, a report must be presented of the work already carried out, indicating the results achieved, as well as reasons justifying the work continuation. The renewal of the exploration license does not depend on the publication of a new license but only on the publication of the decision to renew it.

A final exploration report summarizing the economic viability and technical feasibility of the claim must be supplied to the ANM prior to the expiration of the granted period. Such report must be prepared under the technical responsibility of a legally qualified professional and must also contain the following:

1. Information on the area, means of access and communication.
2. Plan of the geological surveys completed.
3. Description of the main aspects of the deposit.
4. Quality of the mineral substance and definition of the deposit.
5. Genesis of the deposit, as well as its qualification and comparison to similar deposits.
6. Report on the assay results of the collected samples.
7. Demonstration of the economic feasibility of the deposit, and
8. The necessary information for the calculation of the reserve, such as the density, area, volume, and grade.

The final exploration report must be presented independently from the work results and shall indicate the feasibility or non-feasibility of the development and exploitation of the mineralization or the non-existence of the deposit. The holder of an exploration license who does not present a final exploration report within the date established by the regulations will be fined. Nevertheless, the exemption from submitting the report is permitted when the titleholder relinquishes the license. The ANM must confirm the relinquishment, provided it happened in one of the two following instances:

1. at any time, if the titleholder has not been successful at entering the area, despite all the efforts made, including judicial means, or;
2. before one-third (1/3) of the term of duration of the exploration license has passed.

Should the final exploration report conclude that mineral exploitation or development is temporarily non-feasible (due to economic conditions, logistics, and commodities prices). In that case, the license holder may request the postponement of the decision related to the report (Sobrestamento), which the ANM shall review.

A concession holder has one year from the approval of the report to apply for a mining concession or to transfer this right to a third party. The application period may be extended for longer than a year at the discretion of the ANM, if requested by the holder before the expiration

date, with necessary motivations and justifications (for example, more time to obtain environmental approvals or conduct further studies on economic viability and technical feasibility).

Development of mining projects is governed by three phases: Preliminary Licence (LP), Installation Licence (LI) and Operating Licence (LO). Issuance of these licences is governed by the Brazilian Institute of Environment and Renewable Natural Resources (Instituto Brasileiro do Meio Ambiente e dos Recursos Naturais Renováveis, IBAMA), the State Environmental Agencies, which would be the Pará State Environmental Agency (Secretaria de Estado de Meio Ambiente e Sustentabilidade do Pará, SEMAS) for the Luanga Project or the Municipal Authorities.

4.3.2.1 Stage 1 Licencing: Preliminary Licence (LP)

Receipt of the LP requires the licencing agency to evaluate the location and overall design of the project, environmental impact, social/community impact and establish terms of reference for future development. The Luanga Project occurs on predominantly privately owned, cleared land. There are no Indigenous communities within the property boundary or a 10km radius, so there is no consultation requirement under the National Foundation of the Indian (Fundação Nacional do Índio – FUNAI), the federal agency that establishes and manages policies relating to Indigenous communities.

On December 12, 2024, The Company held a public hearing (Public Hearing) in the Municipality of Curionópolis, Pará State, as part of the process to obtain the LP for the entire Luanga PGM + Au + Ni deposit. The Public Hearing provided local communities and key stakeholders with a formal opportunity to contribute to the project and its Environmental Impact Study (EIA) and Environmental Impact Report (RIMA) by sharing suggestions and voicing their opinions. This hearing represents the final stage, and the most important step, of the LP process, which is critical for securing environmental approval for any major development in Brazil. Over 500 people attended the Public Hearing in person as well as over 900 virtually, engaging in productive discussions with the Company's team, our environmental consultant, and representatives from the Pará State Environmental Agency (SEMAS). The Public Hearing was deemed officially valid by SEMAS for the purposes of the LP issuance process. As a subsequent event of the effective date, the LP was approved and published on February 27, 2025.

4.3.2.2 Stage 2 Licencing: Installation Licence (LI)

Receipt of the LI allows earthworks and mine construction to start. Application for the LI must include the layout of the mine, processing plant, tailings dam and all associated infrastructure. It also details mining methods, recovery methods, tailings dam design (and dam failure studies). The LI also expands and updates the environmental and social/community studies included in the LP terms of reference and conditions.

4.3.2.3 Stage 3 Licencing: Operating Licence (LO)

Receipt of the LO allows operating activities to start and is essentially a review of the operation to ensure it was constructed according to the detail provided in the LI.

4.4 Mineral Tenure

On September 5, 1995, the Ministério de Minas e Energia (Ministry of Minerals and Energy – MME) issued Vale Exploration Licence No. 1961 under the process designated ANM.851.966/1992. The ANM administers Exploration Licences. This Exploration License is located 40km northeast of Parauapebas in Para State, Brazil.

The license, which covers the Luanga Project, comprises an area of 7,810.02 hectares, currently in Bravo Mineração Ltda.'s name, as summarized in Table 4-1 and illustrated in Figure 4-3. Exploration License 851.966/1992 remains valid while the Mining License application is pending.

Table 4-1: Mineral tenement summary

ANM Process	Municipality	Stage	Mineral	Title Owner	Size (hectares)	License No.	Expiry Date
851.966/1992	Curionópolis	Application for Mining License	Au, Pd, Pt, Ni	Bravo Mineração Ltda	7,810.02	1961	
				TOTAL	**7,810.02**		

Notes:
Comments: Mining License pending.
ANM = Mining National Agency.
Source: ANM, February 2025.

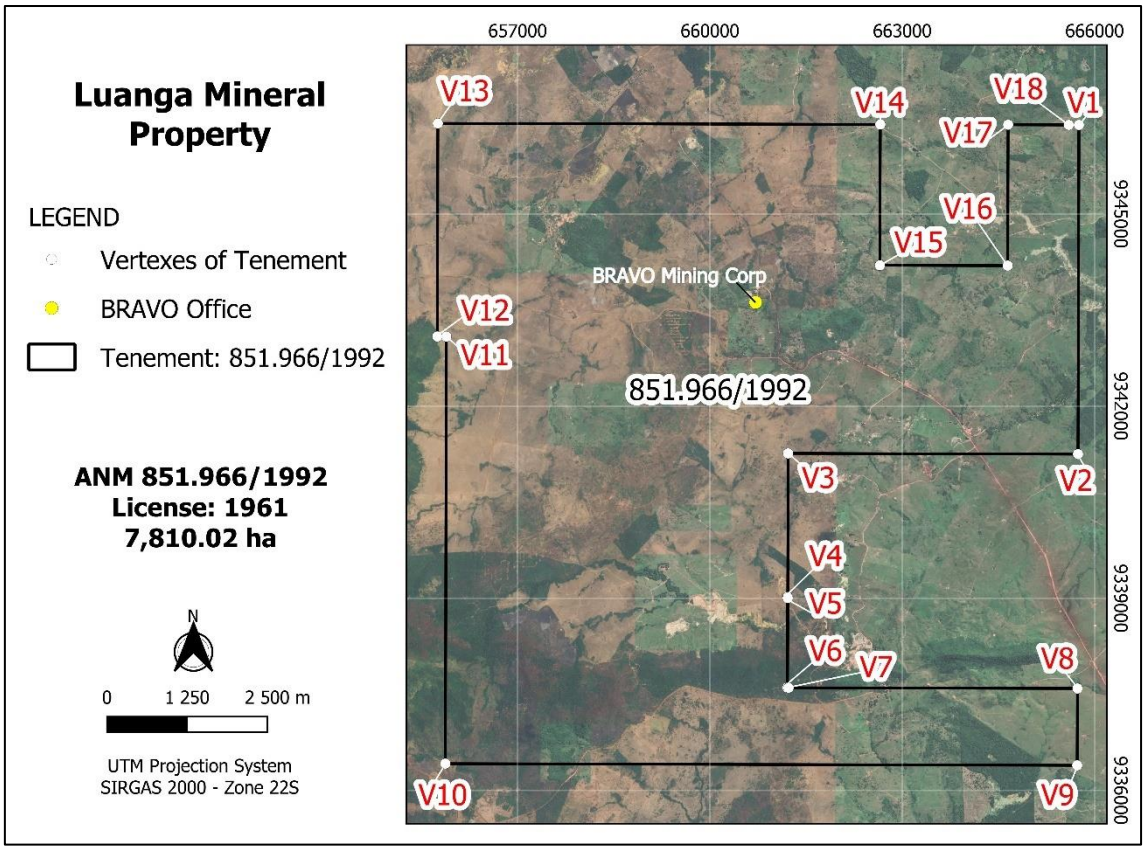

Figure 4-3: Luanga Project tenement map

Source: GE21, 2025.

The Luanga mineral property is centred approximately at coordinates -05º57'24.34" S/-49º32'51.00" W. Bounding coordinates of Exploration License No.1961 from ANM title documents are presented in Vertices of Luanga mineral property (Table 4-2).

Table 4-2: Vertices of Luanga mineral property

Vertex	Latitude	Longitude	Vertex	Latitude	Longitude
v1	-05°54'40"284	-49°30'09"580	v10	-06°00'05"795	-49°35'30"045
v2	-05°57'27"643	-49°30'09"580	v11	-05°56'28"677	-49°35'30"072
v3	-05°57'27"638	-49°32'36"608	v12	-05°56'28"677	-49°35'34"710
v4	-05°58'41"177	-49°32'36"614	v13	-05°54'40"336	-49°35'34"693
v5	-05°58'41"177	-49°32'36"617	v14	-05°54'40"300	-49°31'50"304
v6	-05°59'26"752	-49°32'36"617	v15	-05°55'51"911	-49°31'50"304
v7	-05°59'26"758	-49°32'36"617	v16	-05°55'51"911	-49°30'45"503
v8	-05°59'26"758	-49°30'09"580	v17	-05°54'40"289	-49°30'45"503
v9	-06°00'05"822	-49°30'09"580	v18	-05°54'40"284	-49°30'14"770

Exploration License Nº 1961, ANM.851.966/1992 – Datum SIRGAS 2000
Source: ANM, October 2023.

The first three years of the exploration permit expired on September 5, 1998. Still, the ANM only provided renewal of Exploration License on April 12, 2005, due to its internal bureaucracy, renewing for an additional three years until April 12, 2008. On April 11, 2008, Vale presented a Final Exploration Report to the ANM, and on April 19, 2013, the Company applied for a Mining License.

The ANM continues postponing the decision on the Project's Final Exploration Report. Bravo expects this status to continue until the Company submits a new study that demonstrates the technical and economic feasibility of the Project.

4.4.1 Acquisition or Transaction Terms

On June 3, 2020, Vale, FFA Holding e Mineração Ltda (FFAH) and Brazil Americas Investments and Participation Mineração Ltda (BAIP), where Bravo is the beneficiary party, appointed FFAH and BAIP to acquire the Luanga Project. Payment terms are as follows, with royalties shown in Section 4.5.

- USD300k paid on Dec 7, 2021
- USD500k paid on Nov 09, 2022
- USD500k paid on Nov 19, 2023
- Total: USD1.3 million

On 24 January 2022, Bravo´s wholly owned subsidiary acquired 100% of the shares of AIPL (Americas Investments & Participation Ltd.), giving it a 100%, undivided interest in the Luanga Project.

4.5 Royalties

The following royalties are applicable to the Luanga Project:

- 1% NSR royalty to Vale
- 2% NSR royalty to BNDES
- CFEM Government Royalties:
  - 1.5% NSR royalty Au
  - 2% NSR royalty on precious metals (Pd, Pt, Rh)
  - 2% NSR royalty on base metals (Ni, Cu)
- The Private Landowner Royalty is equal to 50% of CFEM royalties.

4.6 Environmental and Social Liabilities

No environmental liabilities have been identified within the Luanga Exploration License. The current land use at the Luanga Project is solely agricultural cattle grazing. There are no significant rivers within the property. There are also no existing forests on the property thus no deforestation is required. However, it is the stated intention of Bravo to plant 10 trees for every drill hole completed (Figure 4-4).

Figure 4-4: Seedling nursery

Source: Bravo, 2025.

The most significant activity to be completed by the company in the next few years is relatively low-impact drilling. Bravo will concurrently rehabilitate drill sites.

Social or community impact is expected to be negligible since the nearest community is the village of Serra Pelada, which is approximately 8km away. There are no indigenous communities within 25km of Luanga.

The unpaved road to Serra Pelada crosses Luanga in the northern half of the property. Vale is currently in the process of asphalting this road. A low-voltage power line parallels this road. Bravo does not expect to encounter major difficulties in moving the road and associated power line if the Project advances to a construction decision. The location of the road and power line will not impact planned exploration activities.

4.7 SUDAM

Bravo is subject to a corporate income tax rate of 25%, which is applied to the pre-tax profit. The company can apply for a tax incentive under Superintendence for the Development of the Amazon (Superintendência do Desenvolvimento da Amazônia, SUDAM) based on Federal Law Nº 13,799, January 3, 2019. If granted, this reduces the 25% income tax by 75% for a 10-year period, starting from the year in which the Appraisal Certificate from SUDAM is issued. The total tax burden in this case is 15.25% (75% of 25% + 9% social contribution tax), plus royalties as defined in section 4.5.

5 ACCESSIBILITY, CLIMATE, LOCAL RESOURCES, INFRASTRUCTURE, AND PHYSIOGRAPHY

5.1 Accessibility & Physiography

The Luanga Project is located in the municipality of Curionópolis in the central-eastern region of Pará State, approximately 500km south of Belém (a sizeable coastal port city and capital of Pará, Figure 5-1). Luanga is accessible via paved roads from two regional centres, Parauapebas and Marabá (Figure 5-2). Both cities have commercial airports with multiple flights a day to Brasilia and Belém from Parauapebas and to Brasilia, São Paulo, Rio de Janeiro, Salvador, and others from Marabá (Figure 5-3). Access to the Project is via a municipal paved road that turns off Highway PA-275 (Table 5-1).

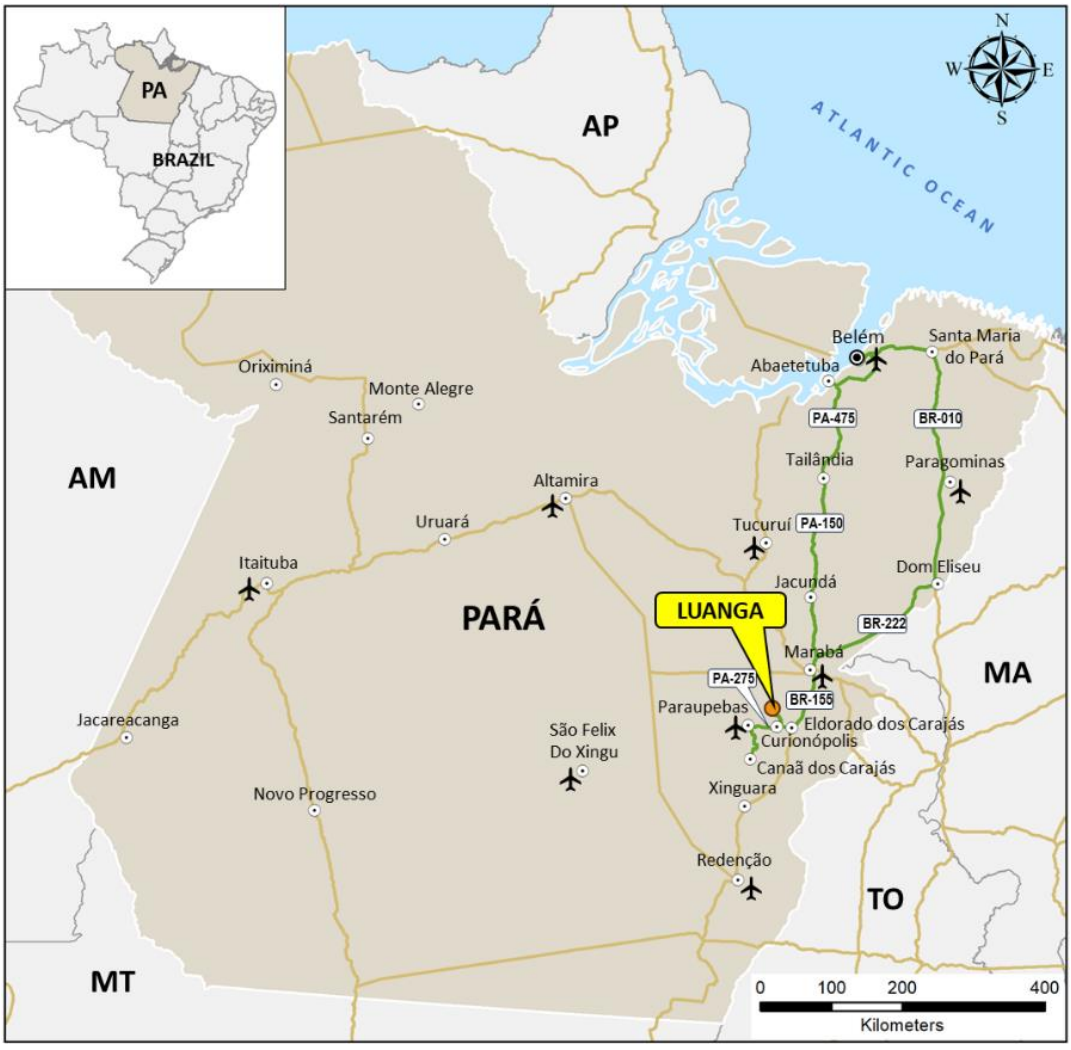

Figure 5-1: Regional location of Luanga Project in Pará State, Brazil

Source: GE21, 2023.

The closest population centres to the Project are the small town of Curionópolis, with a population of approximately 17,846, approximately 17km south-southwest of Luanga and the

mining community of Serra Pelada, approximately 12km west of Luanga. There are no communities within the Project boundary.

Parauapebas, located approximately 40km to the west-southwest of Luanga, is the region's critical service provider and labour source. Parauapebas is the largest mining town in the state, with a significant labour force of residents supporting multiple world-class iron mineralization and copper-gold mines in the Carajás. Parauapebas is also home to all the region's mining-related services and mining infrastructure. Parauapebas was recorded as having a population of 213,576 in 2020. Any future operation is expected to be able to source all labour from the local region.

The nearest rail services are those privately owned by Vale in Parauapebas, which connect to Marabá. Bravo has access to this rail line as part of the Luanga purchase agreement with Vale. The nearest commercial-scale port facility is Vila da Conde, located adjacent to the state capital, Belém, approximately 660km to the north. The port facilities can also be accessed via barge on the Tocantins River, which is also the nearest access point in Marabá.

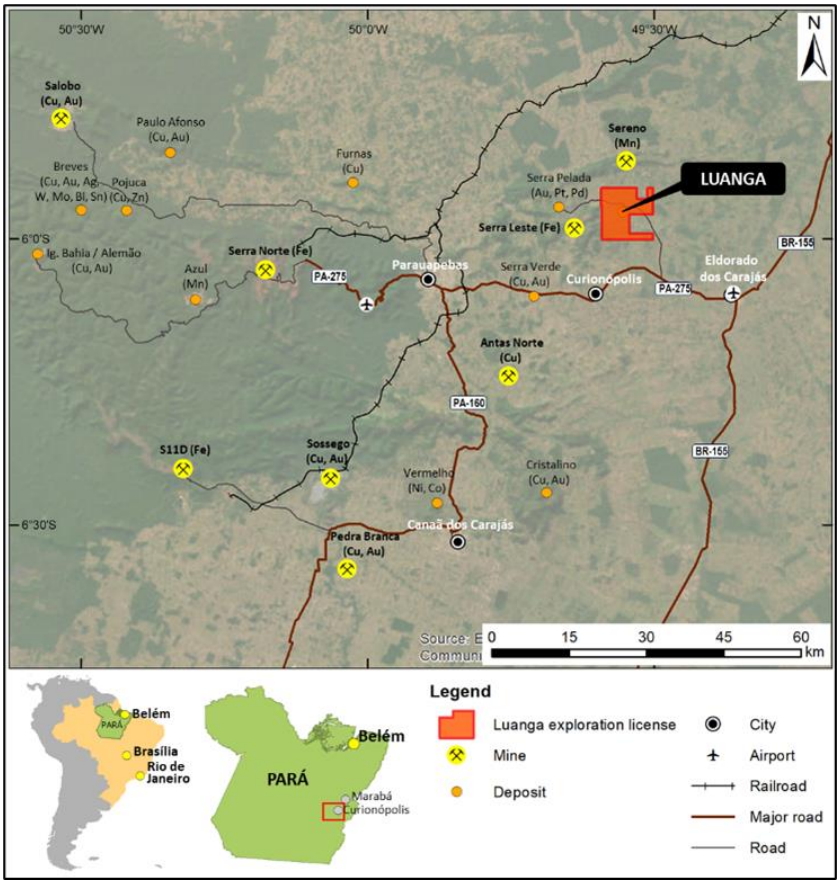

Figure 5-2: Access map for Luanga Project

Source: Bravo, 2025.

Figure 5-3: A) Carajás Airport building view. B) Marabá airport aerial view

Source: Aviação Brasil, 2017.

Table 5-1: Distances for ground access to Luanga Project

Departing (from)	Destination (to)	Road distance (km)	Estimated time (hours)
Marabá town	Eldorado dos Carajás town	102 (on BR-222)	01:30
Eldorado dos Carajás town	Paved road to Serra Pelada	16 (on PA-275)	00:20
Municipal paved road	Luanga property	17	00:20
TOTAL		135	02:10
Departing (from)	**Destination (to)**	**Road distance (km)**	**Estimated time (hours)**
Parauapebas town	Curionópolis town	36 (on PA-275)	00:40
Curionópolis town	Paved road to Serra Pelada	16 (on PA-275)	00:20
Municipal paved road	Luanga property	17	00:20
TOTAL		69	01:20
Departing (from)	**Destination (to)**	**Road distance (km)**	**Estimated time (hours)**
Curionópolis town	Paved road to Serra Pelada	16 (on PA-275)	00:20
Unpaved road access	Luanga property	17	00:20
TOTAL		**33**	**00:40**

Source: GE21, 2025.

The Luanga Project is located in the Carajás Mineral Province, which lies within the South Pará Plateau, where the altitudes vary from 500m to 700m above sea level. A series of NNE-SSW trending ranges project above the plateau, remnants of an older surface that was eroded to a peneplain and uplifted during the Paleozoic. Luanga lies on the southeast flank of the Serra Sereno range, with peaks up to 600m above sea level. The stream banks are terraced and capped with iron-aluminous laterite, which is currently being actively eroded (Figure 5-4).

The drainage of the area flows into the Sereno River, part of the Rio Vermelho system. A system of tributaries flows from Serra Leste to the northeast, crossing the Luanga mineral property, till discharge into the Sereno River.

Inside the Luanga Project area, vegetation has been cleared for pasture and subsistence cultivation, which is indicated in Figure 5-5 by the pink areas, versus dark green, which is forested areas. The Luanga Project covers 7,810 ha, much of which has been deforested to create grazing land for cattle and which is more than sufficient area for any contemplated future mining-related activities, including waste rock and tailings disposal, process plant and related infrastructure. Similarly, the other surface rights agreements discussed in Section 4 and shown in Figure 4-2, will also provide sufficient space within the 7,810 ha for proposed work programs and any contemplated future mining-related activities.

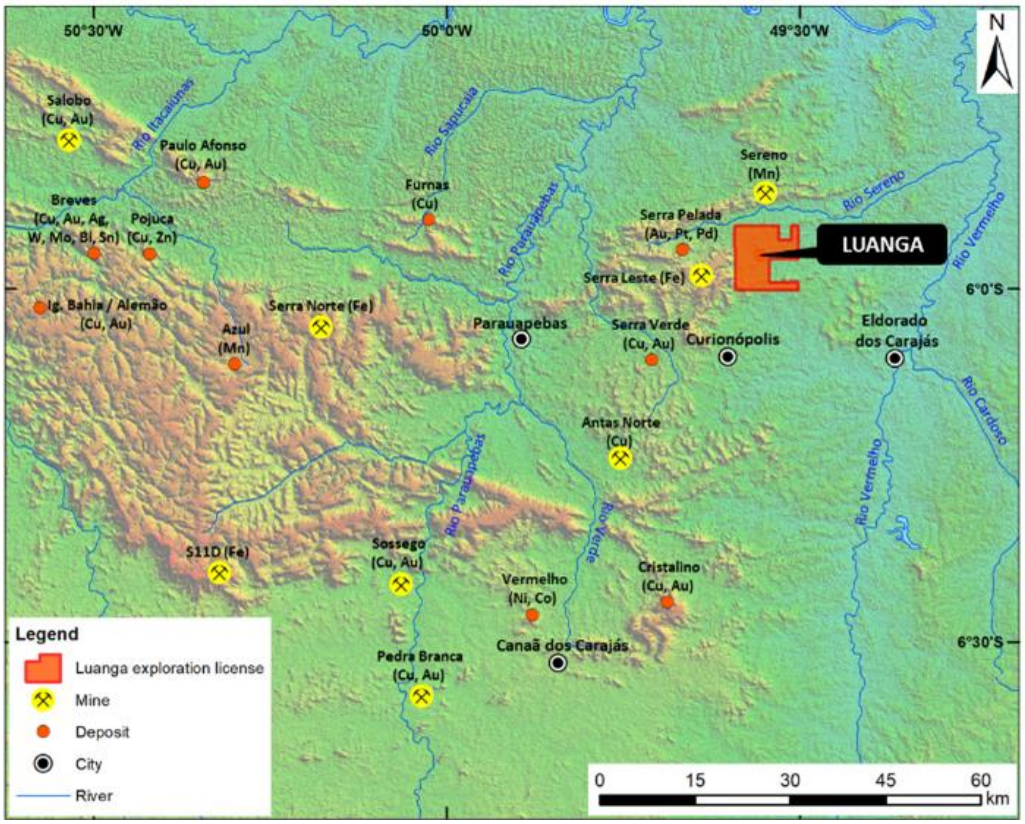

Figure 5-4: Physiography of Carajás region

Source: GE21, 2023.

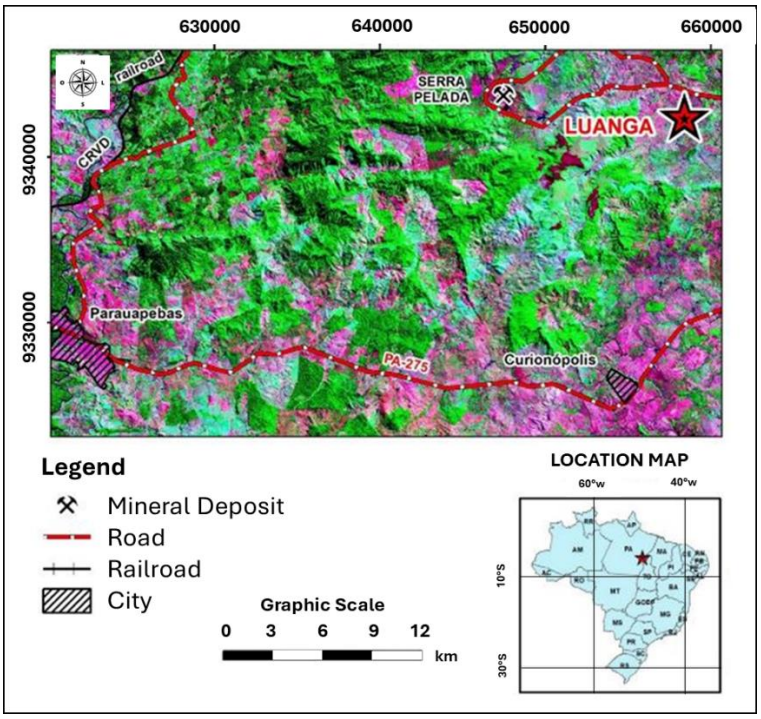

Figure 5-5: Sat image (RGB composition 342) with relief and vegetation of Carajás region

Source: GE21, 2025.

5.2 Climate and Length of Operating Season

Situated approximately 6º south of the equator, the climate at Luanga Project is typically equatorial, with slight variation in mean monthly temperatures throughout the year. The average maximum temperature is 32ºC while the average minimum is 22ºC. There are two distinct seasons: the winter is warm and dry, while the summer is wet and humid. Three-quarters of the annual precipitation falls from December through April. In August, the average rainfall is 10mm, while in January, February and March, the monthly rainfall exceeds 150mm. Rainfall intensity can be high. For these reasons, water availability for any contemplated future mining-related activity in the region is plentiful and readily accessible. Figure 5-6 shows the climate data for Curionópolis. The annual rainfall average is 2,082mm.

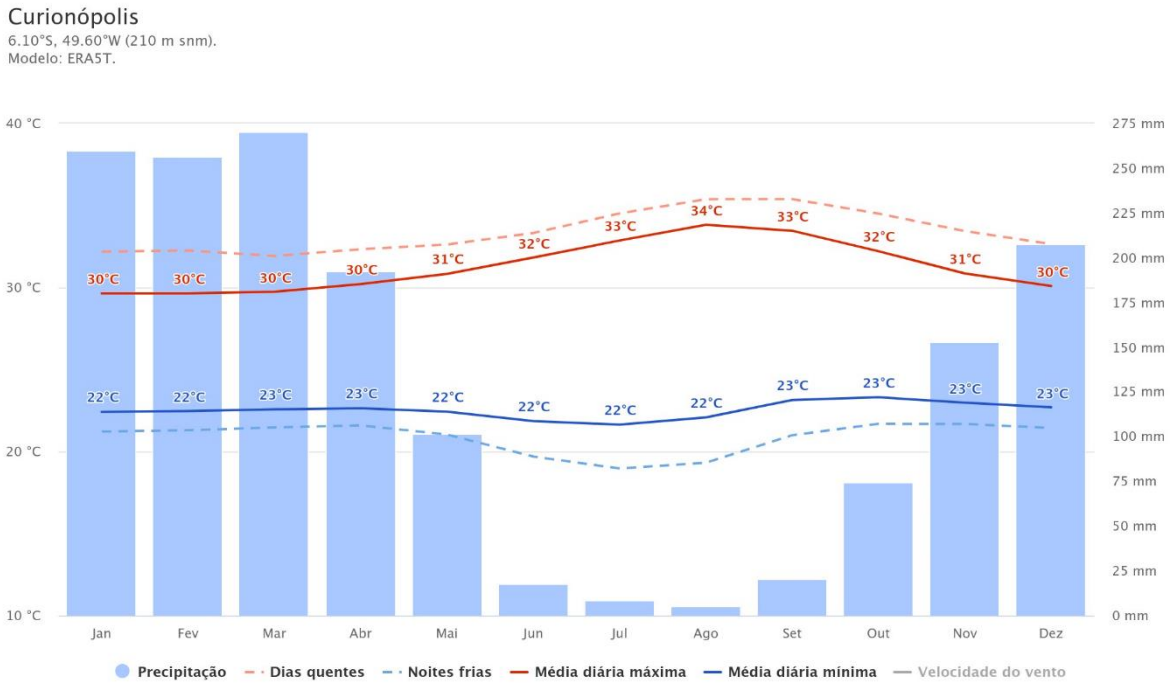

Figure 5-6: Average monthly temperature and rainfall at Curionópolis

Source: Meteoblue.com, 2025.

5.3 Local Resources and Infrastructure

The Luanga Project area is in a moderately fertile red/yellow podsols region. Agricultural production includes rice, corn, beans, palm oil, banana, tomato, watermelon, coffee, avocado, guava and cashew nuts. Throughout the region, there is extensive cattle ranching, producing both milk and meat, using natural pastures that are annually burnt to stimulate the growth of young grasses. Total stock numbers include up to 400,000 head of cattle and 50,000 pigs in the region. The remaining forest areas have been intensively exploited for fuel wood for domestic use and especially to produce charcoal. This is an essential material for producing pig iron for small plants in Marabá.

The burgeoning mining industry in the Carajás Mineral Province required a massive investment in infrastructure to create transport routes for industrial and agricultural exports. One of Brazil's most significant mining projects is based on the iron mineralization deposits in the Serra dos Carajás near Parauapebas. With a reported 18 billion tonnes of mineralization, this is one of the world's most significant iron mineralization deposits. The Luanga Project lies within the Grande Carajás Project Mining and Industrial Zone (Projeto Grande Carajás, PGC) that is reportedly gazetted over an area of 400,000 km^2 and involves a total investment of US$62 billion. The town of Carajás has been completely rebuilt and is closed to all but Vale's workers. Vale constructed a heavy-duty rail line over 892 km from the iron mines to the Atlantic port of São Luís. The nearest railhead to Luanga Project is at Carajás, 55 km by road from Luanga.

Besides iron mineralization, other minerals such as gold, copper, nickel, manganese, and bauxite have been discovered in significant quantities in the Carajás Mineral Province, with

additional discoveries a regular occurrence. Much of the metal mined in the region is exported in its raw form, but there has been some attempt at metal refining. These include the aluminum smelter in Belém (Latin America's most significant industrial plant) and a steel mill in São Luís. Mining developments have led to increased energy demands, spurring the construction of dams for hydroelectric power generation.

The region's economy is heavily dependent on mining, principally from the iron mineralization mines of Carajás. Vale is reportedly developing five projects in Southern Pará located within a radius of 90km from Carajás, three of them to the southeast and two to the northeast.

The city of Parauapebas is equipped with all the local amenities, such as banks, hospitals, hotels, and supermarkets. In addition, the long history of mining in the town has provided the area with a skilled workforce experienced in disciplines that support mining, such as machinery mechanics and general maintenance.

Marabá is the market centre for the region and a hub for road, rail, and river transport. Along with the mining industry, the city economy relies on agriculture, cattle raising, handcraft production and commerce. Many experienced miners are in the vicinity, and the university in Marabá is focused on training professionals for the mineral industry.

The Tocantins River and its tributaries are of vital economic importance to the region, both as a source of fresh water for the population and industry and as a source of hydroelectric power. Downstream from Marabá, the Tucuruí hydroelectric dam expanded its capacity in 2005 to lift output to 8,370MW. Three other hydroelectric plants on the Tocantins River have a combined capacity of 2,630MW, and an additional plant is near completion. Seven more hydroelectric plants are planned on the Tocantins River (Figure 5-7).

A branch of the main 230kV hydroelectric power transmission line from Tucuruí to Carajás has the available capacity to supply the necessary power to the Luanga Project area for any contemplated future mining-related activity. This power transmission line is approximately 25km to the NW of the Luanga property.

However, it is worth noting that Bravo has office facilities close to the Project, on land that is leased by Bravo and is within a local farm close to Curionópolis and Parauapebas (Figure 5-8).

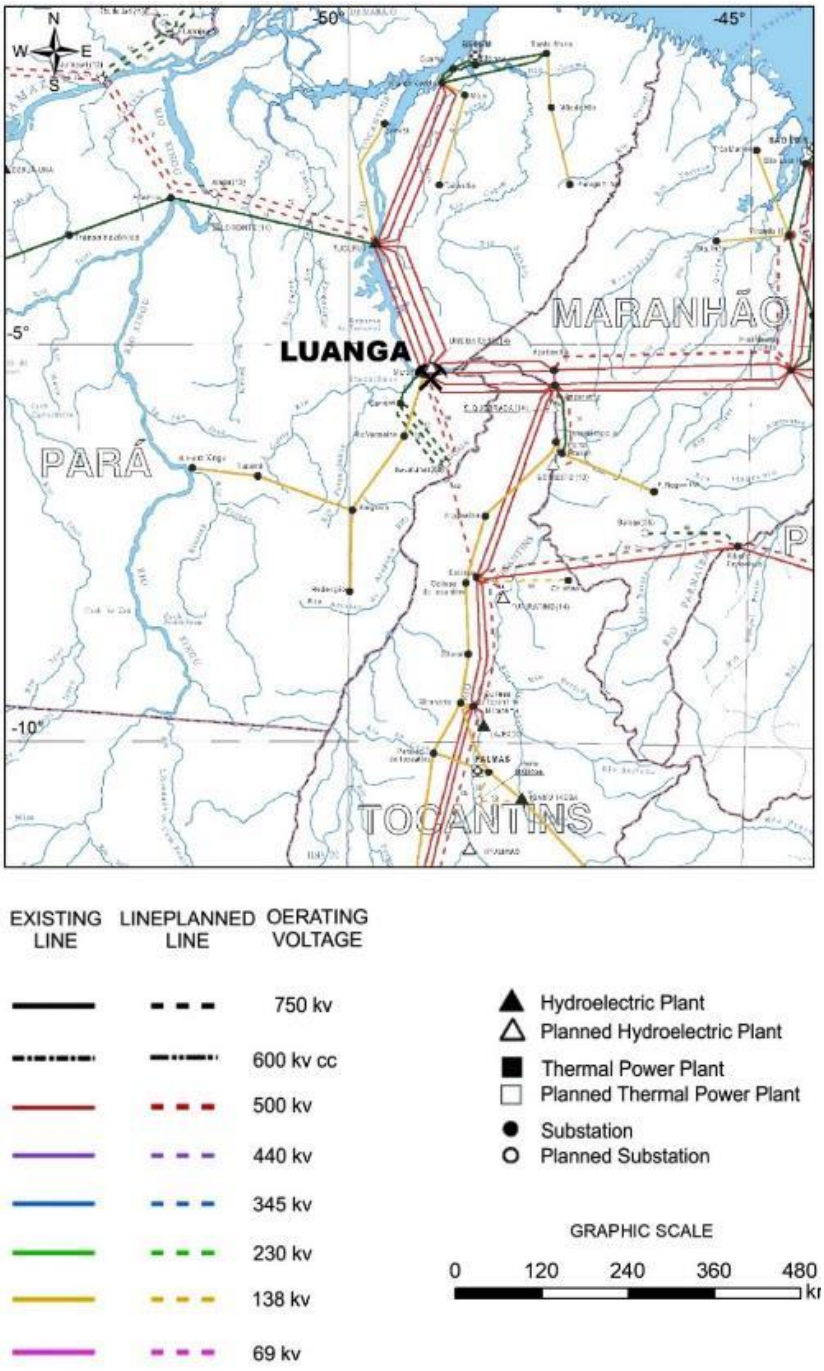

Figure 5-7: Power transmission lines in the region of Luanga Project

Source: Bravo, 2023.

Figure 5-8: Bravo facilities at Luanga Project

Source: Bravo, 2025.

5.4 Social and Community

Bravo has implemented several initiatives related to Environmental, Social, and Governance (ESG) performance during the implementation and development of Luanga. One of the ESG initiatives is related to environmental management. Bravo has implemented measures to minimize the impact of its operations on the environment. For example, it has developed a water management plan that includes monitoring water quality and quantity and implementing measures to reduce water consumption. Additionally, Bravo has implemented a waste management plan that provides recycling and proper disposal of waste material. In order to enhance the natural environment, Bravo created an internal procedure to plant at least ten new trees for each drill hole carried out on the Project area and, to the Effective Date, has planted more than 36,000 trees (or approximately 105 trees per hole drilled). Currently, the company has over 30,000 trees in its local nursery, awaiting planting.

Figure 5-9: Bravo's nursery at Luanga camp

Source: Bravo, 2023.

Figure 5-10: Some of Bravo's social projects at Serra Pelada community

Source: Bravo, 2023

The company is committed to the highest possible health and safety standards to achieve a zero-incident work environment.

The company also provides training programs for residents to develop skills that can be used in the mining industry or in other areas of the local economy, establishing partnerships with local communities to promote sustainable development in the region. Currently, 80% of Bravo's workforce is from the local communities in the Carajás region, exceeding Bravo's goals for local hiring.

Bravo has also set a goal of local spending, with significant contracts such as drilling and assaying being left to companies within the Carajás region. As part of Bravo's ESG strategy, the company developed, approved, and disseminated the following policies:

- Code of Conduct & Ethics Policy.
- Anti-Bribery & Anti-Corruption Policy.
- Disclosure & Confidentiality Policy.
- Diversity & Inclusion Policy.
- Whistleblower Policy.
- ESG Policy (including Health & Safety, and Environment).

6 HISTORY

6.1 The Carajás Mineral Province

The history of the Carajás region is essential to contextualize the discovery and subsequent evaluation of the Luanga deposit. Until the 1960s, geological work carried out in the Carajás region was restricted by a lack of access except in the vicinity of the major rivers. In 1966, DNPM/PROSPEC published the results of Project Araguaia. This involved the acquisition of aerial photo coverage and photo interpretation of the Carajás region. No mineral discoveries were reported as the fieldwork was restricted to the major drainages. The bare patches in the rainforest that later turned out to be high-grade iron ore were interpreted at the time to be calcareous sandstone.

The first mineral exploration in the Carajás region was carried out by Companhia de Desenvolvimento de Indústrias Minerais (CODIM), a subsidiary of Union Carbide, which, in 1966, discovered the manganese deposit of Serra do Sereno. This discovery motivated US Steel to commence broad-scale exploration in the region through its subsidiary Companhia Meridional de Minerações (CMM). In July 1967, a Brazilian team discovered high-grade iron ore with an average grade of 66% Fe. US Steel wanted to develop the Carajás iron deposit. However, the Brazilian Government was unwilling to give a foreign company control over such an important national asset. Instead, the Brazilian Government created in April 1970 a joint venture company, Amazônias Mineração SA (AMSA), of which the Companhia Vale owned 51 percent to Rio Doce (CVRD," which now is "Vale"), the Brazilian Government state enterprise, and 49 percent were owned by CMM. By presidential decree on 6 September 1974, AMSA was granted the rights to all iron ore in the Carajás Mineral Province.

Exploration continued until 1977, when CMM, concerned over the high capital cost and poor outlook of the international market for iron ore at the time, withdrew from the project. Vale purchased CMM's 49% for US$55 million. AMSA, now wholly owned by Vale, was granted the rights for mineral exploration and development of the entire Carajás Mineral Province.

In June 1978, at the commencement of laying the Carajás railroad, linking Ponta da Madeira on the Maranhão coastline to the Carajás reserves effectively launched the implementation of the Carajás Iron Ore Project, which was to cost CVRD US$3 billion in direct investments:

- 56% for the railroad
- 20% for the mine and beneficiation plant
- 14% for the marine terminal
- 10% for infrastructure

With the establishment of the Carajás Iron Ore Project and its associated infrastructure, the Carajás Mineral Province was established and recognized. Decades on, it is one of the largest mineral provinces in the world and the most significant mining region in Brazil. As a result of the

recognition of the global importance of the Carajás Mineral Province, meaningful exploration was undertaken over the following decades by Vale and other domestic and foreign mining companies. This work resulted in the discovery of several deposits in the province and the development of several mines.

6.2 The Luanga Project

Mafic-ultramafic rocks of the Luanga Complex were identified in 1983 during regional exploration developed by DOCEGEO in the Serra Leste region. After discovering up to 2m thick chromitites, DOCEGEO conducted geological mapping, soil geochemistry survey (400m x 40m grid) and ground magnetic survey in the Luanga Complex. Four diamond boreholes were drilled to test the thickness and lateral continuity of outcropping chromitites. The drilling results were not favourable for chromium mineralization but intersected anomalous concentrations of Pt and Pd, including 9 metres at 2.57ppm of Pt+Pd (drill hole PPT-LUAN-FD0004).

In 1997, a joint venture between DOCEGEO-Barrick Gold, carried out a stream sediment campaign over the Luanga Complex area that identified Au anomalism.

In 2000, Vale carried out a new soil geochemistry survey to test the Au anomalies outlined by Barrick Gold. The sampling grid, covering the southern portion of Luanga Complex, defined a 1km long trend of Pt and Pd anomalies. Due to this anomalous trend, Vale carried out an additional soil geochemistry survey in the northern portion of the Luanga Complex (next to chromitite layers), identifying another 1km long Pd and Pt anomalous trend. The geochemical survey was extended to the central portion of the layered complex, adding a further 2km extension, now joining up to form a continuous Pt-Pd anomalous trend along the entire layered intrusion.

In 2001, Vale started an exploration program for PGM in the Serra Leste region. Systematic geological and structural mapping using RADARSAT and Landsat-TM5 integrated data, along with airborne geophysical survey, led to the discovery of several other layered mafic intrusions.

6.3 Vale / DOCEGEO Drilling

Vale completed considerable Diamond Drilling in the 1992, 2001, 2002 and 2003 campaigns. Drill logs and assay summaries and certificates for all historical drill holes are available and have been compiled into a database along with more recent drill data. This historical work has been thoroughly documented.

Historical Vale drilling consisted of 256 diamond drill holes (50,786.74 linear metres) at Luanga between 1992 and 2003 (Table 6-1). Most diamond drilling occurred between 2001 and 2003, and it involved two main targets, Luanga and Luanga South. At Luanga, 232 diamond drill holes (45,599.59 linear metres) were completed, representing approximately 90% of the drilling program. At Luanga South, 24 drill holes (5,187.15 linear metres) were completed.

Most of the Diamond Drilling was carried out by two Brazilian Diamond Drilling companies Geologia e Sondagem S.A. (Geosol) and Rede Engenharia e Sondagem Ltda (Rede). DOCEGEO was responsible for the first four drill holes at the Project.

Table 6-1: DOCEGEO Drilling Summary

Year	Drill Type	Drill Holes	Total Metres	Contractor	Target
1992	DD	4	643.69	DOCEGEO	Luanga
2001	DD	86	14,584.35	Geosol	Luanga
2002	DD	71	15,423.25	Geosol	Luanga
2003	DD	67	14,535.15	Geosol - Rede	Luanga
		4	413.15		Luanga (Met)
		24	5,187.15		Luanga South
TOTAL		**256**	**50,786.74**		

Source: Bravo, 2025.

6.4 Historical Metallurgical Test Work

The Project is an exploration stage project and, as a result, historical metallurgical test work was limited to first-pass (or fatal flaw) metallurgical test work.

This test work was early stage. However, it indicated that a “saleable” Pd-Pt-Au-Ni concentrate could potentially be produced.

Historical metallurgical test work focused on samples from the Sulphide mineralization, since this represented the bulk of the historical PGM mineralization identified at Luanga. Work was performed at several facilities between 2002 and 2007 and can be summarised as follows:

- Mintek, 2002
- CDM (internal Vale laboratory), 2002-2004
- SGS Lakefield, 2003-2004

Initial work by Mintek and CDM used a higher-grade sample (5.0g/t Pt + Pd + Au) from the Sulphide mineralization. Metallurgical test work by both companies demonstrated that recoveries to concentrates of approximately 70% could be achieved using conventional milling, griding and froth flotation, similar to other sulphide PGM deposits globally.

Test work subsequently carried out by SGS Lakefield (Canada) on a lower grade, 200kg sample from the Sulphide mineralization, also indicated recoveries of approximately 70%, with a concentrate from 0.78% of the fed mass of 132g/t PGM + Au. Internal work by CDM using the same sample also supported these results.

Results of historical metallurgical work are summarised in Table 6-2.

Table 6-2: Results of historical metallurgical work

Sample	Lab	Test	Average Grade (g/t 3E*)	Mass	Concentrate Grade (g/t 3E*)	Recovery (%)
M1	Mintek	Lock Cycle Test	5,00	2.2%	137	66.2
M2	CDM	Open Circuit	5,00	3.4%	104	72.1
S1A3	CDM	Lock Cycle Test 1	1.70	1.2%	95	73.0

Sample	Lab	Test	Average Grade (g/t 3E*)	Mass	Concentrate Grade (g/t 3E*)	Recovery (%)
S1A3	CDM	Lock Cycle Test 2	1.70	0.89%	137	69.3
S1A3	Lakefield	Lock Cycle Test	1.49	0.78%	132	69.4

*3E = Pt + Pd + Au. No data is available for Rh or Ni.
Source: Mintek, 2002; CDM, 2002 - 2004; SGS Lakefield, 2003 and 2004.

6.5 Historical Mineral Resource

6.5.1 Historical Mineral Resource (2020)

The “Historical Estimate” of Mineral Resources for Luanga was prepared internally in 2017 by Vale and reported by Mansur et al., 2020:

142Mt@1.24g/t 3E (Pd + Pt + Au) + 0.11% Ni using a cut-off grade of 0.5g/t PGM + Au.

This disclosure is made as per Section 2.4 of NI 43-101, parts 1 to 7 inclusive:

1. The “2020 Historical Estimate” was prepared internally in 2017 by Vale and reported publicly by Mansur *et al*., 2020, with other Vale geologists as co-authors.
2. Bravo acquired the Project directly from Vale and has since conducted a significant amount of infill drilling, resampling of the historical core, metallurgical test work, geophysics and other works. Given these substantive works, the authors believe that the 2020 Historical Estimate was strongly supported by Bravo’s work and is relevant to the reader’s understanding of the status of the Project and its future potential. Further, given that this estimate was prepared by Vale, a major mining company with global operations, the authors believe it is likely to have been prepared to standards a reasonable person would use and is therefore considered reliable for the purposes of defining recommendations for future work.
3. No breakdown of the individual metals contributing to the 2020 Historical Estimate was published and no technical report related to the 2020 Historical Estimate is available to the authors. As a result, aside from the information quoted above, nothing is known about the key assumptions, parameters, and methods used to prepare the 2020 Historical Estimate.
4. The 2020 Historical Estimate used no categories to define it.
5. Until the publication of the 2023 MRE (see 6.5.2 below), there were no more recent estimates or data available to the authors.
6. The work needed to be done before the 2020 Historical Estimate could be classified as a current Mineral Resource was defined in Section 26 of the 2022 Technical Report filed in conjunction with the initial public offering of Bravo, and was subsequently undertaken.
7. A QP has not done sufficient work to classify the 2020 Historical Estimate as a current Mineral Resource.
8. Bravo is not treating the 2020 Historical Estimate as a current Mineral Resource.

Bravo also cautions that the 2020 Historical Estimate was not prepared in accordance with NI 43-101 and should not be relied upon since it has been superseded by the Mineral Resource Estimate detailed in the 2023 Technical Report and, subsequent to that, the MRE

contained this report. Nevertheless, Bravo believes the information is relevant to the reader. Further, readers should be aware that the assay values used to calculate the nickel content in the 2020 Historical Estimate are total Nickel and thus contain both sulphide Nickel (recoverable) and silicate nickel (unrecoverable). It is unknown to Bravo whether the nickel content in the 2020 Historical Estimate had been modified to account for this or not.

6.5.2 Historical Mineral Resource (2023)

Subsequent to the 2020 Historical Estimate, Bravo undertook extensive work programs as recommended in the 2022 Technical Report. The 2023 Technical Report contained Bravo's maiden MRE, prepared in accordance with the requirement of NI43-101, for Luanga Project, which was prepared by GE21 and disclosed by Bravo in 2023:

Table 6-3: Mineral Resource Report – 2023

Mineral Resource Classification	Weathering	Average Grades and Contained Metal Estimates												
		Tonnes	Pd Eq		Pd		Pt		Rh		Au		Ni	
		Mt	g/t	Oz	g/t	Oz	g/t	Oz	g/t	Oz	g/t	Oz	%	Tonnes
Indicated	Oxide	4.6	1.43	212,990	0.91	135,949	0.54	79,901	0.07	10,031	0.08	11,944	n/a	n/a
	Fresh rock	68.5	1.77	3,892,313	0.78	1,705,709	0.53	1,159,078	0.06	131,248	0.07	146,263	0.13	89,539
	Total	73.1	1.75	4,105,303	0.78	1,841,658	0.53	1,238,979	0.06	141,279	0.07	158,207	0.13	89,539
Inferred	Oxide	10.0	1.30	418,810	0.75	241,117	0.72	230,367	0.08	25,738	0.04	12,444	n/a	n/a
	Fresh rock	108.1	1.52	5,286,970	0.60	2,082,479	0.57	1,997,054	0.05	190,746	0.04	122,076	0.10	104,640
	Total	118.1	1.50	5,705,800	0.61	2,323,596	0.59	2,227,421	0.06	216,484	0.04	134,520	0.10	104,640

Notes:

1. The 2023 MRE was prepared by Porfirio Cabaleiro Rodriguez, Mining Engineer, BSc (Mine Eng), MAIG, director of GE21 Consultoria Mineral Ltda., an independent Qualified Persons (QP) under NI43-101. The effective date of the MRE is 22 October 2023.
2. The 2023 Mineral resources are reported using the 2014 CIM Definition Standards and were estimated in accordance with the CIM 2019 Best Practices Guidelines, as required by NI 43-101.
3. Mineral resources that are not Mineral Reserves do not have demonstrated economic viability. There is no certainty that all Mineral Resources will be converted into Mineral Reserves.
4. This MRE includes inferred Mineral Resources which have had insufficient work to classify them as Indicated Mineral Resources. It is uncertain but reasonably expected that inferred Mineral Resources could be upgraded to indicated Mineral Resources with continued exploration.
5. The Mineral Resource Estimate is reported/confined within an economic pit shell generated by Whittle software, using assumptions generated from work completed by Bravo and historical test work:
   - Phase 1 and 2 Metallurgy test work – Metallurgical recovery in sulphide material of 80% Pd, 88% Pt, 59% Rh, 56% Au, 50% Ni to a saleable Ni-PGM concentrate.
   - Phase 1 and 2 Metallurgy test work– Metallurgical recovery in oxide material of 73% Pd, 24% Pt, 61% Rh, 95% Au to a saleable PGM ash residue (Ni not applicable).
   - Independent geotechnical test work – Overall pit slopes of 40 degrees in oxide and 50 degrees in Fresh Rock.
   - Densities are based on 26,898 relative density sample measurements. Averages are 1.58 t/m^3 oxide, 2.71 t/m^3 Saprock and 2.85 t/m^3 fresh rock.
   - External downstream payability has not been included, as the base case MRE assumption considers internal downstream processing.
   - Payable royalties of 2%, (only considering CFEM, for reserves a complete set of royalties must be considered).
6. Metal Pricing
   - Metal price assumptions are based on 10-year trailing averages: Pd price of US$1,380/oz, Pt price of US$1,100/oz, Rh price of US$6,200/oz, Au price of US$1,500/oz, Ni price of US$15,648/t.
   - Palladium Equivalent (PdEq) Calculation
   - The PdEq equation is: PdEq = Pd g/t + F1 + F2 + F3 + F4

     Where: $\boldsymbol{F1} = \frac{(Pt_p * Pt_R)}{(Pd_p * Pd_R)} \boldsymbol{Pt_t}$ $\boldsymbol{F2} = \frac{(Rh_p * Rh_R)}{(Pd_p * Pd_R)} \boldsymbol{Rh_t}$ $\boldsymbol{F3} = \frac{(Au_p * Au_R)}{(Pd_p * Pd_R)} \boldsymbol{Au_t}$ $\boldsymbol{F4} = \frac{(Ni_p * Ni_R)}{(Pd_p * Pd_R)} \boldsymbol{Ni_t}$

     $_P$ = Metal Price $_R$ = Recovery
   - Costs are taken from comparable projects in GE21's extensive database of mining operations in Brazil, which includes not only operating mines, but recent actual costs from what could potentially be similarly sized operating mines in the Carajás. Costs considered a throughput rate of ca. 10mtpa:
     - Mining costs: US$2.50/t oxide, US$3.50/t Fresh Rock. Processing costs: US$8.50/t fresh rock, US$7.50/t oxide. US$2.50/t processed, for General & Administration. US$1.00/t processed for grade control. US$0.50/t processed for rehabilitation.

- Several of these considerations (metallurgical recovery, metal price projections, for example) should be regarded as preliminary in nature, and therefore, PdEq calculations should be regarded as preliminary in nature.
- The current MRE supersedes and replaces the Historical Estimate, which should no longer be relied upon.
- The QP is not aware of political, environmental, or other risks that could materially affect the potential development of the Mineral Resources other than as disclosed in the 2023 Technical Report.
- Totals may not sum due to rounding.

Source: GE21, 2023.

7 GEOLOGICAL SETTING AND MINERALIZATION

The following is summarized from published academic works describing the regional geological framework of the Amazon Craton.

7.1 Regional Geology

The Brazilian Shield extends over much of South America east of the Andes Mountains. The major tectonic units of the Shield are the Amazon, São Francisco and the Rio de la Plata Cratons, surrounded by Neoproterozoic orogenic belts. There are many smaller cratonic fragments, such as the São Luís Craton. Paleoarchean rocks occur as small cratonic nuclei in north-eastern Brazil. The cratons contain voluminous 2,600-3,000 Ma granitic and greenstone belts and a large volume of Paleoproterozoic rocks. The Neoproterozoic orogenic belts are dominantly derived from re-working of older Archean crust but also include Mesoproterozoic sedimentary rocks and volcanogenic sedimentary rocks. Major orogenic activity ceased in the Cambrian. Deformation of the Shield in the Phanerozoic is limited to re-activation of older sub-vertical shear zones.

The Amazon Craton represents one of the main tectonic units of South America (5,600,000 km^2) and is the largest preserved block in the Brazilian Shield. The craton is separated from the Andean orogenic belt by extensive Cenozoic coverage (Colombian Llanos, Venezuelan Llanos, Paraguayan Chaco, etc.), which covers both Paleozoic basins and extensions of the craton. Several Phanerozoic basins in the northeast (Maranhão), south (Xingu and Alto Tapajós), southwest (Parecis), west (Solimões), north (Tacutu) and center (Amazonas) cover the craton area. In the eastern flank, the craton is limited to the Araguaia Orogenic Belt, part of the Tocantins Province, formed during the Neoproterozoic, as result of the convergence and collision of the Amazon Craton, to the west; São Francisco Craton, to the east; and Paranapanema Craton, to the southwest.

Currently, the Amazon Craton is subdivided into 7 geological provinces, based on geochemical and geochronological data (Figure **7-1**):

- Carajás (3.0 – 2.5 Ga)
- Central Amazon (Archean?)
- Transamazonas (2.26 – 2.01 Ga)
- Tapajós–Parima (2.03 – 1.86 Ga)
- Rio Negro (1.82 – 1.52 Ga)
- Rondônia-Juruena (1.82 – 1.54 Ga)
- Sunsás & K'Mudku (1.45 – 1.10 Ga)

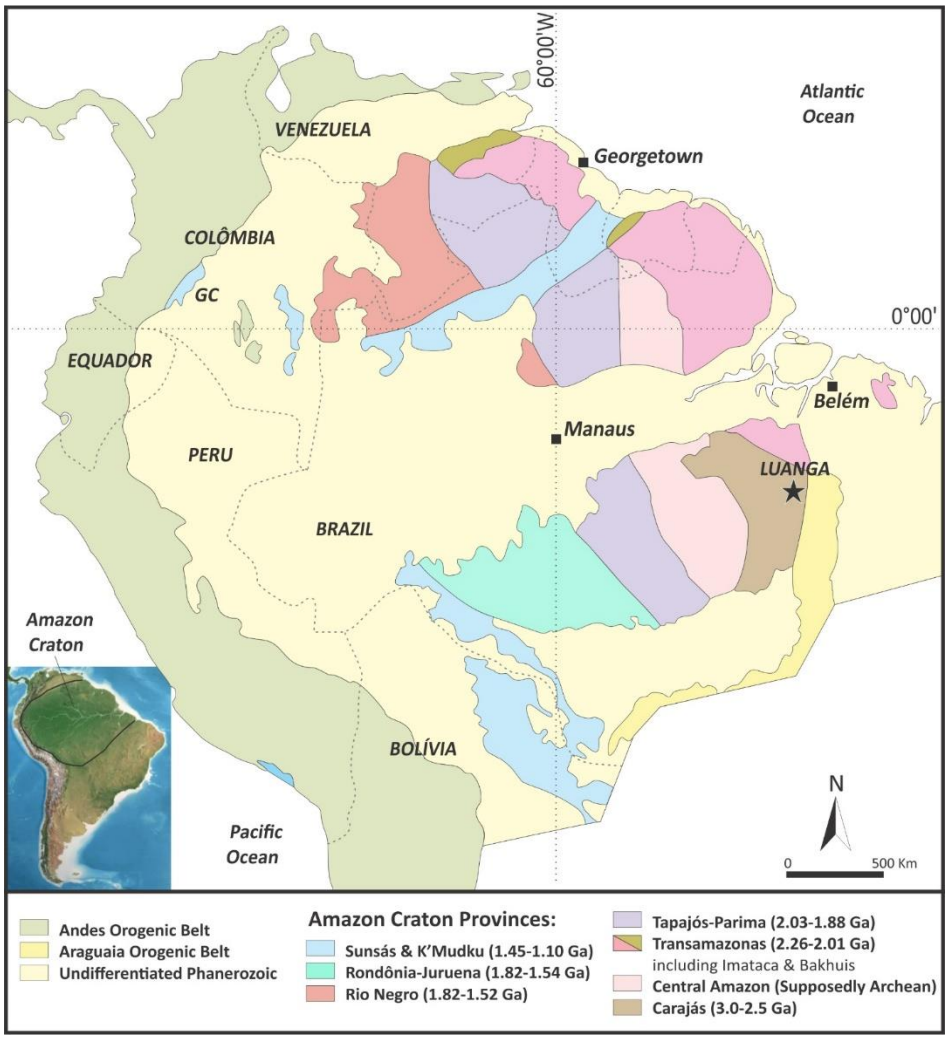

Figure 7-1: Geological provinces of the Amazon Craton

Source: Santos et al., 2008.

The Luanga Project is located within the Carajás Mineral Province (CMP), located in the southeastern margin of the Archean Amazonian Craton (Figure **7-1**). The CMP is composed mostly of granites and greenstone belts and hosts the largest gold deposits in the Amazon Craton, including Serra Pelada and the Salobo and Igarapé Bahia Cu-Au deposits. Gold deposits are concentrated in the Archean and Paleoproterozoic terranes, including the Archean Carajás Mineral Province.

Like other PGE/PGM deposits (such as Chalice's Gonneville deposit – Julimar Project), the Luanga Complex is intruded close to the edge of the Amazon craton, within a dilational splay at the end of the Cinzento Shear.

7.1.1 The Carajás Mineral Province

The Carajás Mineral Province (Figure 7-2) is one of the most important mineral provinces of the South American continent, hosting several world-class Fe, Cu-Au and Ni deposits. It is in the south-eastern portion of the Amazonian Craton, bounded by the Neoproterozoic Araguaia Belt in the east and south, and overlain by Paleoproterozoic sequences generically assigned to the

Uatumã Supergroup in the west (Araújo and Maia, 1991; DOCEGEO, 1988). To the north, where Paleoproterozoic gneiss-migmatite-granulite terrains predominate (Vasquez et al., 2008), geological limits are not precisely defined. The Carajás Mineral Province is subdivided into two Archean tectonic domains: the older Mesoarchean Rio Maria Domain to the south and the younger Neoarchean Carajás Domain to the north (Araújo and Maia, 1991; Araújo et al., 1988; Dall'Agnol et al., 2006; DOCEGEO, 1988; Feio et al., 2013). A regional E–W shear zone, known as the Transition Subdomain (Feio et al., 2013), separates the Rio Maria and Carajás domains (Figure 7-2).

The Rio Maria Domain is a typical granite–greenstone terrain (Vasquez et al., 2008). The Andorinhas Supergroup comprises several individual Mesoarchean greenstone belts (2904 ± 29 Ma) and metasedimentary rocks (Huhn et al., 1986; Souza and Dall'Agnol, 1996; Souza et al., 2001). The recent characterization of spinifex-textured komatiites in a greenstone belt sequence within the Transition Subdomain (Siepierski and Ferreira Filho, 2016) suggests that granite–greenstone terrains extend further north than indicated in previous regional maps.

The basement of the Carajás Domain consists mainly of gneiss-migmatite-granulite terrains of the Xingu Complex (Machado et al., 1991; Pidgeon et al., 2000). Different models have been proposed to explain the evolution of the Archean volcano-sedimentary sequences, which includes the large sequence of metabasalts of the Grão Pará Group (ca. 2.75 Ga). While several studies have proposed an intraplate rift model (Gibbs et al., 1986; Villas and Santos, 2001), others have suggested subduction-related environments (Dardenne et al., 1988; Teixeira and Eggler, 1994). These volcano-sedimentary sequences are covered by low-grade metamorphic sequences of clastic sedimentary rocks of the Águas Claras Formation.

Several mafic–ultramafic complexes intrude into both the Xingu Complex and the Archean volcano-sedimentary sequences (DOCEGEO, 1988; Ferreira Filho et al., 2007). These intrusions host large Ni laterite deposits (e.g., Onça-Puma, Vermelho and Jacaré) as well as PGM deposits (e.g., Luanga, Lago Grande) and were ascribed as part of the Cateté Suite in regional studies. Significant differences in the magmatic structure and evolution of the layered intrusions suggest, however, that they belong to different Neoarchean magmatic suites (Ferreira Filho et al., 2007; Rosa, 2014; Teixeira et al., 2015).

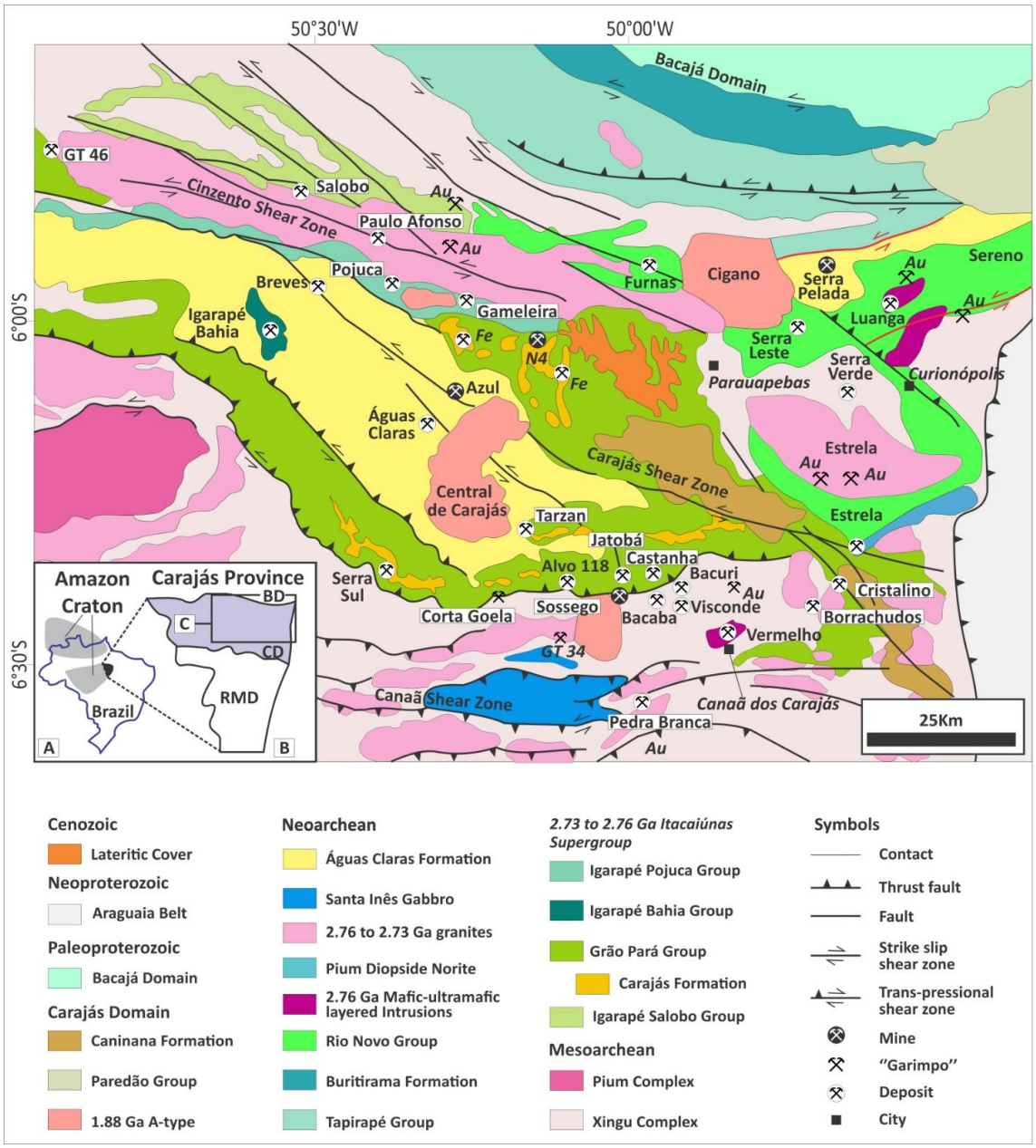

Figure 7-2: Geology and mineral deposits of the Carajás Mineral Province

Source: Trunfull et al., 2020.

7.1.2 The Serra Leste Magmatic Suite

The Serra Leste Magmatic Suite (Ferreira Filho et al., 2007) consists of a cluster of small- to medium-size layered mafic-ultramafic intrusions located in the north-eastern portion of the CMP. Mafic-ultramafic complexes are intruded into gneissic rocks of the Xingu Complex and/or volcanic-sedimentary rocks of the Grão Pará Group. This suite was originally grouped, based on the abundant PGM anomalies in the layered intrusions, disregarding any geological, stratigraphic or petrological consideration (Ferreira Filho et al., 2007). Magmatic ages of the layered intrusions overlap with the age of the bimodal volcanism of the Grão Pará Group (2,759 ± 2 Ma, U-Pb in zircon and 2,760 ± 11 Ma, U-Pb in zircon), supporting the interpretation that they are part of a major Neoarchean magmatic event (Machado et al., 1991; Ferreira Filho et al., 2007).

The architecture of the intrusion and the crystallization sequence described in the Luanga and Lago Grande complexes indicate an overturned layered sequence (Ferreira Filho et al., 2007; Teixeira et al., 2015). Even though the tectonic processes leading to the overturned sequence of layered rocks in the Lago Grande and Luanga complexes have so far not been studied in detail, regional structural studies in the Serra Leste region indicate significant tectonic transport that may lead to major overturned blocks (Holdsworth and Pinheiro, 2000; Tavares, 2015).

7.2 Regional Geophysics

The Luanga Project area is covered by airborne geophysical surveys carried out on behalf of the Brazilian Government and currently available in the public domain. These surveys include magnetic, radiometric and electromagnetic data obtained by Geoterrex-Dighem in 1999, using flight lines oriented along an E-W direct with lines spaced 250m apart. Control flight lines were N-S oriented and spaced 5km apart. Flying height was 120m above the ground.

Magnetic field anomalies highlight the structural framework and main geological features in the area. High signal values are associated with meta-ultramafic rocks of the mafic-ultramafic complexes and magnetite-rich shear zones related to the Serra Pelada Divergent Splay (SPDS). The meta-ultramafic rocks include dunite, meta-peridotite, serpentinite, sulphide-rich zones with pyrrhotite, and shear zones with magnetite. Formation of magnetite in meta-peridotite occurs simultaneously with talc and serpentine as a product of olivine alteration.

The axes of the anomalies appear as anastomosed features that are ductile shear zones. Magnetite-rich, sub-parallel splays related to the Cinzento Transcurrent Shear Zone (CTSZ) crosscut the Luanga mafic-ultramafic complex (Figure 7-3). Magnetic highs are associated with magnetite-enriched meta-ultramafic rocks, such as dunite, peridotite, serpentinite, and talc-schist, as well as shear zones that truncate these complexes and remobilized the magnetite from the meta- ultramafic units. PGM mineralization in the mafic–ultramafic Luanga Complex is associated with pyrrhotite-rich meta-pyroxenite and chromitite layers close to the contact between meta-pyroxenite and peridotite/serpentinite.

Discrete circular high magnetic anomalies can be seen in the central part of the area. These anomalies are associated with shallow depth magnetic banded iron formation sources such as the Serra Leste iron deposit.

Discontinuities in the high values of the N-S or NNW anomaly patterns likely represent magnetite-enriched gabbroic dikes, which are widespread in the Itacaiúnas Supergroup.

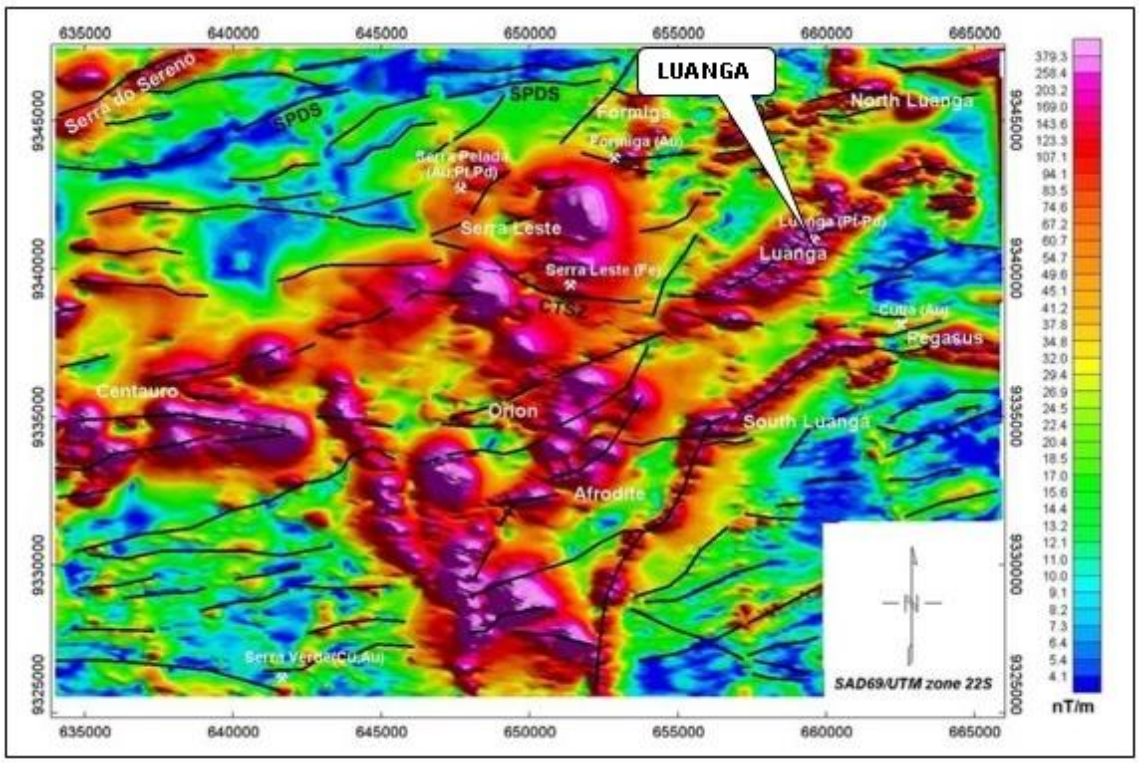

Figure 7-3: Regional aeromagnetic image with interpreted major structures shown as black lines

Source: CPRM data, 1999.

The transient electromagnetic (TEM) data shows conductive zones in: (a) the NE portion of the map, where there are NE-trending aligned features (part of the Serra Sereno), which may represent carbonate and manganese-rich phyllite of the Rio Fresco Group; (b) the surroundings of the Formiga deposit, highlighting the thick alteration mantle, the meta-ultramafic rocks of the Formiga complex as well as banded magnetite-rich formations; (c) the mafic-ultramafic Luanga complex, where sulphide-related PGM mineralization occurs; and (d) the Serra Pelada Au-Pd-Pt deposit, where highly conductive zones occur due to the presence of carbonaceous meta-siltstone (Figure 7-4).

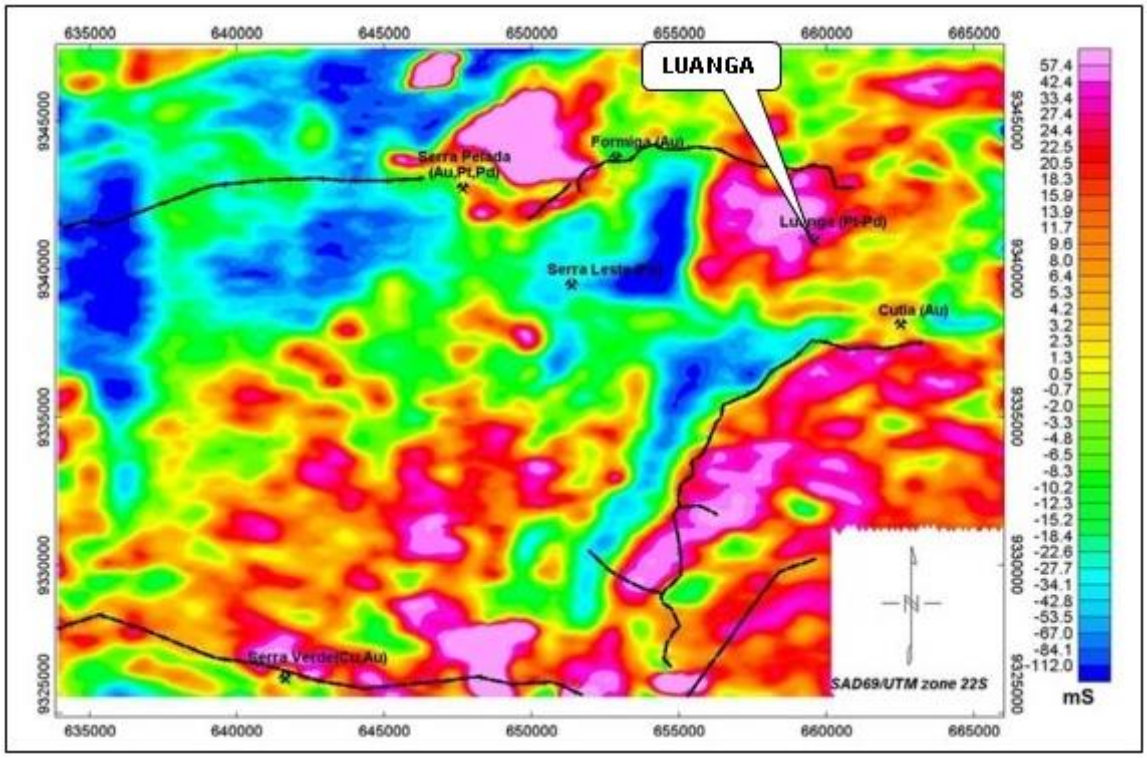

Figure 7-4: Regional airborne TEM image

Source: CPRM data, 1999.

High values of total radiation count in the image below can be related to the presence of Archean granitic rocks of the Estrela Granite Complex, the Xingu Complex and Paleoproterozoic Cigano-type granites. Intermediate to high total radiation count values in the central area reflects the sericite-rich metasiltstones of the Rio Fresco Group.

Low values of total gamma radiation count are associated with outcrops of the mafic–ultramafic complexes (a = Luanga, b = Luanga South) and appear as dark colours (Figure 7-5). It is interesting to note that, immediately east of the Serra Pelada Au-Pt-Pd deposit, there is a small area of low values that is compatible with the radiometric signature of meta-mafic to ultramafic units. The possible presence of buried meta-mafic and meta-ultramafic rocks near this mineralization could provide a source for the Pt and Pd associated with Au in the Serra Pelada deposit.

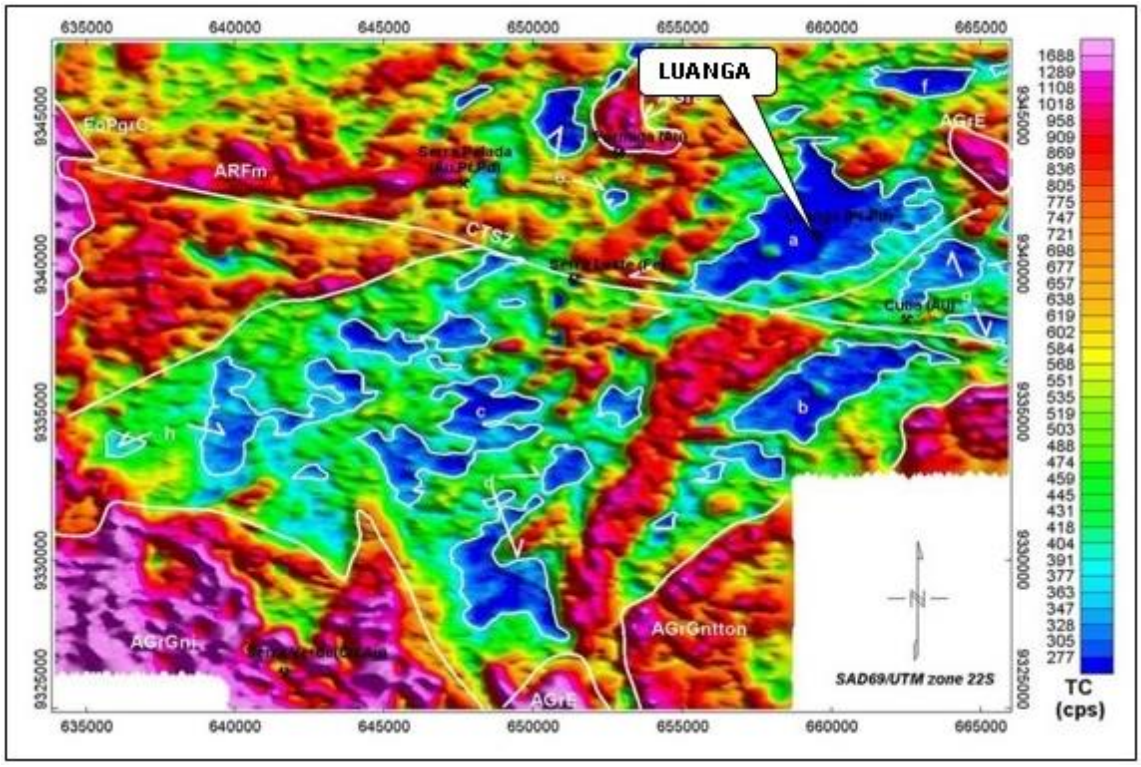

Figure 7-5: Regional air-radiometric image (total count channel) with major domains and structures in white

Source: CPRM data, 1999.

7.3 Local Geology

The principal geological unit on the mineral property is the Luanga Layered Mafic-Ultramafic Complex (Luanga Complex). The Luanga Complex is a 6km long and up to 3.5km wide (~18km²) mafic-ultramafic layered intrusion that belong to the Neoarchean Large Igneous Province (LIP) of the Carajás Mineral Province. The intrusion is characterized by abundant of unweathered outcrops, massive blocks and boulders, relative to adjacent areas of the Carajás Mineral Province, the most prominent geomorphologic feature consists of an elongated arc-shaped smooth hill underlain mainly by ultramafic rocks, up to 60m higher than flat areas where gabbroic rocks prevail. The layering forms an arc-shaped structure that matches the morphology. Host rocks of the Luanga Complex consist of highly foliated gneiss and migmatite of the Xingu Complex in the south/southeast and mafic volcanics and iron formations of the Grão Pará Group in the north/west (Figure 7-6 A).

The central portion of the Luanga Complex has the thickest sequence of layered rocks. To the north and northeast, the layered sequence is truncated by granitic intrusions and to the south, it becomes progressively thinner. The Luanga Complex and host rocks are crosscut by NNW-SSE dolerite dykes. These vertical dykes are up to several metres wide and consist of fine- to medium-grained intergranular to ophitic textured rocks with thin aphanitic chilled margins. Diabase dykes consist mainly of clinopyroxene, olivine and plagioclase, with accessory Ti-magnetite. They belong to a Proterozoic swarm of magnetic mafic dykes that occurs in the Serra Leste region (Teixeira, 2013; Teixeira et al., 2015).

Geological sections (Figure 7-6 B) defined by drilling indicate that igneous layers have steep dips to the SE in the central and southwestern portions of the Luanga Complex. These sections indicate that the Ultramafic Zone overlies the Transition Zone, which overlies the Mafic Zone, suggesting that the layered sequence is tectonically overturned. An overturned layered sequence was previously described for the Luanga Complex (Ferreira Filho et al., 2007) and for the Lago Grande Complex (Teixeira, et al., 2015). These studies suggest the existence of regional scale structures leading to large, overturned blocks in the Serra Leste region.

The Luanga layered sequence is subdivided in three zones, based on the different type and/or proportion of cumulus minerals, Ultramafic Zone (UZ), Transition Zone (TZ) and Mafic Zone (MZ). The estimated thickness of the layered sequence is some 3,500m thick, as indicated in both the stratigraphic column (Figure 7-6 C), which is likely to represent the axial portion of the original magma chamber.

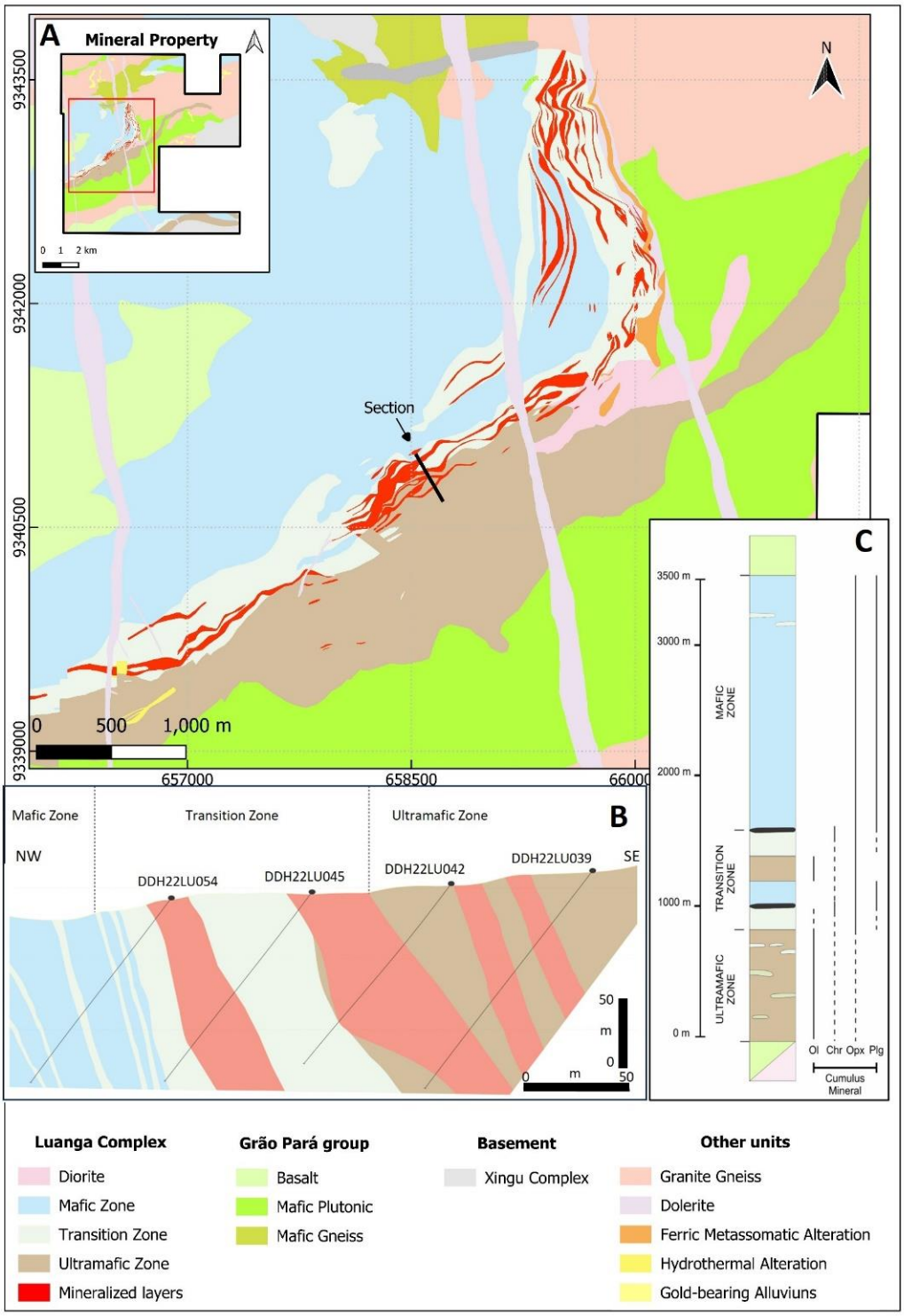

Figure 7-6: Luanga Complex A) Geological map. B) Section of the Central Sector, C) Stratigraphic column

Source: Bravo, 2025.

7.3.1 Ultramafic Zone

The Ultramafic Zone is about 9km long, up to 1km wide and has an estimated thickness of 800m. It consists of wehrlite (Olivine (Ol) + Clinopyroxene (Cpx) cumulates) and lesser dunite and lenses of clinopyroxenite. The Ultramafic Zone follows the stratigraphy of the Luanga

Complex in the southwest and central sectors but extends to the NE of the Luanga Complex as an irregular domain of ultramafic rocks (Figure 7-6 A). The lower contact of the Ultramafic Zone with the Xingu Complex and Grão Pará Group is poorly exposed and was mapped mainly by ground + air magnetic data and soil geochemistry. The contact with the stratigraphically overlying Transition Zone is indicated by a few meters thick transition from Cpx bearing cumulates in the Ultramafic Zone (wehrlite and minor clinopyroxenite) to orthopyroxene (Opx) bearing cumulates (orthopyroxenite and minor harzburgite) in the Transition Zone. Typically, ultramafic rocks in the basal ultramafic zone are extensively sheared and altered, consisting of variable proportions of serpentine, amphiboles, talc and magnetite. Domains where primary magmatic textures and minerals are preserved include wehrlite (Figure 7-7 A) and clinopyroxenite (Figure 7-7 B and C). The NE extension of the Ultramafic Zone is delineated by Cr-Ni in-soil anomalies, blocks of serpentinite and restricted drilling data. This irregular zone of ultramafic rocks may represent the feeder conduits of the Luanga Complex.

7.3.2 Transition Zone

The Transition Zone is about 5km long and up to 1km wide, comprises a pile of interlayered ultramafic and mafic cumulate rocks, which is up to 500m thick. Interlayering of different rock types in different scales (from a few centimetres up to dozens of metres), is a distinctive feature of the Transition Zone. Cumulate rocks have variable textures, from adcumulate to orthocumulate, and variable assemblages of cumulus and intercumulus minerals. The most common rock types are orthopyroxenite and lesser interlayered harzburgite and norite.

Orthopyroxenite is a medium- to coarse-grained orthopyroxene cumulate. The texture varies from adcumulate (Figure 7-7 E and F) to meso- and orthocumulate with plagioclase as the predominant intercumulus mineral. Harzburgite is a medium- to coarse-grained olivine+chromite cumulate with meso- to orthocumulate texture, commonly consisting of abundant oikocrysts of orthopyroxene enclosing several olivine and chromite crystals (Figure 7-7 D). Norite is a medium-grained orthopyroxene+plagiclase adcumulate rock. Primary textures and minerals are variably altered to fine-grained aggregates consisting mainly of talc, serpentine and minor magnetite in the ultramafic rocks.

Chromitite layers with variable thickness (commonly 10cm but up to 60cm) and textures occur mainly in the upper portions of the Transition Zone and the lowermost portion of the Mafic Zone. These layers are commonly discontinuous but intercepts consisting of several chromitite layers are up to 100m in extension. Chromitites are fine- to medium-grained chromite cumulates with variably altered intercumulus plagioclase and orthopyroxene. Chromite crystals commonly have atoll textures or abundant silicate inclusions (Figure 7-7 H and I). The upward transition from massive chromitite, to chain textured chromitite and disseminated chromitite (Figure 7-7 G) is common and provides a facing criterion for the igneous stratigraphy of the Luanga Complex.

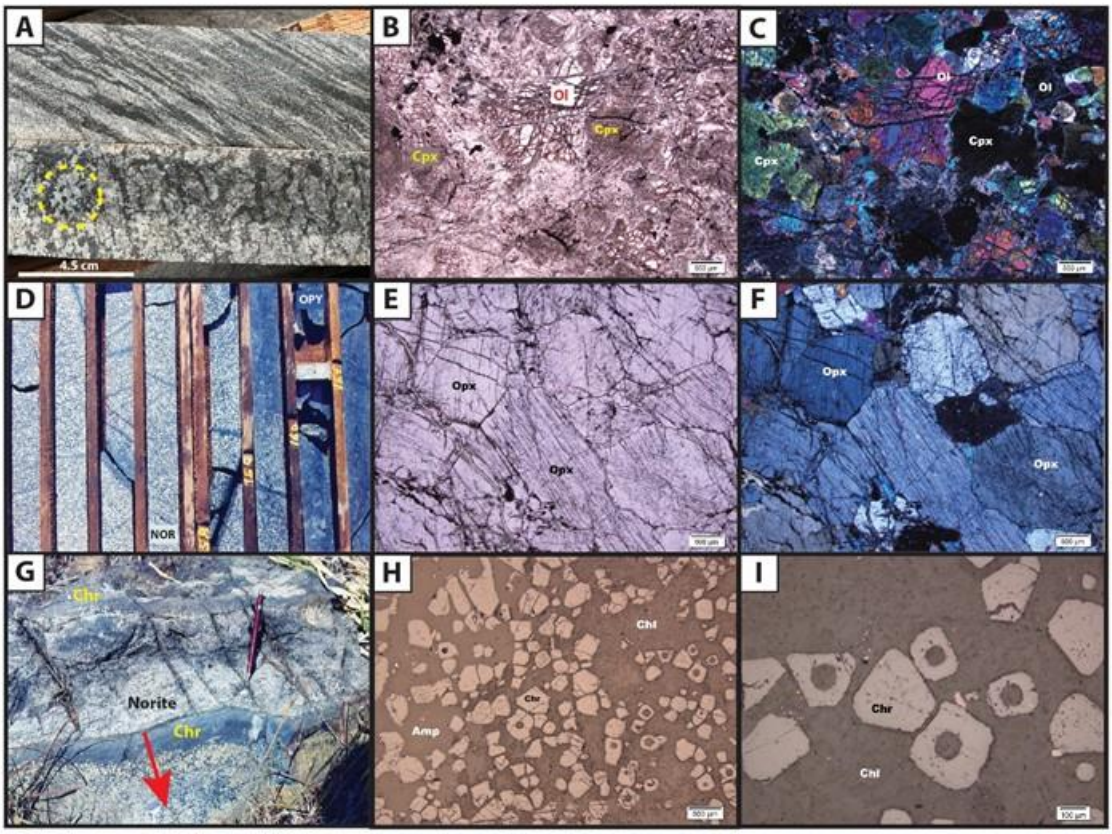

Figure 7-7: Photos and photomicrographs of representative rock types of the Luanga Complex

Legend: A) Drill core samples of the UZ showing wehrlite with primary magmatic texture (lower photo) and a sheared domain (upper photo). The dashed circle shows coarse-grained clinopyroxene (Cpx) (light color mineral) enclosing several euhedral olivine pseudomorphs (dark color mineral). B) and C) Photomicrographs of wehrlite of the UZ under parallel (N//) and crossed (NX) polarized light. D) Drill core section showing a sharp contact between norite (NOR) and orthopyroxenite (OPY) of the TZ. E) and F) Photomicrographs of adcumulate textured orthopyroxenite of the TZ (under N// and NX). G) Outcrop of interlayered chromitite and norite from the lower portion of the MZ. The arrow indicates the base-to-top gradational transition from massive chromitite to chain textured chromitite. H) and I) Photomicrograph of chromitite consisting of fine-grained euhedral chromite with atol texture (observation under reflected light). The matrix consists of an aggregate of chlorite (Chl) and amphiboles (Amp) resulting from alteration of primary orthopyroxene and plagioclase.
Source: Bravo, 2025.

7.3.3 Mafic Zone

The Mafic Zone, about 5km long and up to 3.5km wide, comprises a thick monotonous pile of noritic rocks. Norite consists of medium-grained orthopyroxene + plagioclase cumulates. Primary textures and minerals are variably altered to fine-grained aggregates consisting mainly of amphiboles (hornblende-actinolite), chlorite and epidote-group minerals. Minor interlayered ultramafic rocks in the MZ, including orthopyroxenite and minor chromitite, have petrographic features like those described in the TZ.

7.3.4 Tectonic Setting

The current model of the tectonic evolution of the CMP implies that it is a product of oblique rift evolution (2.76-2.06 Ga) controlled by the Cinzento and Canaã strike-slip system (Figure 7-8). The Carajás rift is hosted in the tonalite-trondhjemite-granodiorite (TTG) terrain which includes the Rio Maria greenstone belt (3.0-2.85 Ga). It is postulated that it overlies a Mantle plume and is filled by the Carajás plutonic-volcanic sedimentary sequences. The rifting

stage (Igarapé Bahia Group + Grão Pará Group) began with intense tholeiitic fissure volcanism with basalt and rhyolite flows, coeval intrusions of alkali granites and mafic-ultramafic bodies, BIFs, shales and restricted tuff beds. The strain developed during passive rifting or plume-initiated active rifting generates deep rooted structural zones which control the migration of magma from the mantle to the surface. The high magnesium and Platinum-Group Metals (PGM) contents of mafic ultramafic complexes indicate extensive partial fusion, conditions that are indicative of a plume origin (Teixeira et al. 2021) (Figure 7-9).

The oblique rifting results in dextral shearing along the Canaã dos Carajás and Cinzento shear zones (Figure 7-8). Stages 1 is responsible for mafic-ultramafic intrusions, alkalic granite emplacement, and early Iron-Oxid Copper Gold (IOCG) mineralization at the Igarapé Bahia, Bacaba, Sequeirinho, and Sossego deposits. In Stage 2 the most important IOCG deposits like Salobo, Alemão and Igarapé Bahia were formed.

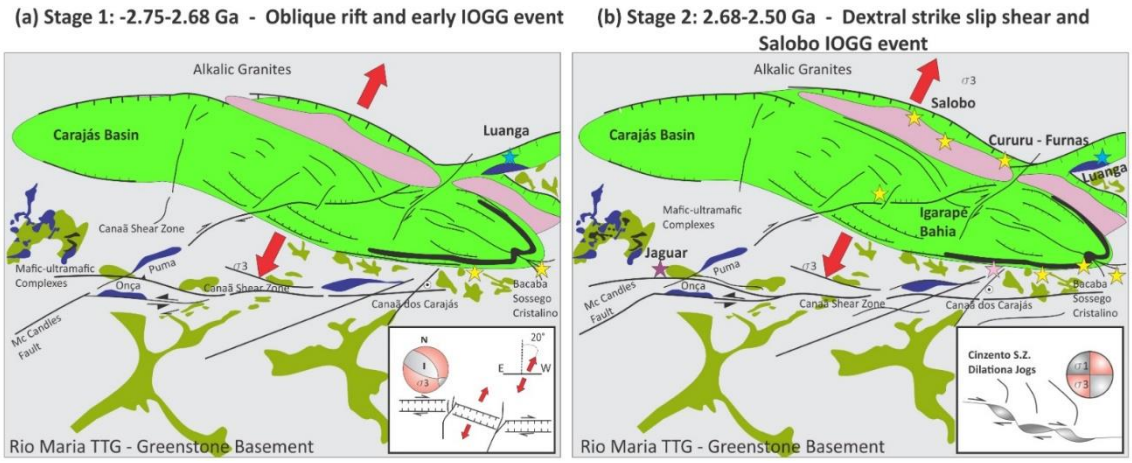

Figure 7-8: Simplified early tectonic evolution of the Carajás Basin and adjoining regions

Source: Teixeira et al., 2021.

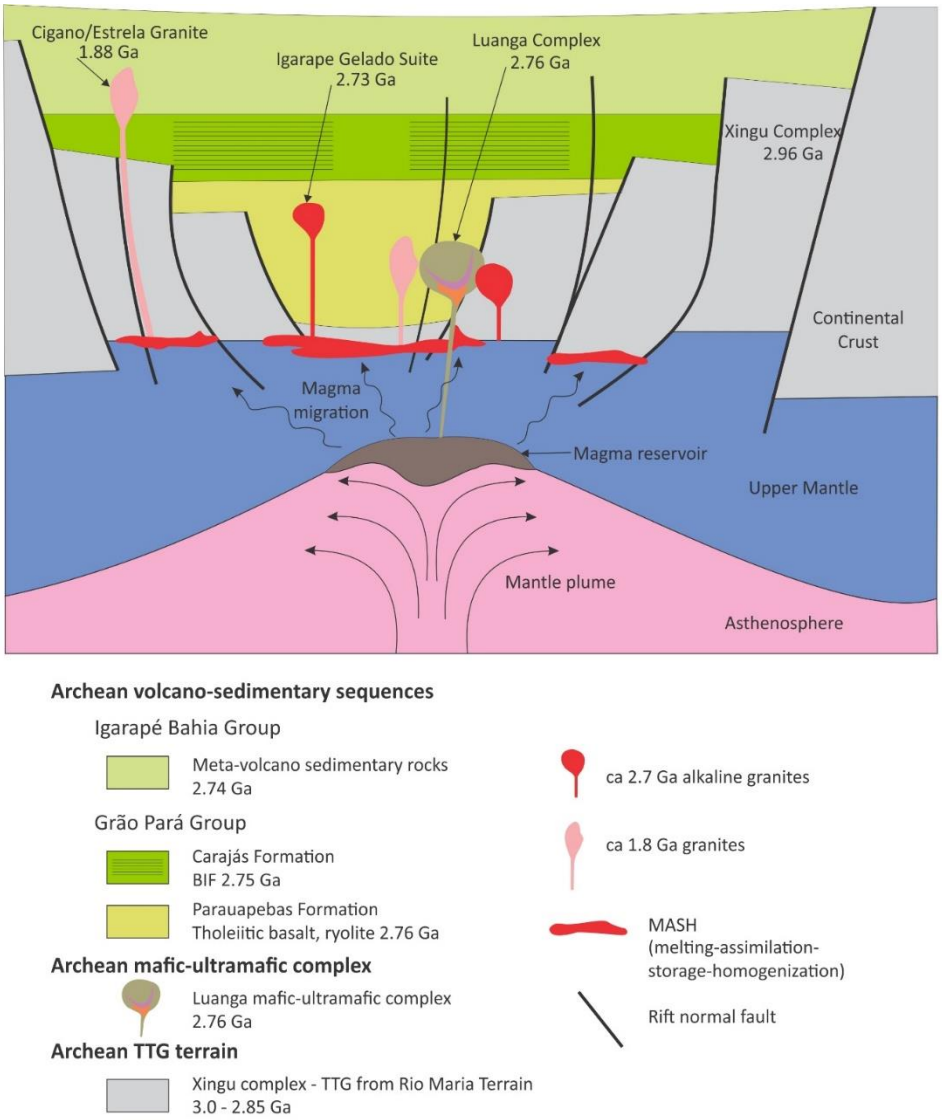

Figure 7-9: Carajás rift system

Source: Teixeira et al., 2021.

The Luanga complex is positioned between the Cinzento and Sereno sinistral strike-slip faults. A transtensional zone of this transcurrent system could generate space and pumping (high pressure zones) or suction forces (low pressure zones) that would favor the entry of mafic-ultramafic magmas of the Luanga Complex (Figure 7-10).

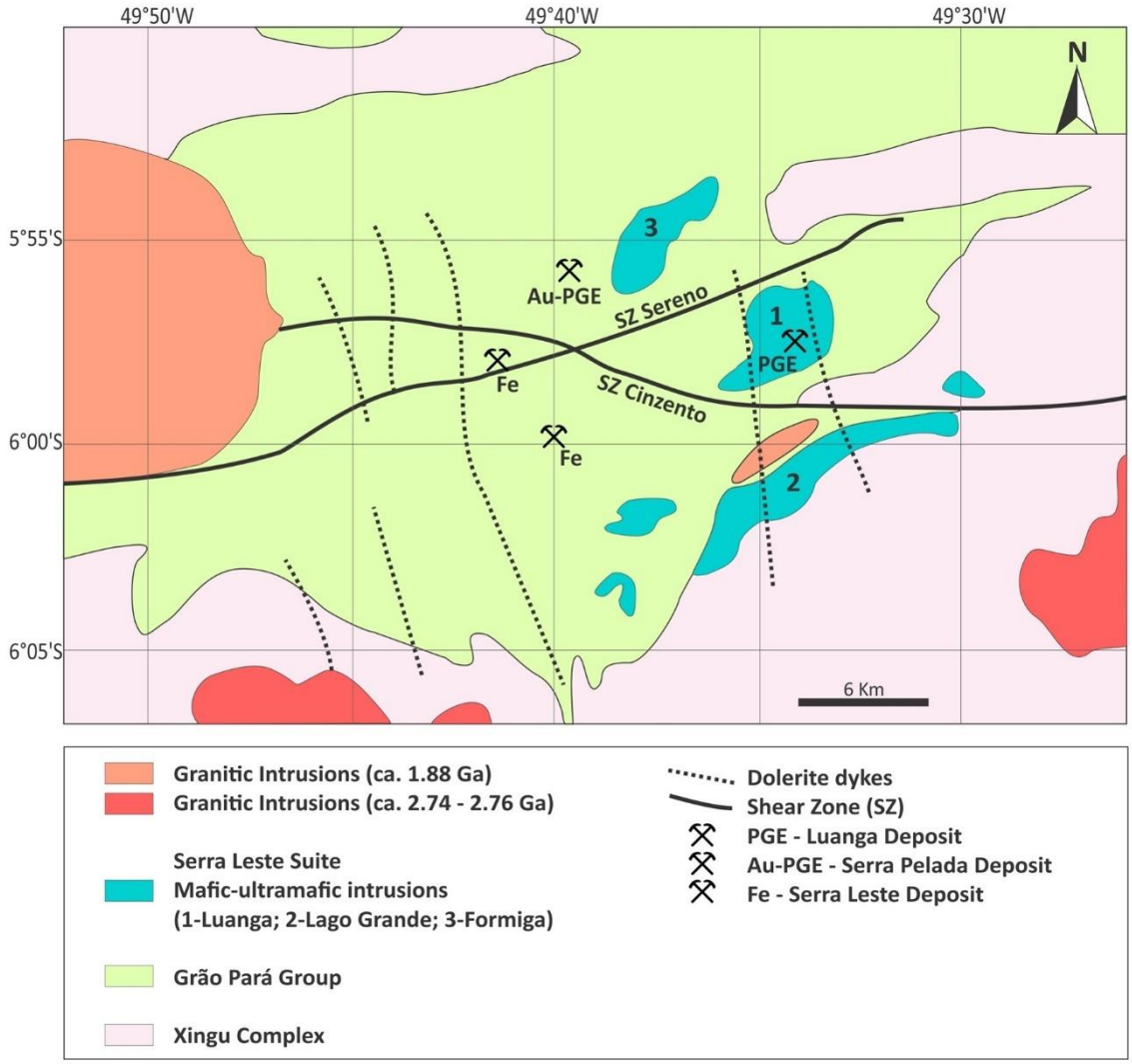

Figure 7-10: Major structures controlling Luanga intrusion

Source: Teixeira & Ferreira Filho, 2015.

Strike-slip faults comprise a sub-set of structures which typically develop in response to anisotropy of the motion of Plate margins. The structures associated with strike-slip motion include both restraining and releasing bends. Within areas of transpression there is no opportunity for structural space to be generated which can be exploited by ascending magma (Lightfoot & Evans-Lamswood 2015).

In contrast, releasing structures at sites of transtension may take the form of rifts and pull-apart basins where the detailed internal geometry of motion of blocks within the rift or pull-apart has a vertical and lateral sense of displacement. Transtension generates local open space in the crust, and sub-vertically connected open spaces provide a pathway through which mantle-derived magmas can migrate from the mantle to the crust (Lightfoot & Evans-Lamswood 2015).

Due to the complex internal structures of ductile shear zones, many igneous bodies intruded into transtension-generated spaces have the plan shape of an asymmetrical rhomboid with the long axis subparallel to a fault zone and contacts that are often structurally modified during and/or after placement of the magma. The typical cross section of these asymmetric

rhomboid intrusion is a downward-closing cone shape with curved walls and often a dyke-like keel at the base.

7.3.5 Metamorphism and Alteration

Metamorphic assemblages commonly replace the primary igneous minerals of the Luanga Complex. This widespread metamorphic alteration is heterogeneous and characterized by an extensive hydration that largely preserves primary textures, bulk rock compositions and the compositional domains of igneous minerals. The penetrative fabric is restricted to narrow domains of up to a few metres across, and igneous textures are identified in adjacent non-deformed domains. These assemblages include: (1) serpentine + talc +magnetite ± cummingtonite commonly overprinting harzburgite/orthopyroxenite, (2) serpentine + tremolite + talc + magnetite overprinting wehrlite/clinopyroxenite and (3) hornblende + chlorite + epidote overprinting norite.

Metamorphic assemblages in the Luanga Complex indicate temperatures at the transition from greenschist to the amphibolite facies of metamorphism (Ferreira Filho et al., 2007; Mansur et al., 2016). The same type of alteration described in the cumulate rocks of the Luanga Complex occurs in other mafic-ultramafic intrusions of the Serra Leste region (e.g., Lago Grande and Formiga layered complexes; Teixeira et al., 2015). Regional metamorphic events in the Serra Leste region, affecting both mafic-ultramafic complexes (e.g., Luanga Complex) and volcanic-sedimentary sequences (e.g., Itacaiúnas Supergroup), are indicated in previous studies (Tavares et al., 2015). The age and type of metamorphism affecting the layered intrusions and their host metavolcanic and metasedimentary rocks in the Serra Leste region, as well as the Carajás Mineral Province, is a debated issue (Tavares et al., 2015, Teixeira et al., 2021).

Apart from the widespread metamorphism affecting the Luanga Complex and host volcanic-sedimentary sequence, the layered rocks are also altered by hydrothermal alteration developed along crosscutting shear zones. Domains of hydrothermal rocks occur along the easter and southeastern border of the Luanga Complex, being particularly robust at the North Sector, where drill intercepts up to 100m thick of metasomatic rocks occur. Two main types of hydrothermal alteration were recognized in the Luanga Complex and adjacent host rocks. An older event of K-Fe-Mg-Cl metasomatism characterized by biotite-amphibole (± scapolite, ± tourmaline) assemblage, and a second event of Fe-Ca metasomatism characterized by magnetite-Ca-amphibole-grunerite-garnet assemblage. These hydrothermal events were first recognized in the Luanga Complex during the exploration program carried out by Bravo and were interpreted to belong to the regional hydrothermal system linked to IOCG deposits in Carajás Mineral Province.

7.3.6 Mineralization

The Luanga PGM + Au + Ni mineralized envelope follows the arc-shaped structure of the Mafic-Ultramafic Complex along approximately 8.1 km. The deposit is subdivided into three separate mineralized sectors, named North, Central and Southwest (Figure 7-11).

The Transition Zone (TZ) of the Luanga Complex hosts several PGM mineralized units, including the MSZ which hosts the bulk of PGM resources of the Luanga Complex. Other mineralized layers are identified within the TZ and on the Ultramafic Zone (UZ).

In addition, several thin chromitites layers or lenses occur in the Luanga Complex either in the upper or in lower stratigraphic portions of the TZ, the latter occurring where they are hosted by ultramafic cumulates. The upper chromitite layers are developed on the immediate contact with the overlying Mafic Zone (MZ), where they are hosted by plagioclase-bearing norite cumulates.

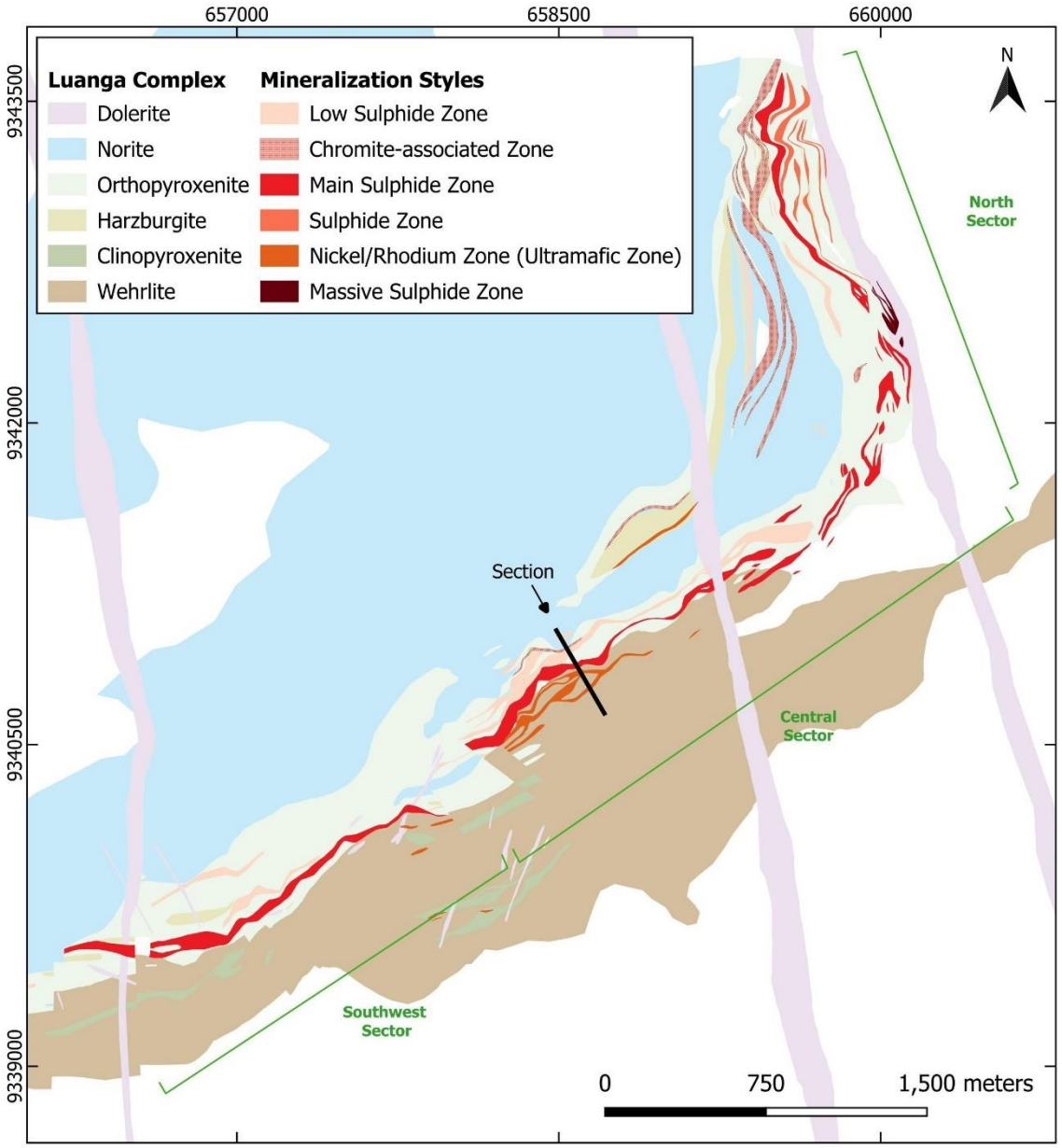

Figure 7-11: Mineralization and lithology map of the Luanga Project

Source: Bravo, 2025

Mineralized zones of the Luanga Complex are grouped into six different styles of PGM + Au + Ni mineralization (Table 7-1). They are named as: (i) MSZ, (ii) Low Sulphide Zone (LSZ), (iii)

Chromite-associated Zone (Chr-PGM) (iv) Nickel/Rhodium Sulphide Zone (Ni-Rh), (v) Sulphide Zone (SZ) and (vi) Massive Sulphide Zone (MASU). An example of the mineralized zones in a cross section from the Central Sector is presented in the Figure 7-13, and the following topics provide an overview of the main characteristics for each style of PGM + Au + Ni mineralization.

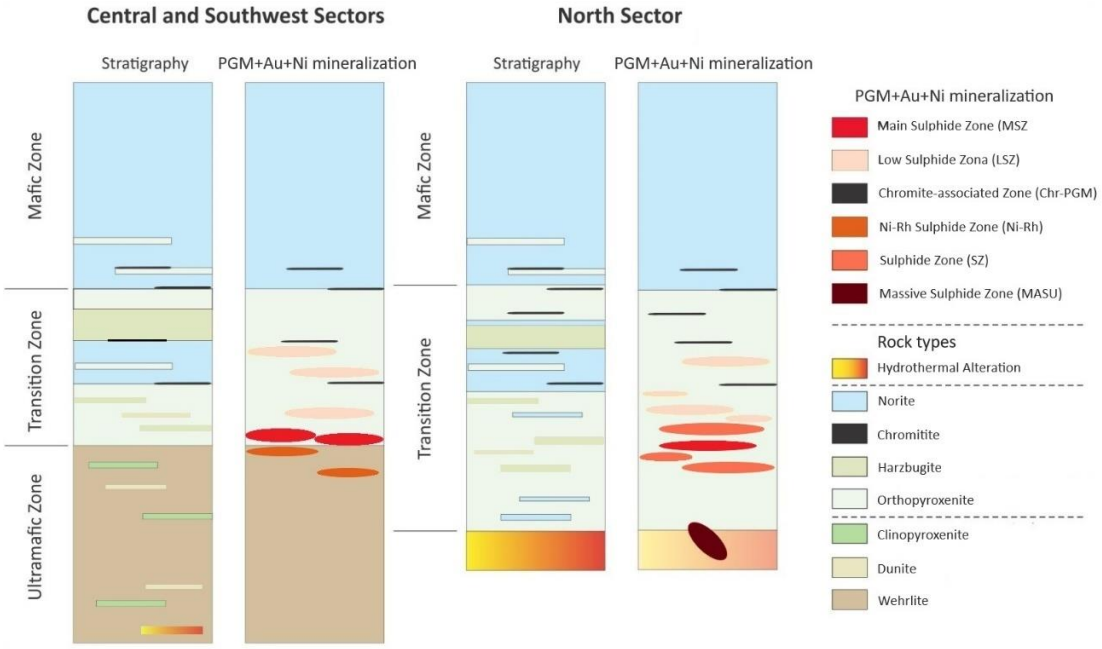

Figure 7-12: Schematic stratigraphic column locating the different styles of PGM mineralization on Luanga Complex

Source: Bravo, 2025.

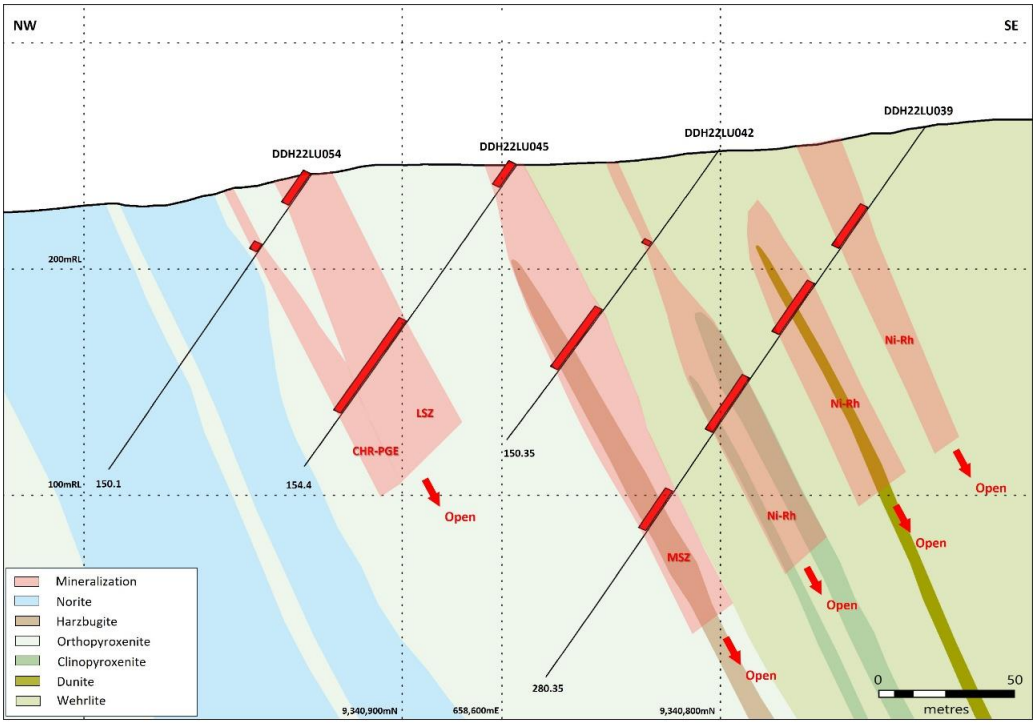

Figure 7-13: Drill section with the mineralized zones identified at Luanga

Source: Bravo, 2025.

Table 7-1: Styles of mineralization on Luanga deposit

PGM + Au + Ni Mineralization	Occurrence	Stratigraphy	Geology	Petrography	Chemical Composition
Main Sulphide Zone (MSZ)	Central and Southwest sectors.	Lower portion of the TZ at the contact with the UZ.	Stratabound disseminated sulphides (1-5%) with variable thickness (up to 50 m) hosted by orthopyroxenite and minor harzburgite.	Sulphide blebs interstitial to cumulus Opx-Ol. Po-Pn and minor Ccp. Pn (25-50% of Sulphide fraction) occurs as fine-grained crystals with rare exsolutions within Po.	Very high Ni (10-15%) and Pt-Pd (up to 100 ppm) tenors, variable very high Ni/Cu (~10), Pt/Pd < 0.5, and Pd/Rh ~0.05.
Low Sulphide Zone (LSZ)	All sectors	Discontinuous stratabound bodies (lenses) distributed throughout the stratigraphy of the TZ.	Several lenses of variable thickness (up to 200 m) hosted by orthopyroxenite, and minor harzburgite. No significant amounts of sulphides.	PGM mineralized lenses occur in Ol-Opx cumulates without any distinctive feature from barren cumulates.	Very low Ni-Cu contents, Pt-Pd contents < 1-2 ppm, and Pt/Pd ~ 1.0-2.0. Pt-Pd show moderate to strong positive correlation.
Chromite-associated Zone (Chr-PGM)	All sectors	Irregular lenses located predominantly at the upper portion of the TZ and lower portion of the MZ.	Chromitite pods (< 60 cm) closely associated with disseminated clusters of chromite within orthopyroxenite, harzburgite and norite. No significant amounts of sulphides.	Chromitite pods consist of fine-grained cumulus Chr commonly with abundant inclusions and/or atol texture.DIS chromite occurs as cluster of several euhedral chromite crystals.	Very low Ni-Cu contents, high Pt/Pd ratio (~4.0), and Rh/Pt ~0.3.
Ni-Rh Sulphide Zone (Ni-Rh)	Central and Southwest sectors.	Discontinuous lenses located only inside the UZ domain.	Sulphide-bearing lenses (up to 25%) with variable thickness (up to 40 m). Hosted by interlayered wehrlite and dunite, and minor clinopyroxenite.	Disseminated to net-textured sulphides consisting of Po (~60-70%), Pn (~30-40%) and minor Ccp. Pn occurs as medium-grained crystals (1-2 mm) with very rare Pn exsolutions within Po.	Pt/Pd ~0.15; Rh/Pd ~0.20. Higher % of sulphides and lower Pt-Pd contents than the MSZ, suggest relatively lower Pt-Pd tenors. Modal % of Pn (~30-40%) indicates very high Ni tenor.
Sulphide Zone (SZ)	North sector	N-S trending zones of massive to semi-massive sulphides. Stratigraphic correlation with the Central and Southwest sectors is hampered by intense tectonism and alteration.	Folded or faulted stratabound bodies of disseminated fine-grained sulphides (1-5%) with variable thickness (up to 40 m). Hosted by orthopyroxenite and minor harzburgite. Layered mafic-ultramafic sequence are crosscut by granitoids at depth.	Pervasively altered rocks with poorly preserved primary textures. Consist mainly of fine-grained aggregates of sulphides (Po-Pn and minor Ccp) interstitial to pseudomorphs of Opx.	Low Pt/Pd (commonly < 0.5, but up to 1.0) and variable Ni contents. Weak positive correlation between Pd-Ni and Pd-Rh possibly results from variably altered sulphides.
Massive Sulphide Zone (MASU)	North sector	Robust intercept of MASU (DDH22-LU047) within a hydrothermal alteration zone at the western border of the North sector.	Host rocks and the footwall sequence consist of hydrothermal rocks with variable proportions of Amp-Grt-Bt-Mag. Sulphide-bearing orthopyroxenite and interlayered norite occur in adjacent drill holes.	Sulphides consist of Po (~80-90%) and Pn (~10-20%) with local Ccp-rich domains. Amp-Bt-Qz-Mag-Bt are enclosed within MASU, with common sulphide-Amp intergrowths. Pn occurs mainly associated with Po as fine-grained crystals or exsolutions.	Variable contents of Ni-Cu-PGM, with Ni>Cu and Pd>Pt. Weak correlation between metals (Ni-Cu-Pt-Pd-Rh). Contents of Ni (< 6.0%), Pd (< 6.0 ppm), Pt (< 2.5 ppm) and Rh (0.2 ppm) indicate lower tenors than those calculated for the MSZ.

Source: Bravo, 2025.

7.3.6.1 Main Sulphide Zone (MSZ)

PGM mineralization associated with disseminated sulphides in the MSZ hosts the bulk of PGM + Au + Ni Mineral Resources of the Luanga Complex. The stratigraphic interval hosting the MSZ consists of a 10–50m thick interval with disseminated sulphides located along the contact of the UZ and TZ (Figure 7-12).

MSZ is strata bound-style PGM mineralization consisting of interstitial sulphides (~1-5 vol.%) hosted by orthopyroxenite and minor harzburgite (Figure 7-13). The MSZ is characterized by very high Ni tenors (10-15%) and Pt-Pd (up to 100 ppm) tenors (content of 100% sulphides), variable very high Ni/Cu (~10), Pt/Pd <0.5, and Pd/Rh ~0.05. Pt-Pd have strong positive correlation that is not affected in variably altered rocks (Figure 7-14 and Figure 7-15). Variable Pt, Pd, and Ni correlation with S (from strong positive to weak) results from variable alteration of sulphides.

PGM mineralization is associated with sulphide blebs (up to few cm) interstitial to cumulus Opx-Ol or their pseudomorphs. Sulphides consist of Po-Pn and minor variably distributed Ccp. Pn (~30-50% of the sulphide fraction) occurs mainly as fine-grained crystals (<1mm) with rare Pn exsolutions within Po (Figure 7-16). PGM grades have a strong positive correlation with the amounts of sulphides. Sulphides are variably altered and commonly occur with intergrowth of magnetite in extensively altered samples.

PGM mineralization on the MSZ consist predominantly of Pt-Pd-bismuth tellurides followed by stannides, arsenides and antimonides (Mansur et al., 2020). The PGM occurs mainly enclosed within sulphide grains, or at the contact between sulphide and silicate grains.

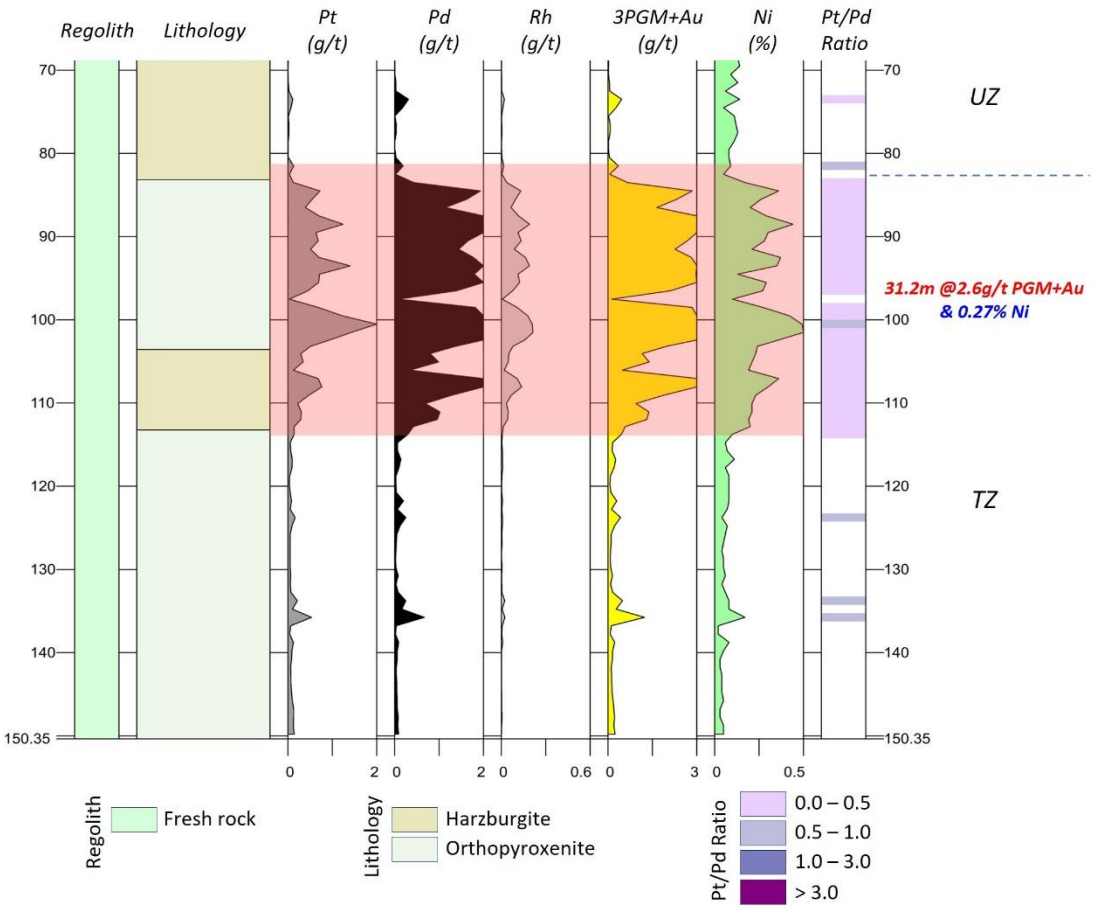

Figure 7-14: Typical log plot of a representative intercept of the MSZ mineralization

Source: Bravo, 2025.

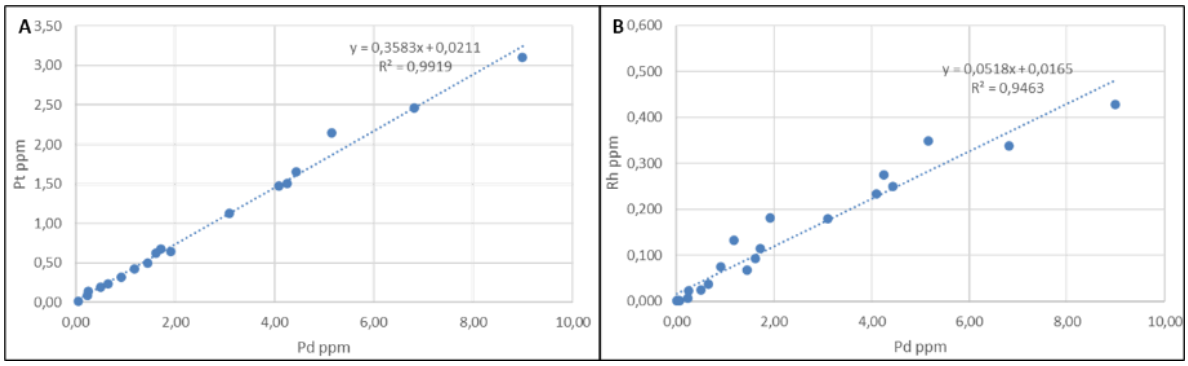

Figure 7-15: Correlation charts for a representative MSZ intercept

Legend: A) Pt (ppm) vs. Pd (ppm) and B) Rh (ppm) vs. Pd (ppm).
Source: Bravo, 2025.

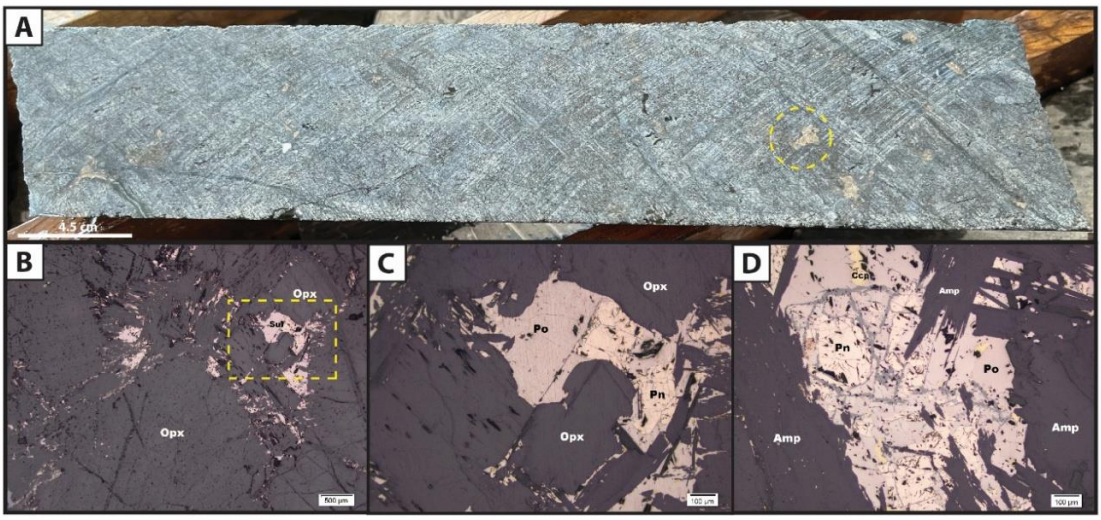

Figure 7-16: Representative photos and photomicrographs of the MSZ

Legend: A) Drill core samples of orthopyroxenite with interstitial disseminated sulphide blebs. The dashed circle shows a sulphide bleb. B) and C) Photomicrographs of sulphide blebs consisting mainly of pyrrhotite (Po) and pentlandite (Pn). Sulphides are interstitial to Opx and partially remobilized along fractures. The dashed rectangle is detailed in B. D) Photomicrograph of a sulphide bleb consisting of Po+Pn and minor Ccp. Sulphides are partially altered to magnetite (gray color lamellae) and occur in a domain where Opx is partially altered to prismatic amphibole (Amp).

Source: Bravo, 2025.

7.3.6.2 Low Sulphide Zone (LSZ)

The LSZ style of mineralization comprises PGM-mineralized rocks devoid of base metal sulphides and/or abundant chromite. The Low Sulphide mineralization of the Luanga Complex consists of up to 30m thick stratabound zones across the TZ. These zones do not show extensive lateral continuity and commonly occur at the contact between layers of distinct cumulate rocks. The hosting rocks, mainly harzburgite and orthopyroxenite, do not show any distinctive texture or change in modal composition that characterizes the PGM enrichment.

The LSZ occurs as several irregular stratabound bodies (lenses) located above the MSZ and throughout the stratigraphy of the TZ in the Central and Southwestern sectors, as well as in the North sector (Figure 7-12). This style of mineralization is hosted by orthopyroxenite, and minor harzburgite and plagioclase-orthopyroxenite, without significant amounts of sulphides (commonly no sulphides were identified during core logging) (Figure 7-17). The LSZ lenses have a high steep dip to the southeast (Central and Southwestern sectors) and to the west (North sector).

The LSZ is characterized by very low Ni-Cu contents, Pt-Pd contents commonly <1-2 ppm (Figure 7-18), and Pt/Pd ~1.0-2.0. Pt-Pd show moderate to strong positive correlation (Figure 7-19).

PGM mineralization on the LSZ consist predominantly by Pt-arsenides (mainly sperrylite, $PtAs_2$), followed by Pt-Pd-stannides, antimonides, and minor bismuth tellurides (Mansur et al., 2020).

Figure 7-17: Representative photo of the LSZ

Legend: Drill core sample of orthopyroxenite with interstitial plagioclase. The dashed circle shows a domain with medium- to coarse-grained Opx pseudomorphs (replaced mainly by talc) with interstitial plagioclase pseudomorphs (replaced by mainly by chlorite). Whitish veinlets consist mainly of talc and minor carbonate.
Source: Bravo, 2025.

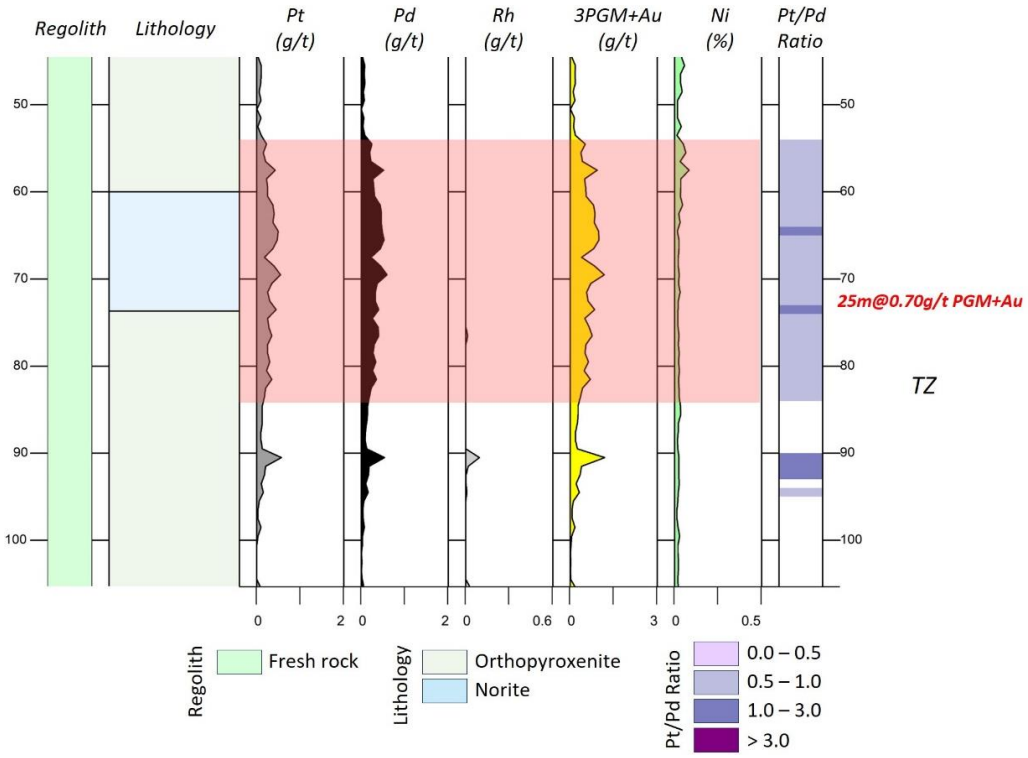

Figure 7-18: Typical log plot of a representative intercept of the LSZ mineralization

Source: Bravo, 2025.

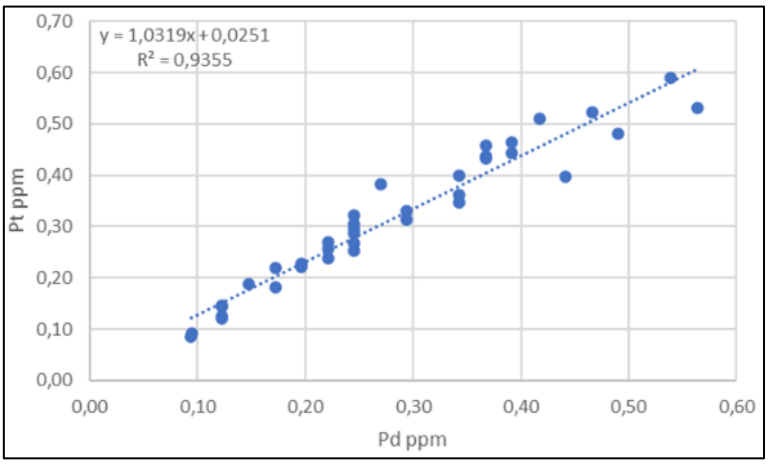

Figure 7-19: Correlation chart for a representative LSZ intercept

Source: Bravo, 2025.

7.3.6.3 Chromite-associated Zone (Chr-PGM)

Chr-PGM mineralization occurs as chromitite pods (< 60cm) closely associated with intercepts with disseminated clusters of chromite within orthopyroxenite, harzburgite and norite (Figure 7-20 A to C). This style of mineralization is stratigraphical located predominantly at the upper portion of the TZ and lower portion of the MZ (Figure 7-12).

Chromitite pods consist of fine-grained cumulus chromite commonly with abundant inclusions and/or atol texture. Disseminated chromite occurs as clusters of several euhedral chromite crystals (Figure 7-20 D to G).

The Chr-PGM mineralization has high Pt and Rh grades and low Pd and Ni contents (Figure 7-21), resulting in a high Pt/Pd ratio (~4.0), and low Rh/Pt ration (~0.3) (Figure 7-22).

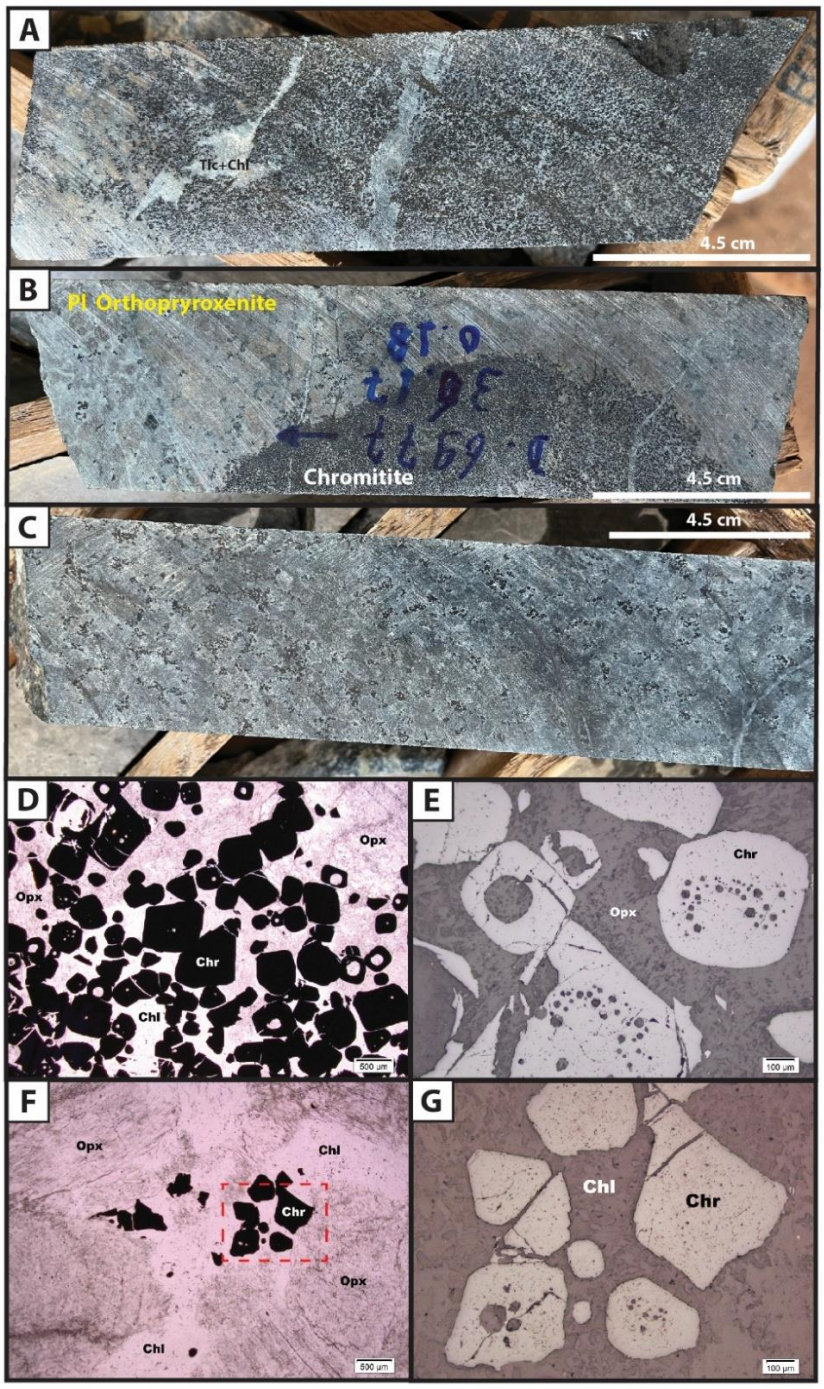

Figure 7-20: Representative photos and photomicrographs of Chr-PGM mineralization

Legend: A) Drill core sample of chromitite. Fine-grained chromite(Chr) occurs as euhedral black crystals in a light gray matrix consisting of chlorite (Chl) and talc (Tlc). B) Drill core sample of a chromitite pod hosted in a plagioclase-orthopyroxenite (pOPY) with disseminate clusters of Chr (black crystals). C) Drill core sample of a pOPY with disseminated clusters of Chr. D) Photomicrograph of a chromitite consisting of fine-grained euhedral chromite with common atol texture. Chr is associated with Opx pseudomorphs (Amp+Tlc) and fine-grained aggregates of Chl. E) Photomicrograph of euhedral Chr crystals hosted in Opx pseudomorphs (Amp+Tlc). F) Photomicrograph of pOPY with disseminated clusters of Chr The rock consists of euhedral Opx pseudomorphs (Amp+Tlc) and interstitial aggregates of Chl (plagioclase (Pl) pseudomorphs). Fine-grained Chr crystals occur mainly associated with interstitial aggregates of Chl. G) Detailed photomicrograph of the dashed red rectangle in (F).
Source: Bravo, 2025.

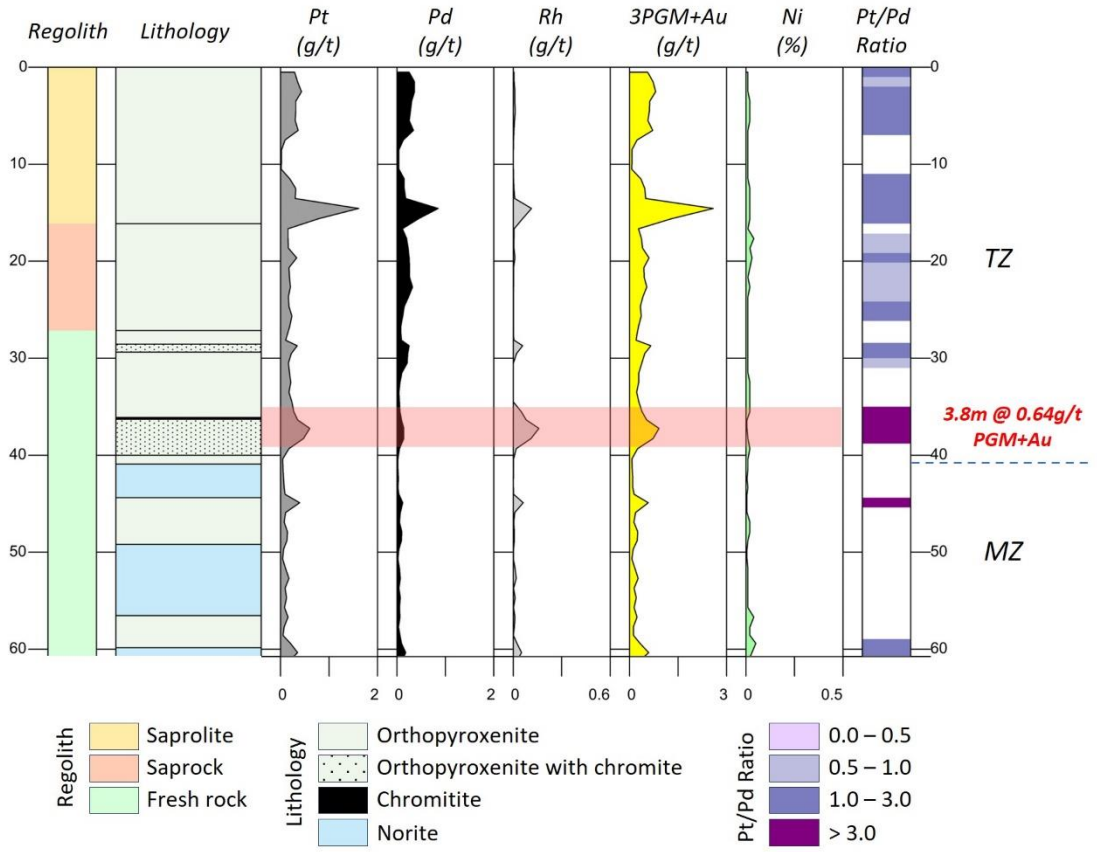

Figure 7-21: Typical log plot of a representative intercept of the Chr-PGM mineralization

Source: Bravo, 2025.

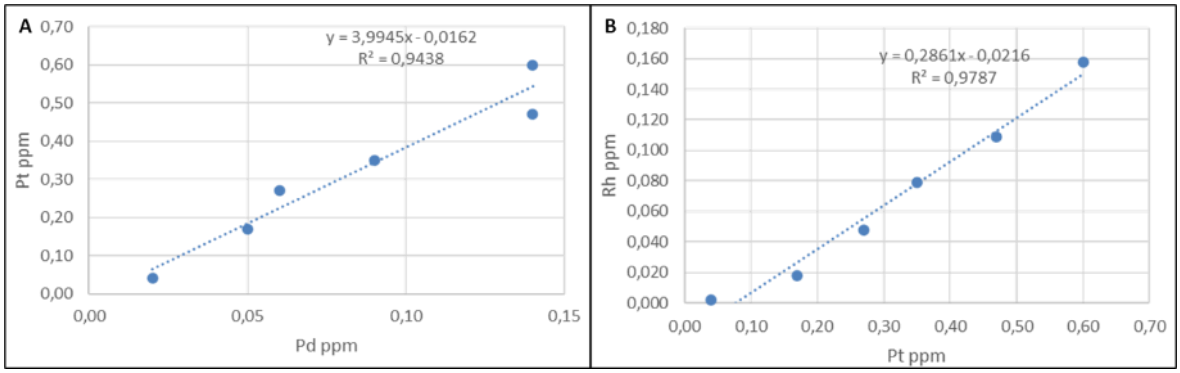

Figure 7-22: Correlation charts for a representative Chr-PGM intercept

Legend: A) Pt (ppm) vs. Pd (ppm) and B) Rh (ppm) vs. Pt (ppm).
Source: Bravo, 2025.

7.3.6.4 Ni-Rh Sulphide Zone (Ni-Rh)

The Ni-Rh mineralized zone has been identified only within the UZ on the Central and on the Southwest sectors (Figure 7-12 and Figure 7-13). It occurs as lenses of disseminated to net-textured sulphides (up to 25%) interstitial to cumulus Cpx and olivine or their pseudomorphs.

Ni-Rh zones have variable thickness (up to 40 m) and are commonly hosted by interlayered wehrlite and dunite, and minor clinopyroxenite.

Sulphides consist of Po (~60-70%), Pn (~30-40%) and minor Ccp. Pentlandite occurs mainly as medium-grained crystals (1-2mm) with very rare Pn exsolutions within Po. Partially altered sulphides, replaced by magnetite and Fe hydroxides are identified within the olivine-rich domains (Figure 7-23). This style of mineralization is represented by very low Pt grades associated with anomalous values of Rh+Pd and higher Ni grades (Figure 7-24).

Chemically, the Pt/Pd and Rh/Pd ratios are around 0.15 and 0.20, respectively (Figure 7-26A and B). Ni-Rh zones have significantly higher proportion of sulphides and lower Pt and Pd contents than the MSZ, which reflects relatively lower Pt-Pd tenors, as indicated by a calculated tenor of 5.8 ppm for Pd (Figure 7-25C). High Ni (~11.11 wt.%) and low Cu (~1.16% wt. %) tenors result in Cu/Ni ratio of ~0.15 (Figure 7-25 D and E).

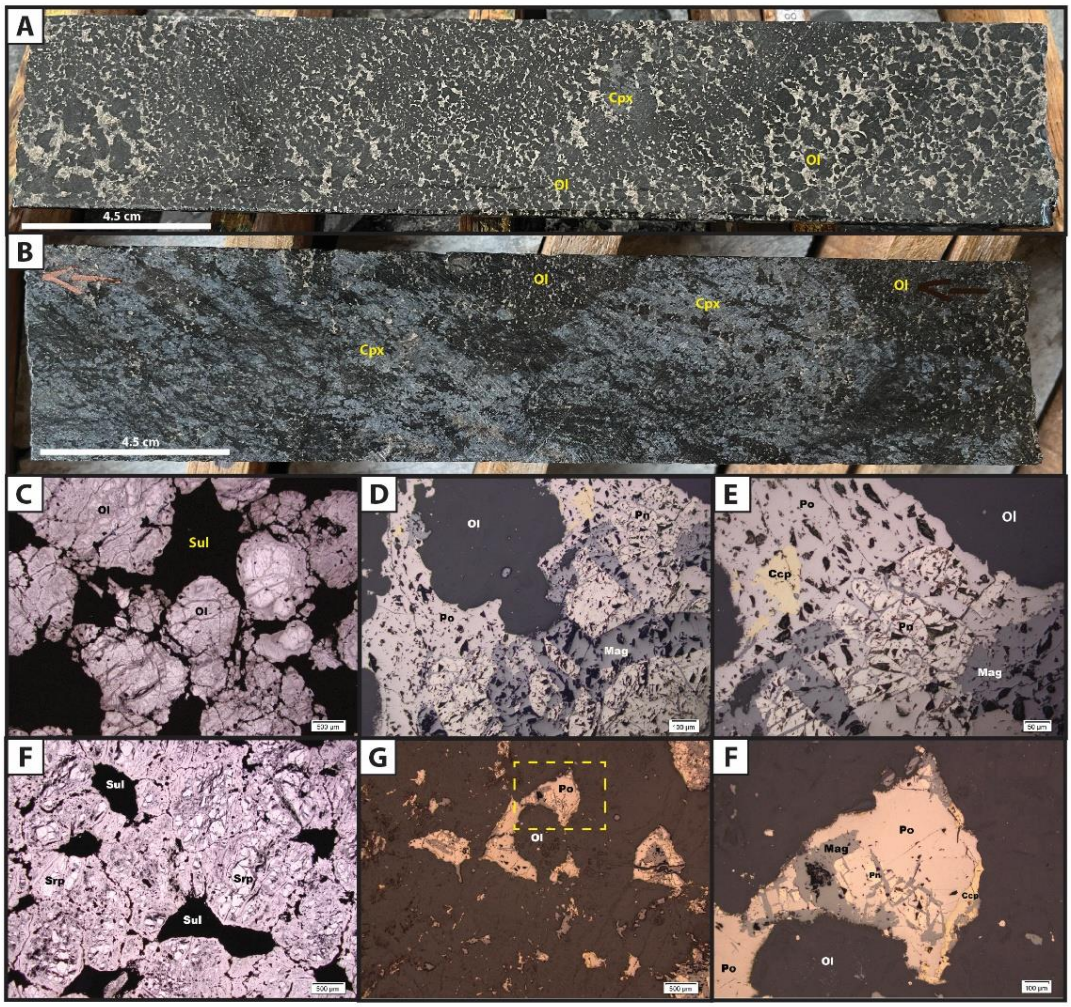

Figure 7-23: Representative photos and photomicrographs of Ni-Rh mineralization

Legend: A) Drill core sample of net-textured to matrix sulphides in dunite. Sulfides enclose euhedral olivine (Ol) pseudomorphs (black color). Minor coarse-grained anhedral Cpx crystals (dark gray color) partially enclose olivine. B) Drill core sample of disseminated interstitial sulphide blebs in wehrlite. The sample has irregular domains with variable amounts of Cpx (gray color) and Ol (black color). C) Photomicrograph of net-textured sulphides (Sul) interstitial to Ol pseudomorphs replaced by serpentine and minor magnetite. D) and E) Photomicrographs of sulphide aggregate enclosing Ol pseudomorph. Sulphides consist of pyrrhotite (Po), pentlandite (Pn) and minor chalcopyrite (Ccp), and are partially altered to magnetite (Mag). F) Photomicrograph of interstitial sulphide (Sul) blebs in a wehrlite altered to serpentinite. G) and H) Photomicrographs of sulphide blebs interstitial to Ol pseudomorph in wehrlite. Sulphides consist of pyrrhotite (Po), pentlandite (Pn) and minor chalcopyrite (Ccp), and are partially altered to magnetite (Mag).

Source: Bravo, 2025.

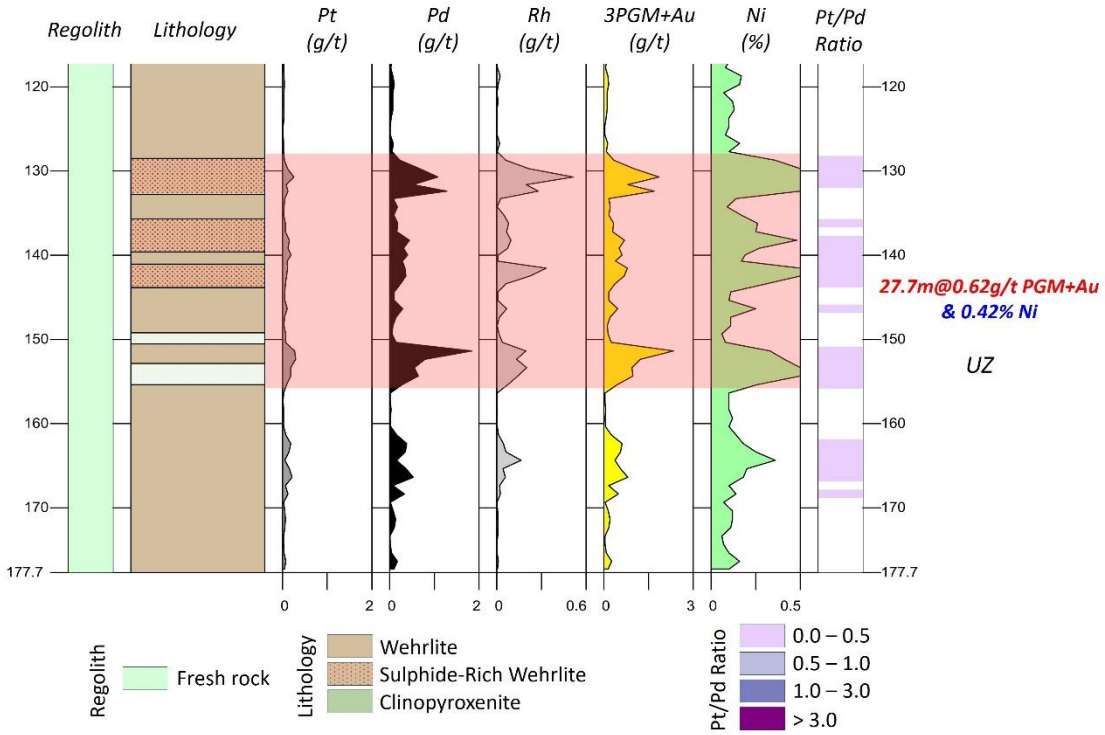

Figure 7-24: Typical log plot of a representative intercept of the Ni-Rh mineralization

Source: Bravo, 2025.

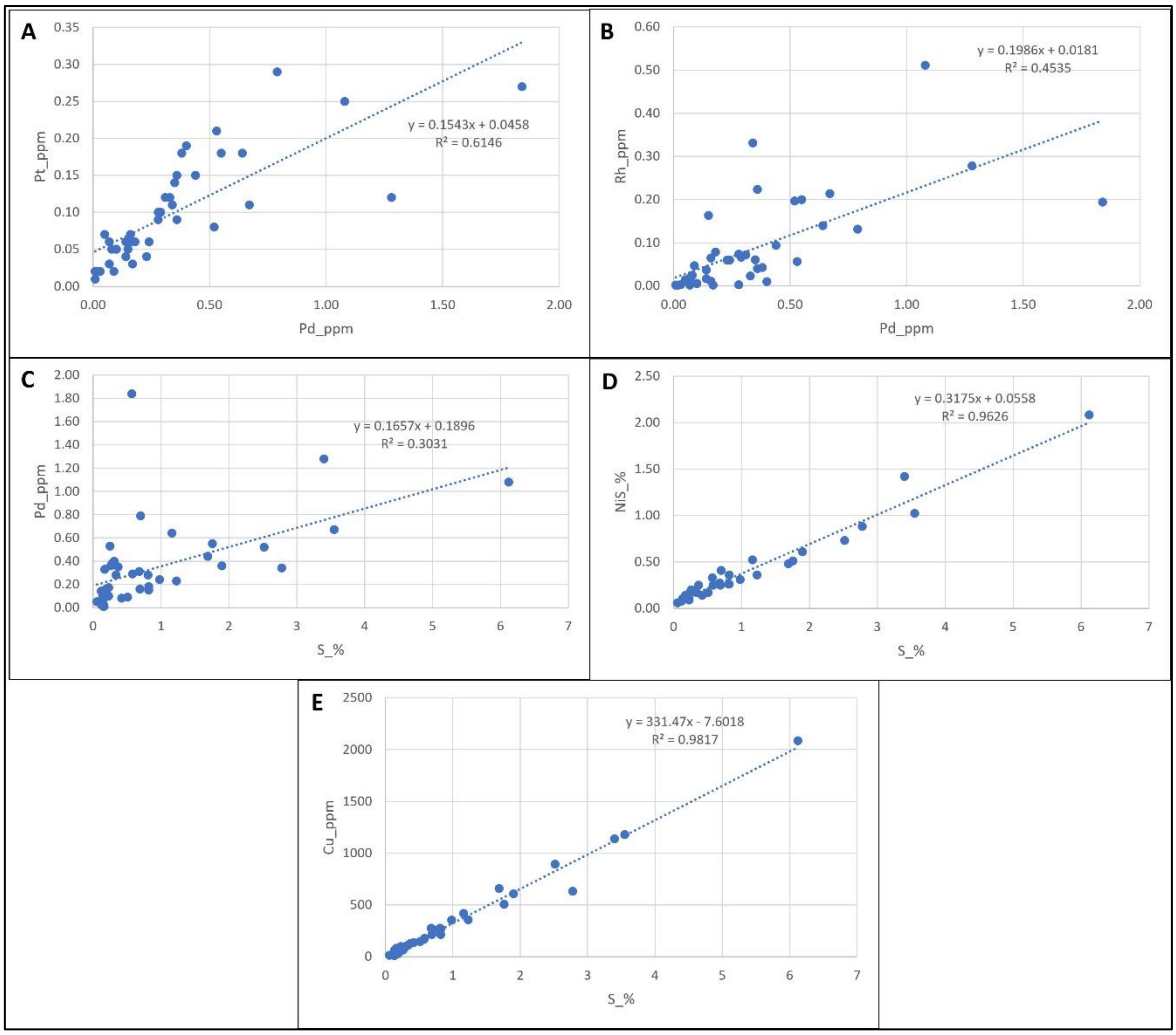

Figure 7-25: Correlation charts for a representative Ni-Rh intercept

Legend: A) Pt (ppm) vs. Pd (ppm), B) Rh (ppm) vs. Pd (ppm), C) Pd (ppm) vs. S (%), D) Ni (%) vs. S (%), E) Cu (ppm) vs. S (%).

Source: Bravo, 2025.

7.3.6.5 Sulphide Zone (SZ)

The SZ mineralization style is recognized exclusively in the Northern sector, characterized by mineralized bands of variable thickness hosted in rocks of the Transition Zone. The SZ occurs as several irregular N-S trending zones of disseminated sulphides hosted mainly in orthopyroxenite and is stratigraphically closely associated with Chr-PGM and LSZ mineralization (Figure 7-12). Correlation of the SZ in the North sector with the stratigraphy of the Central and Southwest sectors is hampered by extensive deformation and alteration of rocks in the North sector.

The SZ occur as a ~2 km-long stacked stratabound bodies of disseminated fine-grained sulphides (1-5%) and this style of mineralization has highly variable thickness, reaching up to 40 m (Figure 7-26 and Figure 7-27). The irregular structure suggests a disrupted (folded or faulted) subvertical strata bound bodies that is some places together with the mafic-ultramafic sequence

are crosscut by granitoids at depth, restricting this kind of mineralized zones to vertical depths around 100 metres.

This style consists mainly of fine-grained aggregates of sulphides interstitial to pseudomorphs of Opx. The sulphide paragenesis is predominantly Po-Pn and minor Ccp.

Chemically, the SZ is characterized by moderate to high PGM contents (30-40 m intercepts with 2-3 ppm of Pt + Pd) with predominantly low Pt/Pd (commonly <0.5, but up to 1.0) and variable Ni contents (up to 0.20%). Weak positive correlation between Pd-Ni and Pd-Rh possibly results from variably altered sulphides (Figure 7-28).

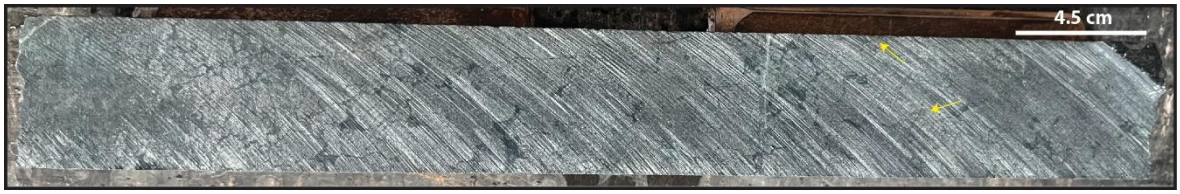

Figure 7-26: Representative photo of the SZ

Legend: Drill core sample of orthopyroxenite with interstitial plagioclase. Coarse- to medium-grained Opx pseudomorphs (replaced by talc and serpentine) are delineated by interstitial plagioclase pseudomorphs (dark color) replaced by chlorite. Fine-grained partially oxidized sulphide blebs are indicated by yellow arrows.
Source: Bravo, 2025.

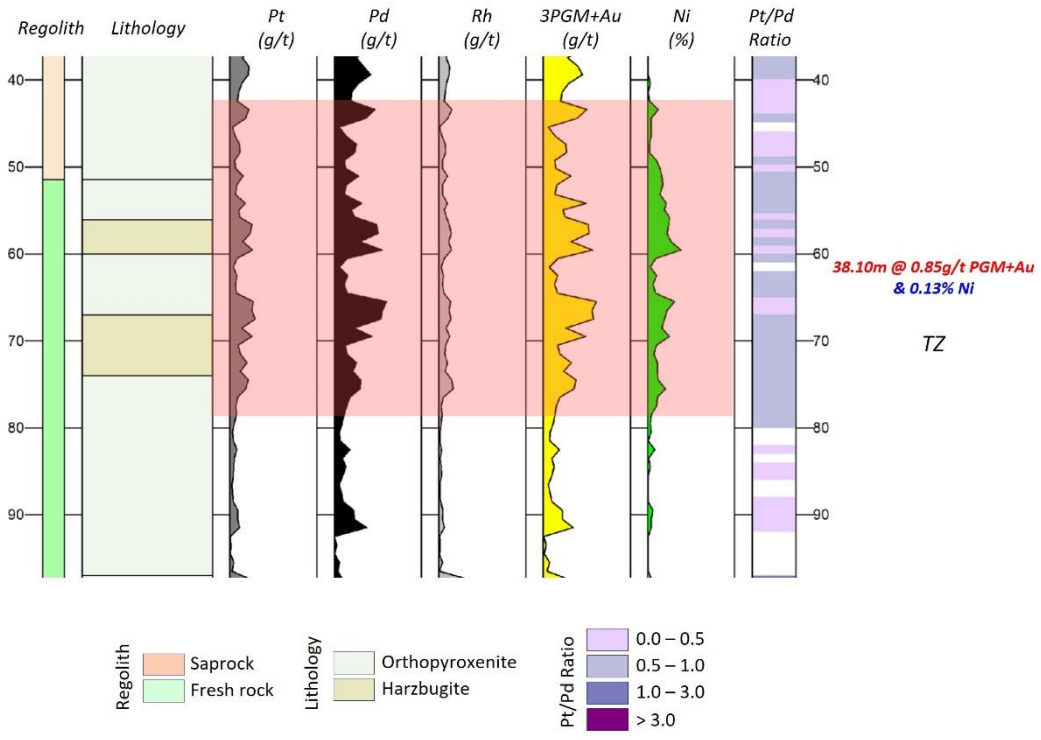

Figure 7-27: Typical log plot of a representative intercept of the SZ mineralization

Source: Bravo, 2025.

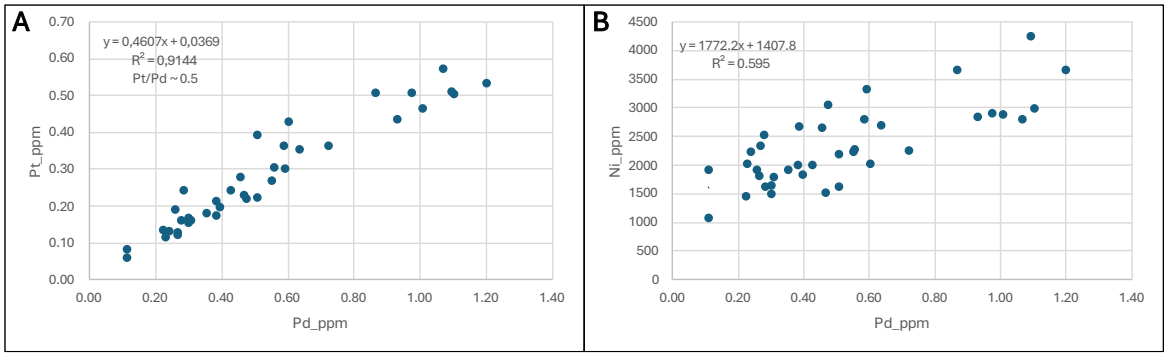

Figure 7-28: Correlation charts for a representative SZ intercept

Legend: A) Pt (ppm) vs. Pd (ppm) and B) Ni (%) vs. Pd (ppm).
Source: Bravo, 2025.

7.3.6.6 Massive Sulphide Zone (MASU)

The MASU style of mineralization was identified in 2022 on the North sector where drill hole DDH22LU047 intercepted 11.0m grading 4.24 g/t 3PGM+Au, 2.04% Ni, 1.23% Cu within a hydrothermal alteration zone at the eastern border of the Luanga Complex (Figure 7-29).

Host rocks and the footwall sequence of the MASU consist of amphibolitite, massive rocks consisting of variable proportions of amphibole-garnet-biotite-magnetite and banded iron formation. Sulphide-bearing orthopyroxenite and interlayered norite occur above the MASU and in adjacent drill holes. Cumulate rocks close to the alteration zone are partially to pervasively replaced by the Fe-Ca-K hydrothermal minerals, including MASU to semi-MASU breccias, suggesting that the Ni-Cu-PGM mineralization originated by hydrothermal remobilization of primary sulphides. The alteration assemblage originated from a pervasive Fe-Ca-K hydrothermal alteration is possibly connected with the regional hydrothermal system associated with the IOCG deposits in Carajás.

Sulphides consist mainly of pyrrhotite (~80-90%) and pentlandite (~10-20%) with local chalcopyrite-rich domains (up to 60-70% Ccp). Variable proportions of amphibole and minor biotite, magnetite and quartz are enclosed within massive sulphides, with common sulphide-amphibole intergrowths. Pn occurs mainly associated with Po as fine-grained (<0.5 mm) crystals or exsolutions (e.g., flames, flakes) (Figure 7-30 A to G).

The MASU has variable contents of Ni, Cu and PGM, generally with Ni>Cu and Pd>Pt (Figure 7-31 A and B). Except for the broad positive correlation between Ni and Pd, correlations between metals are only subtle, including Pd-Pt, Ni-Cu and Pd-Rh (Figure 7-31 C and D). Contents of Ni (<6.0%), Pd (<6.0 ppm), Pt (<2.5 ppm) and Rh (0.2 ppm) in samples of MASU (i.e., close to 100% sulphides) provide approximate tenors for these metals in this style of mineralization.

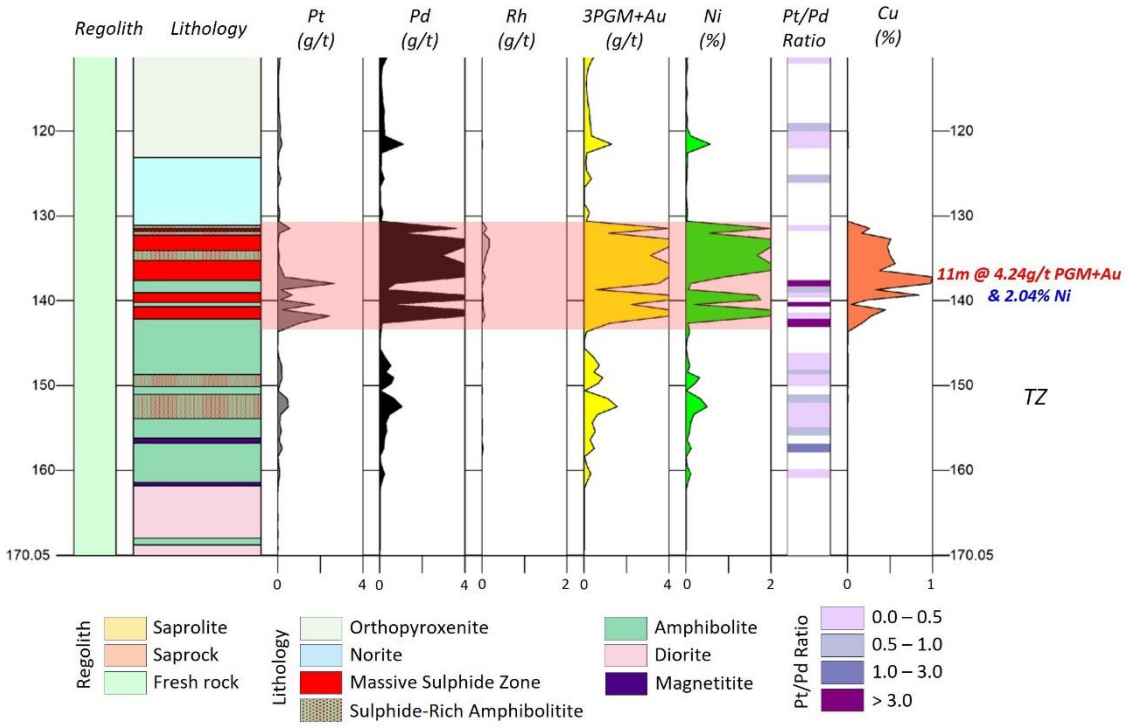

Figure 7-29: Typical log plot of a representative intercept of *the* MASU mineralization

Source: Bravo, 2025.

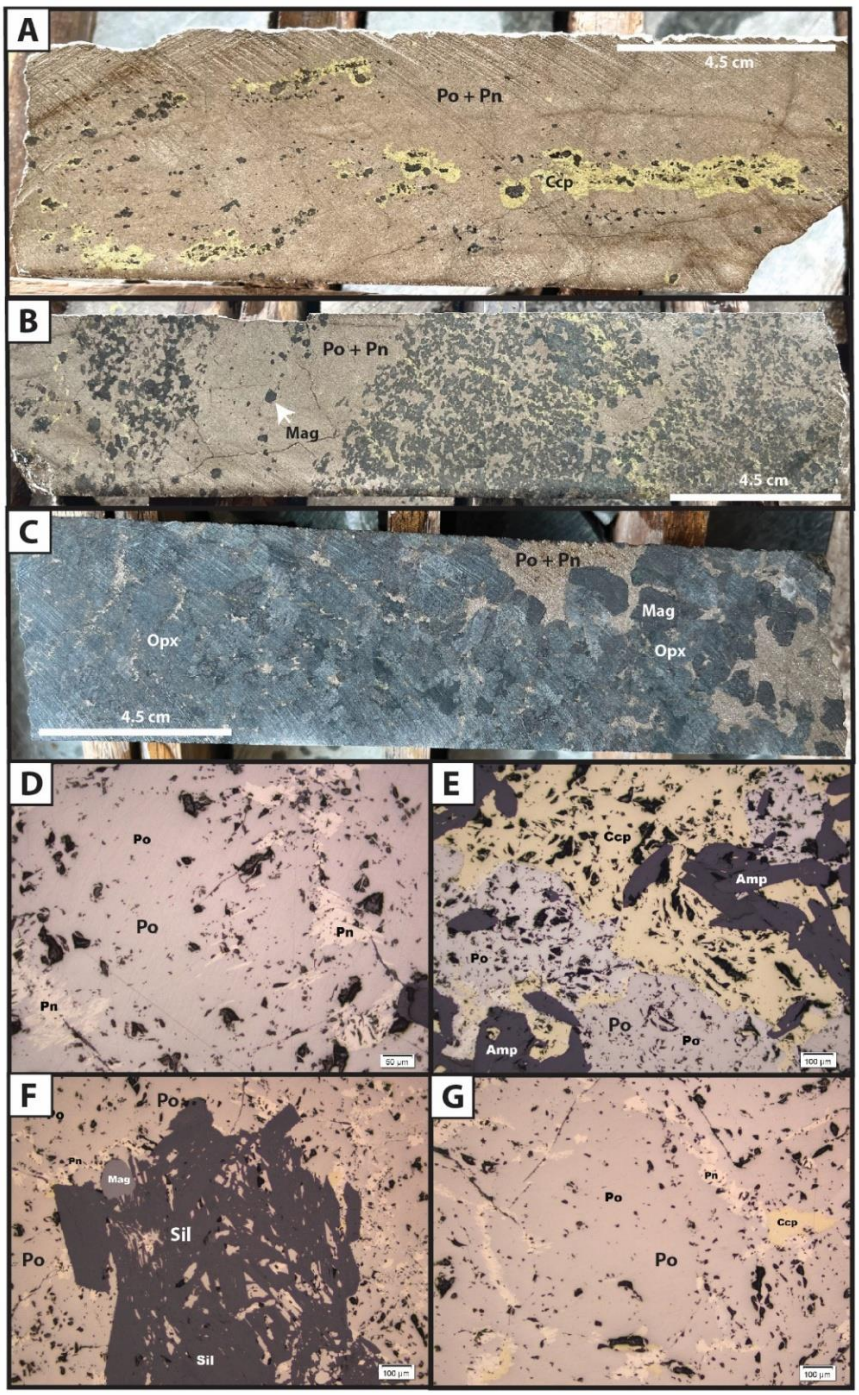

Figure 7-30: Representative photos and photomicrographs of MASU

Legend: A) Drill core sample of MASU mineralization. Sulfides consist of pyrrhotite (Po) and pentlandite (Pn), with minor chalcopyrite (Ccp) domains (yellow color). B) Drill core sample of MASU mineralization. Sulfides consist of Po and Pn, with minor Ccp (yellow color). Gangue minerals consist mainly of prismatic amphiboles (Amp) and minor magnetite (Mag).C) Drill core sample with disseminated and minor MASU mineralization interstitial or enclosing Opx pseudomorphs (replaced by Amp) and minor magnetite (Mag). D) Photomicrograph of MASU consisting of Po with Pn exsolution (flames and flakes). E) Photomicrograph of MASU consisting of Po and a Ccp-rich domain. Sulfides are associated with prismatic amphiboles. F) Photomicrograph of MASU consisting of Po with Pn exsolutions enclosing an aggregate of silicates (Amp+Chl+Bt) and minor Mag. Sulfides are associated with prismatic amphiboles. G) Photomicrograph of MASU consisting of Po with Pn exsolution and minor Ccp.

Source: Bravo, 2025.

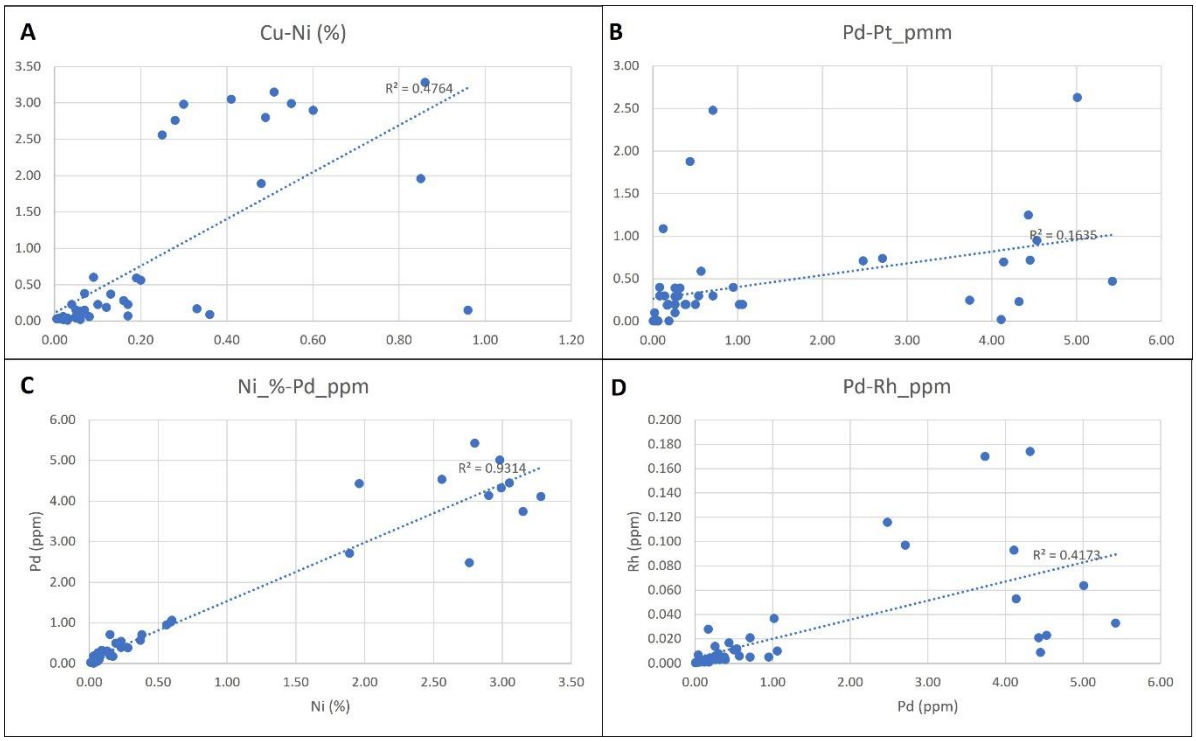

Figure 7-31: Correlation charts for a representative MASU intercept, shown in Figure 7-30

Legend: A) Cu (%) vs. Ni (%), B) Pd (ppm) vs. Pt (ppm), C) Ni (%) vs. Pd (ppm) and D) Pd (ppm) vs. Rh (ppm).
Source: Bravo, 2025.

The bulk of the world's PGM resources are mined from mafic-ultramafic layered intrusions, commonly from stratiform mineralized layers located near the transition from mafic to ultramafic cumulate rocks. Magmatic Ni-Cu-PGM sulphides formed by the accumulation of immiscible sulphide liquid that scavenged chalcophile elements from a coexisting silicate magma. Textural relationships between sulphides and their host silicates are key evidence for their origin as immiscible sulphide liquids. The magmatic origin of the Luanga deposit is supported by textural and mineralogical features described in different styles of PGM mineralization, particularly the MSZ, Ni-Rh and SZ. In these different PGM zones, sulphide blebs consisting of pyrrhotite + pentlandite ± chalcopyrite are interstitial to cumulus olivine and/or pyroxene. In addition, sulphide blebs enclosed in cumulate crystals, as well as their rounded/corroded faces, provide unequivocal evidence for a magmatic origin of sulphides and PGM. Variable litho-chemical features in PGM zones located in distinct stratigraphic horizons of the Luanga complex, including different metal tenors, as well Pt/Pd and Rh/Pd ratios, indicate that several events of mineralization occurred during the magmatic evolution of the Luanga complex. The occurrence of several mineralized horizons in the Luanga complex, including PGM mineralization hosted in chromitites, has remarkable similarity with reef-type productive deposits (e.g., Bushveld and Stillwater).

The widespread alteration of rocks from the Luanga complex has partially disrupted their primary magmatic features. In the Luanga complex, magmatic silicates are partially altered and commonly occur as pseudomorphs. The magmatic sulphides have also been partially altered during the widespread alteration. The most common alteration of primary sulphides (pyrrhotite - pentlandite - chalcopyrite) consists of their replacement by magnetite and Fe-hydroxides.

Because this alteration is heterogeneous at different scales (from mineral crystals up to several hundred meters thick zones) and largely preserves primary textures and compositions of cumulate rocks and PGM mineralized zones, magmatic features can be recognized throughout the layered intrusion.

8 DEPOSIT TYPES

The bulk of the world's PGM resources are mined from mafic-ultramafic layered intrusions, commonly from stratiform mineralized layers located near the transition from mafic to ultramafic cumulate rocks (Naldrett, 2004; Mungall and Naldrett, 2008; Zientek, 2012). This type of mineralization, known as reef-type deposits, has the Bushveld Complex as the leading model for exploration. In addition, layered mafic-ultramafic intrusions can host economic deposits of base metal sulphides (Ni-Cu-Co), chromite and magnetite-ilmenite (Fe-Ti-V). These deposits result from magmatic processes of crystallization, differentiation, and concentration during emplacement and cooling of mafic-ultramafic magmas. In particular, PGM (Ni-Cu) deposits are generally accepted to result from the concentration of variable amounts of sulphides originated as a separate immiscible liquid from the parental magma.

"PGM reefs" are strata bound enriched lode mineralization in mafic to ultramafic layered intrusions. The term "reef" is derived from Australian and South African literature for this style of mineralization and used to refer to (1) the rock layer that is mineralized and has distinctive texture or mineralogy or (2) the enriched sulphide mineralization that occurs within a rock layer.

A schematic model of an ideal layered intrusion is presented on Figure 8-1, showing the relative position and petrological affinities of the differing types of magmatic PGM deposits. A single layered intrusion is unlikely to host all these styles of mineralization, and that PGM deposits with differing magmatic affinities can occur in similar positions within an intrusive system.

Magmatic Ni-Cu-PGM sulfides form by the accumulation of immiscible sulphide liquid that scavenged chalcophile elements from a coexisting silicate magma (e.g., Naldrett, 2004, Barnes et al., 2016). Textural relationships between sulphides and their host silicates are key evidence for their origin as immiscible sulphide liquids (Barnes et al., 2017, 2018). The magmatic origin of the Luanga PGM + Au + Ni deposit is supported by textural and mineralogical features described in different styles of PGM mineralization, particularly the MSZ, Ni-Rh and SZ. In these different PGM zones, sulphide blebs consisting of po+pn±cpy are interstitial to cumulus olivine and/or pyroxene. In addition, sulphide blebs enclosed in cumulate crystals, as well as their rounded/corroded faces, provide unequivocal evidence for a magmatic origin of sulphides and PGM. Variable lithochemical features in PGM zones located in distinct stratigraphic horizons of the Luanga Complex, including different metal tenors, as well Pt/Pd and Rh/Pd ratios, indicate that several events of mineralization occurred during the magmatic evolution of the Luanga Complex. The occurrence of several mineralized horizons in the Luanga Complex, including PGM mineralization hosted in chromitites, has remarkable similarity with reef-type productive deposits (e.g., Bushveld and Stillwater).so

The widespread alteration of rocks from the Luanga Complex has partially disrupted their primary magmatic features. In the Luanga Complex, magmatic silicates are partially altered and commonly occur as pseudomorphs. The magmatic sulphides have also been partially altered during the widespread alteration. The most common alteration of primary sulphides (po-pn-cpy)

consists of their replacement by magnetite and Fe-hydroxides. Because this alteration is heterogeneous at different scales (from mineral crystals up to several hundred meters thick zones) and largely preserves primary textures and compositions of cumulate rocks and PGM mineralized zones, magmatic features can be recognized throughout the layered intrusion.

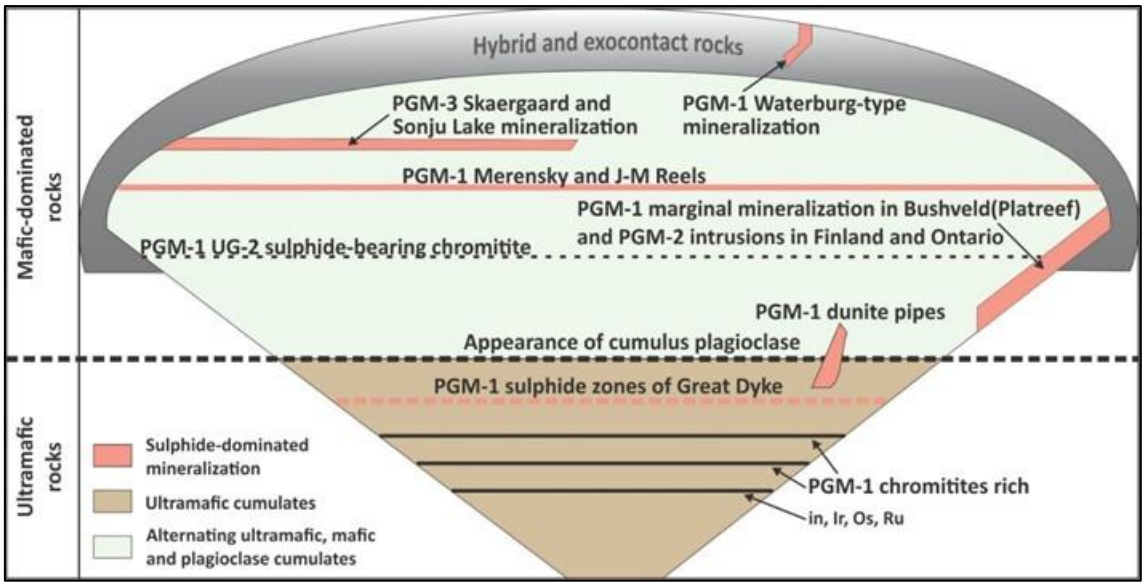

Figure 8-1: Schematic model of a Large Igneous Province (LIP) related layered intrusion

Source: Naldrett, 2010.

9 EXPLORATION

Bravo has been diligently following a systematic approach in its exploration programs for the Luanga PGM + Au + Ni Project.

9.1 Preliminary Works

The earliest exploration completed by Bravo was from the September 2 to 23, 2020. Bravo staff visited Vale´s core facilities where they collected five verification core samples from four historical drill holes (Table 9-1). Samples were ¼ core from mineralized intervals previously sampled by Vale (Figure 9-1). Those samples were cut and bagged in Vale's facilities by Bravo personnel, who were responsible for the identification (the same ID as the original sample) and shipping of the sample bags.

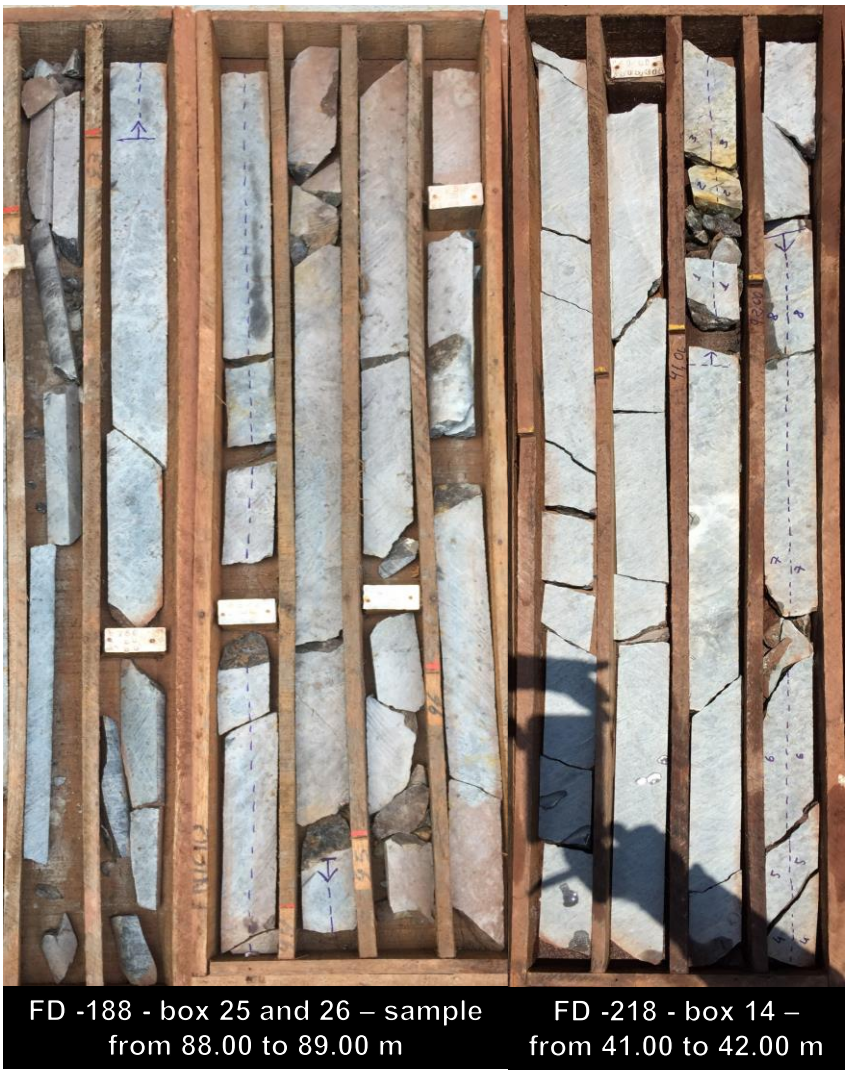

Figure 9-1: Examples of drill holes selected for independent re-sampling

Source: Bravo, 2023.

Samples chosen for assay analysis by Bravo were shipped directly to the analytical laboratory of ALS Brasil Ltda. in Belo Horizonte, Minas Gerais state. ALS Brasil Ltda. is a part of

ALS Global, an international laboratory company with certified labs all over the world. ALS are ISO/IEC 17025:2017 and ISO 9001:2015 certified/accredited. At ALS, all samples were weighed, dried, crushed, split, and pulverized up to 85% <75µm.

All samples were analysed for Pt, Pd, and Au by fire assay with ICP-AES finish, and for Rh by fire assay with ICP-MS finish. The samples also were analysed for 48 elements by four acid and ICP-MS finish.

In 2021, Bravo conducted a detailed review on Vale data, including results from previous Diamond Drilling database campaign and results validation based on chemical results from core resampling conducted in 2020.

After Bravo assumed management of the Luanga Project in 2022, historical drill core, drilled by Vale, has almost entirely been relocated from the Vale N5 core yard to the Bravo core yard. In total, 234 complete diamond drill holes were received at Bravo core yard, representing a significant cross-section of the geology intersected by the historical drilling campaign (Table 9-1).

Table 9-1: Historical drill core transport status

	Vale (N5)	Bravo Camp	% Transported	% Pending
Total Drill Holes	234	234	100	0
Total Metres	46,029	46,029	100	0
Total Boxes	13,047	13,047	100	0

Source: Bravo, 2025.

Following the receipt of the drill cores, Bravo technical staff repaired and cleaned the core boxes, their markings and labels prior to relogging the core geologically (Table 9-2 and Figure 9-2). Following this relogging, the core was cleaned and photographed before the commencement of resampling.

Table 9-2: Historical drill core – quantity of relogging and resampling

Relogging & Resampling				
Received Core	**Bravo Camp**	**Relogged**	**% Relogged**	**% Resampled**
Total Historic Drill Holes	234	202 (all drilling within the Luanga deposit)	87%	87%
Total Metres	**46,029**	**40,065**	**87%**	**87%**

Source: Bravo, 2025.

Figure 9-2: Vale core now at the Bravo facilities

Source: Bravo, 2025.

For the resampling programme (), half core was cut in half again by a standard industry core saw and, in cases where only quarter remains, it was sampled in its entirety. Figure 9-3Certified Reference Materials (blanks and standards) (CRM) were inserted throughout the sample sequence at a ratio of one in every twenty samples for each, resulting in a quality control sample after every ten primary samples. Standards were purchased from both OREAS in Australia and AIMS in South Africa. These standards cover a variety of grades, while also being the best matrix match for the type of mineralization at Luanga. Samples were submitted to ALS Brasil at their sample reception facility located in Parauapebas.

Figure 9-3: Resampling programme

Source: Bravo, 2025.

Historical drill core sample data and Bravo's drill core resampling to date shows an expected positive correlation for the PGM assessed. Minor variations from Vale's original assays to the re-assay are attributed to updated preparation and analytical methods and refined assaying for Rh and Ni. Ni resampling data assays presents two different populations, one probably related to the silicate and other sulphides.

9.2 Soil Samples

9.2.1 Historical Soil Sampling

A total of 5,241 soil samples were collected by Vale during the exploration works conducted at Luanga. All soil samples were submitted to chemical analyses for a suite of 16 elements (in ppb), including: Ag, As, Be, Bi, Ce, Co, Cr, Cu, La, Ni, Pb, Sb, Sn, Te, W and Zn. This suite of elements was analysed by inductively coupled plasma/mass spectrometry (ICP/MS) by the three different laboratories (Nomos, Lakefield and SGS). Soil samples were also analysed for Au, Pt and Pd (in ppb) by fire assay/atomic absorption spectrometry (FA/AAS). Information about the laboratory responsible for the FA/AAS analyses is not included in the database.

The results from historical soil sampling were reprocessed by Bravo (Figure 9-4). Cr and Ni soil anomalies fits very well with mafic and ultramafic rocks of Luanga Complex and Luanga South. Pd and Pt anomalies in soil are coincident with the rocks of Transition Zone of Luanga Complex.

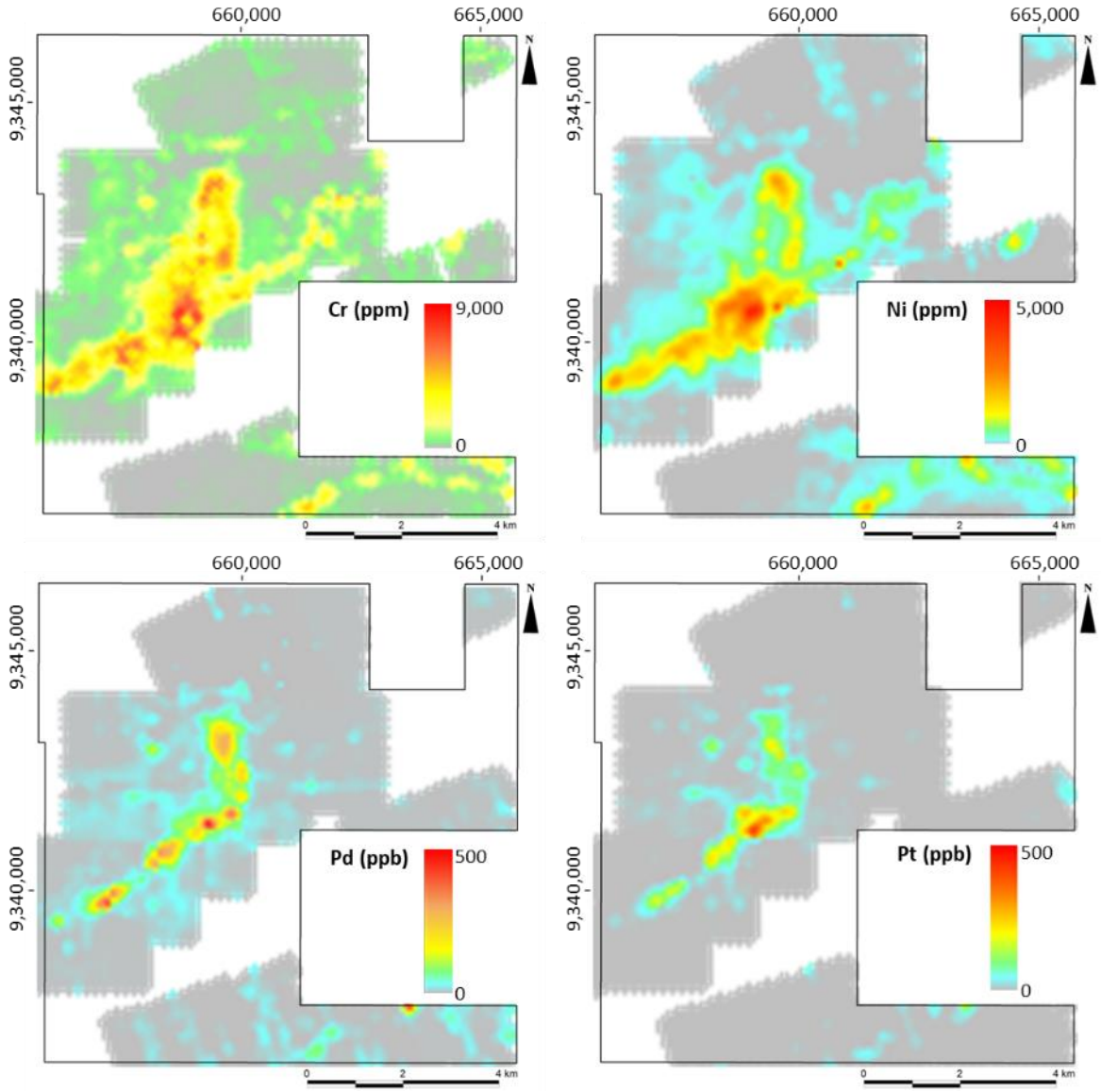

Figure 9-4: Maps with reprocessed results from historical soil sampling campaign

Source: Bravo, 2025.

9.3 Topographic Surveys

In 2022 RR Topografia & Engenharia of Brazil completed the Orthophotography and new Digital Elevation Model (DEM). Commercial drone surveying equipment was used to complete the aerial work, while ground surveying was used for control of accuracy, positioning and georeferencing. A mosaic of the ortho-imagery overlain on the 3D digital terrain model created from the DEM, is shown below in Figure 9-5.

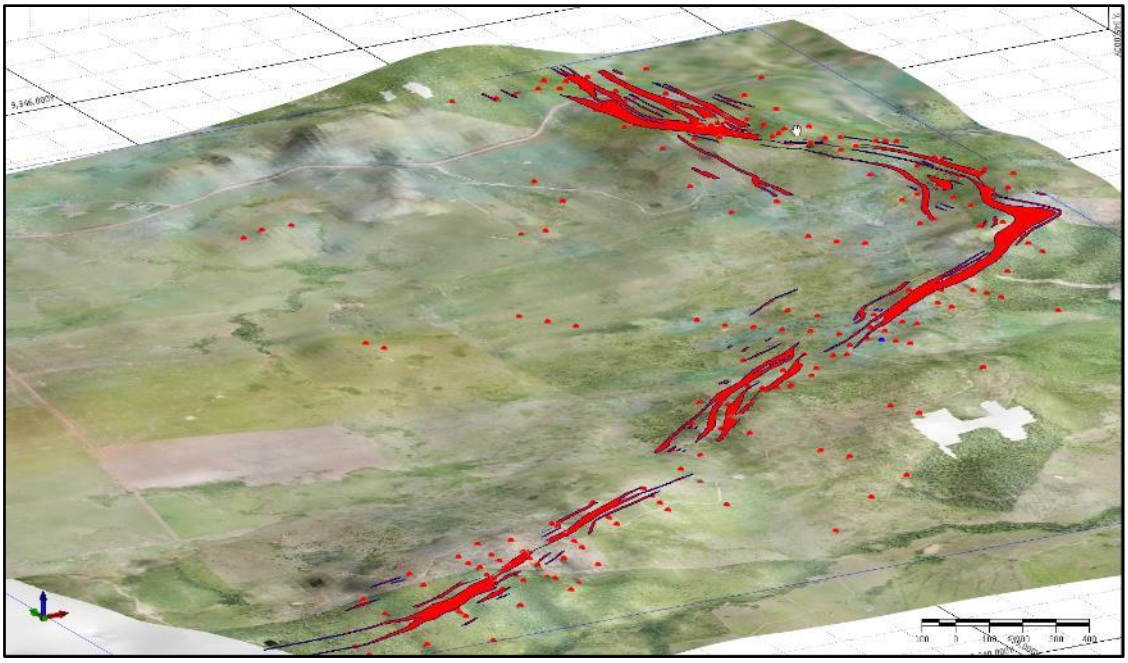

Figure 9-5: Luanga Project: digital elevation model, ortho-image, drill collars and mineralization zones

Source: Bravo, 2025.

In June 2023, Bravo contracted Sul Pará to conduct a new Drone Survey over the Luanga deposit and adjacent areas. The survey covered a total area of 26.96 km^2 over Luanga Complex and provided a detailed (1 m) Digital Elevation Model (Figure 9-6 A) and an ortho-mosaic image (Figure 9-6 B).

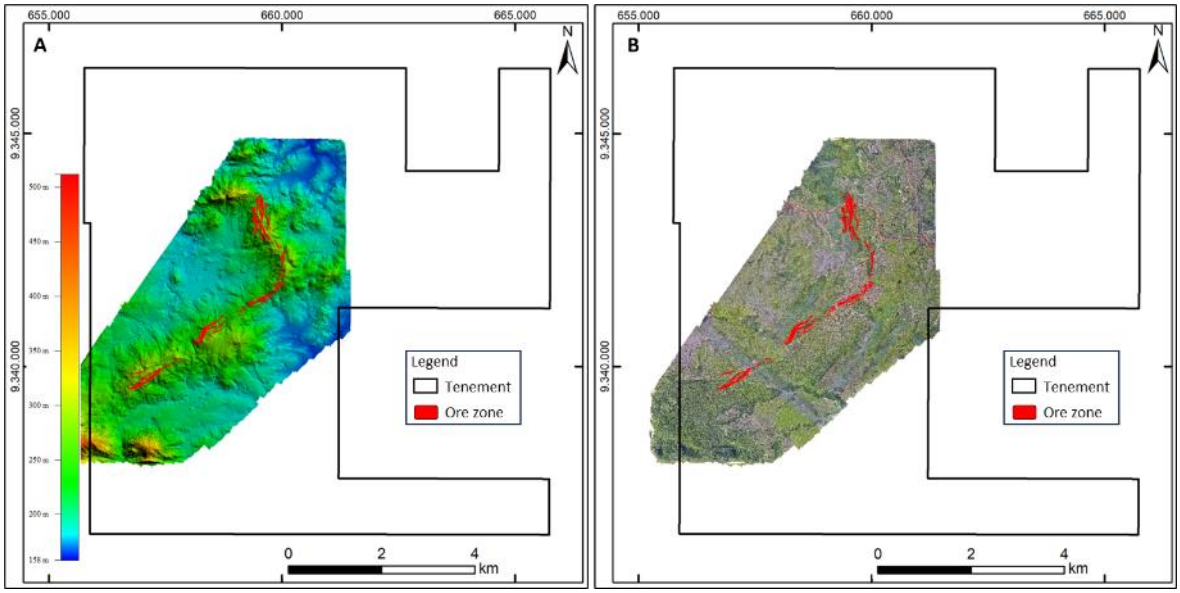

Figure 9-6: Luanga Complex digital elevation model and ortho-mosaic image

Legend: (A) digital elevation model, and (B) ortho-image. Both with identified mineralized zones.
Source: Bravo, 2025.

9.4 Geological Mapping

Bravo conducted a detailed geological mapping over the Luanga Complex at the 1:10,000. Mapping was performed along north-south profiles at intervals of 100m. In more complex zones of the Complex, mapping was completed at a scale of 1:5,000, also using the drilling data and ground geophysics to support interpretations.

Additionally, Bravo hired PRCZth to carry out the geological and structural mapping work at the Luanga Project. This work was performed from November 2022 to July 2023. A total of 88 field points were fully described, and a further 52 stations were marked where observations were made by quick reference to lithologies or contacts. The description, structural measurements, photos and location coordinates of each field point are stored in a spreadsheet. The information provided by PRCZ was compiled by Bravo and used in the compilation of the geological map (Figure 9-7).

Geological units identified in the Project area included rocks from the basement of the Carajás Domain, consisting mainly of gneiss–migmatite–granulite terrains of the Xingu Complex, and metavolcanic and metaplutonic rocks of Grão Pará Group.

The Luanga Complex consist of three main lithological domains: (i) Ultramafic Zone, comprising ultramafic cumulates (wehrlites with lesser dunites and clinopyroxenites), at the lower portion; (ii) Transition Zone, comprising interlayered ultramafic and mafic cumulates (orthopyroxenites, locally with chromite-rich zones/chromitite, and minor norite/harzburgite layers); and (iii) Mafic Zone comprising a monotonous sequence of mafic cumulates (norites) with minor orthopyroxenite layers, in the upper part. Additionally, a late intrusive diorite body is interpreted as part of the complex. The rocks of the Luanga Complex are metamorphized to amphibolite facies, but with largely preserved primary textures.

Dolerite dykes intruded throughout the Luanga complex rocks. Minor quartz veins occur locally.

Recent sedimentary rocks are restricted to alluvial deposits related to water courses. Artisanal gold mines have been mapped surrounding the Luanga Complex.

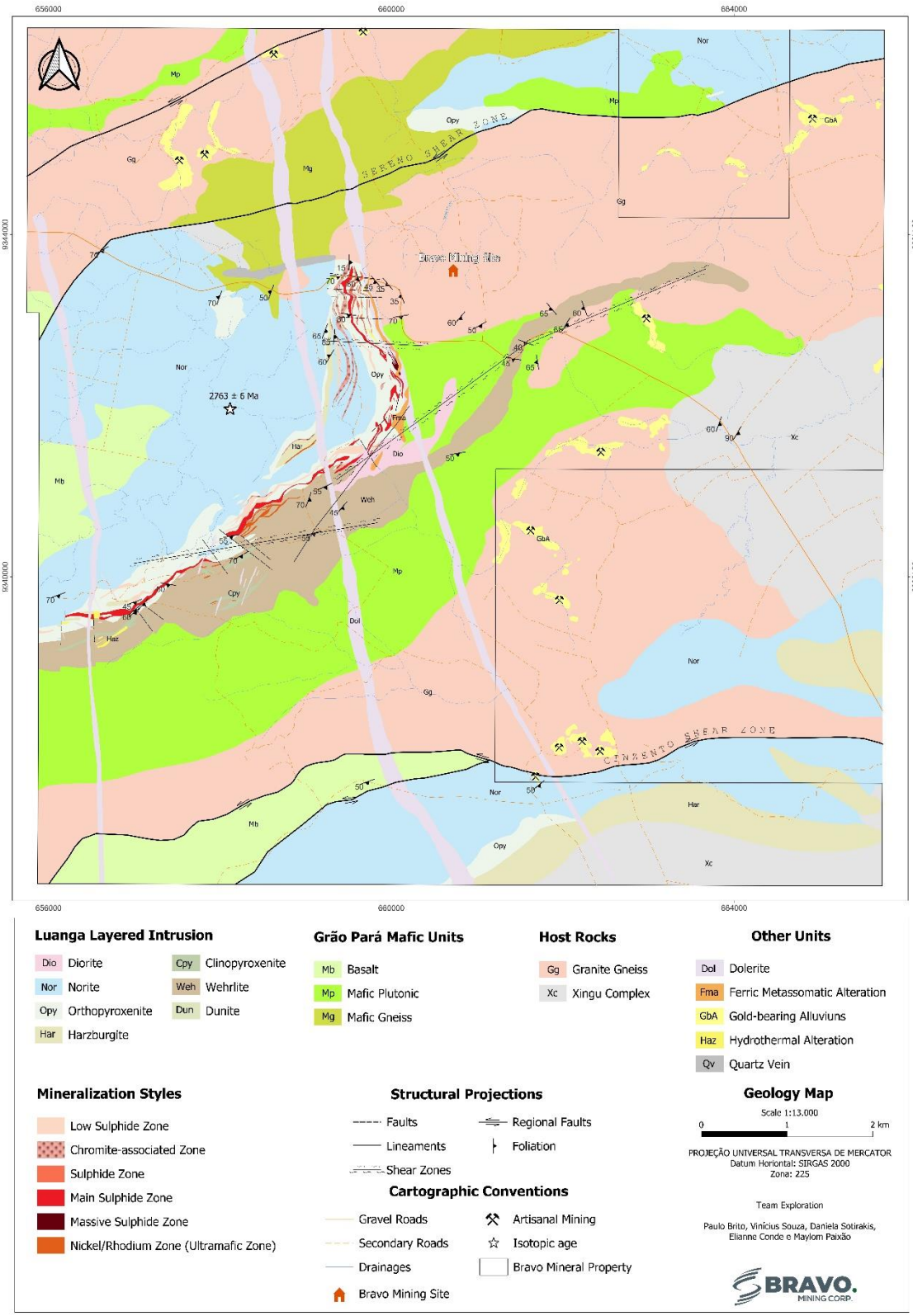

Figure 9-7: Geological map of Luanga Project

Source: Bravo, 2025.

9.5 Petrography

To improve the geological understanding of the Luanga deposit, several petrographic studies were conducted between 2022 and 2024 using 117 selected drill core samples representing the lithological diversity and multiple mineralized styles, polished thin sections were prepared for all of them. The petrographic studies were developed under an academic collaboration with Professor Cesar Ferreira Filho from the University of Brasília. Figure 9-8 and Figure 9-9 show photomicrographs representative of common textures described at Luanga.

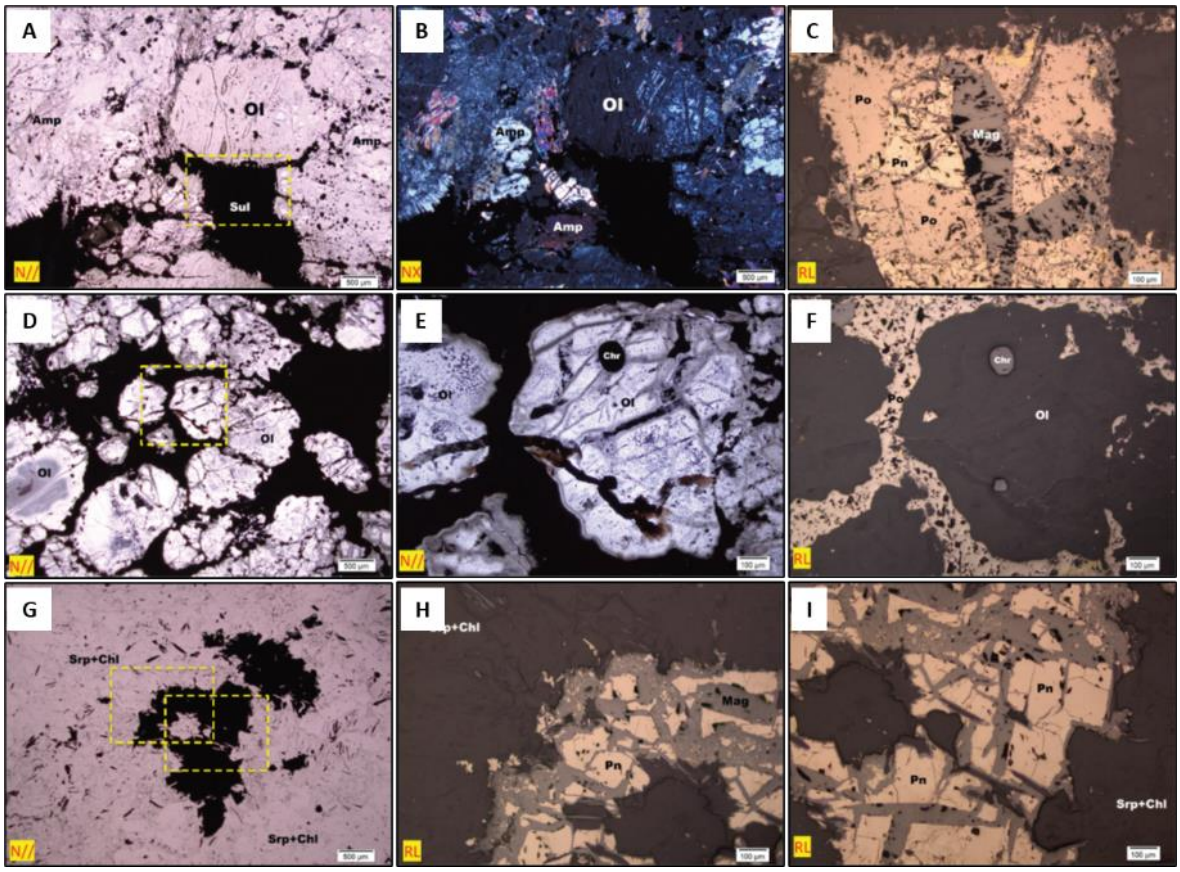

Figure 9-8: Sample Ptr-23 photomicrographs

Legend: (A) and (B) Olivine orthopyroxenite Olivine is altered to fine-grained aggregates of Srp + Mag, while Cpx is altered to colorless amphibole (Amp) and Mag. (C) Po and Pn with minor Ccy. Sulphides are partially altered to Mag - Detail of the dashed rectangle area showed in A. Sample Ptr-09 photomicrographs: (D) Dunite with interstitial to net-textured sulphide. Sulphides (Po + Pn) interstitial to olivine pseudomorphs (Ol). Note euhedral chromite crystals (opaques) enclosed in Ol. (E) and (F) Detail of the dashed rectangle area showed in D. Sample Ptr-15 photomicrographs: (G) Harzburgite (Serpentinite) with fine-grained aggregate of Srp and Chl. Opaques consist of magnetite (irregular elongated crystals) and sulphides. (H) and (I) Sulphide blebs consisting mainly of Pn variably altered to Mag. Note Mag. developed along cleavage planes of Pn - Details of the dashed rectangles area showed in G.
N// = plane polarized light. NX = cross polarized light. RL = Reflected Light. Amp = amphibole, Chl = chlorite, Chr = chromite, Cpy = chalcopyrite, Mag = magnetite, Srp = serpentine, Sul = sulphide, Ol = olivine, Pn = pentlandite, Po = pyrrhotite

Source: Bravo, 2025.

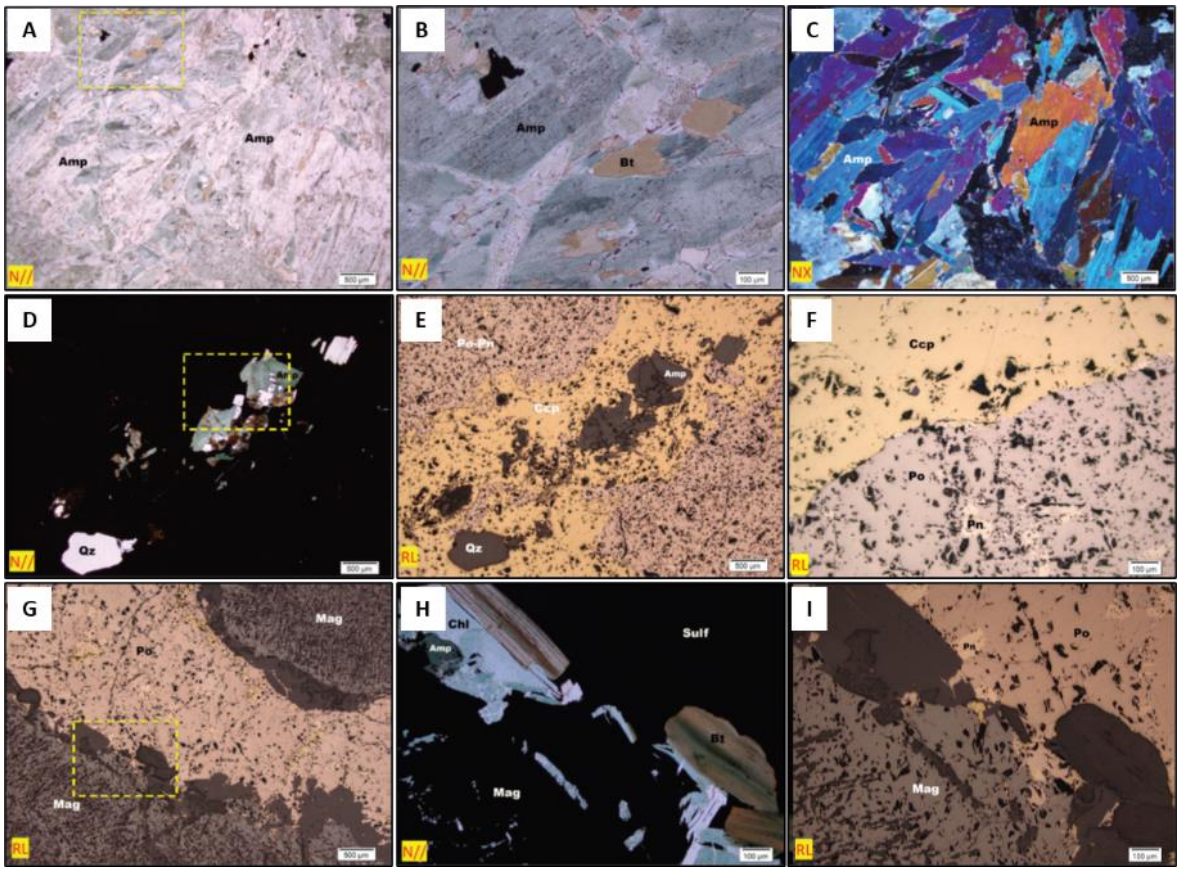

Figure 9-9: Sample Ptr-07 photomicrographs

Legend: (A) Amphibolite (orthopyroxenite/norite) consisting of randomly oriented amphibole (colorless to green pleochroism) and minor Bt (light to dark red pleochroism) and euhedral magnetite-ilmenite (opaques). (B) and (C) Detail of the dashed rectangle area showed in A. Sample Ptr-03 photomicrographs: (D) Massive sulphide zone. Cpy-rich domain with associated Amp, Qz and Bt. (E) Detail of the dashed rectangle area showed in D. (F) Massive sulphide. Cpy with Po with Pn inclusions (crystals and exsolution). Sample Ptr-47 photomicrographs: (G) Coarse-grained orthopyroxenite with Mag crystals associated with sulphides. Alteration minerals (Chl, Bt, Amp) occur at the contact of Mag and sulphides. Trellis exsolutions (Ilm) are abundant in the Mag crystals, except for the outer rim. Sulphides consist mainly of Po and Pn. (H) and (I) Detail of the dashed rectangle area showed in G.
N// = plane polarized light. NX = cross polarized light. RL = Reflected Light. Amp = amphibole, Bt = biotite, Chl = chlorite, Chr = chromite, Cpy = chalcopyrite, Mag = magnetite, Serp = serpentine, Sul = sulphide, Ol = olivine, Pn = pentlandite, Po = pyrrhotite, Qz = quartz.
Source: Bravo, 2025.

9.6 Geophysics

9.6.1 2021 Geophysics

Geophysical processing and interpretation for Luanga was performed by both SGC and Southernrock for Bravo in 2021. Southernrock reprocessed the historical IP data, while SGC reprocessed the historical magnetic data. The images below show the IP from one of the images from the Southernrock work (Figure 9-10) and IP overlaid on reprocessed magnetic image produced by SGC (Figure 9-11). Location of this work is entirely within the property boundary and shown in Figure 9-10.

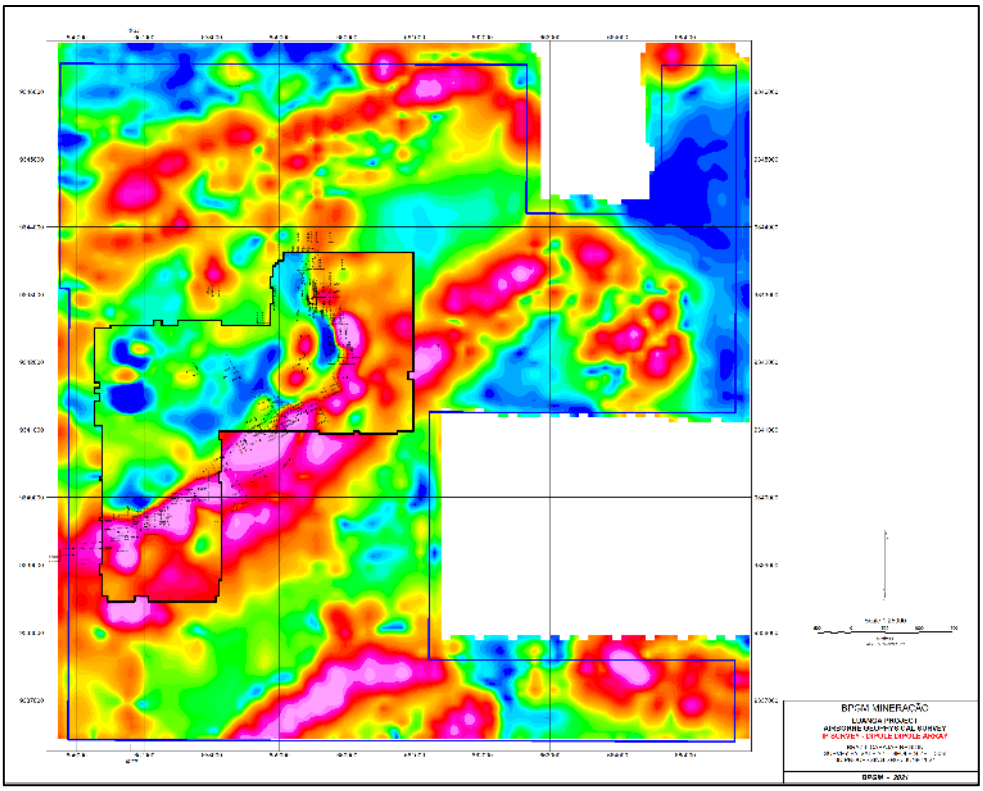

Figure 9-10: Luanga Project: IP over reprocessed magnetic imagery

Source: Bravo, 2025.

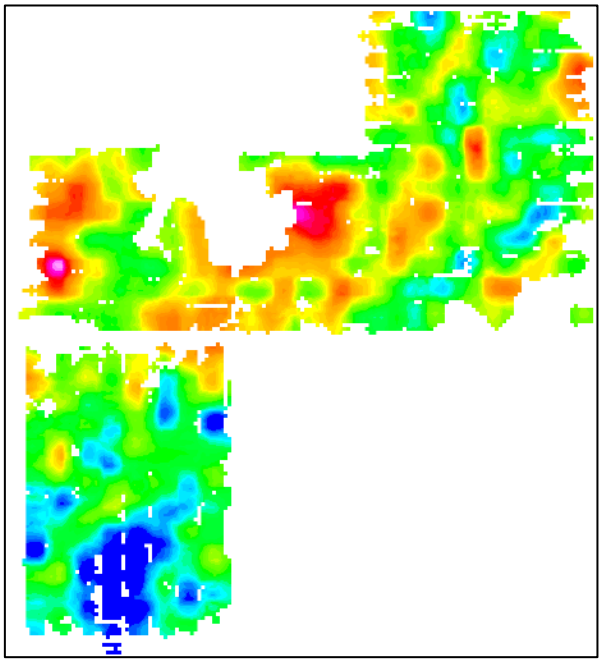

Figure 9-11: Luanga Project: 3D inversion of IP resistivity, depth -125m

Source: Bravo, 2025.

9.6.2 Borehole Electromagnetics

Ground geophysics activities conducted during 2022, and January 2023 included borehole electromagnetics and surface electromagnetic survey. Both surveys were conducted by Geomag S.A. (Geomag).

Borehole electromagnetics (BHEM) were carried out in twenty drill holes (DHH2310T001, DHH2312T001, DDH2317T001, DDH2317T002, DHH2308T001, DDH2305T001, DDH2313T001, DDH23LU224, DDH2315T001, DDH2311T001, DDH2306T001, DDH2316T002, DDH2405T011, DDH2401T001, DDH2415T002, DDH22LU047, DDH22LU052, DDH22LU068, DDH22LU073 and DDH22LU077), totaling 4,265 linear metres (Figure 9-14). The best BHEM response was related to drill hole DDH22LU047 which intersected 11 metres of massive sulphide (Figure 9-12 and Figure 9-13).

Figure 9-12: BHEM survey in DDH22LU047

Source: Bravo, 2023.

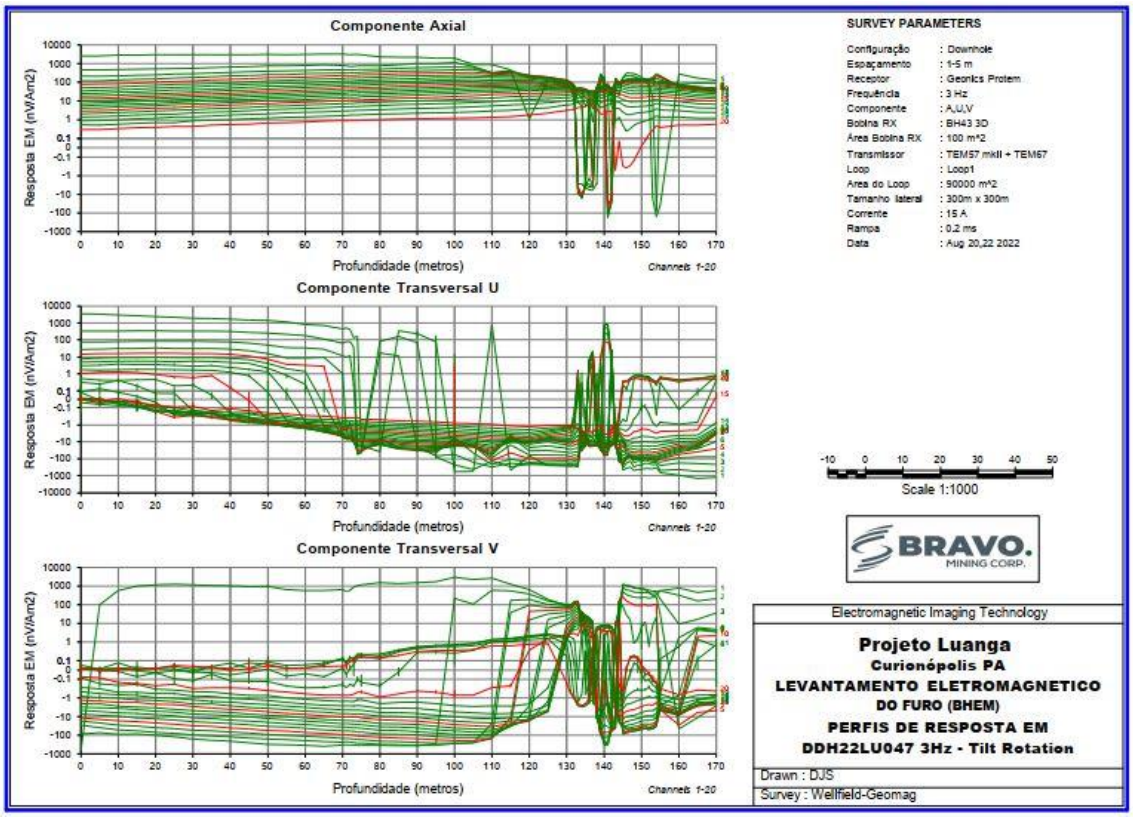

Figure 9-13: BHEM profile on drill hole DDH22LU047

Source: Bravo, 2023.

9.6.3 Fixed-Loop Transient Electromagnetics

Fixed-Loop Transient Electromagnetics (FLTEM) survey was completed on the Central and North Sectors totaling 56 transversal lines (total of 54.62 km) using established loops named as CSL01, CSL02, CSL03, CSL04, CSL05, NSL01, NSL02, NSL03, NSL04, ESL01, ESL02 and ESL03. Loop dimensions were 600 x 400 metres and survey lines were spaced 100 metres apart (Figure 9-14).

The raw data was processed, and several conductive plates have been modelled. Some of them have been tested and other are planned to be drilled.

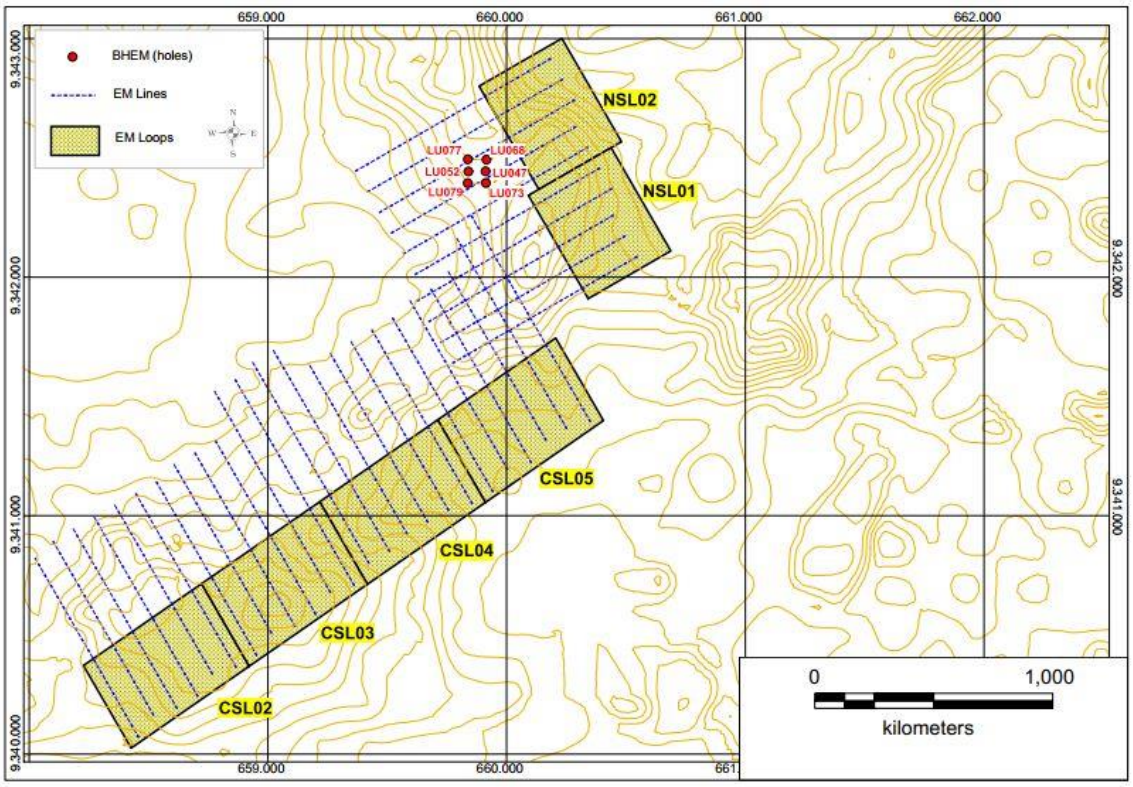

Figure 9-14: Location map of BHEM and FLTEM surveys

Source: Bravo, 2025.

9.6.4 Ground Magnetometry and Gravimetry

A ground geophysics survey consisting of magnetometry and micro-gravity, using 100 m line-spacing grid was performed over an area of approximately 18.7 km^2, covering the ultramafic and transition zones of the Luanga Complex. Ground magnetometry was performed with continuous readings along the lines and the micro-gravity survey was conducted with readings spaced 50m along the lines. The acquisition was carried out by the Bravo team during the period of 2023/2024. The raw data was delivered to SGC for quality control, corrections and processing.

Several thematic maps were produced from the ground-magnetic survey defining high-amplitude trends that partially coincide with the ultramafic rocks mapped at surface and, in some other areas, suggest the presence of other magnetite-bearing lithologies that have no clear exposures at surface.

In general, the magnetic data shows a linear anomalous feature trending SW-NE (Southwestern and Central Sectors) with a flank running S-N (North Sector) and another flank trending NW-SE on the eastern extreme of the survey grid (Figure 9-15 a and B).

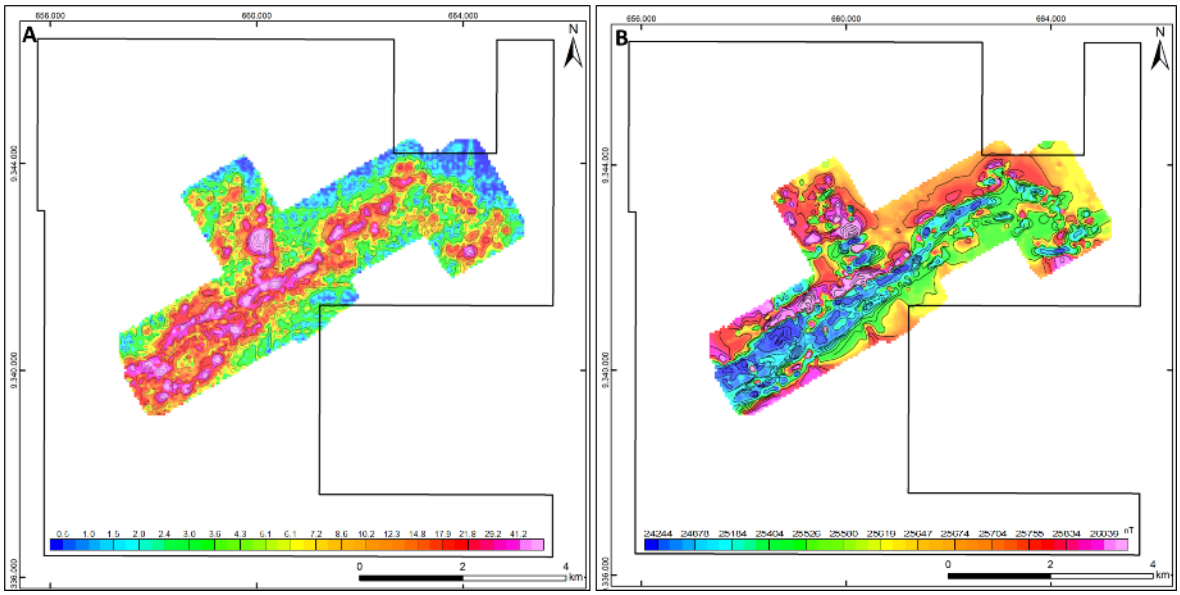

Figure 9-15: (A) Analytical signal image (B) TMI image

Source: Bravo, 2025.

The Bouguer image produced from the micro-gravity survey shows that the highest density rocks occur on the Southwestern and Central Sectors associated with the wehrlites of the so-called basal Ultramafic Zone. Its contact with the hosted metamafic plutonic rocks of the Grão Para Group became clear on the gravity data (Figure 9-16).

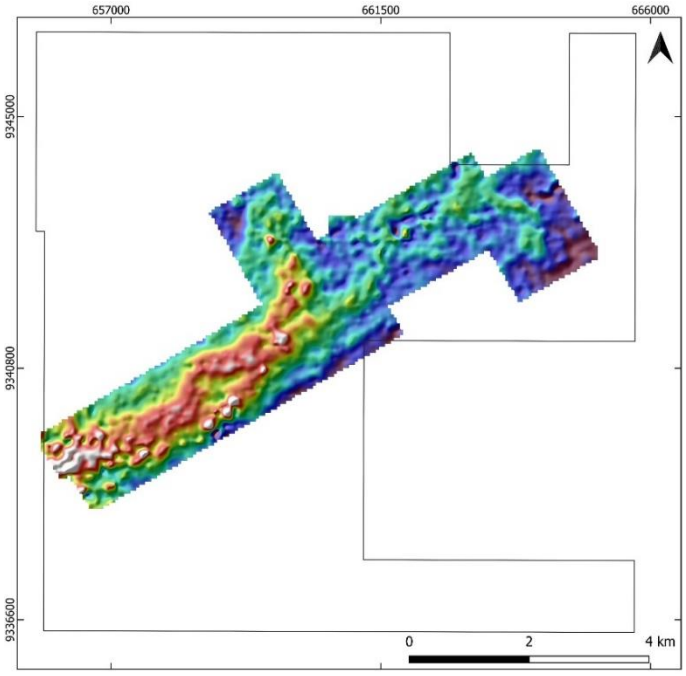

Figure 9-16: Bouguer Residual image with horizontal gradient directed to east

Source: Bravo, 2023.

9.6.5 Time Domain Electromagnetic and Magnetic Survey

Time Domain Electromagnetic and Magnetic airborne geophysical survey (HeliTEM) was carried out over an area of 99.72 km2, covering the whole Luanga mineral property. The survey

was conducted by Xcalibur Multiphysics (Xcalibur) and consisted in a total of 771.2 km of lines, being 697.1km along NW-SE transverse lines, spaced from 150m, and 70.9km along SW-NE tie lines, spaced from 1,500m (Figure 9-17).

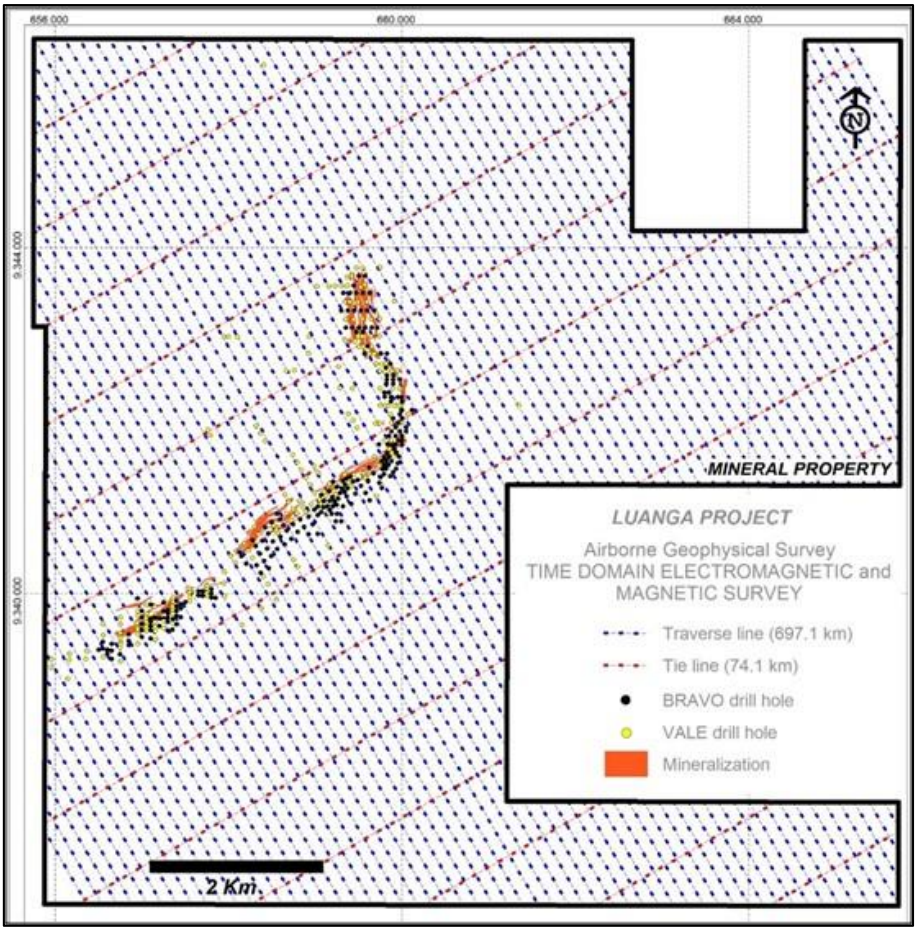

Figure 9-17: Coverage of Bravo HeliTEM survey on Luanga Project

Source: Bravo, 2025.

The configuration system used on the HeliTEM survey is summarized on Figure 9-18 and the final data was processed by Xcalibur

Descriptor	Specification / Comment
EM Transmitter	Vertical axis loop slung below helicopter
Loop area:	m²
Number of turns:	4
EM Receiver	Multicoil system (X, Y and Z)
Recording rate	samples per second of X, Y and Z component
Number of defined windows	channels
Inflight Vertical Rx-Tx separation	0.1 m
Helicopter – Loop separation	35.6 m
EM Waveform	Square pulse
Base frequency:	Hz
Pulse end:	17.2282 ms
Off-time:	16.1051 ms
Transmitter Current:	A
Dipole moment:	5.65 kA□m²

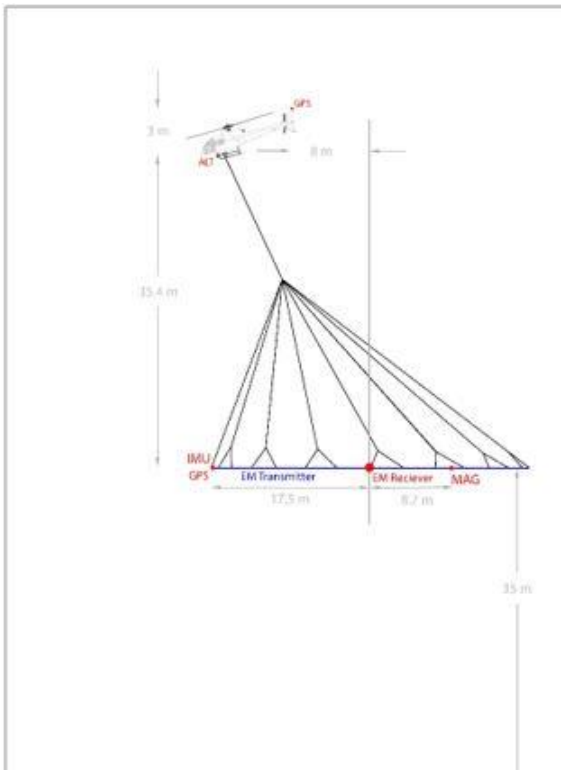

Figure 9-18: HeliTEM configuration

Source: Bravo, 2025.

Bravo engaged SGC to select and provide 3D modelling of the main conductors. As a result of this phase, 17 priority one (Priority 1) targets plus 16 priority two (Priority 2) targets were identified (Figure 9-19). These targets were ranked based on their electromagnetic (EM) response together with ground micro-gravity and magnetic surveys, detailed geological/structural interpretations, soil geochemistry data and the existing drilling database.

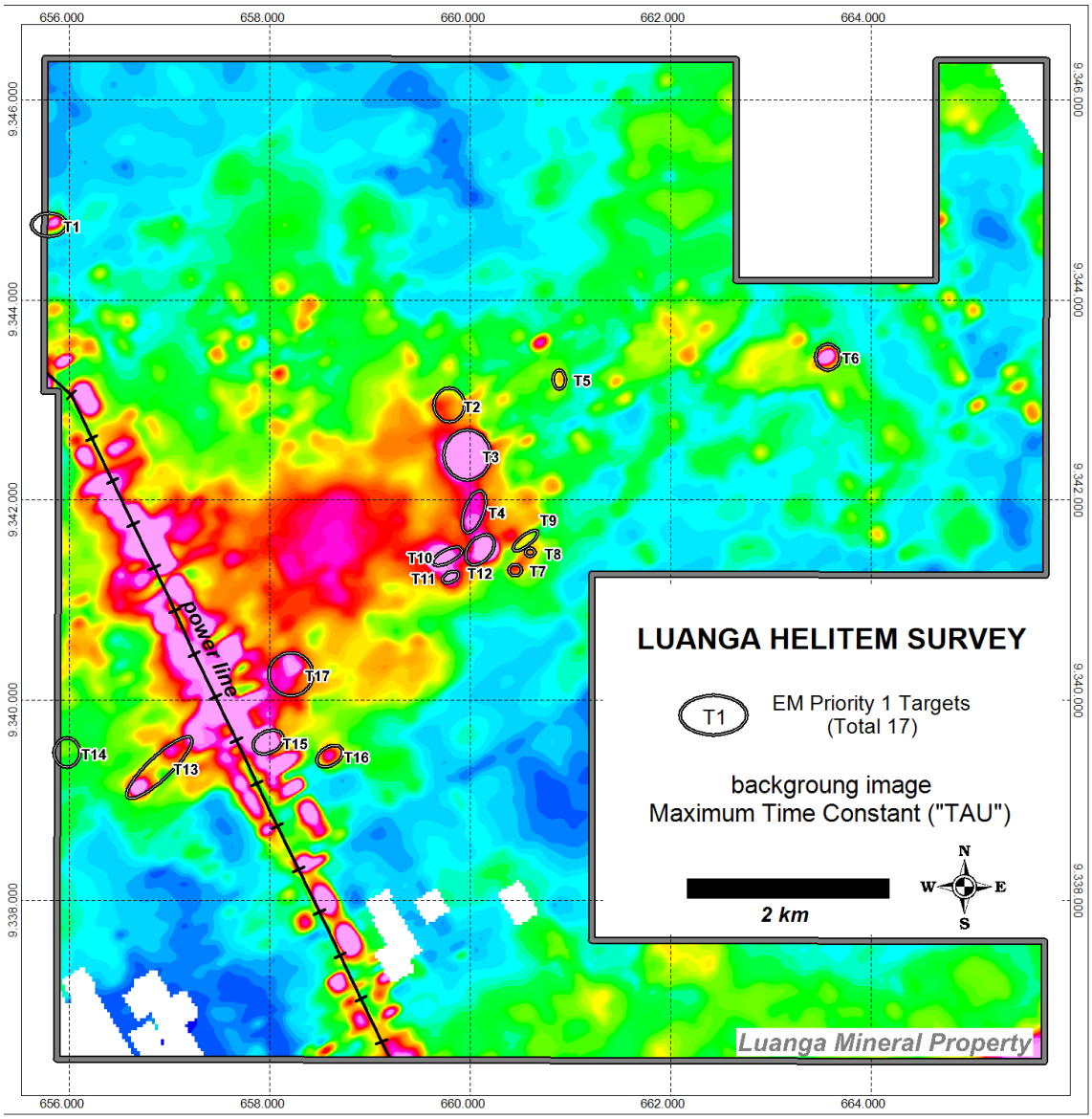

Figure 9-19: EM priority 1 targets

Source: Bravo, 2025

9.7 In Situ Density Sampling

From June 2023 to the Effective Date, Bravo's field team has collected 112 density samples in regolith material such as saprolite and soil. The first step for the sampling is the identification of the regolith horizon to be sampled and the pedological and geological description of the physical aspects of the material.

A sampling location is selected by a Geologist or Technician and the location is then cleaned, leaving a flat vertical surface exposed. A cylinder measuring 15 cm in height and 6 cm in internal diameter, is positioned perpendicularly to the vertical surface and then pressed against the matrix of the weathered material using a small metallic sledgehammer (Figure 9-20). After the cylinder is completely dug into the soil or saprolite, it is then removed, using a spatula to excavate the material above and next to the cylinder. The spatula is also used to remove excess material from the open ends of the cylinder, carefully avoiding sample material loss (Figure 9-21)

Figure 9-20: Cylinder insertion into weathered material

Source: Bravo, 2025.

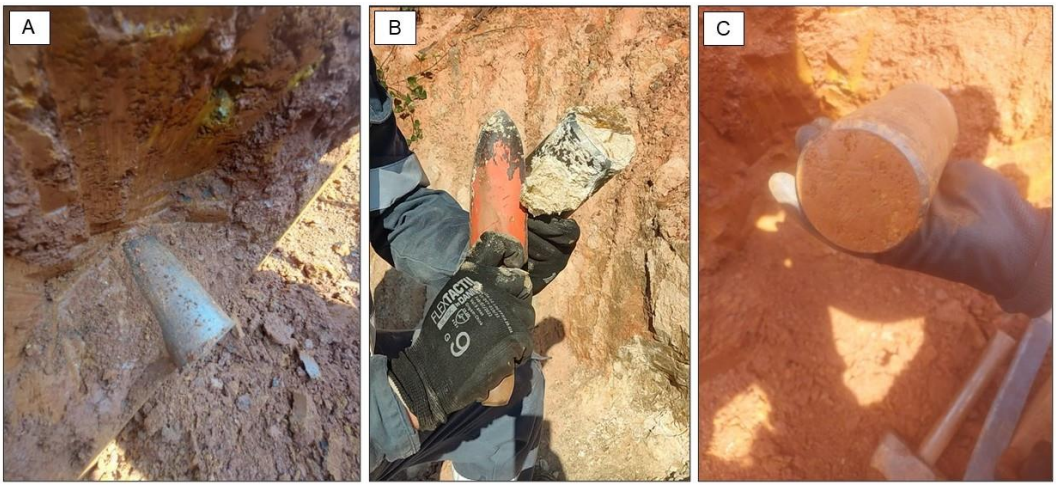

Figure 9-21: Cylinder removal

Source: Bravo, 2025.

Once the samples are collected, they are sealed in plastic bags, clearly labelled with sample identifiers (Figure 9-22). The samples are transported to the core shed, where they are weighed, dried at 105°C for 24 hours, and reweighed (Figure 9-23). Density is calculated using the formula:

$$Density\ (g/cm^3) = \frac{Dry\ Weight\ (g)}{Volume\ of\ the\ Cylinder(cm^3)}\ Volume\ of\ the\ Cylinder = 423.9cm^3$$

Moisture content is calculated using the formula:

$$Moisture\ Content\ (\%) = \frac{Wet\ Weight - Dry\ Weight}{Dry\ Weight}\ x\ 100$$

The sample location coordinates, the experimental data, and the calculated densities and humidities are all entered an Excel spreadsheet.

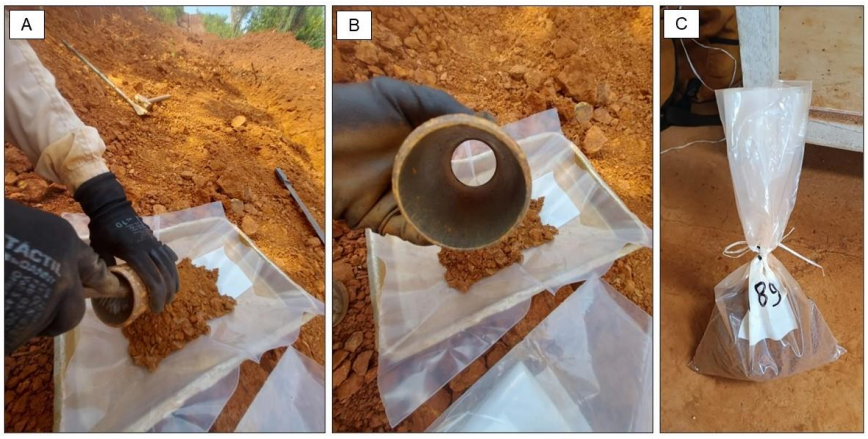

Figure 9-22: Sample material collection

Source: Bravo, 2025.

Figure 9-23: Weighing and drying procedures

Source: Bravo, 2025.

9.8 Trenching

The trenching program started in Q4/2022 aiming to provide detailed information about the mineralized zones at the surface level. Up to the Effective Date of this report, 45 trenches were opened totaling 9,065 linear meters. The location of the trenching program is shown on Figure 9-24.

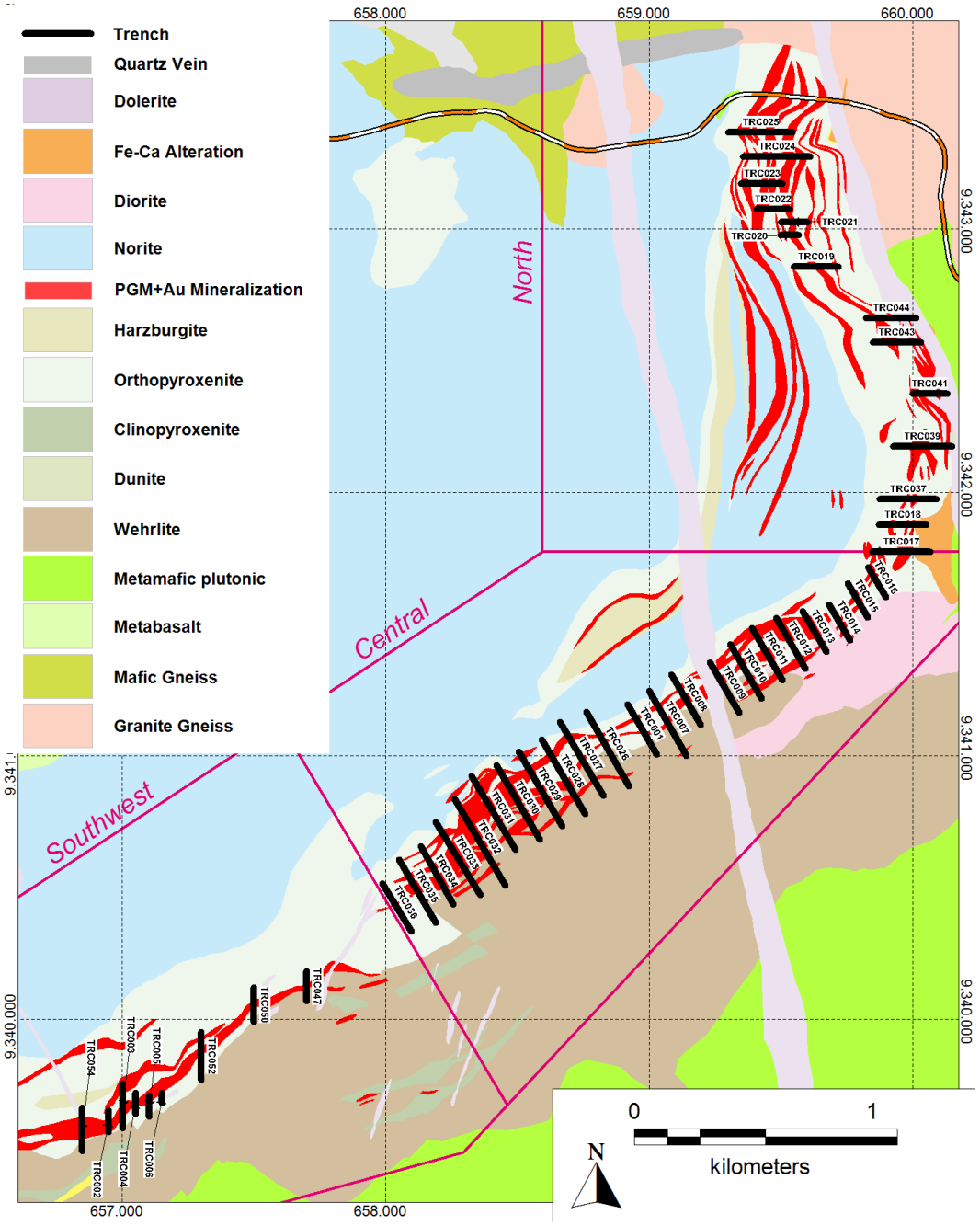

Figure 9-24: Trench opening program

Source: GE21, 2025.

The trench opening procedures adopted by Bravo are based on NBR 9604, a Brazilian regulation of trench opening and sampling procedures. Trenches are 80 cm wide (the size of the backhoe's rear shell) and have a maximum height of 120 cm (Figure 9-25). All opened trenches were geologically described, mapped, sampled, and their channel samples were precisely surveyed with RTK GNSS. Geologic description is logged on site into Micromine 'GeoBank For Field Teams', an application that is linked to the main Project Database.

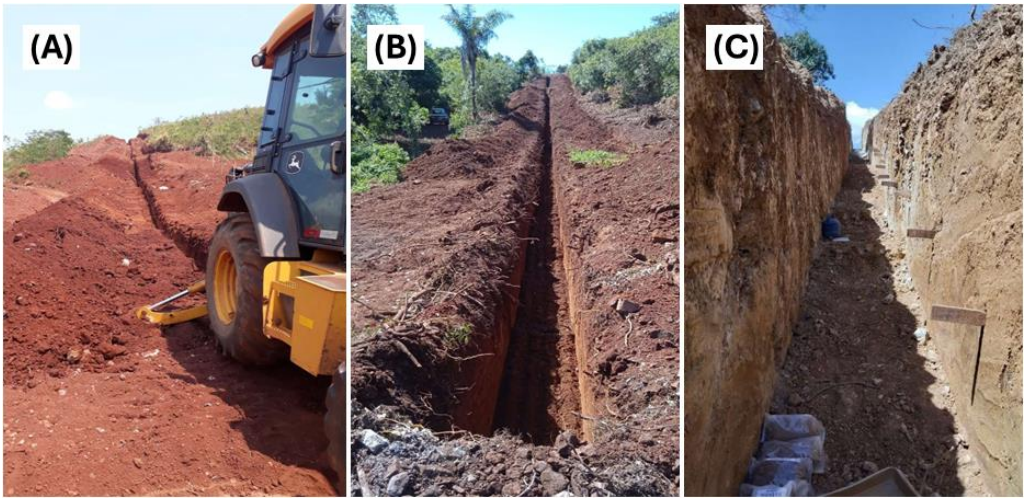

Figure 9-25: Trench opening and channel sample marking

Source: Bravo, 2025.

Sampling takes place using a 1 m standard sample size, varying from 0.7 m to 1.2 m where geological contacts must be respected. In general, the opening of the sampling channel is 40 to 50 cm away from the trench floor, aiming to sample the saprolite and avoid sampling soil. Sample collection is performed using chisels and sledgehammers to disintegrate the material and collect it on an aluminum tray, placed under the channel. A total of 9,521 channel samples, including QA/QC samples, were collected and analyzed for 3PGM and Au at independent laboratories.

After the work was completed, all trenches were closed.

Figure 9-26 illustrates the cross section with a shallow mineralized zone of 175.7m @ 1.71 g/t PGM + Au identified in the Trench TRC23LU024.

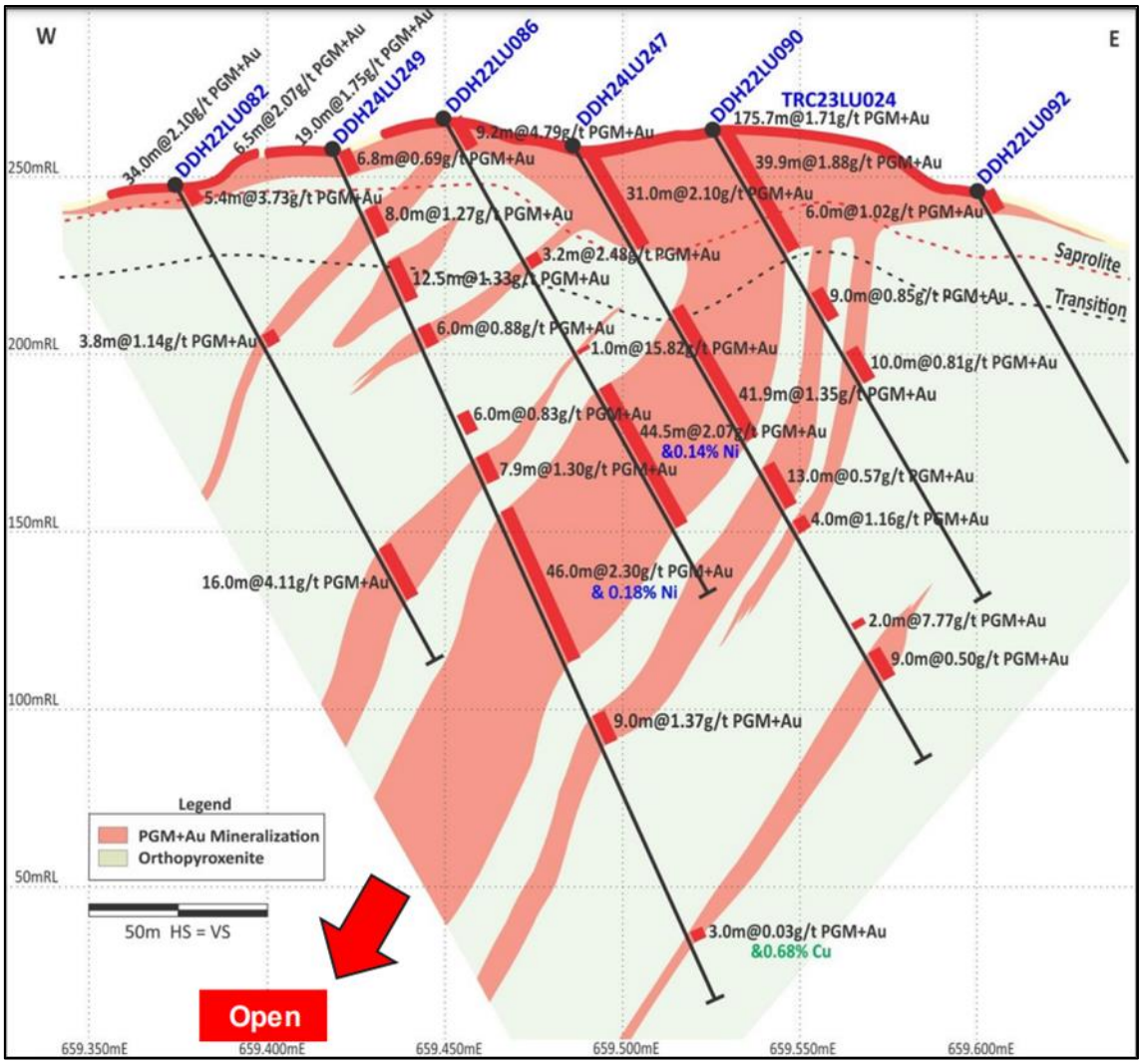

Figure 9-26: Section Bravo DDH22LU014 with trench TRC22LU003

Source: Bravo, 2025.

10 DRILLING

10.1 Introduction

Approximately 123,610 m in 601 drill holes have been drilled on the Property since 1992. Of these, 256 (50,787 m) are diamond drill holes (DDH) executed by DOCEGEO (Vale) and include Luanga's North, Central, and Southwest geological targets. Bravo's drilling corresponds to 72,823 m and 345 holes, representing 59% of the project's drilled length.

Details of the various drilling programs are summarized in Table 10-1, drill hole locations are shown in Figure 10-1. Table 10-1 also includes drilling executed in the *exploration targets*, presented in Section 9 of this Report.

The drilling by Vale in 1992 was for early-stage exploration while the drilling between 2001 and 2003 was for exploration-focused programs and for initial resource estimates. Holes were drilled using HQ, NQ, BQ and ZWF diameters.

Drilling by Bravo started in March 2022, and has continued since then and the program was designed primarily for infill drilling, step-out and resource definition at Luanga. Bravo also performed 8 drill holes with geometallurgical purposes. In 2023/2024, Bravo´s drilling program also included some exploration drill holes over several geophysical targets located outside the Luanga PGM + Au + Ni deposit. The whole diamond drilling program carried out by Bravo was performed using a mixture of HQ and NQ2 diameters. The drill holes that were included in the Mineral Resource estimate are discussed in Section 14 of this report.

Table 10-1: Drilling summary for Luanga

Year	Drill Type	Drill Holes	Total Metres	Company	Contractor
1992	DD	4	643.69	DOCEGEO	DOCEGEO
2001	DD	86	14,584.35		Geosol
2002	DD	71	15,423.25		Geosol
2003	DD	95	20,135.45		Geosol / Rede
2022	DD	135	23,258.20	Bravo	Servdrill
2023	DD	116	30,296.60		Servdrill
2024	DD	94	19,268.65		Servdrill
TOTAL		**601**	**123,610.19**		

Source: Bravo, 2025.

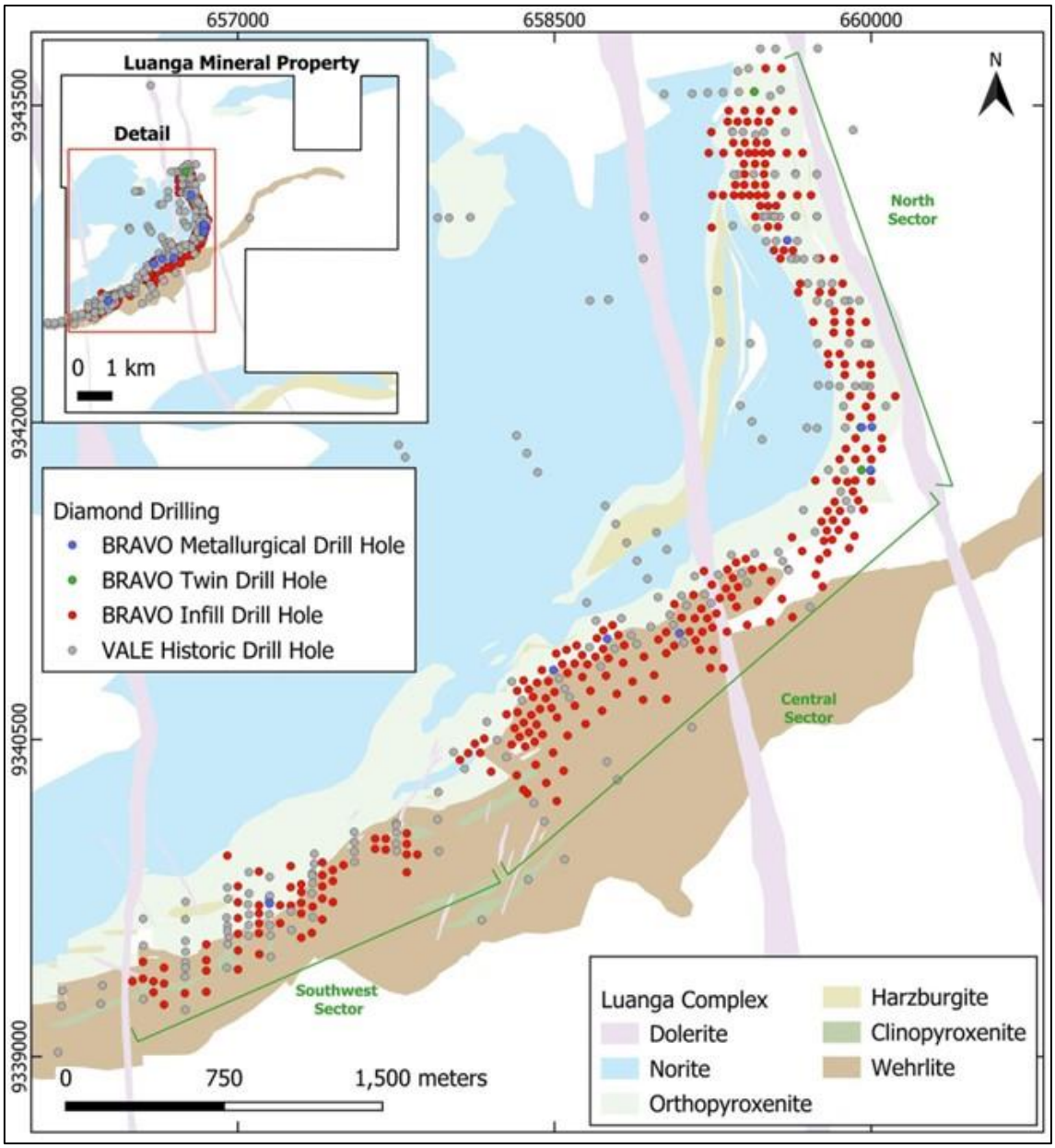

Figure 10-1: Drill hole locations at Luanga

Source: Bravo, 2025.

10.2 DOCEGEO Drilling

The drilling conducted under DOCEGEO administration consists of 256 diamond drill holes (50,787 linear metres) at Luanga between 1992 to 2003 (Table 10-2). Most of the Diamond Drilling occurred between 2001 and 2003 over two main targets, Luanga and Luanga South. At Luanga, 232 diamond drill holes (45,600 linear metres) were completed, representing approximately 90% of the entire DOCEGEO drilling program. At Luanga South, 24 drill holes (5,187 linear metres) were completed.

Most of the Diamond Drilling was carried out by two Brazilian Diamond Drilling companies Geologia e Sondagem S.A. (Geosol) and Engenharia e Sondagem Ltda (Rede). DOCEGEO was responsible for the first four drill holes at the Project.

Table 10-2: Historical drilling summary

Year	Drill Type	Drill Holes	Total Metres	Contractor	Target
1992	DD	4	643.69	DOCEGEO	Luanga
2001	DD	86	14,584.35	Geosol	Luanga
2002	DD	71	15,423.25	Geosol	Luanga
2003	DD	67	14,535.15	Geosol - Rede	Luanga
		4	413.15		Luanga (Met)
		24	5,187.15		Luanga South
TOTAL		256	50,786.74		

Source: Bravo, 2025.

Most of the diamond drill holes (248 holes) were drilled with inclinations varying from -55.0º to -70.0º, with the predominant inclination at -60.0º (Figure 10-2). Only four diamond drill holes were drilled vertically or close to vertical (-90.0º to -80.0º).

Figure 10-2: Drilling under DOCEGEO administration at Luanga Project, angled drill hole

Source: Vale.

The maximum drill hole length in historical drilling was 497.6m and the average hole length was 198.4 metres. The Diamond Drilling (DD) holes were drilled with a HQ (96.40mm) diameter in the weathered zone, changing to NQ (76.20mm) diameter in the fresh rock. There is no information about the drilling recovery in the historical database. However, from visual inspection of available core from these programs, recoveries appear to have been excellent.

The near surface portion of Luanga has been oxidized to depths of a few meters to a few tens of metres and is underlain by a thin transition zone before fresh sulphide mineralization is encountered. PGMs and Au are potentially recoverable from both oxide and sulphide mineralization, based on comparable deposits, whereas Ni would typically only be recovered from sulphide mineralization, in which sulphide minerals are present.

The location of the drill holes carried out by DOCEGEO at Luanga and Luanga South targets are illustrated on Figure 10-3 and Figure 10-4, respectively.

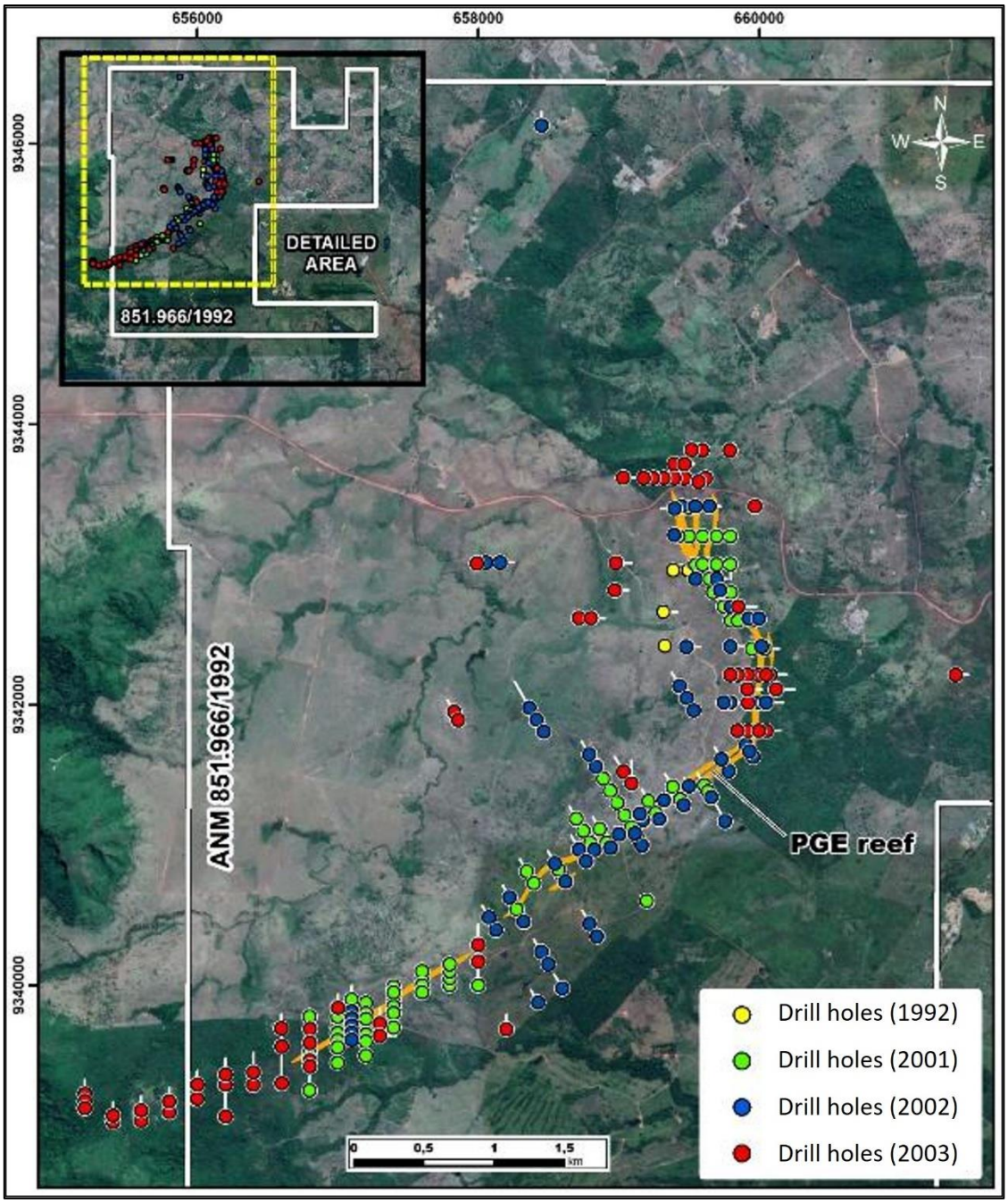

Figure 10-3: DOCEGEO drill hole location map for Luanga target, Luanga Project

Source: GE21, 2025.

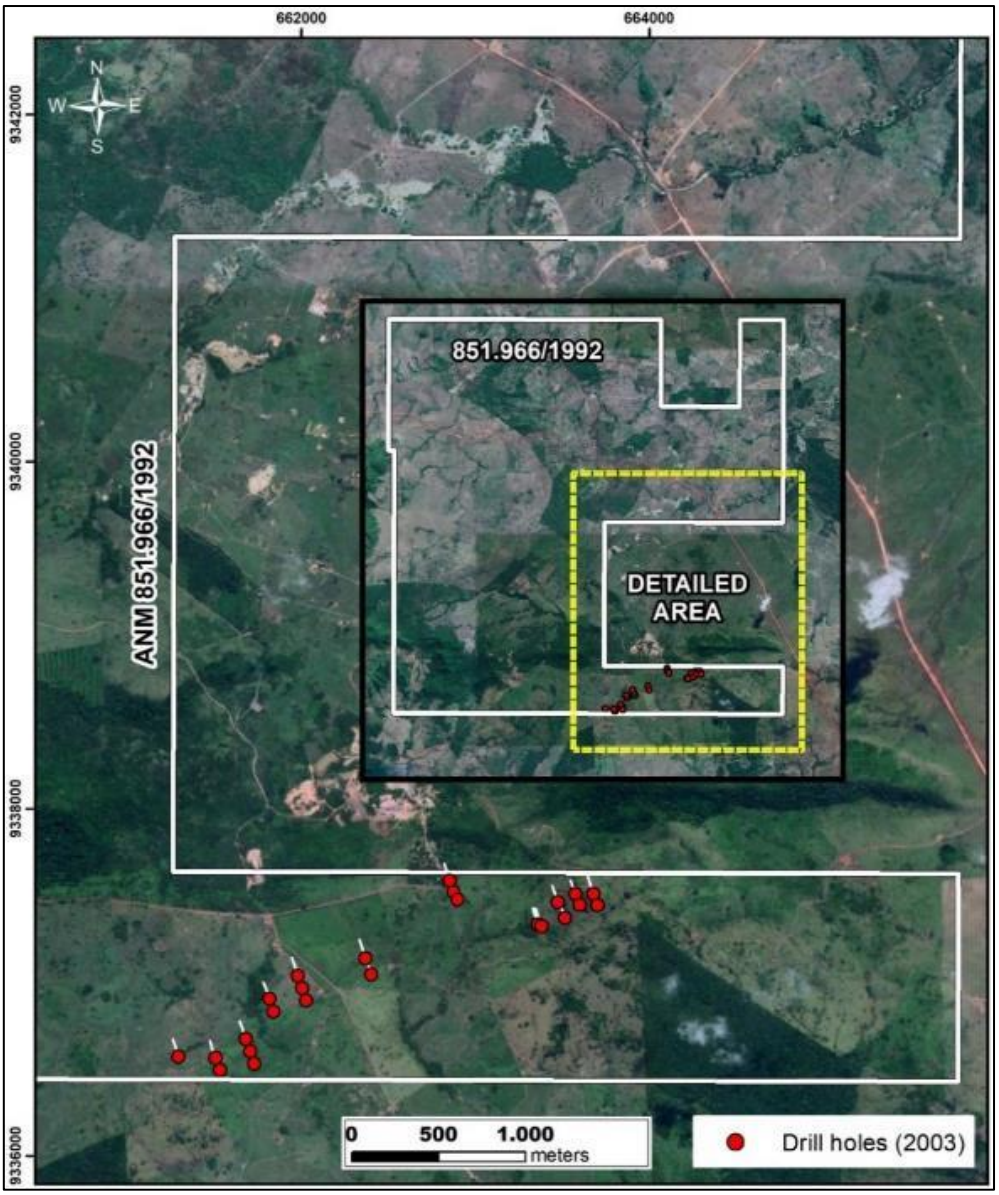

Figure 10-4: DOCEGEO drill hole location map for Luanga south target, Luanga Project

Source: GE21, 2025.

10.2.1 DOCEGEO Drill Collar Survey

The drill holes collars were sited based on the Instituto Brasileiro de Geografia e Estatística (IBGE) base datum. All the drill holes collars were surveyed at the end of each drilling campaign, using Total Station TOPCOM GTS 229 equipment with the final location entered into the drilling database. The survey Datum used for the Luanga Project was SAD69.

All the drill holes collars were capped with cement blocks, including a PVC tube and aluminium plates, including drill hole number. Information related to hole ID, coordinates, elevation, dip, azimuth and final depth data are included on the collar plugs on the aluminium plates.

Bravo re-located the majority of Docegeo's drill holes, using the Datum SIRGAS 2000. The collars that were not found on the area, their original coordinates were converted from SAD69 to SIRGAS 2000.

10.2.2 Downhole Survey

Downhole deviation surveys were carried out along the length of 240 diamond drill holes with readings collected at 3 metres intervals. The downhole survey covered approximately 95% of the total drill hole population.

10.3 Bravo Drilling Program

Bravo has been carrying out its Diamond Drilling program using equipment from third-party company Servdrill Perfuração e Sondagem (Servdrill), reaching 6 drill rigs at the same time. Drill inspection is carried out by Bravo's own employees (Figure 10-5).

To the Effective Date, 345 drill holes have been completed within the Luanga PGM + Au + Ni deposit area and, also outside as part of the regional exploration over other targets. In total, 72,823.45 metres of diamond drilling have been completed by Bravo (Table 10-3 and Figure 10-6). Of these, 299 drill holes (63,364.1m) were drilled with the objective to intercept the Luanga PGM + Au + Ni mineralized system and this program included 8 twin holes and 8 geometallurgical drill holes. In general drill holes intercepted the same lithologies and the 2 styles of mineralization previously described by DOCEGEO on its drilling program. However, other four (4) different styles of mineralization were identified by Bravo and some lithological units were renamed based on petrographic studies, as described in detail on Section 7 of this report.

Geometallurgical drill holes (total of 8 and 882,15m) were drilled for the purpose of obtaining volumetric samples for metallurgical tests and did not follow the systematic assaying routine used in the drilling program. Consequently, these drill holes were not used in the Mineral Resource estimate.

A part of the drilling program on Luanga PGM + Au + Ni deposit, Bravo also carried out 46 drill holes (9,459,35 metres) over 14 geophysical targets defined by the HeliTEM survey. Some of these holes are in the proximity of the Luanga PGM + Au + Ni deposit and other are located far away from the PGM + Au + Ni deposit.

Table 10-3: Diamond drilling quantitative

Year	Drill Type	Drill Holes	Total Metres	Company	Contractor	Phase
2022	DD	119	21,241.55	Bravo	Servdrill	Luanga new holes
		8	1,134.50			Luanga twin holes
		8	882.15			Luanga met. holes
2023	DD	103	27,878.50		Servdrill	Luanga new holes
		13	2,418.10			Regional targets
2024	DD	61	12,227.40		Servdrill	Luanga new holes
		33	7,041.25			Regional targets
TOTAL		**345**	**72,823.45**			

Source: Bravo, 2025.

Figure 10-5: Drill rig in operation

Source: Bravo, 2025.

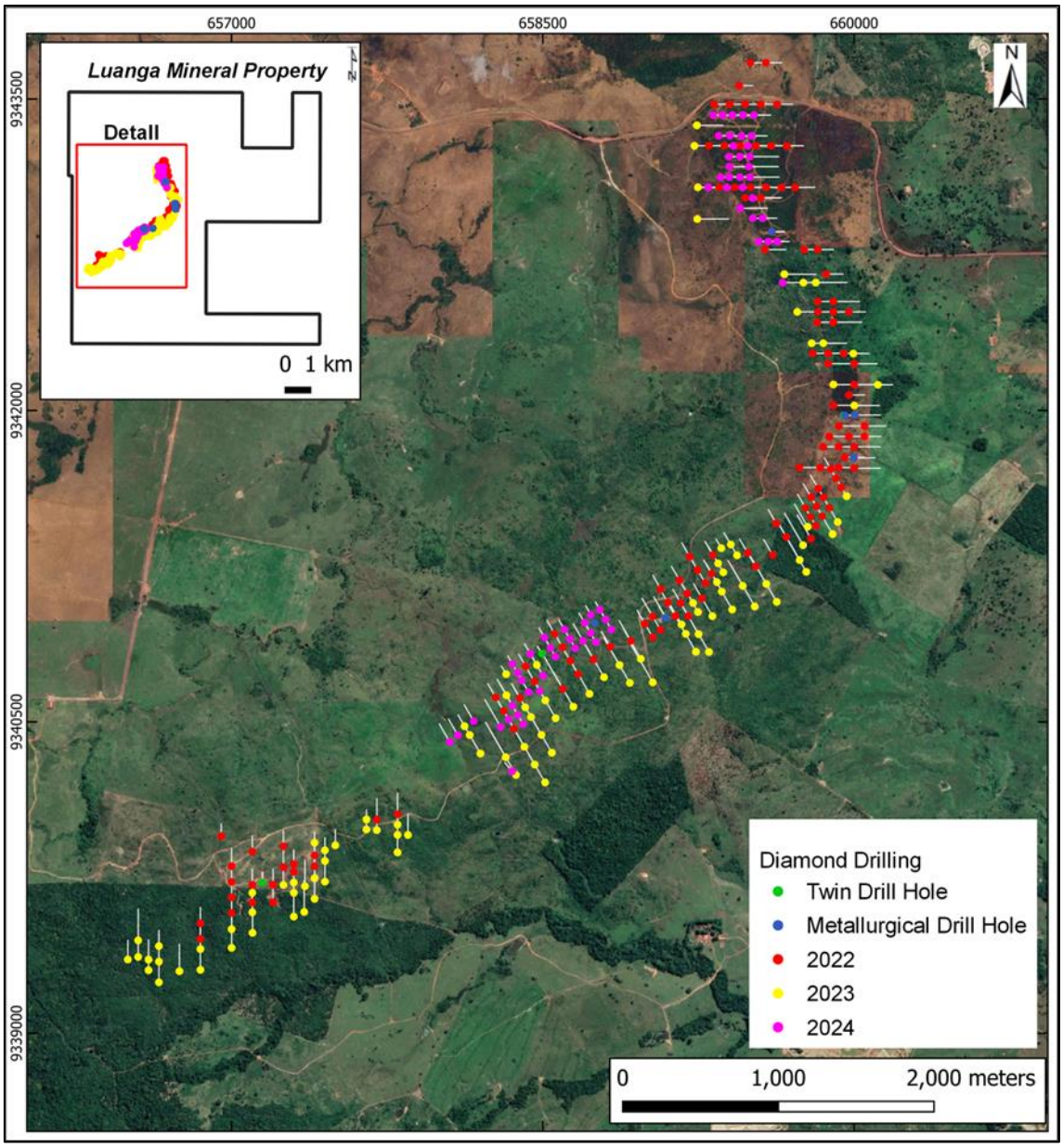

Figure 10-6: Bravo drill hole location map for Luanga target, Luanga Project

Source: Bravo, 2025.

The shallowest drill hole drilled by Bravo was 76.55m and the deepest hole was 625.35m, with an average depth of 214m. Drilling used a HQ sized diamond core from surface, until reaching competent fresh rock, from where drilling changed to NQ2 sized diamond core. Core recoveries are generally excellent, with averages of >98% in the fresh rock and 94% for oxidized rocks. Mineralization is finely and evenly disseminated, thus it is believed that there will be no nugget effects or issues affecting accuracy and reliability, as was the case in the historical core.

In the Southwest Sector of Luanga, drill holes were drilled in a northerly direction, with a dip of 60º. In the Central Sector, drill holes were drilled at azimuth 330º, except for drill hole DDH24LU291, (drilled at an azimuth of 320º) and DDH2309T001, DDH2317T002, DDH2417T003 which were drilled at azimuth 150°, with a dip of 70°, 60° and 50°, respectively. It is worth noting

that drill holes DDH2309T001, DDH2317T002, DDH2417T003 were drilled for a regional exploration purpose and not planned to evaluate the Luanga magmatic mineralization.

The standard dip in the Central Sector was 60º, except for drill holes DDH22LU110, DDH22LU112 and DDH23LU174 which were drilled with a dip of 70º, while drill holes DDH23LU171 and DDH23LU211 were drilled at dips of 50º and 65º, respectively.

In the North Sector, drill holes were drilled at azimuth 090°, with a dip of 60º, except drill holes DDH24LU249 which was drilled with dip -65°.

10.3.1 Bravo Drill Collar Survey

All drilling holes collars are geolocated with GPS with geodetic accuracy, being initially outsourced through the company RR Topo and, subsequently, done by Bravo's own team. The survey Datum used for the Luanga Project was SIRGAS 2000.

All the drill holes collars were capped with cement blocks, including a PVC tube and aluminium plates, showing drill hole identification codes (hole ID). Information related to the drill hole, such as coordinates, elevation, dip, azimuth and final depth data are included on the collar marks in aluminium plates.

10.3.2 Bravo Downhole Survey

Once the drill hole is finished, deviation surveys are conducted for all holes by the drilling company itself using REFLEX GYRO SPRINT-IQ device. In addition, runs are guided whenever possible with Reflex ACT3 device (Figure 10-7).

Figure 10-7: REFLEX GYRO SPRINT-IQ device used for guided run

Source: Bravo, 2023.

10.3.3 Core Transport

At the end of each drilling shift, the wooden boxes containing the drill cores are taken to the drilling shed by the outsourced drilling company or by Bravo employees. The boxes are always transported securely tied and covered (Figure 10-8).

Figure 10-8: Safe transport of drill core boxes

Source: Bravo, 2023.

10.3.4 Core Loging

In the core shed (Figure 10-9), the boxes are placed on racks for checking the depth, advance and recovery information, in addition to meter-by-meter marking. Then, magnetic susceptibility measurements are taken with the KT-20 S/C device. Marking of the oriented intervals is carried out to then proceed with the taking of structural measurements using the IQ Logger device (Figure 10-10).

Figure 10-9: Core shed at Luanga Project

Source: Bravo, 2023.

Figure 10-10: Marking of the oriented intervals

Legend: (A) Checking the core boxes and (B) taking structural measurements with IQ Logger.
Source: Bravo, 2023.

A geotechnical description of the holes is completed, focusing on obtaining the RQD measurement, which consists of adding the length of all core fragments greater than 10cm, within the same run, dividing this sum by the length of the run. Information about the strength and weathering of the rocks is also collected.

In the geological description, the following information is collected: granulation, texture, colour, mineralogy, magnetism, geological contacts, lithology, geological structures (fractures, faults, veins and crenulations), among others. Magnetic susceptibility and conductivity are measured in the core at each 0.5 m with a handheld KT-20 S/C magnetic susceptibility/conductivity meter.

After the geological description, a sampling plan is drawn up (discussed in detail in Section 11). Then the numbering of the samples is marked on the boxes. A marking is also made to guide the sawing of the core into two equal halves (Figure 10-11). Photographs are taken of all core boxes, which are then sawed and sampled.

Figure 10-11: Core logging

Legend: A) Drill cores with core orientation markings and B) Core Photography Table.
Source: Bravo, 2023.

Given the orientation of the holes and the mineralization, the intercepts are estimated to range from approximately 130 to 100% of true thickness.

Drilling completed by Bravo is shown Figure 10-12. Figure 10-13 to Figure 10-15 exemplify cross sections with mineralized intersections in the North, Central and Southwest sectors of Luanga, respectively.

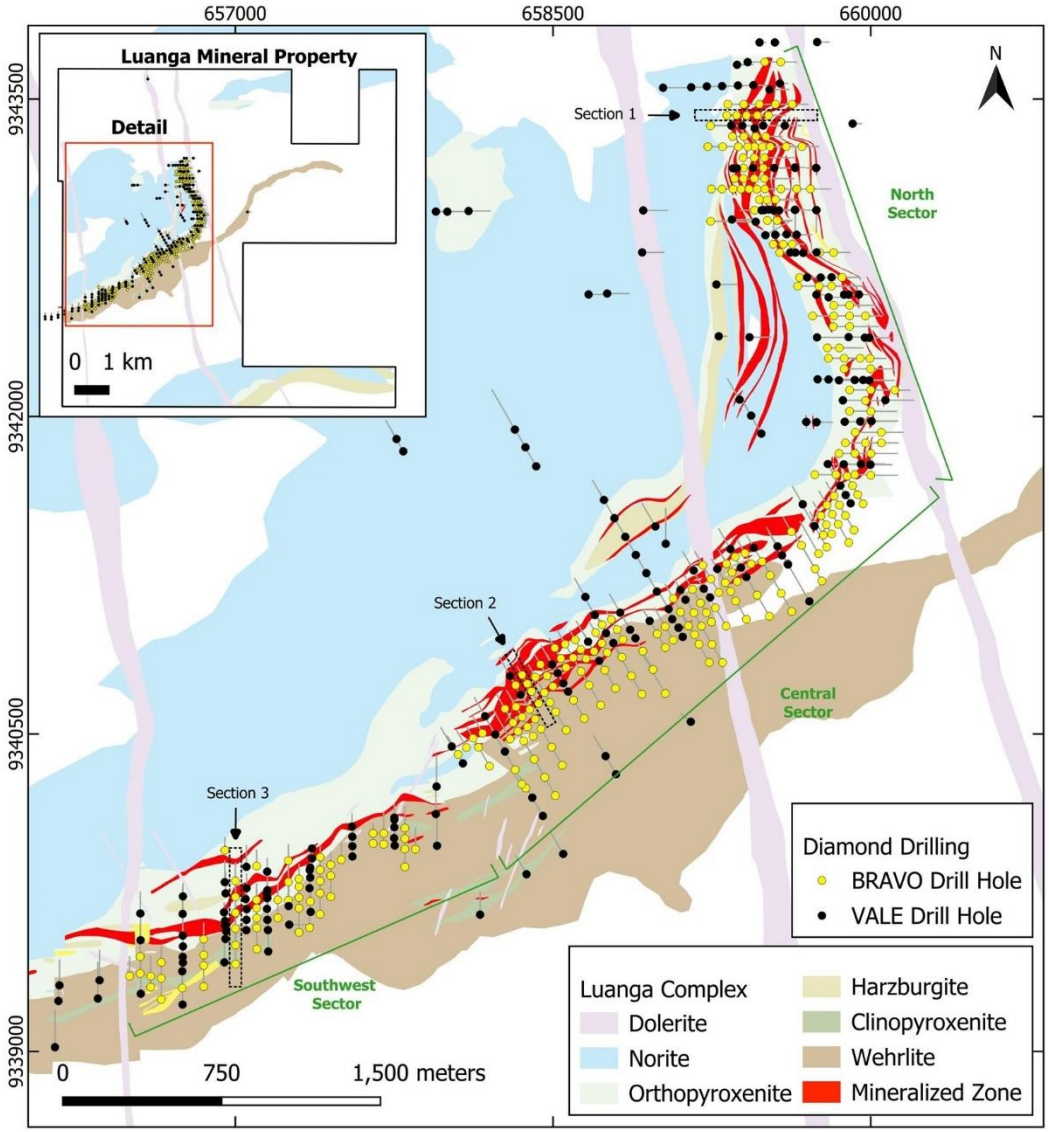

Figure 10-12: Diamond drill holes (DOCEGEO/Vale + Bravo) within the Luanga Mafic-Ultramafic

Legend: Complex, showing location of the drill sections presented on this Section.
Source: GE21, 2025.

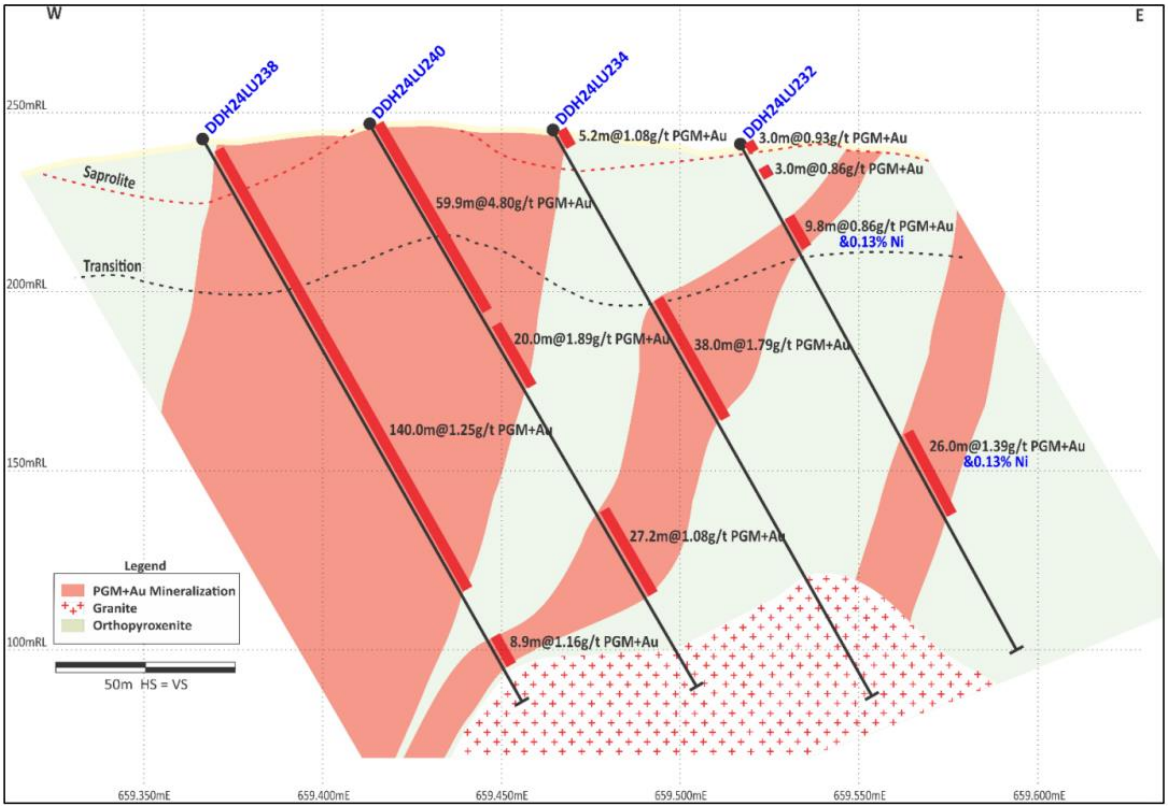

Figure 10-13: Cross section 1 – North Sector

Legend: Multiple stacked mineralization zones (open at depth). Refer to Figure 10-12 for location.
Source: Bravo, 2025.

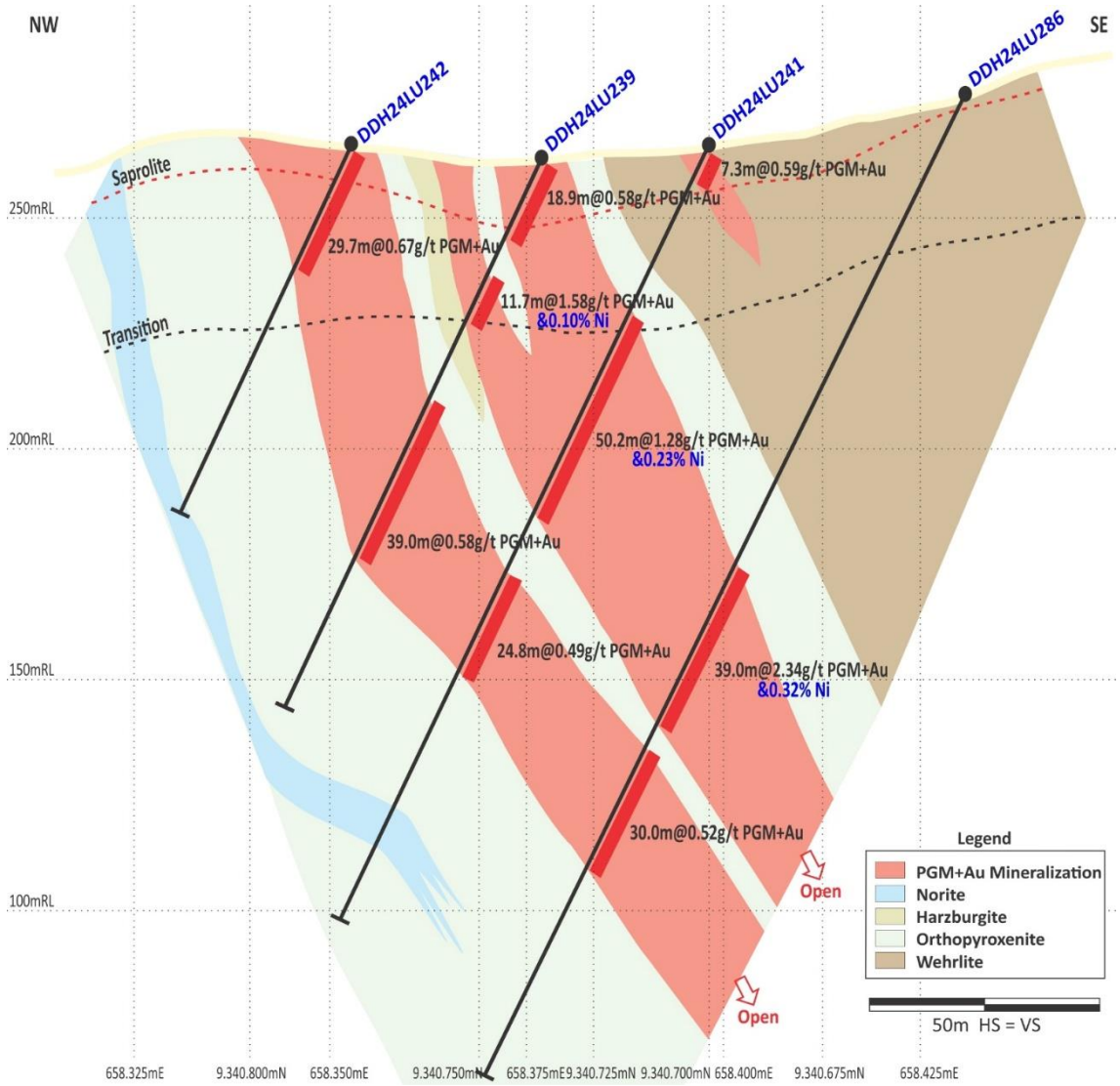

Figure 10-14: Cross section 2 (Central Sector) – Increasing nickel grade to the SE (open at depth)

Legend: refer to Figure 10-12 for location.
Source: Bravo, 2025.

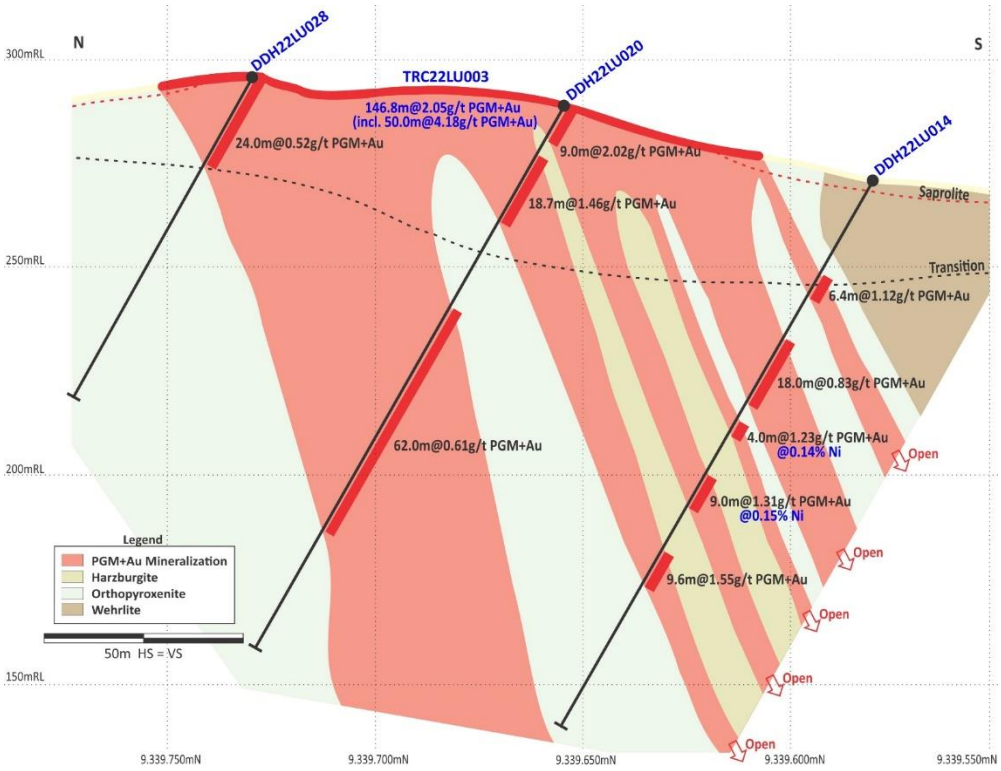

Figure 10-15: Cross section 3 (Southwest Sector) – Multiple mineralization zones (open at depth)

Legend: refer to Figure 10-12 for location.
Source: Bravo, 2023.

10.4 Twin Holes

A twin hole program was designed to validate the historical drilling (Table 10-5). The objective was to support the insertion of historical drilling into Bravo's database with the same degree of quality and confidence in the geological, geochemical, and sample information. This program includes the drilling of 8 "twin holes" against historical drilling, following the coordinates surveyed in the field in SIRGAS 2000 format.

Table 10-5: Selection of results from Bravo twin hole drilling

HOLE-ID	From (m)	To (m)	Thickness (m)	Pd (g/t)	Pt (g/t)	Rh (g/t)	Au (g/t)	DOCEGEO PGM + Au (g/t)	Bravo PGM + Au (g/t)
TWIN of Historical Hole PPT-LUAN-FD0136									
DDH22LU043	0.00	16.70	16.70	15.92	16.51	3.63	0.05		36.12
PPT-LUAN-FD0136	*0.00*	*17.00*	*17.00*	*17.36*	*18.36*	*2.94*	*0.17*	*38.73*	
DDH22LU043	34.90	86.50	51.60	0.84	0.56	0.08	0.12		1.60
PPT-LUAN-FD0136	*24.00*	*78.00*	*54.00*	*0.46*	*0.36*	*0.11*	*0.07*	*0.93*	
TWIN of Historical Hole PPT-LUAN-FD0095									
DDH22LU083	0.00	93.00	93.00	1.80	1.15	0.20	0.02		3.17
PPT-LUAN-FD0095	*0.00*	*93.00*	*93.00*	*1.60*	*1.01*	*0.10*	*0.01*	*2.71*	
TWIN of Historical Hole PPT-LUAN-FD0145									
DDH22LU006	0.00	37.22	37.22	1.93	0.83	0.13	0.26		3.15
PPT-LUAN-FD0145	*0.00*	*40.00*	*40.00*					*2.92*	

Notes:
1. All ‘From’, ‘To’ depths, and ‘Thicknesses’ are downhole.
2. Intercepts are estimated to be 75% to 85% of true thickness.
3. NA: Not Applicable as intercept is oxide, or a mix of oxide and fresh rock mineralization.

Source: GE21, 2025.

11 SAMPLE PREPARATION, ANALYSES AND SECURITY

The procedures carried out by Bravo's sampling program since 2022 are summarized below.

11.1 Sample Security and Chain of Custody

The Company's QA/QC Policy outlines the key procedures implemented by Company personnel to ensure the reliability of exploration data and laboratory analytical results. These measures also maintain an accurate and secure database for the Company's exploration and development projects.

Core boxes and RC sample bags containing samples for analysis are transported from the drill site to the Company's core shed in a manner approved by the Qualified Person (QP). Each delivery is accompanied by a Chain of Custody Form, which includes the names and signatures of transferring parties, the date and time of transfer, the drill hole number and sample interval, and the box sequence with the total number of boxes and bags transferred. Upon arrival at the core logging facility, the samples received are verified against the Chain of Custody Form, and any discrepancies are reported to the QP.

The core shed and office area, where the database and records for exploration and development projects are stored, are restricted to authorized Company personnel and individuals specifically approved by the QP. These areas remain locked when not in use. Staff handling core samples must remove or tape off hand jewelry to prevent contamination or loss of sample integrity. Visitors are not permitted to handle core unless supervised by Company personnel.

Drill cores are laid out in sequential order and cleaned before geological logging and sample selection, which is conducted by authorized project geologists. Once samples are selected for sawing or splitting, a guideline is drawn on the core to ensure mineralization is equally split between halves. If required, one half may be further split into quarters. Technicians, under the supervision of the Core Logging Supervisor, saw or split the core along these guidelines. All portions of the split core are returned to the core box in their original order and orientation.

After logging and sample selection, the core is marked, and sample numbers are stapled to the core boxes. Photographs are taken to ensure that core blocks, including length and sample numbers, are clearly visible. The portion of the core selected for analysis, typically half and always the right-side piece, is placed into pre-labeled and tagged sample bags following QP-approved procedures. Sample bags are secured with zip ties and then placed into larger bags sealed with tamperproof safety seals. These samples are sent to the assay laboratory along with assaying instructions. The Chain of Custody Form and lab submittal documents instruct the recipient to notify the sender immediately if any tamperproof seals are broken or compromised.

The remaining half of the core sample is retained in the original core box and stored in a secure location, with its location recorded. No core samples may be removed for re-assaying,

metallurgical testing, or any other purpose that could lead to sample destruction without prior approval from the QP. If a sample is removed following QP approval, a record is inserted in the core box at the sample's original location, detailing the sample length and interval removed, the purpose of removal, the name of the responsible individual, and the date of removal. A digital record with the same details is maintained in the database.

These measures ensure the security and traceability of all samples from collection through analysis, maintaining compliance with industry best practices and regulatory requirements.

11.2 Sampling

The standard sample size is typically 1-meter length, with a tolerance of 0.70 m to 1.20 m length sample, respecting lithological contacts, weathering zones, and intervals with low recovery.

After drawing up the sampling plan, the samples are identified in the core boxes with the respective numbers. Then the core boxes are photographed, with drill core dry and wet (Figure 11-1).

Figure 11-1: Example of photographic record of drill core box with marks and sampling ID

Source: Bravo, 2023.

Sampling takes place on the right side of the cut of the core and organized in plastic bags closed and sealed with identified seals. Each sample is weighed individually the information is registered at the sampling plan and the database.

The assay request is prepared by the geologist responsible for the sampling plan, which is accompanied by a letter of custody with volumes sent with the list of samples and their respective seals. Each analytical batch is transported by Bravo's technical team to ALS or SGS Geosol laboratory at Parauapebas-PA (Brazil) by truck from Bravo's site. The relogging and resampling and analysis executed as of the Effective Date is described in Figure 11-2.

Drill core samples are prepared in Parauapebas-PA and analyzed in Lima (Peru) by ALS laboratories (ALS), or at Vespasiano-MG (Brazil) by SGS Geosol Laboratórios Ltda (SGS). Until December of 2022 SGS was used as the secondary laboratory but, in January 2023, Bravo started using SGS as the primary laboratory and ALS as the secondary laboratory.

Drill core samples are dried, crushed (90% passing the 2mm), split (riffle splitter) and pulverized (200 mesh). Analytical methods applied are fire assay with ICP-AES finish (Pt, Pd, Au), nickel sulphide leach with ICP-AES finish (Ni) and fire assay with ICP-MS finish (Rh).

ALS' Fire Assays use the Pb Collection method, while SGS' Fire Assays use the NiS method for metal collection. ALS and SGS are ISO-accredited (ISO: 17025:2005) commercial laboratories, completely independent of Bravo.

Bravo's drilling and sampling campaign procedures flowchart is described in Figure 11-2.

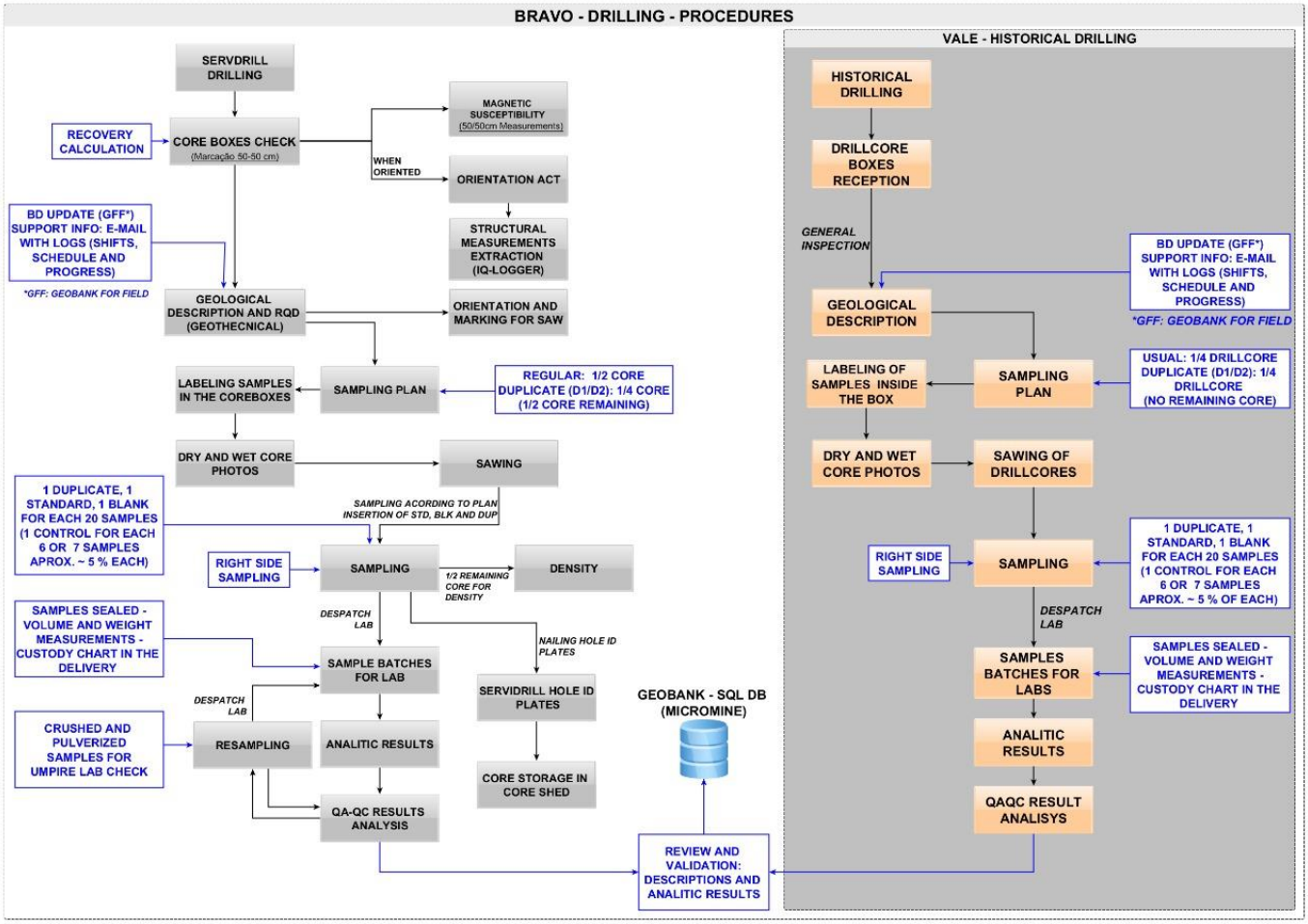

Figure 11-2: Bravo's drilling and sampling procedures

Source: Bravo, 2023.

The assay database used in the Project accounts for both Vale and Bravo samples. Vale samples which were reanalyzed by Bravo have their original grades replaced by the new reanalyzed grades in the database.

The Table 11-1 shows the proportion of assay results present in the database from Vale and Bravo programs.

Table 11-1: Assays proportions by company

Company:	# Samples:	% Samples:
Bravo	75,249	63%
Vale	43,683	37%
TOTAL	**118,932**	**100%**

Source: GE21, 2025.

11.3 Density Sampling

Density sampling in the drill cores executed by Bravo's technical team is conducted after sawing and sampling for chemical analysis. A half-drill core sample is collected every meter, corresponding to half of the remaining core in the box. The selected samples are 10 to 35 cm in length and marked with the sample number and core orientation. Subsequently, the samples are submerged in water and weighed on a 0.001kg precision scale to obtain the wet weight.

The samples are then dried in an oven for 24 hours at 105 °C and weighed for a second time to obtain the dry weight. After the dry weight measurement, the samples are wrapped in cling film and subjected to volume measurement using the water displacement method (Figure 11-3). Finally, the samples are returned to the core box. Bravo has performed a total of 27,170 density assays as of the Effective Date of this report.

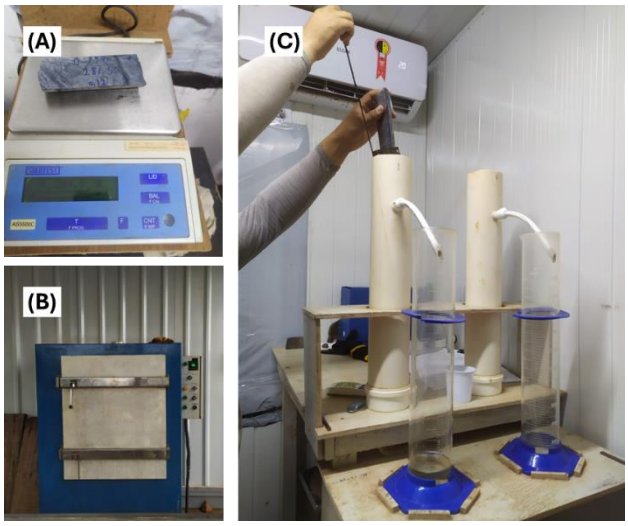

Figure 11-3: Sample density

Legend: A) Scale; Bottom left. B) Drying oven. C) Volume calculation.
Source: GE21, 2023.

Bravo's drill core density statistics for the Luanga Project are summarized in Table 11-2.

Table 11-2: Bravo's drill core density results on fresh rock

Target	Number of Samples	Length (m)	Mean	Minimum	Median	Maximum	Standard Deviation
			g/cm³				
North Mineralization	2,486	585.0	2.83	1.51	2.85	4.47	0.20
Central Mineralization	2,895	672.3	2.88	1.43	2.91	5.31	0.18
Southwest Mineralization	1,532	407.7	2.84	1.43	2.88	4.32	0.16
Host Rock	20,257	4,537.1	2.83	1.30	2.84	4.87	0.20
TOTAL	**27,170**	**6,202.1**	**2.84**	**1.30**	**2.85**	**5.31**	**0.19**

Source: GE21, 2025.

11.4 Quality Assurance and Quality Control

QA/QC procedures for assays adopted in Bravo's Diamond Drilling campaign include Field Duplicates, insertion of Certified Reference Materials (CRMs), Blank samples and Umpire Assay samples. The adopted QA/QC procedures follow the guidelines of the Company Technical Assurance Statement.

Blank and CRM samples are commercial, acquired from OREAS, AMIS and Brasil Minas suppliers. Control samples (blank, CRM and duplicate) are inserted in the analytical batch at the site at a ratio of 1:20 regular samples.

Bravo's QA/QC program accounts for 14,159 control samples, including CRMs, Blank Samples, Field Duplicates and Umpire Check Assays, representing 10.7 % of the total samples. Table 11-3 presents a summary of the QA/QC samples, including the Vale QA/QC program.

Table 11-3: Bravo's QA/QC summary

Bravo	CRM	4,060
	Blank	4,126
	Field Duplicate	4,417
	Umpire Check	1,556
	Total Bravo QC Samples	14,159
	Total Bravo Samples	75,249
	Total Bravo Database	89,408
	Total QC Samples | Bravo Database (%)	**15.8%**
Vale	Duplicate	2,836
	Blank	720
	Total Vale QC Samples	3,556
	Total Vale Samples	43,686
	Total Vale Database	47,239
	Total QC Samples | Vale Database (%)	**8.7%**
Vale – Resampled	Resampled by Bravo	2,162
	Resampled by Bravo | Vale Database (%)	4.6%
	Vale QC + Resampled by Bravo | Vale Database (%)	**12.1%**
Total	Total Samples	118,932
	Total QA/QC	19,877
	Total	138,809
	Total QA/QC percentage	**14.3%**

Source: GE21, 2025.

Bravo's QA/QC program also accounted for a Resampling Campaign, aiming to validate the Vale database and establish a correlation between total (silicate, oxide and sulphide) Ni grades analyzed by Vale and recoverable sulphide Ni grades. A total of 2,056 core intervals were resampled and analyzed, representing 5% of the Vale samples. The analyzed resample results were entered into the drilling database, replacing the previous total Ni grades. Twin Holes were also drilled to evaluate the quality of Vale's previous drilling, sampling, and assaying.

Bravo's team produces regular QA/QC internal reports to constantly monitor the quality of the received assay results. GE21 has accessed the reports from May 2022 to November 2024. These reports are also used as a Quality Assurance measure, specifying batches or parts of batches to be reanalyzed.

It is important to note that the selected samples are only reanalyzed if the Laboratory is available, and priority is given to unanalyzed batches. The selection and priority for reanalysis is based on the following guidelines:

Full Batch Re-assay:

- Number of failed field duplicate samples (Absolute Difference < 10% of the Pair Mean + 2x Detection Limit).

Partial Re-assay (5 previous and 5 next samples, relative to the failed control sample):

- Number of failed CRM Samples (> 3x SD)
- Number of failed Blank Samples (>20x DL)

Priority is given for the batches or sub-batches with (more) Pt and Pd failed assays. Fails in control samples do not necessarily generate a re-assay request.

11.4.1 Blank Samples

The Blank samples used in the Luanga Project are commercial materials. A total of 6 types of blanks were used. Table 11-4 presents the number of blank samples used in. Blanks AMIS0793 and OREAS 22d are CRMs, while BLK, BLK1, BLP2 and Q403 are Brasil Minas' blank materials.

Table 11-4: Bravo's blank samples summary

Blank Material	Number of Samples
Q403	1,798
BLK	9
BLK1	315
OREAS 22d	215
BLP2	930
AMIS0793	859
Total Blank Samples	4,126

Source: GE21, 2025.

GE21 has generated control charts from the Blank samples' data, using 3x the Detection Limit as the acceptance level. The data was divided into SGS and ALS analysis for the control charts construction. Considering all the Blank samples analysis for PGMs, Au and Ni, results have presented more than 98% of the assay grades below the "3x Detection Limit" acceptance level. The results indicate there was no significant or systematic contamination during the sample preparation and analysis stages.

11.4.2 Certified Reference material – CRM

Bravo's QA/QC includes a range of different Certified Reference Materials (CRM), 25 in total. Of these, 16 are from AMIS, 7 from OREAS, and 2 from CDN. The variety of Standard Materials aims to cover low, medium, and high-grade ranges of the main analyzed elements: Pt, Pd, Rh, Au. Table 11-5 presents the quantitative of Reference Materials included in the QA/QC program.

Table 11-5: Bravo's CRM samples summary

CRM	Number of Samples
AMIS0279	33
AMIS0486	407
AMIS0502	283
AMIS0504	214

CRM	Number of Samples
AMIS0606	332
AMIS0723	49
AMIS0749	275
AMIS0759	351
AMIS0760	114
AMIS0771	277
AMIS0822	153
AMIS0853	49
AMIS0854	23
AMIS0874	150
AMIS0876	293
AMIS0890	4
CDN-ME1310	25
OREAS 085	55
OREAS 083	57
OREAS 680	35
OREAS 681	145
OREAS 682	164
OREAS 683	166
OREAS 684	37
CDN-PGMS29	23
Total CRM Samples	**4,060**

Source: GE21, 2025.

GE21 has generated Control Charts for all the Certified Materials used, dividing assay results by laboratory and by assay method. This assay method separation is essential since the SGS laboratory uses the NiS Fire Assay method while ALS uses the Pb Collection Method. Due to differences in the target metals collection, CRMs have different certified grades and Standard Deviations for Pb Collection Fire Assay and NiS Fire Assay.

Nickel control charts have shown inconsistent behavior since none of the CRMs used by Bravo have certified grades for sulphide nickel analysis, which is the current Ni assay method. Bravo's CRMs are only certified for total Ni analysis, which includes Ni present in silicates and oxides. As a result, a direct comparison between these two assay methods is not possible, making it difficult to objectively evaluate the accuracy of the nickel analysis in the database. GE21 recommends that Bravo acquire Certified or Standard Reference Materials certified for sulphide Ni assay methods.

In the QA/QC Internal Reports from December 2022 and January 2023, Bravo identified and reported to ALS a non-conformance related to an excessive number of failed AMIS0504 samples on 12 different batches. As results of this non-conformance, an internal investigation was conducted by ALS. Bravo also conducted its own investigation on the matter. Both investigations resulted in similar conclusions: the high content of refractory oxides (i.e., Al_2O_3, Fe_2O_3 and Cr_2O_3) in the material require higher fusion temperatures to the complete metal recovery. ALS has also reported three main possible causes for the low PGMs and gold recovery: differences in the collection methods using NiS and Pb, indicating higher recovery in the NiS method; mineralogical

complexity and high refractory oxides content; the weight reduction procedure was considered below optimal, suggesting the need for further mass reduction of the sample and/or the addition of reagents to improve fusion.

GE21 analyzed the CRM data using the Certified Grades and Standard Deviations reported in each Reference Material's Certificate and found that the CRMs AMIS0279, AMIS0504, AMIS0606, AMIS0749, AMIS0760, AMIS0771, AMIS0890, OREAS085, OREAS086, OREAS680, and OREAS684 have consistently shown negative bias. GE21 has reviewed the certified values for Al_2O_3, Fe_2O_3, and Cr_2O_3 in all these CRMs and found that most of them contain a significant combined amount of these elements, which could explain the observed negative bias (as pointed out on the investigations carried out by Bravo and ALS).

The AMIS standards data used by Bravo were revised for QA/QC programs. The recommendation states that new Reference Grades and Standard Deviations should be obtained from the data acquired during the Project (after outlier treatment). After this procedure, new reference values were generated. No significant biases were found after the correction of Reference Values. Bravo discontinued the use of OREAS CRMs.

11.4.3 Field Duplicates

Bravo uses Field Duplicates to evaluate the precision of the sampling procedures. Duplicate samples are generated using ¼ drill cores. The Field Duplicates control charts were generated only for the duplicates with both original and duplicate grades above 3x the Detection Limit of the analytical method evaluated. This measure removes analytical artifacts that occur near the Detection Limit. Table 11-6 summarizes the Control Charts generated. GE21 carried out an additional Exploratory Data Analysis (EDA) of Field Duplicates.

Table 11-6: Bravo's duplicates samples summary

Laboratory	Sample Count	Element:	Assay Method
ALS	1,217	Au	PGM-ICP27
		Pd	PGM-ICP27
		Pt	PGM-ICP27
		Rh	Rh-MS25
		Ni	Ni-ICP05
		Ni	ME-ICP61
SGS	3,200	Au	FAI515
		Pd	FAI515
		Pt	FAI515
		Rh	FAA35J
		Rh	FAI30V_RH
		Ni	AAS04B
		Ni	ICP40B
		Ni	AAS04B

Source: GE21, 2025.

Duplicated samples show a good correlation with the original samples. The PGMs and gold duplicate results range between 60% and 90% below the 15% Half Average Real Difference (HARD) limit.

GE21 recommends to Bravo, the inclusion of course and fine duplicates as control samples of its QA/QC program. Coarse and fine duplicates might be collected as an aliquot from the material after the mass reduction processes employed after crushing and milling, respectively. This measure should help to evaluate the quality of the sample preparation processes.

11.4.4 Umpire Check

Umpire Check assays are used to evaluate the reproducibility of a Project's primary laboratory procedures and results. An umpire lab is used to analyze the samples and cross-check the results, like a duplicate quality control procedure. As mentioned, the Luanga Project's Primary Laboratory was ALS until, in January 2023, Bravo decided to use SGS as the primary laboratory.

GE21 has produced control charts to evaluate the reproducibility of PGM and Au assays. The control charts were generated only for the check assays with original and duplicate grades above 3x the Detection Limit of the analytical methods evaluated. This measure is taken to remove analytical artifacts that occur near the Detection Limit. Palladium and platinum presented the best results, with practically 90% of the sample data below the 15% HARD limit.

Rhodium assays resulted in nearly 60% of samples below the 15% HARD limit. Gold check assays present the most dispersion when compared to the PGMs. This element has presented approximately 80% of the sample pairs below the 15% HARD limit.

11.5 Validation of DOCEGEO (Vale) Diamond Drilling Data

Part of Bravo`s mineral exploration campaign is aimed to check the historical Vale DD campaign. Logging, sampling, sample preparation and analysis procedures were the same as the ones employed at Bravo's infill drilling campaign.

11.5.1 Twin holes

Historical drilling is checked through relogging and resampling historical drill holes, and with 8 twin drill holes executed by Bravo (Table 11-7).

Table 11-7: Historical drill holes and their respective twin drill holes executed by Bravo

Historical					Bravo			
HOLE-ID	EASTING	NORTHING	RL		HOLE-ID	EASTING	NORTHING	RL
PPT-LUAN-FD0145	658,495.3	9,340,827.8	243.2	Vs.	DDH22LU006	658,495.8	9,340,828.1	243.0
PPT-LUAN-FD0069	659,092.5	9,341,001.7	241.3	Vs.	DDH22LU007	659,092.9	9,341,002.1	241.2
PPT-LUAN-FD0220	659,997.3	9,341,771.9	276.4	Vs.	DDH22LU026	659,998.8	9,341,772.0	254.7
PPT-LUAN-FD0136	659,950.6	9,341,976.3	290.3	Vs.	DDH22LU043	659,950.7	9,341,976.0	268.5
PPT-LUAN-FD0221	659,954.0	9,341,774.6	268.7	Vs.	DDH22LU081	659,954.1	9,341,775.1	247.5
PPT-LUAN-FD0095	659,603.1	9,342,861.4	288.4	Vs.	DDH22LU083	659,602.8	9,342,861.0	289.3
PPT-LUAN-FD0036	657149.3	9,339,723.8	272.1	Vs.	DDH22LU001	657,148.3	9,339,726.1	272.0
PPT-LUAN-FD0173	659,446.0	9,343,565.3	226.0	Vs.	DDH22LU113	659,446.0	9,343,564.9	225.9

Source: GE21, 2025.

The visual analysis of the twin pairs shows a good correlation of the PGMs, gold, and nickel grades between the holes. The spatial correlation observed indicates that the data acquired by Vale is of sufficient quality to characterize the deposit and its geochemical features.

11.5.2 Resampling - Vale Samples

Bravo previously relogged and resampled the historical DD holes. After the geological/structural description, the photograph of core boxes and magnetic susceptibility measurements, the geologist prepares the sampling plan respecting lithological contacts, weathering profile, drill core diameter and drilling recovery. Relogging and resampling activities follow Bravo's Diamond Drilling campaign's same operational procedures and QA/QC protocols. The historical drill core sample data and Bravo's drill core resampling of the historical core show an expected positive correlation for the PGM assessed. Correlated assay data shows spreading due to the difference in preparation and analytical laboratory methods.

The resampling campaign undertaken by Bravo aimed to validate the Vale database. Due to the big contribution of Vale samples in the database, testing the reproducibility and the precision from the Vale ownership period is of material importance. It is important to note that the resampled Vale samples have their grades updated to the reanalyzed grades in the database. Resampling is carried out on half of the stored Vale half-drill cores, resulting in a ¼ drill core new sample.

GE21 has evaluated the assay results of resampled drill cores by generating control charts for Pt, Pd, Rh, Au and Ni. The control charts were generated only for the samples with original and reanalyzed grades above 3x the Detection Limit of the analytical methods evaluated. Due to the difference in analytical methods used for Nickel readings, a strong bias is detected in the Ni charts.

The Resampling data of ALS and SGS were evaluated separately. ALS data shows a good correlation between original and reanalyzed grades. Pd and Pt resampled pairs present more than 70% of the data below the 40% HARD limit. Rhodium data is 60% below the same HARD limit, while Au data is 55% below. The SGS reanalysis data accounts only for Pt, Pd and Rh. More than 70% of the Palladium and Rhodium sample pairs are below the 40% HARD limit. In comparison, Platinum has over 55% of samples below the limit.

11.5.3 Correlation Between Vale and Bravo Grades

GE21, at the request of Bravo, has conducted a correlation study between the grades analyzed by Bravo and Vale. This procedure aims to correct some discrepancies between the Vale and Bravo databases by transforming the Vale-analyzed grades using a linear regression equation. Linear regressions were generated using the Resampling data for Au, Pd, Pt, Rh and Ni.

For the PGMs and Gold, the grade shell modelled by Bravo was used as a spatial constraint for the regression data. Only the resampled pairs with both grades above 0.03 ppm were used for the regression. This grade limit corresponds to 3x the Detection Limit of the applied

assay methods and was used to reduce the impact of analytical noise near the Detection Limit. Figure 11-4 to Figure 11-7 presents the correlation for Au, Pd, Pt and Rh after the transformation of Vale data.

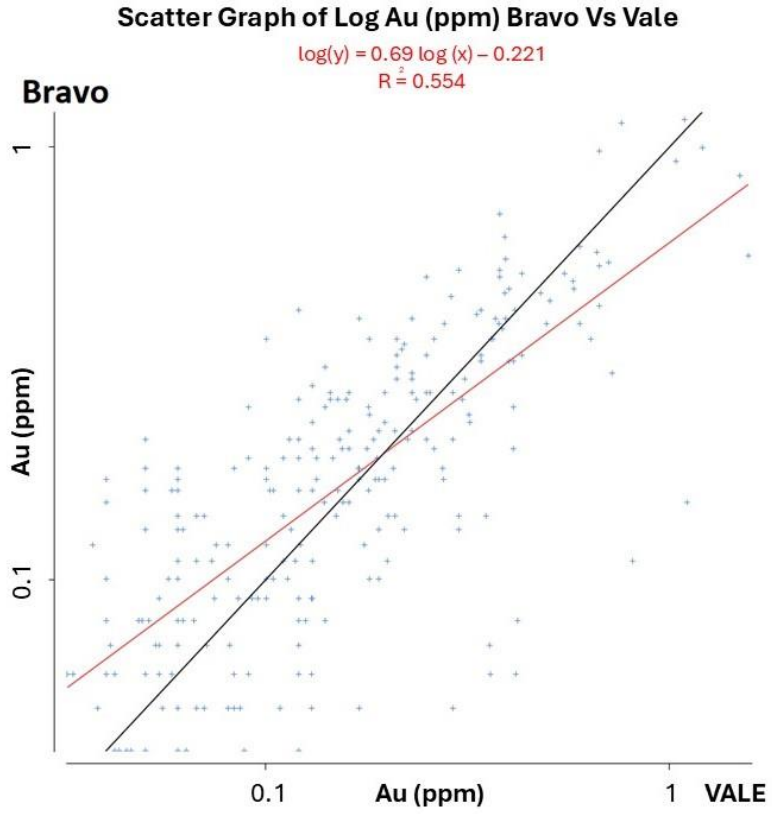

Figure 11-4: Chart correlation of Au assays from Bravo x Vale samples

Source: GE21, 2025.

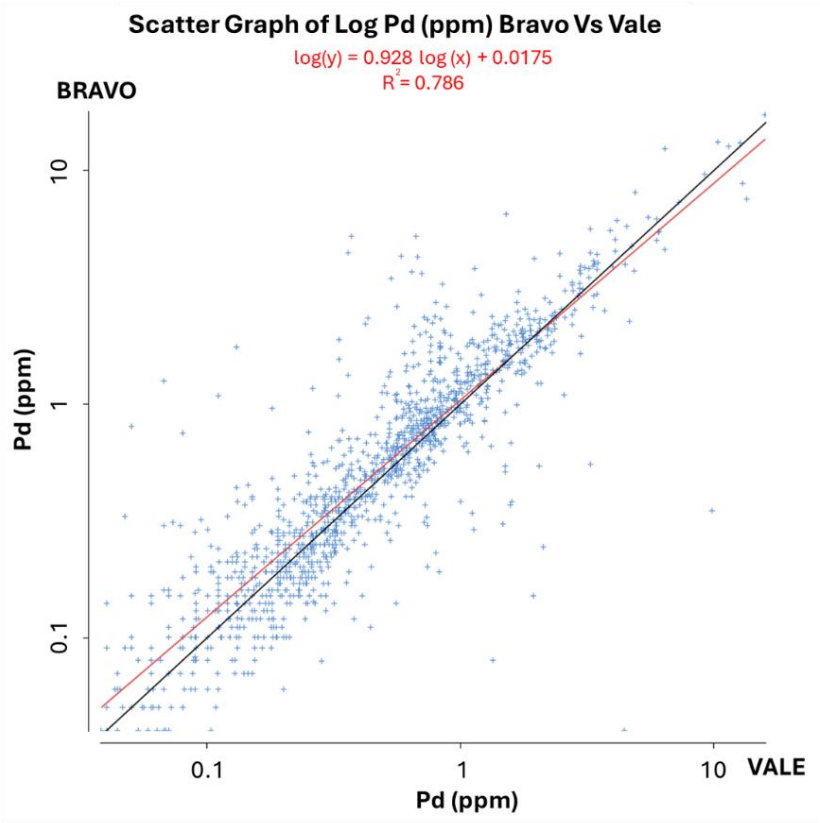

Figure 11-5: Chart correlation of Pd assays from Bravo x Vale samples

Source: GE21, 2025.

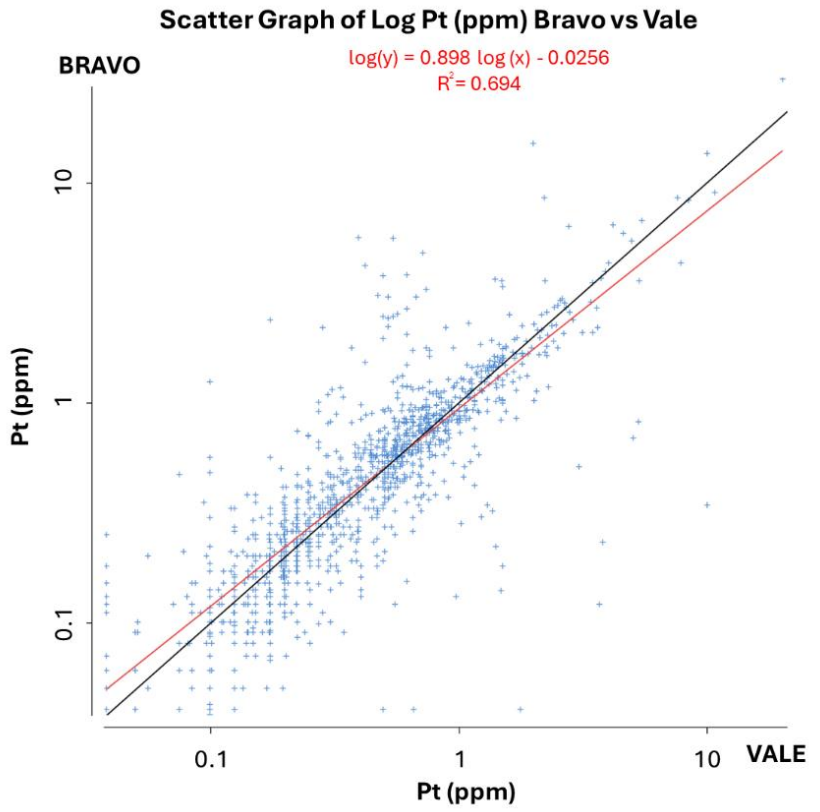

Figure 11-6: Chart correlation Pt samples Bravo x Vale

Source: GE21, 2025.

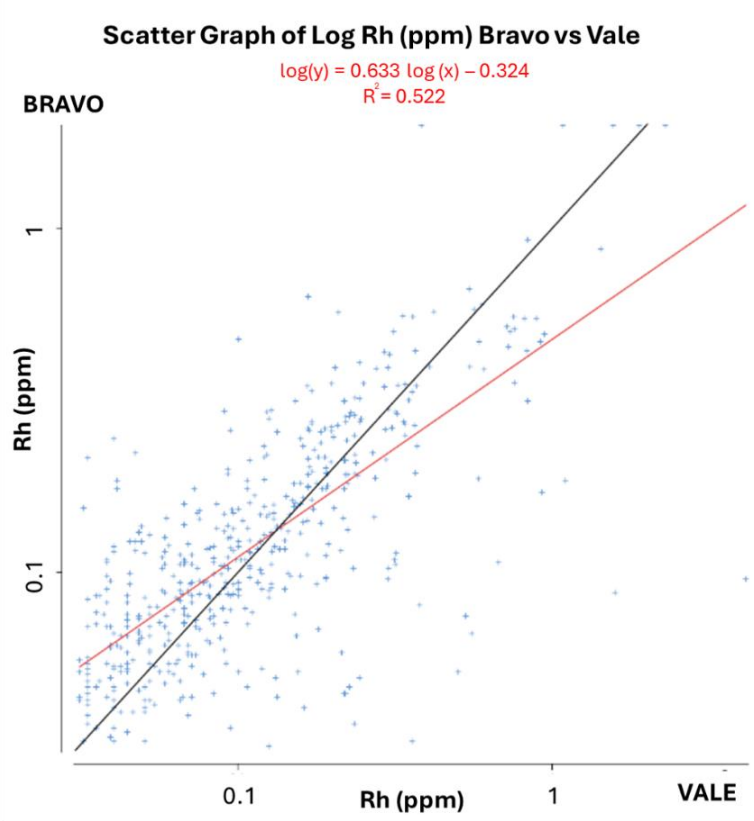

Figure 11-7: Chart correlation Rh samples Bravo x Vale

Source: GE21, 2025.

As mentioned, the Nickel grades analyzed by Vale account for total Nickel: silicate Ni, oxide Ni and sulphide Ni. In contrast, the Bravo grades correspond to the sulphide Ni only. For this reason, additional steps were taken to ensure a valid correlation between the Vale Ni and Bravo Ni grades. Those steps were:

Data was split into two subsets, one above and one below the 1:1 line. The subset below the line was named Negative Bias, and the one above was called Positive Bias.

- Linear regressions were applied in both the subsets.
- The Negative Bias regression was adjusted to make the Angular Coefficient equal to 1. This adjustment was made to reflect a fixed (constant) proportion between the total Ni and the sulphide Ni.
- Data below 100 ppm Ni was removed from the datasets. This grade corresponds to the higher Detection Limit used in the resampled pairs.
- The data constrained between the Positive Bias and the adjusted Negative Bias lines was used for a third linear regression. This regression was used to correlate the Vale and Bravo grades.

Figure 11-8 present the final linear regression for Ni and the Ni grade distribution, after the transformation of Vale data.

The Table 11-8 presents a summary of the transformations applied to the Vale grades.

Table 11-8: Summary of the transformations applied to the Vale grades

Element	Correlation Equation	R2
Au	[Au Bravo] = 10^(0.690*(Log10 [Au Vale]) - 0.2210)	0.554
Pd	[Pd Bravo] = 10^(0.928*(Log10 [Pd Vale]) - 0.0175)	0.786
Pt	[Pt Bravo] = 10^(0.898*(Log10 [Pt Vale]) - 0.0256)	0.694
Rh	[Rh Bravo] = 10^(0.633*(Log10 [Rh Vale]) - 0.3240)	0.522
Ni	[Ni Bravo] = 10^(1.050*(Log10 [Ni Vale]) - 0.2280)	0.941

Source: GE21, 2025.

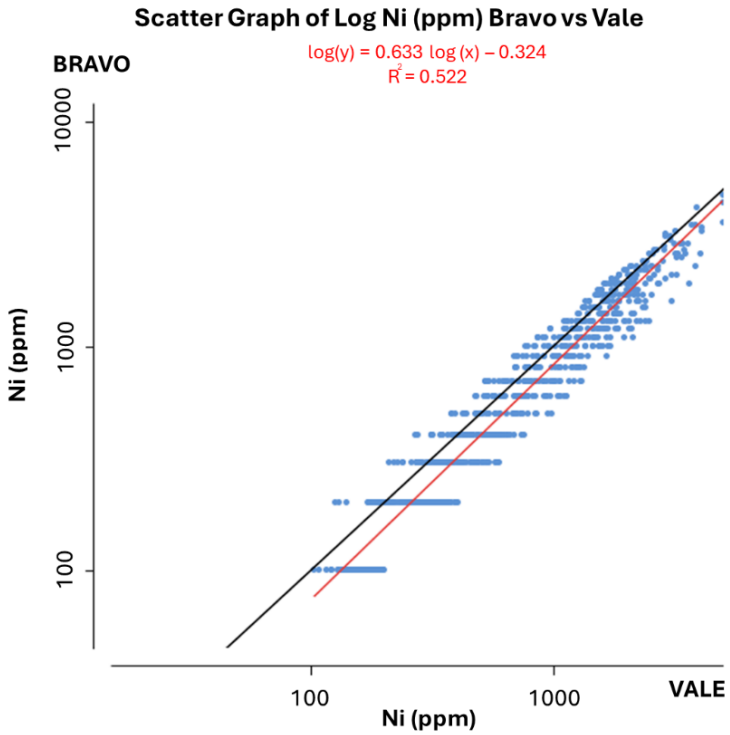

Figure 11-8: Chart correlation Ni samples Bravo x Vale

Source: GE21, 2025.

11.6 QP Opinion

Although the Vale database was historical in nature, the validation and correlation procedures applied and the results obtained, enable the QP of this report to consider this database to be valid for estimation works. It is important to notice that the Vale QA/QC program did not include any CRM) insertion. GE21 and Bravo have, unsuccessfully, tried to obtain the internal QA/QC results from the laboratory used by Vale (SGS).

QA/QC procedures, sampling methodology, and analytical methods applied by Bravo are within the industry's best practices standard. The QP responsible for this report, considering the data presented in this section, is of the opinion that the Luanga Project's Database is suited for a Mineral Resource Estimation work.

Recommendations:

- Acquisition of Certified Reference Materials that are certified for sulphide Ni assay methods.
- Production of CRMs using materials from the Luanga mineralization.
- Implementation of Coarse/Crusher Duplicates and Fine/Pulverized Duplicates.

12 DATA VERIFICATION

GE21 team members have conducted several field visits since 2022 at Luanga to verify the company's infrastructure, the procedures in the course, and the results obtained from the activities that are carried out by Bravo staff.

Engineer Porfirio Rodriguez is an independent consultant and has conducted field visits to the project in 2023 and 2025. Mr. Rodriguez has accompanied Bravo personnel in the development of the resource estimate activities.

Three site visits were conducted in the period from July 4 to 7, 2023, October 3 to 6, 2023, and January 27 to January 31, 2025. In the last two visits, GE21's Qualified Persons Team was composed by Geologist Bernardo Viana and Mr. Rodriguez.

12.1 Site Visit

The site visits included the review of the QA/QC program, field tours (Figure 12-1), exploration of the core shed, drilling in progress, review of density procedures, and discussions of the current geological interpretations with geologists of Bravo.

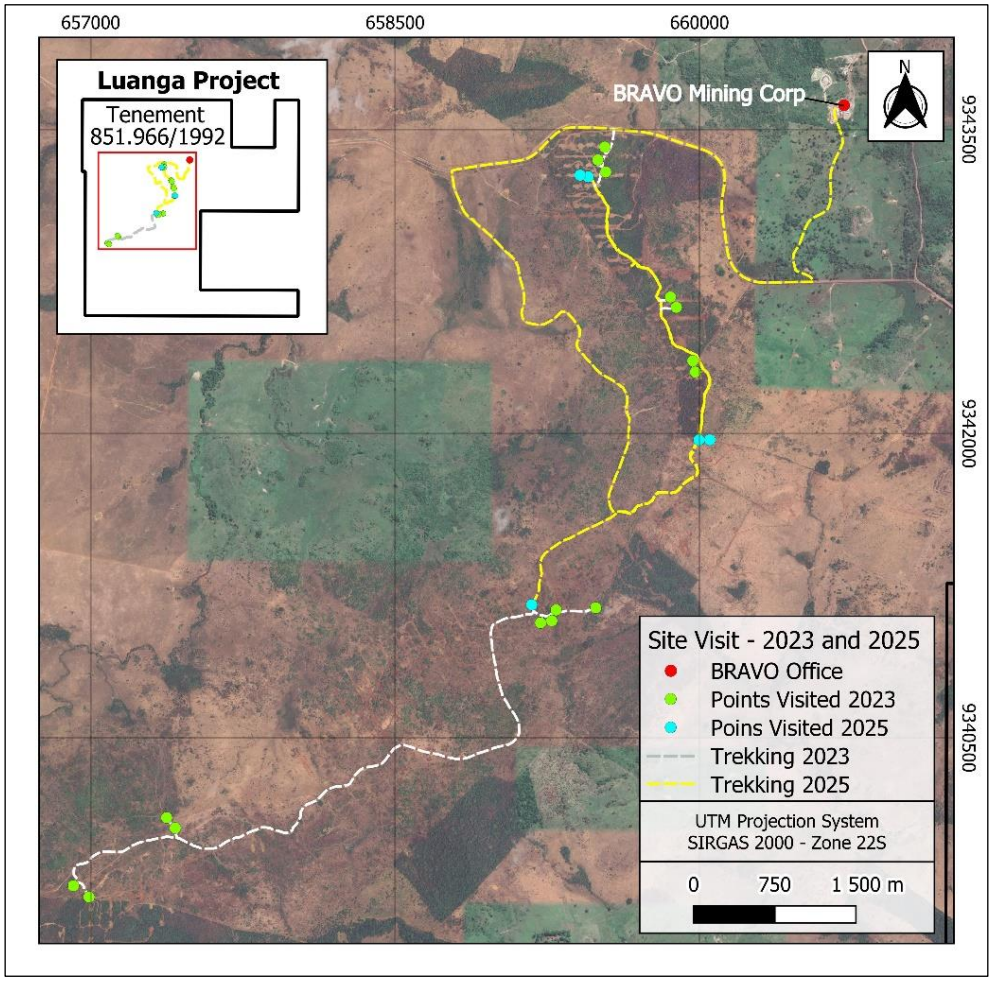

Figure 12-1: Points visited during January 2025

Source: GE21, 2025.

12.1.1 Density Test Laboratory

GE21 visited the Bravo internal density laboratory, where they observed the installation and equipment used for density test measurement (Figure 12-2).

Discussions held with on-site geologists allowed to confirm procedures were adequately applied. More details about Bravo procedures are available in Sections 10 and 11 of this report.

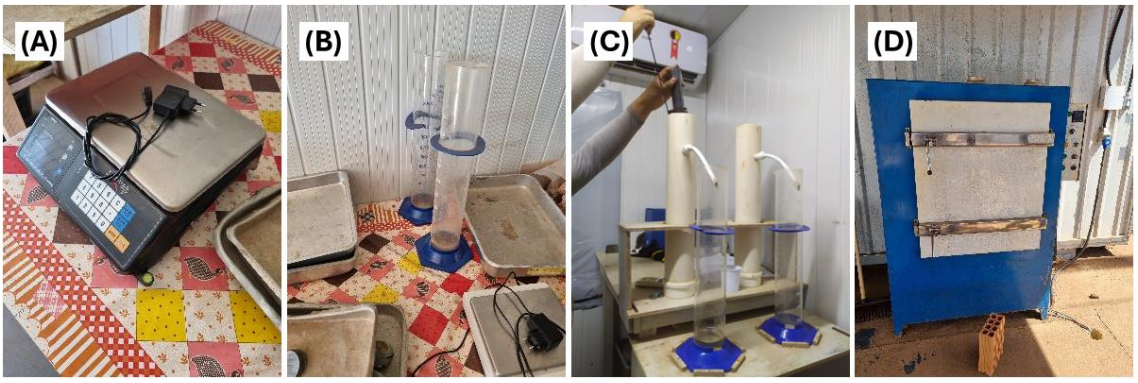

Figure 12-2: Density test equipment

Legend: A) Electronic Weight Scale. B) Test tubes and trays used in density tests. C) Water displacement method for volume calculation. Equipment for determining density by volume displacement. D) Drying Oven.
Source: GE21, 2023.

12.1.2 Drill Hole Location

GE21 verified drill hole collars in the field, checked with handheld GPS units, and compared them to the exploration database (Figure 12-3). GE21 visited the location and collar marks of:

- Metallurgic drill holes 901, 902, and 905.
- Drill holes 086, 249, 001, 007, 044, 047 and 189.
- Trench 004, 022, 024 and 037.

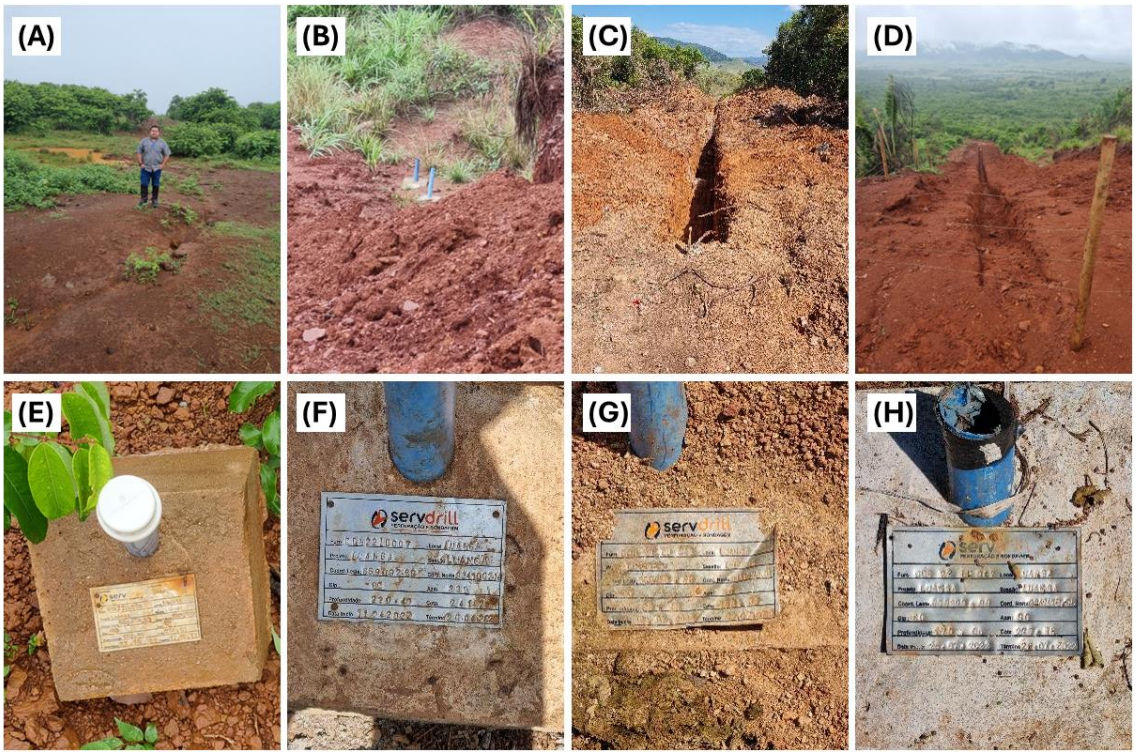

Figure 12-3: Drill hole location evidence

Legend: A) Mr. Viana ion the Field Visit B) Drilling Collar Marks. C) Trench 004. D) Trench TRC24LU037. E) Drill hole DDH22LU086 Mark. F) Drill Hole DDH22LU007 Mark. G) Drill Hole DDH22LU044 Mark. H) Drill hole DDH22LU047 Mark.

Source: GE21, 2023 and 2025.

Drill hole collars have an identification physical marker. The markers are comprised of a concrete pad with a metal plate designating the drilling contractor, drill hole number, drilling area, orientation, coordinate location, start and end date drilled, and total depth. A PVC pipe protruding from the marker provides a physical record of the drill hole orientation.

12.1.3 Core Shed

All core boxes were labelled and properly stored. Sample tags were present in the boxes, and it was possible to validate sample numbers and confirm the presence of mineralization in witness half-core samples from the mineralized zones.

During the core shed visit, the Bravo team explained in detail the entire path of the drill core, from the drill rig to the logging and sampling facility and finally to the laboratory (Figure 12-5).

GE21 visited the core shed of the Luanga Project (Figure 12-4) and did a visual inspection of the historical Vale core. The drill holes were previously selected by the GE21 team, to review sections of the mineralized core (Figure 12-6). The mineralization observations agree favourably in the extent and type of mineralization logged in the exploration database.

Figure 12-4: Core Shed installation during 1st visit, and after complete construction on 2nd visit

Legend: A) Front view of the Core Shed. B) Lateral view of the Core Shed. C) Inside the Core Shed. D) Vale Core Shed. E) Core box storage area. F) Drill core description and sampling shed.
Source: GE21, 2023 and 2025.

Figure 12-5: Sampling and QA/QC procedures

Legend: A) Labelled Drill core samples. B) Labelled Drill core samples batches. C) Standards for QA/QC program. D) Coarse Blank for QA/QC program.

Source: GE21, 2023.

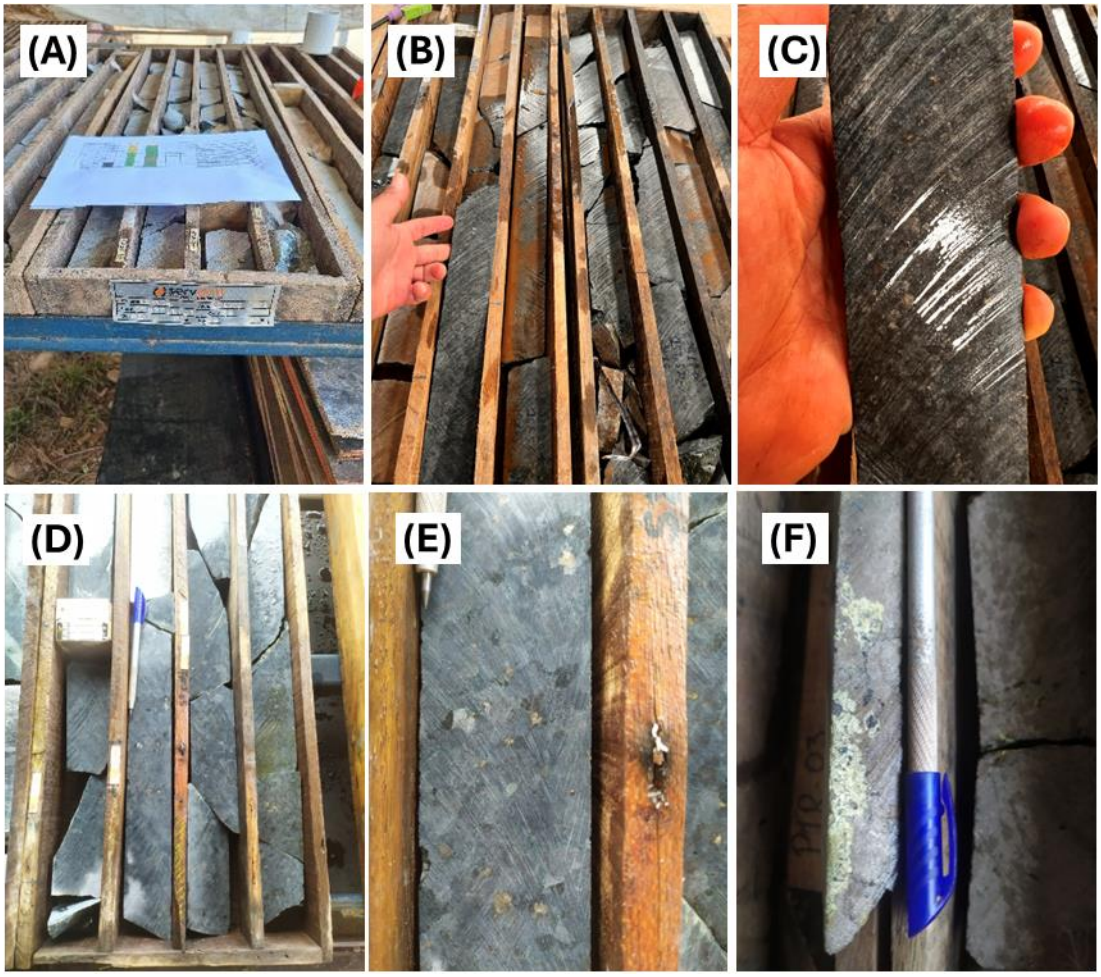

Figure 12-6: Checking drill holes

Legend: A) Personal checking on core description. B) Core box of the drill hole DDH23LU162. C) Disseminated sulphide in the drill hole DDH23LU162. D) Core box of the drill hole DDH23LU162. E) High sulphide PGM mineralization in hole DDH22LU083. F) Massive sulphide range in hole DDH22LU047 with high Ni (pentlandite) and Cu (chalcopyrite) grades.

Source: GE21, 2023.

12.1.4 Witness Samples

During the visit on the first period, in 2023, Mr. Porfirio Cabaleiro collected a sample selected among the previous drill holes checked, to configure as a witness sample.

The sample on consideration was:

- Drill hole: DDH22LU007
- Interval: from 128.58 m to 128.96 m
- Sample BPGM-101433)
  - Ni: 0.31%
  - PGM + Au: 6.60 ppm

GE21 independently submitted the sample to a chemical analysis in the certified laboratory SGS Geosol in Vespasiano, receiving the result presented in Figure 12-7.

SGS GEOSOL LABORATÓRIOS LTDA.

CERTIFICADO DE ANÁLISES

GQ2308925

INFORMAÇÕES DO CLIENTE

NOME: BRAVO MINERACAO LTDA

ATTN.: Paulo Brito

ENDEREÇO: EST ESTRADA DA VILA ALTO BONITO S/N ZONA RURAL 68523000 PA CURIONOPOLIS

CPF/CNPJ: 37.262.942/0002-39

REFERÊNCIA DO LOTE DE AMOSTRAS

REF. CLIENTE: ACES-BRAVO-0050-23

QTE. AMOSTRAS: 1

RECEBIDO: 11/07/2023

PRODUTO: TESTEMUNHO

COMPLETADO: 07/08/2023

PROJETO: Luanga

EMITIDO: 07/08/2023

REFERÊNCIA ANALITICA

AA

AAS04B: Lixiviação com Citrato De Amônio e Peróxido de Hidrogênio por 2 horas.

FA

FAI30V_RH: Determinação de Ródio por Fire Assay - ICP0ES - Fusão 30 g

FAI515: Determinação de Au, Pt e Pd por Fire Assay - ICP - 50g

PREP

DRY105: Secagem de amostras à 105°C

PREPQC: Controle de Qualidade - Preparação Física

PRPCLI: Preparação Física conforme definição do cliente

LEGENDA: SIGLAS

L.D. = Limite de Detecção | BLK = Branco | REP = Replicata | DUP = Duplicata

L.N.R. = Listado e não Recebido | I.S. = Amostra Insuficiente | N.A. = Não Analisado | STD = Padrão

L.N.I. = Não reportado devido a interferentes | OVR = Não Analisado devido ao alto teor

SGS GEOSOL LABORATÓRIOS LTDA.

CERTIFICADO DE ANÁLISES

GQ2308925

ANÁLISES	Peso_bruto	Ni	Cu	Au	Rh	Pd	Pt
MÉTODO	PRPCLI	AAS04B	AAS04B	FAI515	FAI30V_RH	FAI515	FAI515
UNIDADE	G	%	%	PPB	PPM	PPB	PPB
LIMITE DETECÇÃO	0,00	0,01	0,01	5	0,002	5	5
BRANCO_PREP	N.A.	<0,01	<0,01	<5	<0,002	<5	<5
BPGM-101433	1011,00	0,26	0,02	90	0,572	5039	3387
* REP BPGM-101433		0,25	0,02				
* STD HO_AM_01		0,49	0,29				
* STD AMIS0323				145		647	1083
* STD AMIS0388				8		164	356

Figure 12-7: Analysis certificate of 2023 witness sample

Source: SGS, 2023.

During the visit in January 2025, GE21 QPs Mrs. Bernardo Viana and Porfirio Cabaleiro collected three sample reserves, selected from previously sampled trenches, and sent for chemical analysis as witness samples. Table 12-1 presents the selected samples and the original results, retrieved from the Project Database. Figure 12-8 presents a graphical comparison between original grades and witness sample grades, and Figure 12-9 presents the laboratory certificate of analysis for the witness samples. GE21 concludes there is a good correlation between results on all witness samples.

Table 12-1: Original Witness Samples Results

Trench ID	Sample ID	Interval		Au	Pd	Pt	Rh
		From	To	ppb			ppm
TRC24LU027	BRAV-704468	124.15	125.15	22	643	203	0.044
	BRAV-704476	131.15	132.15	46	827	438	0.097
	BRAV-704491	144.05	145.05	162	5102	2958	0.749

Source: GE21, 2025.

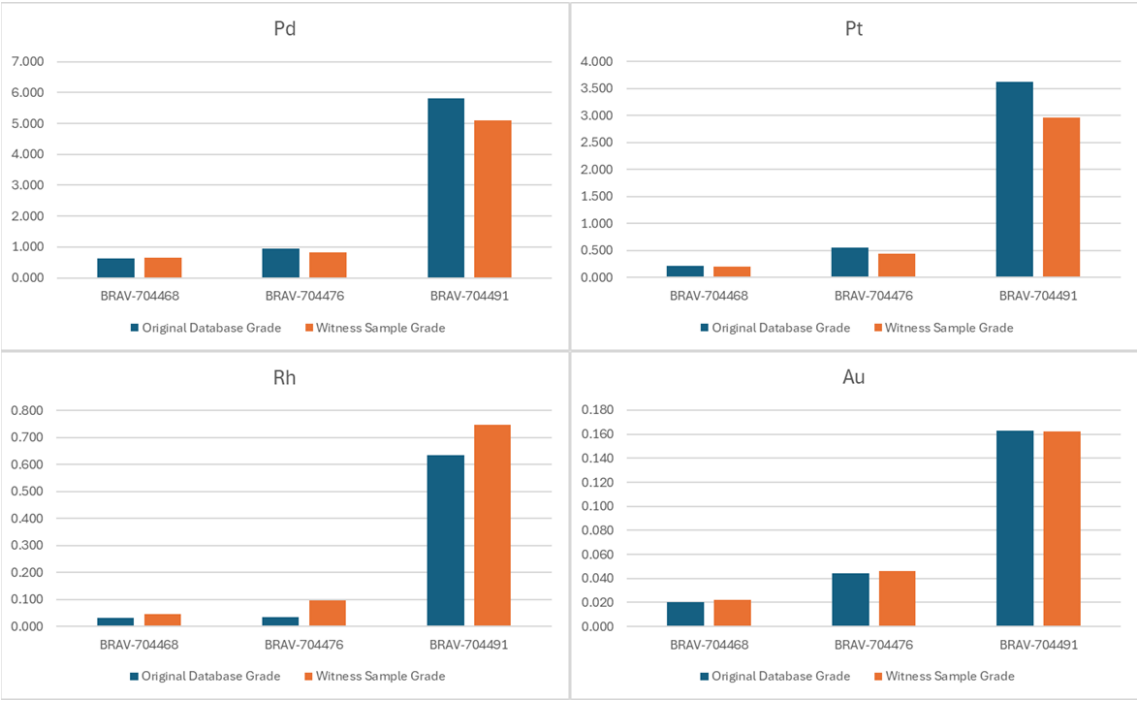

Figure 12-8: Comparison between original database grades and witness sample grades

Source: GE21, 2025.

SGS GEOSOL LABORATÓRIOS LTDA.

CERTIFICADO DE ANÁLISES

GQ2501058

INFORMAÇÕES DO CLIENTE

NOME: BRAVO MINERACAO LTDA

ATTN: Paulo Brito

ENDEREÇO: ESTRADA ESTRADA DA VILA ALTO BONITO S/N ZONA RURAL 68523000 PA CURIONOPOLIS

CPF/CNPJ: 37.262.942/0002-39

REFERÊNCIA DO LOTE DE AMOSTRAS

REF. CLIENTE: ACES-BRAVO-0248-25

QTE. AMOSTRAS: 3

RECEBIDO: 04/02/2025

PRODUTO: POLPAS

COMPLETADO: 10/02/2025

PROJETO: Luanga

EMITIDO: 10/02/2025

REFERÊNCIA ANALITICA

FA

FAI30V_RH: Determinação de Ródio por Fire Assay - ICPOES - Fusão 30 g

FAI515: Determinação de Au, Pt e Pd por Fire Assay - ICP - 50g

LEGENDA: SIGLAS

L.D.= Limite de Detecção | BLK = Branco | REP = Replicata | DUP = Duplicata

L.N.R. = Listado e não Recebido | I.S. = Amostra Insuficiente | N.A. = Não Analisado | STD = Padrão

I.N.F. = Não reportado devido a interferentes | OVR = Não Analisado devido ao alto teor

Marcos Filipe Gonçalves Silva

CRQ II 02202046

Responsável Técnico

Os ensaios foram realizados na SGS GEOSOL Laboratórios Ltda. - Rodovia MG 010, Km 24,5 - Bairro Angicos - Vespasiano - MG - Brasil - CEP: 33.206-240

Telefone +55 31 3045-0261 www.sgsgeosol.com.br

Certificados ISO 9001:2015 e ISO 14001:2015 (ABS 32982 e ABS 39911)

Os resultados expressos neste Certificado se referem somente ao material recebido. Proibida a reprodução parcial deste documento.

Relatório impresso em: 10/02/2025 16:00:49 Página 1 de 2

CERTIFICADO DE ANÁLISES

GQ2501058

ANÁLISES	Au	Rh	Pd	Pt
MÉTODO	FAI515	FAI30V_RH	FAI515	FAI515
UNIDADE	ppb	ppm	ppb	ppb
LIMITE DETECÇÃO	5	0,002	5	5
BRAV-704468	20	0,032	623	210
BRAV-704476	44	0,035	956	550
BRAV-704491	163	0,636	5813	3626
* REP BRAV-704468		0,036		
* REP BRAV-704468	17		578	183
* STD AMIS0769		0,063		
* STD GPP-04	81		92	86

Figure 12-9: January 2025 witness samples laboratory certificate

Source: SGS, 2025.

12.1.5 QP Opinion

GE21 is of the opinion that the exploration data is adequate for use in the Mineral Resource estimate. What follows below are some observations that were recorded by GE21

personnel during visits as it relates to the generation, collection, control and storage of exploration data on-site at Luanga:

- Drill hole Logging: This task was considered as standard industry practice logging procedures, which has been standardized by Bravo. GE21 performed a review of logging procedures for randomly selected drill cores and verified the completeness of the logs. Considering all the evaluated content, Bravo has demonstrated that it understands the geology, and some located omissions are not considered significant.
- Database: recent data is stored in a standard commercial database. Historical Vale records are well-managed and are currently being migrated to the Bravo database. Data storage procedures at Bravo are considered within standard industry practice. As part of the validation process, GE21 verified 8 holes. Database validation was conducted with the help of Bravo staff according to standard validation procedures including review of collar locations, drill hole deviations and database check-assay review. No inconsistencies were found in the database.
- Density: A large database of density information has been collected during the exploration phase. The process whereby density data is obtained is considered within standard industry practice.
- Witness sample: Random samples were collected during the site visits; the results obtained from a certified laboratory were consistent with the original sample results recorded on the database.

13 MINERAL PROCESSING AND METALLURGICAL TESTING

13.1 Introduction

This section reports on the results of preliminary metallurgical test work on PGM+Au+Ni mineralization from the Luanga Project and records recommendations on metallurgical input parameters considered for the Mineral Resource Estimate (MRE). The scope of test work completed to date includes:

1. Historical test work completed for Vale (see section 13.2).
2. Extensive comminution and flotation test work on fresh (sulphide) rock samples conducted for Bravo from 2022 to 2025 including work to review and validate historical work conducted by the previous project owner between 2001 and 2004.
3. Several test programs conducted on oxide material including exploratory leaching and physical separation tests and parameter optimization tests conducted for Bravo between 2022 and 2025.
4. Preliminary tests to evaluate the downstream treatability of Luanga concentrates on site or nearby.

13.2 Review of Historical Metallurgy Work

Historical Metallurgical testing on the Luanga material had been initiated at various stages of its development with the bulk of the work having been completed between 2002 and 2004. Test work was completed at bench scale and pilot plant scale on core samples from diamond drilling. The studies completed include:

- 2001/2002 – CABRI: Mineralogical Characterization Study
- 2002 – MINTEK: Flotation Studies and Mineralogical Characterization Study
- 2003/2004 – LAKEFIELD: Flotation Studies and Mineralogical Characterization Study
- 2003 – HDK ENGENHARIA: Preliminary Milling Circuit Sizing Study
- 2002/2004 – AVEC: Evaluation of the Global PGM Market

Historical metallurgical efforts reported for Luanga were summarized in Vale's final evaluation report as follows:

"The studies of mineral processing carried out with samples of fresh sulphide mineralization have indicated that the traditional flowsheet, involving crushing/grinding and flotation, produces a concentrate with commercially accepted grades [80-154g/t] and PGM recoveries in the order of 74%. The closed-circuit (lock Cycle Test LCT) study obtained a (single) bulk concentrate for Luanga comprising PGM + Ni + Au "

13.2.1 MINTEK Studies

In 2002 a sulphide mineralization sample of 100kg was sent to Mintek in South Africa for the first characterization and concentration studies. The initial sample reported a feed grade of

4.8g/t PGM+Au and the mineralogical analysis showed that the main PGM-bearing minerals were Sperrylite, PGM-Bithmotellurides, and Stibiopaladinite.

Mintek defined the standard mill-float-mill-float (MF2) flowsheet as likely appropriate for preliminary tests. Primary milling was performed to p60 -75µm, followed by rougher, cleaner, and recleaner flotation stages in a “course” circuit. The rougher tailings, together with the cleaner tailings, were then reground to p80 -38µm followed by secondary rougher, cleaner and recleaner, in the “fines” circuit.

The reagents used in the flotation were NaSH (sulfidizing agent), Cu504 (activator), Depramin 267 (silicate depressant), SIBX (collector) and Dow 200 (frother). The Mintek flowchart is shown on Figure 13-1.

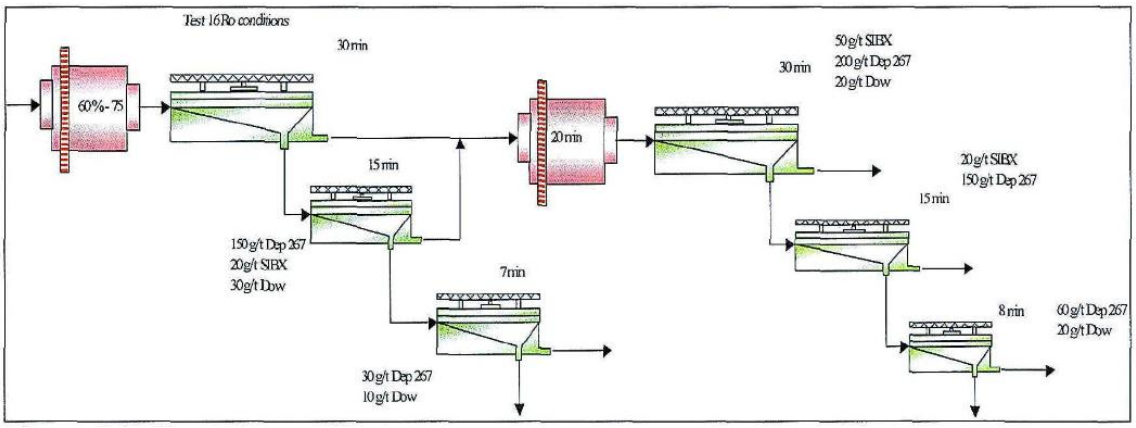

Figure 13-1: Mintek flowchart

Source: Bravo, 2023.

The final concentrate from Mintek’s open-circuit tests reported a mass pull of 3.8%, concentrate grade of 87.2 g/t PGM + Au and recovery of 70.6%. Two locked cycle tests were also carried out at Mintek and produced a concentrate content of ca. 150 g/t PGM + Au with 75% recovery.

Mintek’s grinding investigation concluded that the recovery of PGM from Luanga material into a flotation concentrate is much dependent on grind size with results demonstrating an improvement from 52% to 72% in PGM recovery by grinding finer from 40 to 60% passing 75um.

The mineralogical investigation concluded that the PGM’s occur in various modes, associated with base metal sulphides (inclusions and attached at boundaries), at silicate boundaries, and as inclusions within silicates.

13.2.2 CDM (Vale) Studies

CDM performed tests on 4 fresh sulphide samples with lower PGM+Au grades, S1 with 1.07 g/t, S2 with 2,03 g/t, S3 with 2.67 g/t and S4 with 4.14 g/t head grade.

The flotation testing in open circuit and using the MINTEK process with two stages and high reagent additions produced concentrates with grades varying between 20 and 50 g/t PGM’s

for samples S-1 to S-3, with recoveries 70.4 % < 72.3 %. The S-4 composite delivered an 83 g/t concentrate with 75.4 % recovery (Table 13-1).

Table 13-1: Feed sample analysis and concentrate qualitative analysis from CDM studies

Chemical analysis samples S1 to S4 - PGM & Au (g/t)					
	Pd	Pt	Rh	Au	PGM + Au
INITIAL SAMPLE S1	0.57	0.45	<0.05	0.05	1.70
INITIAL SAMPLE S2	1.05	0.81	0.09	0.08	2.03
INITIAL SAMPLE S3	1.50	0.97	0.10	0.10	2.67
INITIAL SAMPLE S4	2.34	1.43	0.22	0.15	4.14

	SiO2 (%)	Mg (%)	Fe (%)	Al2O3 (%)	Ni (%)	Cr (%)	S (%)
AMOSTRA INICIAL S1	47.10	14.80	7.73	4.29	0.17	0.28	0.40
AMOSTRA INICIAL S2	47.00	15.30	7.00	3.86	0.19	0.29	0.34
AMOSTRA INICIAL S3	47.40	15.10	7.87	4.08	0.26	0.28	0.50
AMOSTRA INICIAL S4	46.50	14.60	8.67	3.37	0.31	0.31	1.18

	Co (%)	Cu (%)	Sb (ppm)	As (ppm)	Ag (ppm)
AMOSTRA INICIAL S1	0.01	0.02	6	1	<1
AMOSTRA INICIAL S2	0.01	0.02	5	2	<1
AMOSTRA INICIAL S3	0.02	0.02	5	2	<1
AMOSTRA INICIAL S4	0.02	0.04	5	2	<1

Feed grades PGM, Au, Ni, Co &Cu							
Pd (g/t)	Pt (g/t)	Rh (g/t)	Au (g/t)	PGM + Au (g/t)	Ni %	Co %	Cu %
1.02	0.66	<0.1	0.09	1.77	0.19	0.01	0.02
Final concentrate grades PGM, Au Ni, Co & Cu							
Pd (g/t)	Pt (g/t)	Rh (g/t)	Au (g/t)	PGM + Au (g/t)	Ni (%)	Co (%)	Cu (%)
54.3	42.9	3.8	3.6	105	7.5	0.35	1.66

Chemical recovery (%)					
Pd	Pt	Au	PGM + Au	Ni	Co
71	79	47	73	44.6	30

Source: Bravo, 2023.

CDM (Vale) increased concentrate grades by additional cleaning by introducing additional cleaning stages – 3 in total. The tests S-1 to S-3 produced concentrates with 50 to 97 g/t PGM's with recoveries between 56 and 64%.

CDM performed two locked cycle tests (LCT). LCT1 was performed on sample blend of S1 to S3 grading 1.77 g/t and consisted of a circuit with two stages of grinding and flotation, with a finer grind at p90 -38 μm. Rougher stages were followed by three cleaner stages, with a total of 8 flotation stages. The concentrate produced in LCT1 after 10 cycles graded 104 g/t PGM+Au with 73% recovery at a mass pull of 1.2% (Table 13-2).

LCT2 used a simpler flotation scheme, a rougher stage fed with mineralization milled to a p90 -38 μm, with concentrates cleaned in two stages. The cleaner tails fed a cleaner scavenger stage. Scavenger cleaner tails were recycled to rougher feed. Recleaner tails and cleaner scavenger concentrate returned to the cleaner feed, joining the rougher concentrate.

Table 13-2: Summary of results in LCT1 and LCT2

Element	Unit	LCT 1	LCT 2	Feed
		grade	grade	grade
Pd	ppm	54.3	72.8	1.02
Pt	ppm	42.9	52.1	0.66
Rh	ppm	3.8	3.8	< 0.1
Au	ppm	3.6	5.34	0.09
PGM + Au	ppm	104.6	135.03	1.77
Ag	ppm	4	< 1	< 1
Al2O3	%	1.08	0.51	4.07
As	ppm	< 1	< 1	< 1
Ca	%	0.59	0.3	2.32
Co	%	0.35	0.45	0.01
Cr	%	0.35	0.39	0.29
Cu	%	1.66	2.59	0.02
F	ppm	< 100	< 100	122
Fe	%	33.3	39.7	7.86
Mg	%	5.3	2.13	15.4
Mn	%	0.06	0.05	0.14
Ni	%	7.5	9.8	0.19
S	%	21.3	29.4	0.47
Sb	ppm	62	119	7
SiO2	%	18.7	7.85	51.8
Zn	%	0.03	0.09	0.01
Mass Recovery		1.20%	0.89%	
Metallurgical Recovery		73%	69,36%	

Source: Bravo, 2023.

CDM did 12 cycles for circuit stabilization in LCT2, resulting in a mass pull of 0.9%, concentrate grade of 134 g/t PGM+Au and 69.4% recovery.

The nickel recoveries in these tests were 46-48%. Nickel is entrained in the crystalline structures of silicates was highlighted by a mineralogical characterization conducted at CDM.

CDM conducted mini-plant tests in February 2004 to generate concentrates for hydrometallurgical refinery tests. A total of 400 kg of sample grading about 1.64 g/t 4PGM was processed and produced a concentrate grade of 124 g/t for a mass pull of 0.8% at a recovery of 63 %.

A 200kg composite sulphide sample was sent to SGS Lakefield in Canada for replication of CDM LCT using a MF1 circuit. The results obtained include a final concentrate mass pull of 0,78% grading 132 g/t PGM+Au and a recovery of 70%. The sample grade was 1,49 g/t PGM+Au.

Vale, through CDM also attempted to test flotation efficacy on oxidized and blended fresh sulphide/oxide mineralization. These tests were generally unsuccessful reporting low recoveries and or poor concentrate quality Sample Selection

13.3 Bravo Sample Selection

Detailed mineralogy was completed on Luanga samples from various locations by the previous project owner. Sample locations for Bravo's 2022/2023 metallurgical test program were aligned with the location of the aforementioned mineralogical study. This facilitated Bravo's

sample preparation, test work configuration, and results allowing interpretation to be directly supported by the historical mineralogical data. The mineralogy study was completed on drill core samples sourced from Vale' previous drill programs. The same drill hole locations used for Bravo's metallurgy sampling with new sample material being generated through twin-hole, HQ, diamond core drilling completed in 2022.

Sample locations extended along the strike length of the mineralized body including the north, central and southwestern Sectors. A bulk oxide/saprolite sample was taken from the central Sector. Sample localities are shown on Figure 13-2.

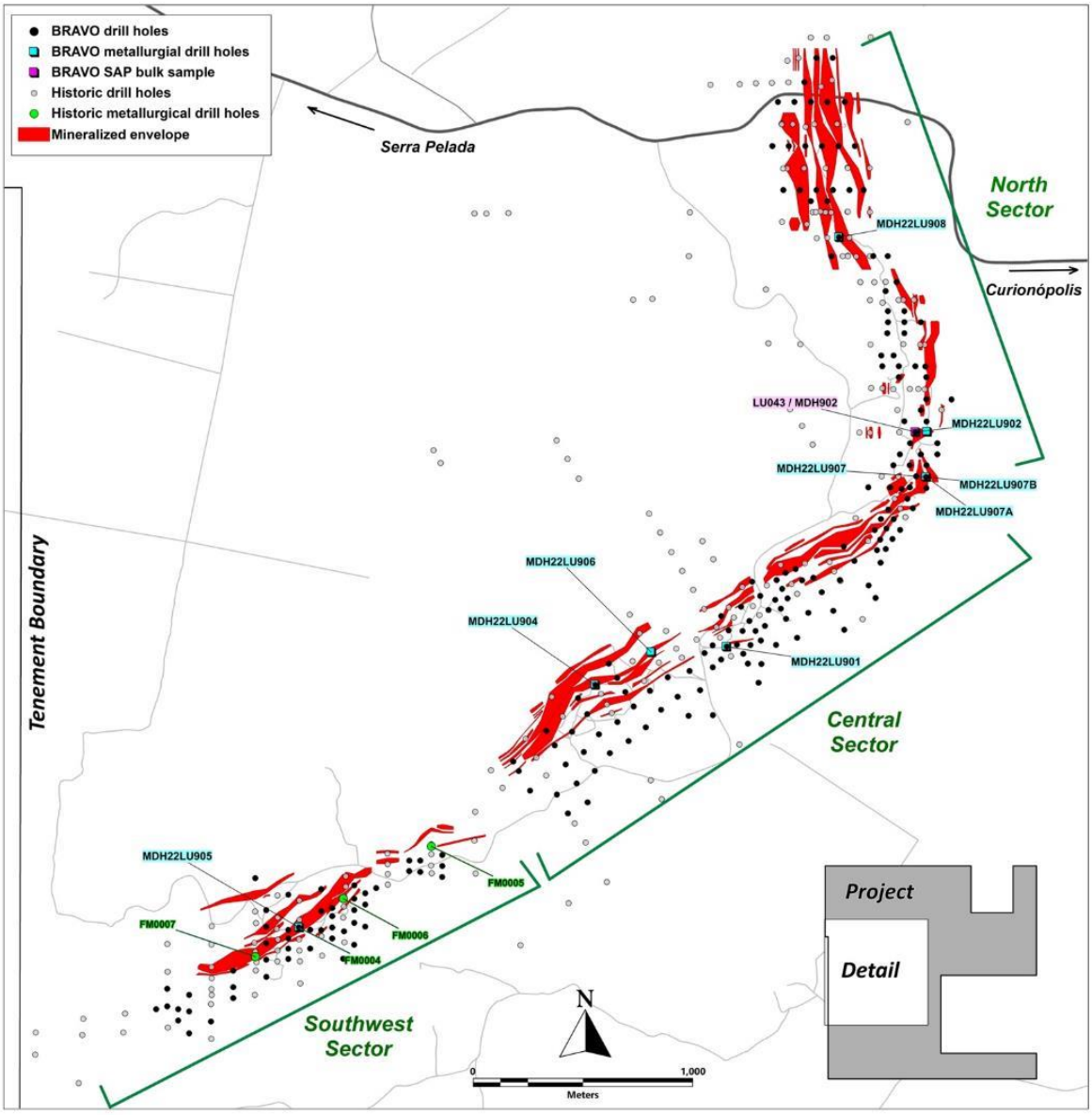

Figure 13-2: Location of metallurgical samples

Source: Bravo, 2023.

13.3.1 Sample Variance Selection

Twin drill core samples for flotation and leaching test program were selected to be representative of the Luanga deposit. This included fresh sulphide, transition and oxide samples. Grade variance has also been taken into consideration with sample grades ranging 0.5 -11 g/t.

The bulk sample for optimization leaching tests was collected at the northern edge of the Central Sector of the Luanga deposit. The Central Sector is considered to contain most oxide resources by attributable tonnes.

13.4 Bravo Metallurgical Program 2022/2023

At the initiation of the 2022/2023 program, Bravo submitted approximately 3 tonnes of fresh-sulphide metallurgical samples and 150kg of oxide samples to the CETEM and TESTWORK Ltd. laboratories respectively, for metallurgical studies.

13.4.1 Sulphide Material

Standard milling tests were conducted to establish comminution curves and size distribution relative to grinding times.

- Bond Ball Mill Grindability Tests

Two individual BBWi tests were performed on samples of Luanga mineralized material to determine preliminary grinding power requirements. The methodology was consistent with the standard Bond method. The tests were performed on composite blends from two major mineralized zones at Luanga, namely the central and southwest Sectors. One composite of fresh sulphide mineralized material and one sample of transitional mineralized material were submitted for analysis. The preliminary BBWi results indicate a hardness classification of “medium” for both samples (Table 13-3). Table 13-4 below shows sample composite details used on the BBWi tests.

Table 13-3: BBWi results

Test	WI
	kWh/t
1 Fresh	13.94
2 Transition	10.29

Source: Bravo, 2025.

Table 13-4: Sample composite – BBWi test

Sulphide Composite Samples	Drill hole ID	Zone	Sample Depth
600014	MDH22LU901	Central	106-112m
600015	MDH22LU901	Central	112-119m
600030	MDH22LU905	SW	49-55m
600031	MDH22LU905	SW	56-62m
Transition Composite Samples	**Drill hole ID**	**Zone**	**Sample Depth**
600006	MDH22LU904	Central	26-27m
600028	MDH22LU905	SW	29-34m

Source: Bravo, 2025.

13.4.1.1 Flotation Tests

Bravo's Flotation testing progressed through various series of study to establish material behaviour, characterization, equipment and reagent calibration. Testing was guided by historical data, with the earlier objectives of replicating and validating historical work. potential areas of improvement and optimization were also identified.

Flotation tests were carried out considering differing reagents, primary grind size and circuit flotation cell configurations. This included: pre-flotation of talc, fast rougher, staged roughers, scavenger-roughers, cleaner, cleaner-scavengers and recleaners.

A flotation test was also carried out on a sample of oxide mineralization. The test reported low recoveries with excessive mass pull resulting in low-grade concentrates. Its believe that the presence of clays in the oxide sample inhibits flotation selectivity and explains the poor results. No other tests were performed with oxide samples.

13.4.1.2 Preliminary Exploratory and Characterization Flotation Tests (Series T, TD)

Initial tests used coarse grinding, short flotation times, and lower additions of collector and frothing reagents relative to the historical work. Initial tests also used an amount of depressant (CMC) as required to control the amount and tenacity of talc minerals which are known to inhibit good flotation.

Only the rougher stage was tested in the first three tests of the T series. A cleaner stage was added in the final three tests. The rougher circuit was, as a first pass, a fast flotation stage to produce concentrate with higher concentrations. This represented a preference to generate saleable concentrates as early in the circuit as possible. Moreover, historical data indicated fast flotation of coarse-grained PGM and is supported by observations from the historical Mintek tests.

Results and interpretation from tests T-01 and T-02 demonstrated that talc depression should occur pre-flotation and that a finer grind is required to improve liberation. The initial grind was coarse relative to historical work, at p48 -74µm.

Tests T-03 and T-04 were carried out with a higher dosage of PAX collector, increasing from 20 to 60 g/t. A cleaning stage was also introduced. The introduction of a cleaner stage in the T-04 decreased the final concentrate mass pull dropping to ca. 1%. A similar mass recovery was achieved on the T-01 in fast rougher flotation. Test T-05 saw the introduction of a blend of two collectors, Aero 208 and Aero 3894, known for high selectivity in sulphide, PGM and gold ores.

Furthermore, the TD test series demonstrated that testing was progressing with increasing selectivity, replicating rougher results achieved by Mintek but using lower reagent addition rates. In general, the metallurgical performance of the TD series varied between concentrate grades of 28.7 – 444.0 g/t and 17 – 83.2% recovery. Feed grades varied between 1.0 g/t and 8.7 g/t (Table 13-5).

Table 13-5: Summary of the best results on flotation tests

Test	Sample	Analytical Lab	Feed		Concentrate	
			Grade (g/t PGM+Au)	Mass Recovery	Grade (g/t PGM+Au)	Final Recovery
TD-12	600015	QLS	1.0	0.3	209	79.7
TD-08	600016	QLS	2.6	1.9	443.9	50.8
TD-19	600006/28	QLS	3.3	5.9	44.8	81.1
TD-20	600006/28	QLS	4.8	12.4	28.7	74.5

Source: Bravo, 2025.

13.4.1.3 Comparative Flotation Tests (Series TC)

For the comparative tests, three bench scale flotation tests were carried out. This series aimed to compare the Bravo open circuit general arrangement with the historical closed-circuit arrangement. The comminution time for this series of tests was 80 min, targeting 80% passing -30 µm based on milling times and particle sizes obtained with partial compounds that participated in the compound used in this (TC) series. The TC-Bravo circuit comprised a 6-stage rougher, followed by 5-stage cleaner. This configuration is believed to provide for the same outcome as the circuit design applied in the historical Mintek/Vale closed circuit (three roughers followed by, cleaning, recleaning and cleaner scavenger). An Aero 65 frother was trialled but it did not perform as well as MIBC.

The above tests' best results include 82 g/t concentrate grade with 75% recovery (TC-01) and 189 g/t concentrate grade with 78% recovery (TC-02). The Feed grades were 2.6g/t and 4.6 g/t PGM respectively.

The feed material was a blend of samples 600013, 600015, and 600031.

13.4.1.4 Preliminary Process Circuit Tests (Series TB, TH)

The TB test series represented a circuit configuration of 6-stage rougher with combined rougher concentrates reporting to 5-stage cleaner. The TH circuit evaluated the configuration using reagent dosages as per the historical Vale test work (higher CMC, higher PAX, higher MIBC).

In the TH tests, two circuit options were used: a) suitable for samples with very little or no copper sulphide and b) where a first rougher flotation and a first cleaner adequate to generate a copper concentrate with commercial grade of the order of 25% Cu. This was due to sample 600031 demonstrating higher than anticipated Cu values.

TB and TH tests demonstrated increasing recovery values with the TB process, outperforming on recovery with lower reagent consumption.

Flotation tests using various reagent suits applied to samples assaying 4.4 g/t 3PGM+Au showed a weighted average concentrate grade of 138 g/t with recoveries averaging 74.5%. The performance compares well with, and constitutes a slight improvement, over results in the

MINTEK and VALE historical work, where a concentrate of around 123 g/t PGM+Au with 73.8% recovery was reported.

The TB test series examined the impact of grind size on rougher recoveries applied a new flowsheet configuration. It was shown that, although a finer grind might be expected to improve recoveries slightly, the improvement was marginal and probably does not justify a p80 finer than -38um.

Previous mineralogy studies by L. Cabri indicated that the equal bimodal PGM grain size distribution was around 15-20µm and 45-50µm, whereas Mintek's study indicated that the majority of PGM are less than 15µm. Mineralogy studies indicate that average grain size likely diminishes with decreasing grade.

The preliminary conclusions from these tests are that the different grade profiles within the Luanga deposit may benefit from differing milling parameters. It is expected that a coarser grind will be required for feed grades above 2g/t and finer grind for lower grade material. further testing is required to determine the economic trade-off between the lower grade mineralization profiles, relative to recovery and the need for a grind finer than p80 -38µm (Table 13-6).

Table 13-6: Preliminary results of Process Circuit Tests (Series TB, TH)

Test	Sample	Analytical Lab	Feed		Concentrate	
			Grade (g/t PGM+Au)	Mass Recovery	Grade (g/t PGM+Au)	Final Recovery
TH-07B	600026	SGS	0.7	1.5	39	61.3
TB-05	600015	SGS	1.57	1.9	78.2	74.0
TB-04	600030	SGS	3.7	0.67	475.2	75.3
TB-07* Rgh Only	600031	SGS	7.7	8.6	136	74.7
TB-08* Rgh Only	600032	SGS	7.4	11.1	74.1	81.8

Source: Bravo, 2025.

13.4.1.5 Fines Flotation Tests

Historical mineralogy and flotation test work on Luanga mineralization established that a significant component of the PGM grain size distribution is concentrated in the range of 3-15 µm. It is well-known that fine and ultrafine liberated valuable particles are often lost to flotation tailings due to inefficient flotation mechanisms and the passivation of their surfaces by oxidation products and slimes. Fine particle recovery is recognized as an area where potential improvement and optimization may be possible.

Extensive research and development covering a diverse range of technologies have been undertaken over the years to find feasible solutions with the most widely adopted, extra-cellular technology being hydrodynamic cavitation devices (HCDs), causing the nucleation of ultrafine nano bubbles (NBs) on the surfaces of fine valuable particles, thus aiding their agglomeration and subsequent recovery by micro-bubbles (MBs) and normal sized (macro) flotation bubbles. The Mach Reactor HCD has found wide adoption, particularly in flotation plants recovering PGM from tailings dams through the demonstration of material improvement in flotation performance from feedstock with low grades (0.3-1g/t) and ultrafine grain size distributions (-5 to -10µm).

HCDs have been demonstrated to increase recovery (+10%) and lower capital and operating costs. The Mach reactor is now a frequent addition to commercial PGM flotation plants in South Africa.

Bravo submitted to Mintek in South Africa a 30kg sample for hydrodynamic cavitation testing using the Mach reactor (Figure 13-3). The reactor consists of an array of venturi nozzles in series or a multitude of parallel, restricted apertures in which intimate contact is achieved between the fine particles and the distribution of very fine bubbles that are formed due to cavitation and the conditions of high shear. This results in a hydrodynamic environment in the pulp zone which contrasts markedly with that observed with conventional flotation equipment.

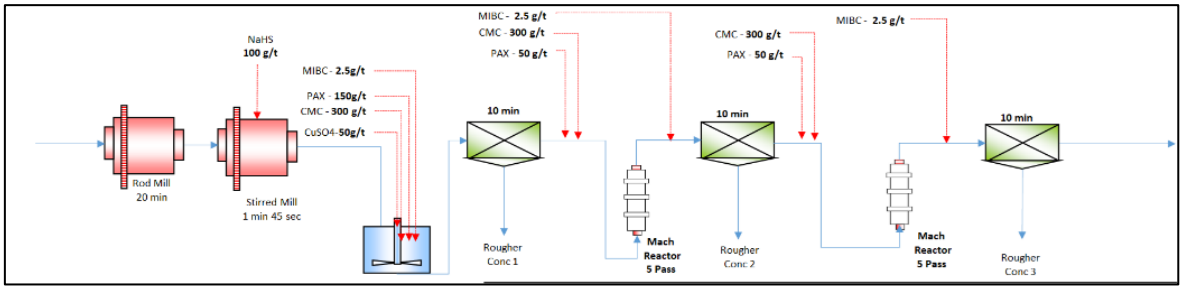

Figure 13-3: Test flowsheet and parameters used by Mintek.

Source: Bravo, 2023.

Three control tests and 5 active Mach reactor tests were performed using a sample feed of 2,66 g/t. Test 4 demonstrated a 6.1% improvement in recovery with similar mass pull and concentrate grade metrics for the three stage rougher circuit.

Results below in Table 13-7 demonstrate the potential improvements achievable by incorporating the Mach Reactor for Luanga ores, particularly lower grade ores where fine PGM particles predominate. Further recovery improvements are anticipated at varying grind sizes and with revisiting floatation cleaner stage performance. In commercial plant Mach Reactors are typically installed in the rougher, cleaner and scavenger stages.

Table 13-7: Results from fines flotation tests

Scenario	Description	Mass Pull (%)	4E grade (g/t)	Recovery (%)	Average Recovery (%)	Rec. Improve (%)
1	0 Pass 1A	9.17	22.27	74.74	74.5	-
	0 Pass 1B	10.2	20.9	73.9		
	0 Pass 1C	10.2	20.8	74.8		
2	10 Pass 2A	18.5	10.6	76	75.9	1.4
	10 Pass 2B	19.3	9.9	75.9		
	10 Pass 2C	18.9	9.5	75.8		
3	5 Pass + N CMC dosage	11.8	18.3	78.8	78.8	4.3
4	2 x 10 Pass + N CMC dosage	11.5	19	80.5	80.5	6.1

Source: Bravo, 2023.

13.4.1.6 Associated Base Metals

Historical Luanga test work had almost exclusively focused on the recovery performance of the platinum group metals. Generally, this is attributed to the very low mass pull on bench scale tests which produce only enough sample to analyse for PGM's. However, two locked cycle tests performed by Vale did produce adequate concentrate to examine the performance of nickel-sulphide recovery in the flotation process (Table 13-8).

Table 13-8: Nickel sulphide flotation results

CDM Vale LCT Tests 2003	Feed Grade Ni (%)	Conc Grade Ni Sulphide (%)	Ni Sulphide Recovery (%)
LTC1	0.19	7.5	47.3
LTC2	0.19	9.8	45.9

Source: Bravo, 2023.

Bravo encountered similar nickel analysis challenges due to low concentrate weights so will only be able to confirm in future testing programs.

13.4.2 Transition Material

Historically, a component of the mineralized body below the oxide horizon was classified as "transition" material based on geological observations including surficial, oxidative staining on host rock samples. Bravo investigated the metallurgical amenability of this domain by performing comparative rougher flotation tests using a coarse grind benchmarked against the abovementioned T series tests and additional comparative flotation results.

22 Transition flotation tests were performed through a grade range of 0.38 – 7.95 g/t PGM's. Samples were milled to p60 -74µm. Table 13-9 shows Test T1-2 as benchmark, fresh rock, control tests vs TBS 19, 11 and 16 as transition material flotation tests (Table 13-9).

Table 13-9: Results of transition material on flotation tests

Rougher Comparative Test	Feed grade (g/t)	Mass Pull (%)	Recovery (%)	Concentrate Grade (g/t)
T1	2.18	10.9	38.0	7.2
T2	2.21	8.7	35.6	9.1
T3	2.23	12.6	47.2	8.4
TBS19	1.81	3.7	36.0	18.0
TBS11	1.36	4.4	51.0	16.0
TBS16	1.94	6.2	37.0	12.0

Source: Bravo, 2023.

The comparative results above demonstrate that the previously classified "transition" domain mineralization responds similarly to the rougher performance of fresh rock material at Luanga and thus it is concluded, from a process metallurgy perspective, that the "transition" domain be considered as fresh rock material.

13.4.3 Oxide Material

The Luanga PGM deposit is characterized at surface by an extensively weathered mineralization zone constrained from surface down to depths of 5 to 30m. It is a sensu stricto oxide horizon with most, if not all, sulphide mineralization minerals (including nickel sulphides) altered to oxide phases with the host rock altered to limonitic/saprolitic phases. Historical mineralogy and test work had led the previous owner not to consider the possibility of recovering PGM from the oxide zone. This was attributed to the oxidized state of metallic mineralization minerals and the abundance of clay material, contributing to poor flotation recoveries, low selectivity and high concentrate mass pulls.

The oxide horizon at Luanga does however account for approximately 10% of historically stated resources by tonnes. Three salient points have led Bravo to review and investigate the possibility of recovering PGM from the oxide mineralization.

PGM grades in the historical oxide horizon appear to be on average, higher than those reported in the fresh rock horizon. Thus, the resource ounce contribution of the oxide mineralization to the total resource is higher than observed from a resource tonnes perspective. The oxide horizon demonstrates some ultrahigh PGM grade intersections, not commonly seen elsewhere in the world.

Due to their refractory nature, platinum group minerals tend not to respond strongly to atmospheric induced weathering, even within deeply weathered profiles. This mineral character presents an opportunity to explore recovery methods that recognise the characteristics of the preserved platinum group minerals, considering either their physiochemical properties and/or gravimetric properties.

The oxide horizon was considered sterile and thus represents an additional waste stripping expenditure item by the previous owner. Should sufficient value be unlocked by establishing an economic processing route that returns capital and operating costs, potential economic benefit can be realized for the global Luanga mineralized body/project by partial stripping cost offset.

Sighter flotation tests, including pre-desliming, were also performed but were condemnatory in nature. The results re-affirmed low recoveries, high mass pulls and low concentrate grades. However, Bravo identified gravimetric separation and cyanide leaching as processing routes that may hold potential to treat oxide mineralization at Luanga.

Note that in the current MRE estimate, the oxide component has been revised and reduced to 5%, so significantly reducing the potentially commercial importance of the oxide zone

13.4.3.1 Gravimetric Tests

Three gravity concentration tests were performed using a Knelson concentrator with sample feed grades of 1.45g/t - 1.91g/t (Figure 13-4).

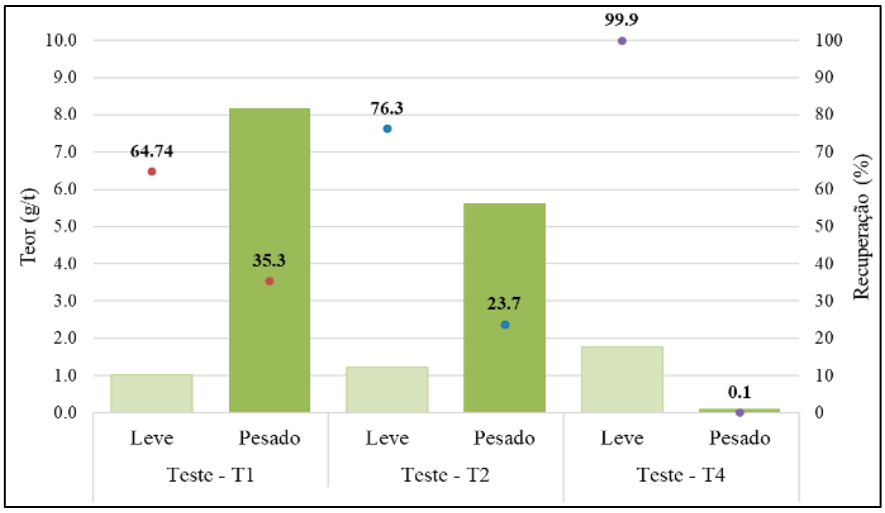

Figure 13-4: Results of gravimetric tests

Source: Bravo, 2023.

The above results demonstrate improved recoveries to the underflow but is still insufficient to envisage that an economic recovery process and saleable product can be developed using a centrifugal concentrator

cyclone tests were carried out using a 40mm Weir hydro-cyclone. Two tests were performed using split material with similar grades from the gravimetric sample feedstock. The hydro-cyclone apex and vortex finder diameters were 4.0 and 10.0 mm, respectively. Table 13-10 presents the operating conditions including mass and volumetric flows, percentage of solids in the streams, as well as mass partition results and desliming efficiency data.

Table 13-10: Operating conditions – hydro-cyclone test

Test	P (KPa)	t (s)	Corrente	mpolpa (g)	msólio (g)	mágua (g)	Vpolpa (ml)
1	250	5.8	Overflow	3,550	127.8	3,422.22	3,470
			Underflow	984	263.2	721.11	819
			Feed	4534	391	4,143.33	4,288
		Qp (L/h)	Wp (kg/h)	Ws (Kg/h)	% Ws	% sol.	ET (%)
		2153.5	2,203.4	79.3	32.7	3.6	67.3
		508.1	611	163.4	67.3	26.7	
		2661.6	2,814.4	242.7	100	8.6	

Source: Bravo, 2023.

After optimizing conditions, a mass recovery for the underflow stream in the first stage desliming of 67.3% was obtained using a feed pressure of 250 KPa. The percentages of solids obtained in the underflow and overflow in the first stage were 26.7% and 3.6%, respectively.

The overall recovery of PGM+Au was 86.7% in the underflow stream, after two desliming stages, the first with a hydro-cyclone and the second stage with siphoning using Stokes' Law of sedimentation. The overall mass recovery considering the two steps was 55.3% (Table 13-11). It is interesting to note that the global metallurgical recovery of Pt was 96.4%, being 97.2% in the first stage and 99.2% in the second stage.

Similar to the Knelson tests, the concentrate grades produced were only marginally above the feed grade and are below commercial requirements.

Table 13-11: Results of hydro-cyclone tests

Products	Mass Balance		Grades (g/t)					
1º Stage – T1	m (g)	%	Rh	Pd	Pt	Au	PGM	PGM+Au
Over 1	127.8	32.7	0.005	0.41	0.08	0	0.5	0.5
Under 1	263.2	67.3	0.006	0.45	1.4	0.05	1.86	1.91
Totais	391	100	0.006	0.44	0.97	0.03	1.41	1.45
2º Stage – T1	m (g)	%	Rh	Pd	Pt	Au	PGM	PGM+Au
Over 2 (sifonado)	1,708.1	17.87	0.003	0.14	0.06	0.04	0.21	0.25
Under 2	7,850.9	82.13	0.007	0.516	1,696	0.052	2,219	2,270
Totais	9,559	100	0.006	0.45	1.4	0.05	1.86	1.91
	Global Rec.	55.3						

	Met. Recovery (%)					
	Rh	Pd	Pt	Au	PGM	PGM+Au
	28.8	30.76	2.82	0	11.55	11.28
	71.2	69.24	97.18	100	88.45	88.72
	100	100	100	100	100	100
	Rh	Pd	Pt	Au	PGM	PGM+Au
	9.83	5.61	0.78	15.26	1.97	2.32
	90.17	94.39	99.22	84.74	98.03	97.68
	100	100	100	100	100	100
Global Rec.	64.2	65.4	96.4	84.7	86.7	86.7

Source: Bravo, 2023.

13.4.3.2 Hydrometallurgical Cyanide Leaching – Phase 1 Exploratory Program

Exploratory leaching tests were performed on oxide samples 600004 and 600005. These samples were collected from Bravo twin metallurgical drill hole MDH22LU904 (Central Sector) from approximately 9-18m depth within the oxide mineralization. Samples were homogenized and split samples from each volume were generated for head grade assay analysis at SGS Geosol. Average grades across the three samples for respective volumes and elements are presented on Table 13-12.

Table 13-12: Average grades obtained on hydrometallurgical cyanide leaching tests

Sample	Au (g/t)	Pd (g/t)	Pt (g/t)	Rh (g/t)	4E Total (g/t)
Volume A (4)	0.22	1.11	0.49	0.06	1.88
Volume B (5)	0.25	0.95	1.95	0.09	3.24

Source: Bravo, 2023.

- Direct Leaching and Carbon-in-Leach Tests

Direct leaching and Carbon-in-Leach (CIL) tests were performed to investigate the response of PGM's at differing grind sizes (p80 -1/8"and p80 -75µm). Sodium cyanide (CN) addition rates were also varied to establish concentration, influence and effective consumption rates. These tests were done at cyanide addition rates of 1000, 5000, and 10000 g/t to evaluate

PGM solubility. The tests were undertaken using 35% solids to promote an amenable pulp viscosity conducive for a good leaching environment. The influence of desliming and leaching with activated carbon were also evaluated.

13.4.4 Study Conclusions and Results

Generally, metal recoveries improved with CN concentration and as the grind size was decreased from p80 -1/8”to p80 -75µm. The later was credited to improved liberation, especially from remnant rock fragments within the oxide material.

The addition of activated carbon improved the final recoveries of PGM. The following percentage improvements in recovery were observed in Table 13-13:

Table 13-13: Recovery with the addition of activated carbon

DL vs CIL	Au	Pd	Pt	Rh
Recovery Improvement (above direct leach)	+1.4 %	+5.5 %	+235%	+74.4%

Source: Bravo, 2023.

Desliming by gravity prior to either direct or CIL leaching showed further improvements in global recoveries due to the purported removal of potential preg-robbing, ultrafine clays. The following better recoveries are reported below (Table 13-14):

Table 13-14: Recovery with the addition of activated carbon and desliming by gravity

DL vs CIL	Au	Pd	Pt	Rh
Recovery CIL (onto carbon)	93.7 %	51.1 %	6.7 %	30.0 %
Deslimed CIL	Au	Pd	Pt	Rh
Recovery CIL (onto carbon)	93.3 %	62.7 %	23.8 %	60.8 %

Source: Bravo, 2023.

In general, it was observed that cyanide concentration does not impact gold and rhodium recoveries but increasing cyanide concentrations improved platinum and palladium recoveries.

Effective consumption rate for cyanide varied between 900 and 4000 g/t across tests. Lime consumption varied between 17 and 20 kg/t across tests. To reduce net cyanide consumption, future consideration should be given to the inclusion of a cyanide reclamation/recovery circuit.

Gold, palladium and rhodium leach kinetics were relatively high compared to the substantially lower kinetics seen for platinum.

The conclusion of this exploratory test program demonstrates that PGM’s from the Luanga oxide zones are potentially amenable to cyanide leaching. It was strongly recommended that a more detailed and comprehensive test program be undertaken to further develop and optimize processing parameters.

13.4.4.1 Leaching at Lower pH

Preliminary tests have been concluded investigating the impact of lower pH on PGM recoveries, particularly on palladium. Using lower pH is well documented in published technical reports which highlight improved palladium recoveries at lower pH. For these tests, lime consumption varied between 3.4 – 11.0 kg/t, lowered from the Phase 1 lime consumption range of 17 – 20 kg/t. All tests demonstrated material improvement in palladium recovery, with the best achieved recovery totalling 81.4% at a lime consumption rate or 11.0 kg/t and effective cyanide consumption of 4.3kg/t.

Gold, platinum and rhodium recoveries under these conditions were negligible and demonstrated the potential for effective sequential PGM leaching under differing pH and cyanide concentration conditions.

13.4.4.2 Carbon Loading and Ashing Tests

Following the encouraging leaching results described above, Bravo investigated the loading potential of PGM onto carbon in a CIL circuit and the potential to produce a final “ashed” residue saleable product. Both loaded carbon and ashed carbon residue represent a saleable product. To achieve sufficient product for analysis (particularly the ashing product) a large volume solution sample was prepared to generate sufficient loaded carbon mass.

The sample was prepared in the following manner:

A tailings oxide pulp sample was analyzed and charged with dissolved gold, platinum, palladium and rhodium such that the final precious metals in-solution concentrations equalled the solution concentration of a direct leach according to observed recovery rates in tests from Phase 1. The average recoveries considered in this calculation were as follows (Table 13-15):

Table 13-15: The average recoveries considered in tests from Phase 1

Element	Au	Pd		Pt	Rh
Recovery	95 %	60 %		20 %	40 %

Source: Bravo, 2023.

Activated carbon was introduced to the system and maintained for 24 hours.

Filtered carbon was homogenized and split with duplicate samples submitted to SGS for fire assay analysis and CETEM for ICP-OES analysis and muffle furnace ashing.

PGM showed high levels of loading onto carbon with high carbon PGM grades and high adsorption recoveries. The analytical results from SGS and CETEM are summarized below (Table 13-16). Due to equipment constraints, rhodium could not be analyzed, and grades were calculated based on mass balance.

Table 13-16: Average grades obtained on Carbon Loading and Ashing Tests

Laboratory	Au (g/t)	Pd (g/t)	Pt (g/t)	Rh (g/t)	3E PGM
SGS Geosol	41.6	819.6	384.3	134.9	1380.4
CETEM	43.2	846.3	404.7	135.0	1429.2
Adsorption Recovery	99.7 %	99.7 %	92.5 %	n/d	

Source: Bravo, 2023.

13.4.4.3 Ashing Tests

In order to investigate the production of a high-grade ashed residue final product in place of a sequential elution or doré product, two ashing tests were conducted to support marketing studies.

Two 20g loaded carbon samples split from the CETEM carbon analysis samples were ashed in a bench-scale muffle furnace at CETEM

For both tests, the residual fraction mass was 0.24 grams representing a 98.8 % reduction in mass. The resultant final product grade was calculated on mass balance and summarized below (Table 13-17):

Table 13-17: Average grades obtained on ashing tests

Ashed Residue	Au (g/t)	Pd (g/t)	Pt (g/t)	Rh (g/t)	4E_PGM+Au (g/t)
Grade	3 600	70 525	33 725	11 250	119 100

Source: Bravo, 2023.

The final product was highly enriched in PGM, demonstrating a total PGM grade of 119.1 kg/t or 11.91% by weight.

Note - whilst the above various oxide tests are very encouraging and warrant further investigation in the current MRE, the oxide tonnage component as a proportion of the total tonnage, has been revised down, reducing the importance of the oxide zone

13.5 Bravo 2024/2025 Program – Fresh Sulphide

13.5.1 Sampling

A global bulk composite from the north Sector of the Luanga deposit, totalling approximately 3.6 tonnes, was constituted from diamond drill core samples. Samples totalling 947 were collected by quarter-core from the MSZ unit of the deposit (Figure 13-5). A homogenized sub-sample analysis reported an average grade of 2.4 g/t 4E PGM and 0.19% Ni.

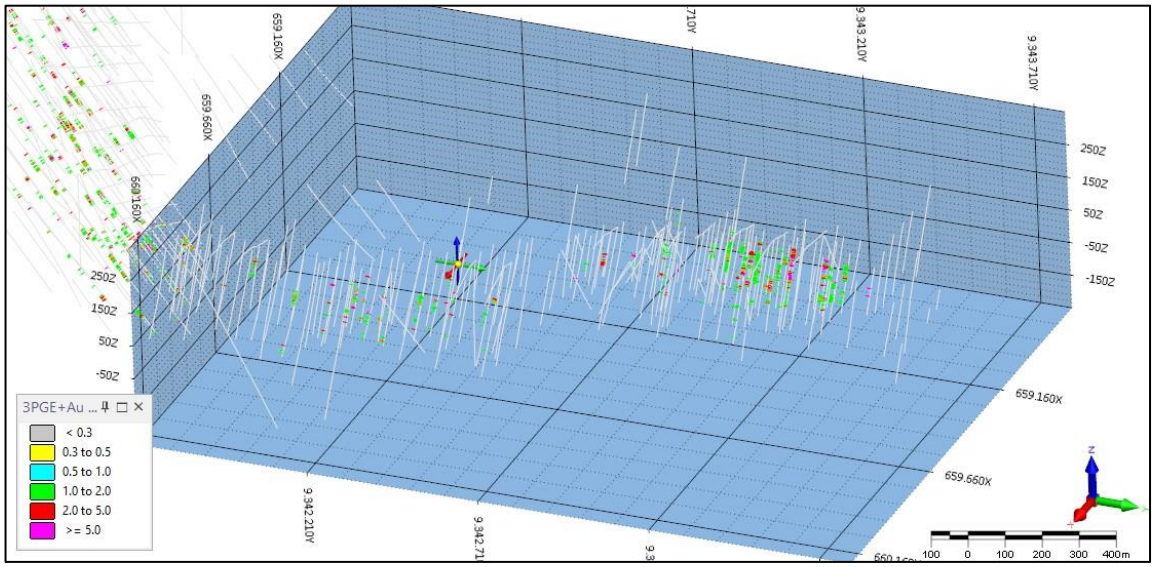

Figure 13-5: Image showing the distribution of samples collected in the north global bulk sample constitution

Source: Bravo, 2025.

Similar global composites were prepared for the Central and Southwest Sectors of the deposit. The Central and SW Sector composite was used in conjunction with the North Sector composite for detailed comminution test work, while only the North composite was used in further minerals processing tests thus far. It is envisioned that a similar scope of work will be applied to the Central and Southwest Sector global composites subsequently.

13.5.2 Comminution

Metso Brazil was contracted to perform detailed comminution tests on North, Central and Southwest Sector global composite material. A sub-sample of 200kg from each composite was selected and sent to Metso in Belo Horizonte. The scope of work was to conduct industry-standard laboratory tests to obtain physical material characteristics that will assist in process route definition and equipment sizing. Tests completed on samples from each deposit Sector include:

- Bond Abrasion Index
- Macon Abrasion Index
- Macon Crushability
- Bond Work Index
- Bulk Density
- Specific Gravity
- Volumetric Capacity Index
- Strength Index
- Product Flakiness Index

The results of tests 1 -9 are summarised in the table below (Table 13-18).

Table 13-18: Comminution test results

Test	Deposit Sector					
	North	Comment	Central	Comment	SW	Comment
Bond Abrasion Index (Ai)	0.07	Low Abrasive	0.091g	Low Abrasive	0.044g	Low Abrasive
Macon Abrasion Index (Ai)	228 g/t	Low Abrasive	502 g/t	Low Abrasive	148 g/t	Low Abrasive
Macon Crushability (Cr)	32.40%	Medium	29.10%	Medium	37.70%	Medium
Bond Standard Ball Mill (Wi)	14.98 kW/t	Med-Hard	18.91 kWh/t	Hard	14.43 kW/t	Med-Hard
Bond Standard Rod (Wi)	16.4 kWh/st	Hard	19.3 kWh/st	Very Hard	16.5 kWh/st	Hard
SAG Circuit Specific Energy	10.56 kWh/t		11.75 kWh/t		9.44 kWh/t	
Bulk Density (Y)	1.68 t/m3		1.73 t/m3		1.71 t/m3	
Specific Gravity (Yr)	2.95 t/m3		3.03 t/m3		2.91 t/m3	
Volumetric Capacity Index (C)	83.13%	Minimum	77.89%	Minimum	75.46%	Minimum
Strength Index (R)	190.64%	Minimum	248.31%	Minimum	161.97%	Minimum
Product Flakiness Index (L)	1.69%	Cubical Material	14.16%	Cubical Material	14.16%	Cubical Material

Source: Bravo, 2025.

The North and Southwest Sectors exhibit material which has low abrasion qualities, moderate crushability and medium to hard indices for ball milling. The Central Sector exhibits a higher material hardness, with higher abrasion, crushability and milling indices. All three sectors exhibit very similar SAG Circuit Specific Energy values.

13.5.3 Flotation

Bravo conducted several flotation optimization programs: including testing at CETEM, independent verification and optimization program at Base Metal Laboratories (BML) in Canada and a series of mini-plant flotation tests at CETEM.

13.5.3.1 Parameter Optimization Program – CETEM

Basic rougher kinetic style tests were conducted investigating conditioning time, cell energy input, pH and pulp density impact on rougher performance (Figure 13-6).

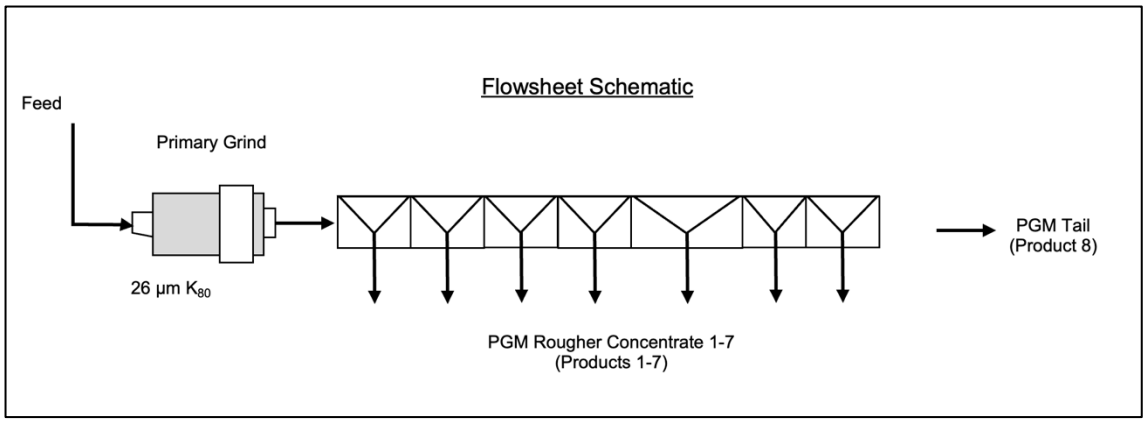

Figure 13-6: Image showing the distribution of samples collected in the north global bulk sample constitution

Source: Bravo, 2025.

Base line conditions included a 60 min grind time to achieve p80 -28µ grind size. CMC addition was 400 g/t with a 1 min conditioning time. Collector, frother, individual conditioning and

flotation times are demonstrated in the table below (Table 13-19). Tests were conducted in a 3l cell using a Denver flotation machine with base line impeller speed at 1050 rpm.

Table 13-19: Collector, frother, individual conditioning and flotation times

Stage	Reagents - g/tonne				Time Minutes		Electrochemistry	
	CMC	MIX AERO 3894 + SENXOC 2	PAX	MIBC	Condition	Float	pH	Eh-mV
Primary Grind					60			
Rougher Condion	400				1			
Rougher 1		20		30	30''	2		
Rougher 2			20		30''	3		
Rougher 3			20		30''	5		
Rougher 4			20		30''	5		
Rougher 5			20		30''	5		
Rougher 6			20		30''	5		
Rougher 7			20		30''	5		

Source: Bravo, 2023.

Longer conditioning times demonstrated improvements in fast rougher recovery, fast rougher concentrate grade and final concentrate grade but only marginal improvement in total rougher recovery.

Higher cell rotation velocities improved performance in fast rougher recovery, concentrate grade and total rougher recovery, while the final rougher concentrate was lower than base line. Nickel recovery improved materially.

Highly alkaline cell conditions adversely affected performance while acidifying the naturally alkaline pulp to 7.5 marginally improved total recovery for PGM while adversely affecting Ni recovery.

Higher pulp density positively impacted total rougher recovery for PGM and Ni but adversely affected selectivity with a drop in concentrate grade relative to a lower 20% pulp density, which showed improved selectivity in both the fast and total rougher concentrate grade (Table 13-20).

Table 13-20: Average grades obtained on mini-plant flotation tests at CETEM

Test	Parameter	FRgh Rec %	Fast Rgh Conc g/t	Total Rgh Grade	Total Rgh Rec % PGM	Total Rgh Rec % Ni	Tail Grade
Baseline K		16.60	19.70	8.90	79.60	58.80	0.79
Test 1	Cond 1'30"	8.06	125.47	8.20	81.49	57.82	0.69
Test 2	Cond 5'	9.05	158.13	10.10	77.73	53.84	0.81
Test 3	Cond 10'	10.02	252.02	12.20	80.02	50.34	0.72
Test 4	Rot 1200 rpm	16.41	101.93	6.90	87.07	64.64	0.54
Test 5	Rot 900 rpm	3.70	52.03	9.50	71.89	47.00	0.98
Test 6	pH 11.5	8.12	35.99	6.50	73.20	51.46	0.99
Test 7	pH 7.5	17.00	116.52	8.20	83.12	52.08	0.71
Test 8	pH 4.5	13.10	91.13	7.90	82.10	54.07	0.69
Test 9	Sol 20%	14.09	120.43	12.80	79.54	48.83	0.74
Test 10	Sol 40%	18.77	49.24	6.80	86.88	61.40	0.57

Source: Bravo, 2025.

13.5.4 Base Metal Laboratories

Base Metal Laboratories in Kamloops, Canada, were contracted to independently perform flotation test work, principally on the North Sector global composite. Initial exploratory tests were also conducted on the Central Sector global composite.

13.5.4.1 Sample Characteristics

Analyses were performed to measure feed characteristics. These included chemical analysis using standard analytical techniques as well as fiber analysis on the North Sector composite. A summary of the chemical data is shown in Table 13-21.

Table 13-21: Average feed samples before the tests

Sample	Assays - percent or g/t						
	Pd	Pt	Au	3E	Ni	Cu	S
North Zone Composite	1.45	1.09	0.08	2.61	0.21	0.049	1.28
Central Zone Composite	1.73	0.56	0.05	2.35	0.25	0.045	0.64

Source: Bravo, 2025.

The North Sector composite measured 1.45 g/t Pd, 1.09g/t Pt, and 0.08 g/t Au for a combined content of 2.61g/t (denoted as 3E throughout this program). The Central Sector composite measures higher Pd and lower Pt at 1.73 and 0.56 g/t, respectively, resulting in a slightly lower 3E of 2.35g/t. Nickel was about 0.21 to 0.25 in both composites. The sulphur content was quite different between the two, measuring 1.28 percent in the North Sector composite and 0.64 percent in the Central Sector composite.

The ratio of sulphur to other elements may be an important consideration when considering concentrate grade from a bulk sulphide flotation process; higher PGM and nickel concentrate grades may be possible from the Central Sector composite, provided the non-sulphide gangue can be reasonably rejected.

13.5.4.2 Metallurgical Tests

Metallurgical testing was conducted on the samples to evaluate currently considered processing options, and to conduct optimization of the conditions and flowsheet. Development testing focused on the North Sector composite and investigated various parameters. Two locked cycle tests were conducted on the North Sector composite. The Central Sector composite was tested with the same (North Sector) flowsheet, including a single locked cycle test. The metallurgical test data is discussed in the following sub-sections.

13.5.4.3 Rougher Test Work

Rougher kinetic tests were conducted to determine the mass recovery versus metal recovery for various conditions. Historical testing on the project indicated fine-grained PGMs and sulphides were present, and a fine primary grind was required. A primary grind series of tests and some alternative flowsheet configurations, including multistage grinding (MF2 – mill float), were

tested. Talc, a naturally hydrophobic gangue mineral, was present and will need to be controlled to avoid dilution of the final concentrate. PE26, a CMC starch-based depressant was used in testing. Talc Pre-flotation was also briefly evaluated in select tests. A summary of the rougher flotation test conditions and results are shown in Table 13-22 and Table 13-23

Table 13-22: Rougher test work parameters

Composite	Test	General Description	PG	g/t		Time
			µm K80	PE26	PAX	Min
North Zone	T01	Effect of PG*	46	425	88	20
	T02	Prefloat	46	0	98	25
	T03	Grav	46	400	88	20
	T04	Effect of PG	30	550	88	20
	T05	Effect of density	30	550	88	20
	T06	Effect of PG	82	400	88	20
	T08	Effect of PG	20	750	215	25
	T10	H2S04 pH 7.5	30	750	165	20
	T12	Calgon	30	550	328	30
	T13	MF2	46/18	900	228	23
	T14	Prefloat	30	200	118	20
	T21	Effect of density/Collector	30	650	328	24
	T22	Effect of density/Collector	30	700	328	24
	T23	800g/t Calgon	30	650	328	24
	T25	Fine/Coarse Circuit	46/43	770	106	31
Central Zone	T28	Baseline	33	475	88	25
	T31	Increase PE 26	33	825	88	25
	T32	Effect of PG	27	725	88	25

*PG = primary Grind
Source: Bravo, 2025.

Table 13-23: Average grades obtained on rougher test work

Composite	Test	Mass %	Assay - percent or g/t							Distribution - percent					
			Pd	Pt	Au	3E	Ni	Cu	S	Pd	Pt	Au	3E	Ni	Cu	S
	T02	14.6	5.8	5.0	0.2	11.1	0.9	0.2	5.6	57.0	59.0	39.0	57.0	59.0	64.0	63.0
	T03	34.2	2.7	1.4	0.7	4.8	0.3	0.1	1.2	72.0	61.0	97.0	71.0	56.0	93.0	32.0
	T04	22.6	5.0	3.4	0.2	8.7	0.6	0.2	1.9	77.0	76.0	77.0	77.0	65.0	94.0	34.0
	T05	12.2	7.7	7.8	0.5	15.9	1.2	0.4	3.5	73.0	77.0	62.0	74.0	66.0	94.0	33.0
	T06	37.1	3.1	2.3	0.2	5.6	0.3	0.1	0.8	74.0	74.0	77.0	74.0	54.0	92.0	22.0
	T08	16.7	5.5	5.0	0.3	10.8	1.0	0.3	6.4	80.0	81.0	72.0	80.0	76.0	95.0	82.0
	T10	19.4	5.0	4.7	0.2	10.0	0.8	0.2	3.4	77.0	81.0	72.0	79.0	70.0	95.0	53.0
	T12	18.0	8.3	5.4	0.3	14.0	0.9	0.3	3.5	87.0	81.0	71.0	84.0	71.0	92.0	51.0
	T13	15.3	8.4	5.3	0.3	14.0	1.0	0.3	3.4	90.0	75.0	62.0	83.0	70.0	91.0	40.0
	T14	17.3	6.7	4.1	0.3	11.1	0.8	0.3	3.4	78.0	70.0	48.0	73.0	64.0	89.0	45.0
	T21	29.9	4.9	3.1	0.1	8.1	0.5	0.2	1.9	86.0	85.0	76.0	86.0	70.0	95.0	46.0
	T22	11.9	11.7	8.4	0.4	20.6	1.2	0.4	4.7	84.0	80.0	75.0	82.0	70.0	94.0	43.0
	T23	15.6	8.6	6.5	0.4	15.4	0.9	0.3	3.7	85.0	83.0	77.0	84.0	75.0	92.0	47.0
	T25	14.6	10.0	5.6	1.2	16.7	1.0	0.3	5.4	85.0	78.0	92.0	83.0	70.0	95.0	56.0
Central Zone	T28	16.5	8.3	3.1	0.8	12.2	1.1	0.3	2.1	74.0	67.0	94.0	73.0	66.0	91.0	49.0
	T31	9.6	13.1	5.3	1.0	19.4	2.1	0.4	4.0	78.0	76.0	91.0	78.0	71.0	93.0	63.0
	T32	13.6	9.3	4.1	0.8	14.1	1.4	0.3	2.6	80.0	76.0	93.0	79.0	68.0	90.0	55.0

Source: Bravo, 2025.

The 3E rougher recovery ranged from 57 to 86 percent, at mass recoveries of 10 to 37 percent. The Mass Versus recovery for 3E is shown in Figure 13-7. In general, there was a significant component of the metals of interest that was fast floating. Past a certain point, the

incremental recovery was quite low, with only a marginal increase in recovery with significant mass recovery. Production of a flash concentrate, producing final concentrate from rougher 1 may be possible. Jameson flotation technology may be a suitable means to recover a portion of the final concentrate material from the rougher.

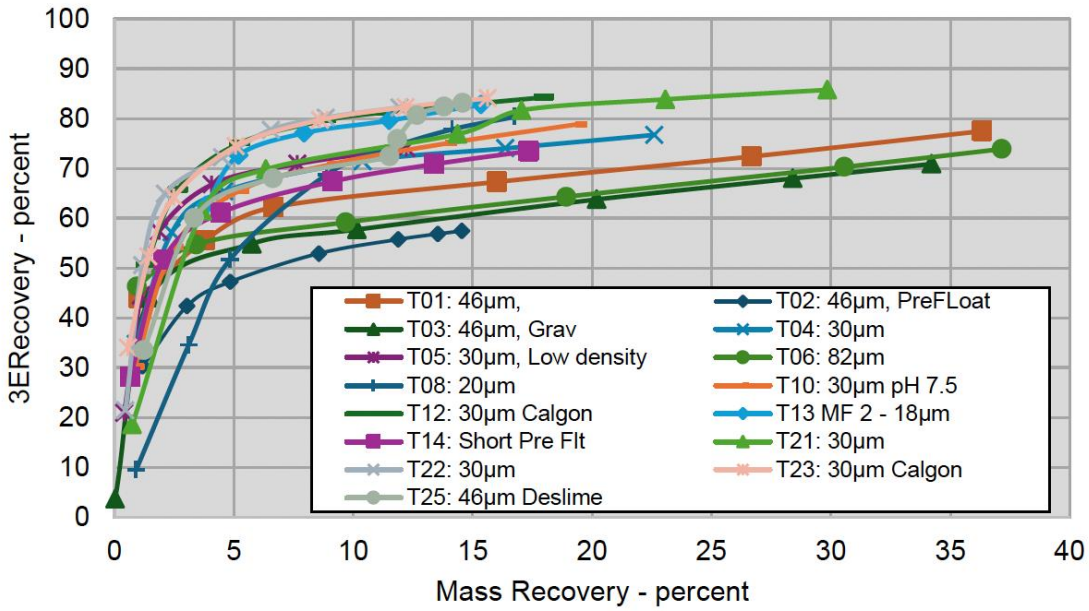

Figure 13-7: The mass versus recovery for 3E

Source: Bravo, 2025.

The primary grind was confirmed to be a significant contributing factor to recovery. The highest recoveries were generally achieved at 30µm K80 or finer primary grinding. Figure 13-8 displays the grade of the rougher tailings versus the primary grind sizing for Pd, Pt, and 3E. Although there is some noise in the data from other changing variables and inherent test variation, there is a clear trend of decreasing PGM tails grade with finer grinding. The tails data is also presented in Table 13-24.

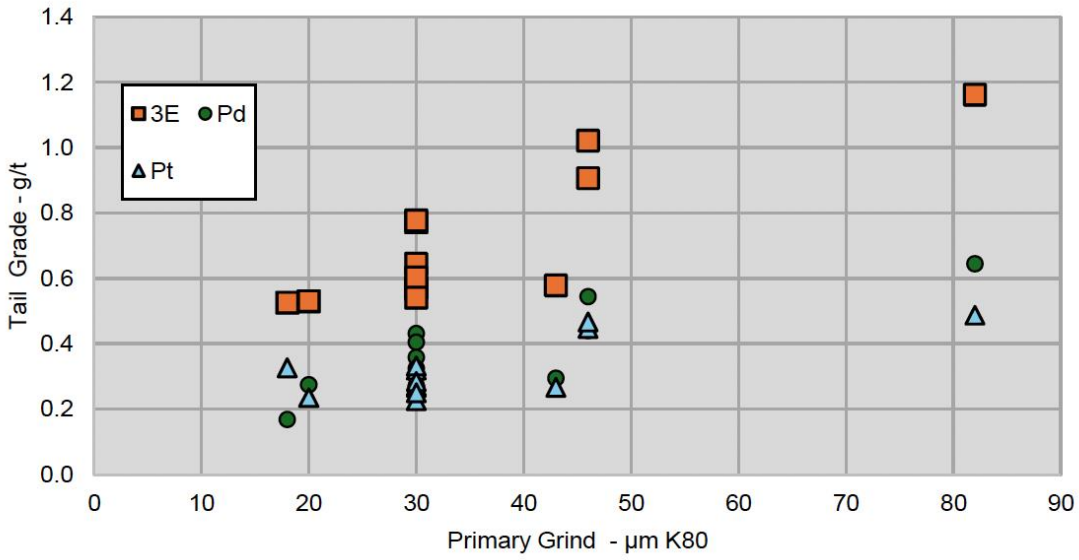

Figure 13-8: Grades of the rougher tailings versus the primary grind sizing for Pd, Pt, and 3E.

Source: Bravo, 2025.

Table 13-24: Average grades obtained on rougher test work in tails

Composite	Test	General Description	Sizing	Rougher Tail Assay - percent or g/t					
			µm K80	Pd	Pt	Au	3E	Ni	S
North Zone	T08	Effect of Primary Grind	20.00	0.27	0.24	0.02	0.53	0.06	0.28
	T04		30.00	0.43	0.32	0.02	0.77	0.10	1.08
	T01		46.00	0.44	0.45	0.02	0.91	0.14	1.42
	T06		82.00	0.64	0.49	0.03	1.16	0.14	1.58
	T05	Effect of density (2kg/8L)	30.00	0.40	0.33	0.04	0.78	0.08	0.97
	T21	Effect of density/Collector (2kg/4L)	30.00	0.32	0.23	0.02	0.57	0.09	0.95
	T22	Effect of density/Collector (2kg/8L)	30.00	0.30	0.28	0.02	0.60	0.07	0.84
	T12	Calgon	30.00	0.27	0.27	0.03	0.57	0.08	0.72
	T23	800g/t Calgon	30.00	0.27	0.25	0.02	0.54	0.06	0.80
	T03	Gravity Included	46.00	0.54	0.47	0.01	1.02	0.14	1.35
	T10	H2S04 pH 7.5	30.00	0.36	0.27	0.02	0.65	0.08	0.74
	T13	MF2	18.00	0.17	0.33	0.03	0.53	0.08	0.94
	T25	Fine/Coarse Circuit	43.00	0.29	0.27	0.00	0.58	0.08	0.70
Central	T28	Baseline	33.00	0.56	0.30	0.01	0.87	0.1 1	0.43
	T31	Increase PE 26	33.00	0.40	0.18	0.01	0.59	0.09	0.25
	T32	Effect of Primary Grind	27.00	0.37	0.20	0.01	0.59	0.10	0.33

Source: Bravo, 2025.

13.5.4.4 Cleaner Test Work

Cleaner testing was conducted to determine the concentrate quality and recovery in the open circuit and to guide conditions for locked cycle testing. Multiple flowsheets were tested with various reagent dosages and with and without regrinding. The main flowsheets tested include a split high-grade (HG) and low-grade (LG) circuit and a single circuit (Bulk). Table 13-25 and Table 13-26 show a summary of conditions and results (Figure 13-9). The following points are of note when reviewing the data:

- For the North Sector, recovery of 3E to the final concentrate measured between 46 and 71 percent at a grade of 70 to 682 g/t 3E. Nickel performance was variable, with recoveries ranging from 5 to 63 percent.

- Only two cleaner tests were conducted on the Central Sector composite due to mass constraints. In both tests, 63 percent of the 3E was recovered to the concentrate at a grade of between 154 and 198 g/t 3E.
- There is some indication performance is related to the dosage of PE26. PE26 is primarily used to depress talc to reduce dilution in the concentrate. While this is a key reason, higher PE26 dosages are also assisting with recovery, indicating there may be other interactions of the PE26 beyond just talc depression; the exact mechanism is unknown. Calgon was evaluated as an additional gangue control mechanism. Calgon is a detergent that is efficient at complexing calcium and magnesium ions in solution, potentially reducing the slime coating of the sulphide surfaces. The impact of Calgon was inconclusive and did not provide a significant boost to performance.
- Higher density resulted in higher mass recovery due to more talc floating under similar conditions. The increased talc recovery could be controlled with increased PE26 addition. A trade-off evaluating the differences in low-density versus higher reagents, among other parameters, should be considered.
- When significant regrinding was used in Test 17, significant increases to concentrate grade were measured; however, recovery was reduced. Given the saleable grades without regrinding, it is not required for the tested samples.
- A portion of the PGMs and nickel is fast floating. However, long flotation times are required for high recovery.

Table 13-25: Cleaner test work parameters

Conditions											
Composite	Test	Flow Sheet	General Description	µm K80		g/t					Ro Cell L
				PG	Rgd	PE26	Calgon	PAX	3894	A208	
North Zone	T09	Bulk	Baseline	30	29	660	-	153	-	-	8
	T11	HG/LG	HG/LG	30	30	695	-	133	-	-	8
	T15	HG/LG	HG/LG	21	21	695	-	133	-	-	8
	T16	HG/LG	HG/LG - Calgone	21	15	695	750	133	-	-	8
	T17	HG/LG	T16 - no Rgd	21	-	695	750	133	-	-	8
	T18	HG/LG	T11 - no Rgd	30	-	695	-	133	-	-	8
	T19	HG/LG	T11 Closed Clnr	30	32	695	-	133	-	-	8
	T24	Bulk	T09 No Rgd, add Scav	30	-	805	-	173	-	-	8
	T26	Bulk	T24, Rgd	30	17	875	-	173	-	-	8
	T27	Bulk	Higher Density	30	-	930	-	173	-	-	4
	T29	Bulk 1 clnr	Clnr 1 kinetic, selective collectors	30	-	650	-	105	25	25	8
	T33	Bulk	Low er PE26, Mag sep on TIs	30	-	400	-	153	-	-	4
Central	T31	Bulk	Preliminary Test	33	-	930	-	173	-	-	4
	T32	Bulk	Finer Primary Grind	27	-	830	-	173	-	-	4

Source: Bravo, 2025.

Table 13-26: Average grades obtained on cleaner test work

Final Concentrate														
Composite	Test	Mass	Assay - percent or g/t						Distribution- percent					
		%	Pd	Pt	Au	3E	Ni	MgO	Pd	Pt	Au	3E	Ni	MgO
North Zone	T09	0.5	192	75.5	14.4	282	6.8	12.8	66	41	73	57	17	0.3
	Til	1.7	71.2	47.7	2.66	122	6.1	17.6	73	69	67	71	47	1.2
	T15	1.1	95.2	33.9	3.25	132	2.9	20.7	70	36	62	56	15	1
	T16	1.3	75.5	33.4	2.61	111	2.4	20	69	42	60	57	14	1.1
	T17	1.2	78.9	37	3.4	119	3.4	21.6	68	46	57	59	20	1.2
	T18	2.5	45.3	29	1.06	75	5.4	12.6	78	61	46	70	63	1.5
	T19	1.8	62.1	39.2	8.16	110	6.5	11.7	71	64	74	69	54	1

Final Concentrate														
Composite	Test	Mass	Assay - percent or g/t						Distribution- percent					
		%	Pd	Pt	Au	3E	Ni	MgO	Pd	Pt	Au	3E	Ni	MgO
	T24	0.9	109.5	71.5	4.68	186	10.3	2.1	72	66	80	69	47	0.1
	T26	0.2	460.1	187	35	682	4.6	3.9	60	36	81	51	5	0
	T27	0.9	122.9	95.8	5.3	224	10.3	3.6	72	71	55	71	45	0.2
	T29	1.6	60.8	39.3	1.63	102	4.2	17.9	63	55	41	59	33	1.3
	T33	1.9	43.3	25.9	1.2	70	3.5	13.6	49	41	57	46	34	1.1
Central	T31	1	103.5	42.9	7.99	154	14.2	7.8	62	62	77	63	49	0.3
	T32	0.8	128.2	57.4	12.4	198	14.9	6.9	62	60	82	63	42	0.2

Source: Bravo, 2025.

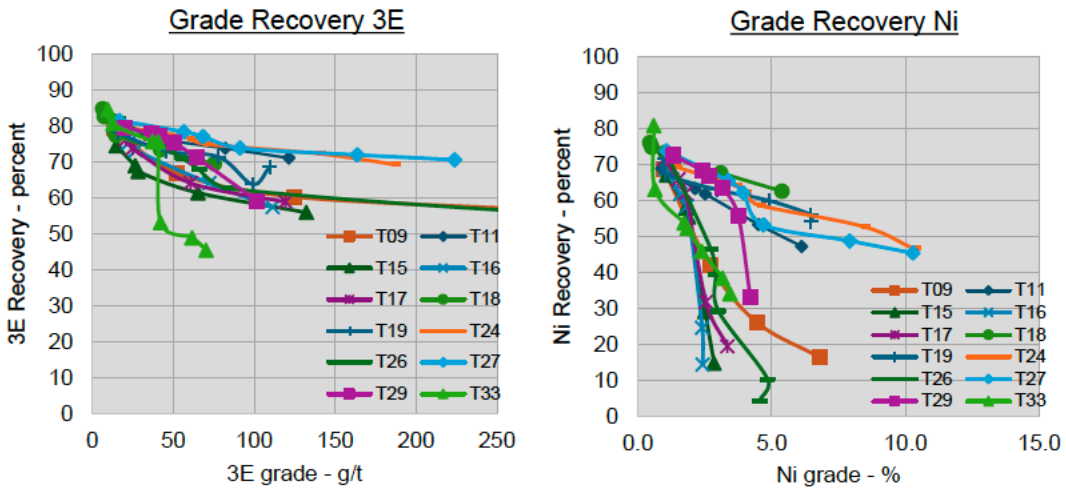

Figure 13-9: Recovery obtained on cleaner test work

Source: Bravo, 2025.

13.5.4.5 Locked Cycle Tests

Locked cycle tests were conducted to determine the overall performance in closed circuit operation. Two locked cycle tests were conducted on the North Sector composite and a single locked cycle test on the Central Sector composite. The flowsheet, conditions, and results are shown in Table 13-27 to Table 13-29, and Figure 13-11 and Figure 13-11.

For the North Sector, two flowsheet configurations were used, including a split feed circuit with lower density, higher collector, and Calgon in Test 20. Following this test, additional batch optimization was conducted, and a subsequent locked cycle test with a simplified circuit, including only one circuit, higher rougher flotation density, no Calgon and lower collector. Slightly higher PE26 was used as established by higher density batch tests. The measured overall performance for these tests was quite similar. In both tests, the 3E recovery measured 78 percent for the North Zone composite. The concentrate graded 121 g/t 3E for the split circuit (Test 20), and 154g/t 3E for the simplified flowsheet (Test 20). Nickel recovery measured 62 percent, resulting in a concentrate grade of 9.4 percent nickel for Test 30.

The simplified circuit was also used for the Central Sector composite, Test 30. For this test, 3E was 68 percent recovered to the bulk concentrate at a 3E grade of 202 g/t. The rougher

recovery was similar to the North Sector composite, but higher cleaner tailings losses were measured. Nickel recovery measured 44 percent, at a concentrate grade of 16 percent nickel.

An opportunity exists to further improve recovery, particularly for the Central Sector composite. According to client provided targets, a concentrate grade closer to 80 g/t 3E is still favourable, so there may be potential to improve recovery, while slightly lowering concentrate grade with more aggressive conditions. A Trace Mineral Search is in progress on Test 20 rougher tailings. It is likely that some of the losses are liberation constrained, but fine liberated particles may be a further target to exploit.

A single cleaner flotation test was conducted after locked cycle tests, evaluating a reduced PE 26 dosage, as well as magnetic separation from the flotation tailings. The lower PE26 significantly reduced both recovery and grade; further optimization with a systematic evaluation of various PE26 dosages and other gangue depressant is recommended. The magnetic concentration recovered a significant amount of mass, at some upgrading of the PGM and significant recovery of Ni and S. Magnetic separation warrants further investigation, possibly on a feed sample which could have the potential to reduce the mass to fine grinding and flotation, provided the metals of interest are adequately recovered to the magnetic concentrate.

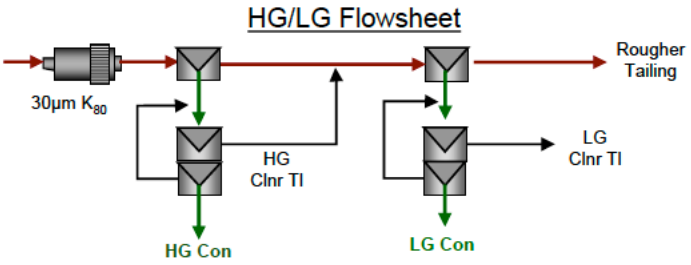

Figure 13-10: HG and LG flowsheet

Source: Bravo, 2025.

Table 13-27: HG and LG flowsheet parameters

Test	Product	Stage	Cell Size	g/t					pH	Time
			L	PE26	PAX	Calgon	MBC	W31		min
T20	HG Rougher	1	8	550	48	-	84	-	8.9	9
	HG CLnr	2	2.5/ 1.5	40	25	-	21	10	8.9	6/4
	LG Rougher	1	8	150	200	500	-	-	8.6	15
	LG Clnr	2	2.5/1.5	135	35	-	14	-	8.6	7/4

Source: Bravo, 2025.

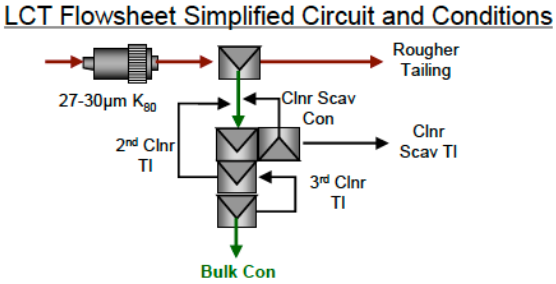

Figure 13-11: HG and LG flowsheet simplified

Source: Bravo, 2025.

Table 13-28: HG and LG Flowsheet simplified parameters

Test	Product	Stage	Cell Size	g/t					pH	Time
			L	PE26	PAX	Calgon	MIBC	W31		Min
T30	Rougher	1	4	825	88	-	49		9.0	25
	Cleaner	3	4/2.5/1.5	105	75	-	56	60	8.7	12/7/9
	Clnr Scav	1	4	-	10	-	-		8.3	4
T34	Rougher	1	4	725	88	-	49		9.2	25
	Cleaner	3	4/2/1	105	75	-	56	10	9.0	12/7/9
	Clnr Scav	1	4	-	10	-	-		8.7	4

Source: Bravo, 2025.

Table 13-29: Average grades obtained on locked cycle tests

LCT Results Cycle D+E																
Test/ Composite/ Flow sheet	Product	Mass	Assay - percent or g/t							Distribution - percent						
		%	Pd	Pt	Au	3E	Ni	Cu	S	Pd	Pt	Au	3E	Ni	Cu	S
T20: North Zone HG/LG Flow Sheet	Cycles D + E															
	Feed	100	1.64	1.2	0.07	2.9	0.21	0.05	1.2	100	100	100	100	100	100	100
	Comb. Con	1.8	71.7	47	2.5	121	6.9	2.7	19.1	81	74	69	78	62	94	29
	HG Con	0.6	190.8	115.3	6.89	313	13.1	7.7	30.4	72	61	65	67	39	92	15
	LG Con	1.2	11.4	12.8	0.24	24.4	3.7	0.1	13.4	8	13	4	10	22	2	14
	LG Clnr Tis	7.8	0.7	0.7	0.03	1.47	0.16	0.003	1.4	3	5	3	4	6	0	9
	Ro Tls	90.4	0.29	0.3	0.02	0.59	0.07	0.003	0.8	16	21	27	18	32	5	62
T30: North Zone Simplified Flow sheet	Cycles D + E															
	Feed	100	1.4	1.1	0.05	2.54	0.2	0.05	1.2	100	100	100	100	100	100	100
	Bulk Con	1	86.3	65.4	2.74	154	3.39	3.39	29.1	79	76	78	78	62	95	31
	Clnr Scav Tis	12	0.54	0.54	0.01	1.1	0.004	0.004	1.4	5	6	3	5	11	1	15
	Ro Tls	86.7	0.27	0.22	0.01	0.5	0.002	0.002	0.7	16	18	19	17	27	4	54
T30: Central Simplified Flow sheet	Cycles D + E															
	Feed	100	1.62	0.64	0.1	2.36	0.29	0.04	0.7	100	100	100	100	100	100	100
	Bulk Con	0.8	137.2	54.3	10.49	202	15.95	4.22	29.4	67	67	86	68	44	83	34
	Clnr Scav Tis	13.4	1.98	0.68	0.04	2.69	0.55	0.021	1.2	16	14	6	15	25	7	23
	Ro Tls	85.8	85.8	0.14	0.01	0.46	0.1	0.005	0.3	16	19	9	17	30	10	43

Source: Bravo, 2025.

13.5.5 Mini Plant Program

A mini plant test program was also initiated to:

1. Produce larger quantities of concentrate to evaluate potential downstream processing opportunities.
2. Further evaluate parameters determined from the bench scale program.
3. Evaluate detailed concentrate chemistry and mineralogy.

Downstream processing of Luanga concentrates is an important consideration since the size of the Luanga deposit is anticipated to support a large tonnage, long life operation. Sample concentrates will be used in a range of pyrometallurgical and hydrometallurgical smelting and refining tests to inform technical and strategic options.

The sample used for this program originated from a large-diameter diamond core (ZW) acquired from the previous project owner. The core was sourced from holes FM004, FM005, FM006 and FM007, drilled in the SW sector of the deposit. These holes were drilled into a localized, high talc area and the core material had subsequently been archived and stored for approximately 20 years.

The drill core was sampled and composited to achieve a target grade of 2g/t 4E PGM.

13.5.6 Phase 1 Concentrate Production Run

Bravo Mining contracted CIT SENAI Laboratory and Frank Rezende Consulting to conduct a concentrate production program using the mini pilot plant equipment at CIT SENAI in Belo Horizonte, Brazil.

Six-grade profile bulk samples were prepared from the historical ZW drill core acquired from Vale. A total of 2.5t of material was prepared for processing with the intention of producing a wide arrangement and volume of concentrate grades for further downstream processing test work (Table 13-30).

Table 13-30: The feed samples' average grades do Phase 1

COMPOSITE	Au(g/t)	Pt (g/t)	Pd(g/t)	Rh(g/t)	4 E (g/t)	Ni (%)	Cu(%)
A	0.041	0.310	0.764	0.033	1.148	0.138	0.014
B	0.046	0.373	0.907	0.041	1.377	0.147	0.021
c	0.045	0.470	1.171	0.058	1.744	0.179	0.019
D	0.066	0.645	1.610	0.090	2.410	0.192	0.021
E	0.125	0.879	2.181	0.155	3.339	0.182	0.022
F	0.128	1,609.000	3.467	0.240	5.444	0.176	0.017

Source: Bravo, 2025.

The circuit configuration composed 3 mechanical rougher cells. The first cell was used as a fast, rougher float, producing a high-grade concentrate. The remaining rougher cells produced a lower-grade combined concentrate, while tailings were treated with a single-stage scavenger to produce a third concentrate.

The feed material was milled to p90 -38μm while general rougher cell reagent conditions were maintained as per the Bravo standard conditions as determined in the 2023 flotation program, which included the addition of 500 g/t of CMC as depressant, 40g/t of A208/A3894 (50/50) and 80g/t staged collector addition and 40g/t MIBC frother.

Resultant concentrates were composited for trace and deleterious element analysis. All trace elements were found to be below smelter thresholds including As, Sb, Bi, Cd, Pb, Te, Zn, F, Hg, and Cl (Table 13-31).

Table 13-31: Typical smelter threshold for trace elements

Element	Bravo Analysis (%)	Typical Smelter Threshold (%)
As	0.015	0.2
Sb	0.0018	0.05
Bi	0.0048	0.01
Cd	0.00007	0.02
Pb	0.0007	0.6
Te	<0.001	0.03
Zn	0.0005	2.5
F	0.0135	0.03
Hg	<0.05	0.001
Cl	0.014	0.05

Element	Bravo Analysis (%)	Typical Smelter Threshold (%)
Cr2O3	0.22	0.90

Source: Bravo, 2025.

A concentrate with a target grade of 60 g/t was also prepared from the produced material for pyrometallurgical test work.

13.5.7 Phase 2 Parameter Circuit Run

Due to equipment sizing and low mass pull from the Phase 1 mini-plant program sufficient cleaner stage investigations could not be undertaken. A remnant feed sample (Sample B) was delivered to CETEM in Rio de Janeiro to conduct further test work, including cleaners, into the processing circuit. The process configuration is shown in Figure 13-12.

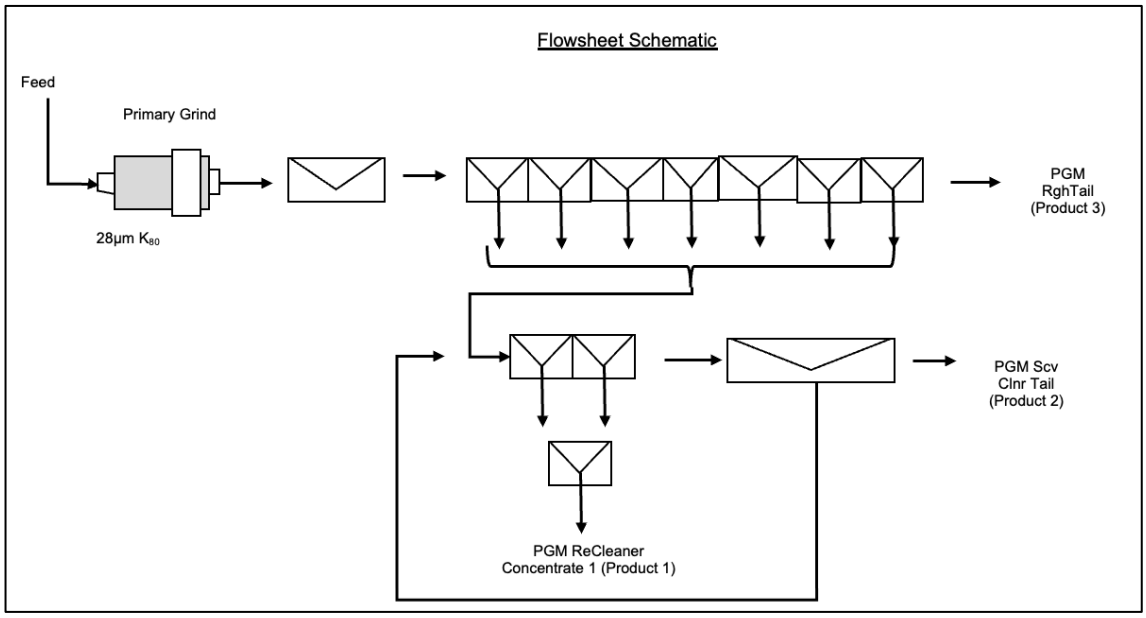

Figure 13-12: Flowsheet schematic of the Phase 2

Source: Bravo, 2025.

The circuit configuration is a primary grind followed by a 7-stage rougher, 2-stage cleaning and a single-stage recleaner and scavenger.

The primary grind was performed to p80 -28µ. Additional reagent conditions are presented in the test sheet below (Table 13-32).

Table 13-32: Phase 2 parameter circuit run

Stage	Reagents - g/tonne				Time Minutes	
	CMC	MIX (AERO 3894 + SENKOL 2)	PAX	MIBC	Condition	Float
Primary Grid						
Talc Condition	700					
Rougher 1 MIX		20		30		
Rougher 2 PAX			90			
Rougher 3 to 4 PAX						
Rougher 5 PAX	200		90			
Rougher 6 to 7 PAX						

Stage	Reagents - g/tonne				Time Minutes	
	CMC	MIX (AERO 3894 + SENKOL 2)	PAX	MIBC	Condition	Float
Cleaner 1 to 2 PAX			20			
ReCleaner						
Scavenger Cleaner			5			

Source: Bravo, 2025.

Metal recoveries are shown in Table 13-33. Recoveries were broadly in line with anticipated results from a localized, high-talc historical sample. Target concentrate grade was not achieved, with a final concentrate grade of 36 g/t 4E and 3.7% Ni. The lower concentrate grade was attributed to excessive gangue contamination and lower selectivity.

Table 13-33: Metal recoveries in Phase 2

Element	Recovery
Pd	73%
Pt	77%
Rh	39%
Au	87%
Ni	59%

Source: Bravo, 2025.

13.5.7.1 Oxide Material Leaching

13.5.7.1.1 Leaching – Phase 2 Parameter Definition and Optimization Program

TESTWORK Process Development were contracted to perform a Phase 2 metallurgical study on Luanga oxide samples.

The Phase 2 sample material was collected as a bulk excavated sample of approximately 2 tonnes, collected at sample location MDH902. The location coincides with the collar location of metallurgical twin diamond drill hole MDH22LU902, situated at the northern edge of the Central Sector of the Luanga mineralized body (refer to sampling map).

The sample was delivered to TESTWORK, where it was homogenized and split into workable sample sizes. Representative split samples were sent to SGS Geosol in Belo Horizonte for head grade analysis (Table 13-34).

Table 13-34: Head grade analysis results – leaching Phase 2

Head Grade	Au (g/t)	Pd (g/t)	Pt (g/t)	Rh (g/t)	4E_PGM+Au (g/t)
Split Sample Average	0.03	1.32	1.58	0.28	3.20

Source: Bravo, 2025.

The scope of the Phase 2 program investigated (Table 13-35):

1. Initial Exploratory Priority Tests
2. Influence of NaCN Initial Concentration
3. 2-Stage pH Augmentation Influence
4. Temperature Influence

5. Influence of Contact Time
6. Size-by-Size Leaching
7. Influence of Additives
8. Oxide/Altered/Fresh Blend Leach
9. Additional Standardized Tests

Table 13-35: Parameters and recoveries of t Phase 2

Regime	Conditions	Tests	Best Elemental Recoveries			
			Pd	Pt	Au	Rh
Exploratory	pH 9.5 – 10.5 NaCN 2500 – 5000 ppm ZTPOLY, H2O2, NaCO3	LT1 – LT11	82%	5%	74%	2%
NaCN Concentration	500 – 10000 ppm ZTPOLY, H2O2	LT 12 – LT21	78%	7%	89%	5%
2-Stage pH	12h pH 9.5 + 12h pH 11.0	LT22 – LT23	74%	*	65%	10%
Temperature	pH 10.5 35°C and 50°C	LT24 – LT25	55%	4%	73%	*
Contact Time	2, 4, 8, 24, 48, 72 hr	LT26 – LT27	84%	*	65%	*
Size by Size	>1/4", >1mm, <1mm 5000ppm NaCN	LT28 – LT33	71% 78% 67%	3% 3% 7%	84% 65% 73%	1% 2% 15%
Additives	Glycine 2g/L Glycine 2g/L + H2O2 1g/L NaOH Turbo 2g/L LeachAid 2 g/L	LT34 – LT45	83%	15%	79%	5%
Blend Leach	NaCN 9281 pH 10.5 24/48hr Direct Leach 48hr CIL	BRF LT1 – LT4	75%	8%	87%	95%
Supplementary Standardized	NaCN 11670 ppm pH 10.5 24 hr	SP1 – SP12	66%	21%	90%	25%

Source: Bravo, 2025.

13.5.8 Palladium

Palladium generally showed good recoveries across a range of conditions with best recoveries at pH 10.5 and NaCN dosages of 5000ppm. Lime consumption was 5kg/t to maintain pH. Longer leaching times favoured improved recoveries with the leaching curves showing potential for further recovery improvement at extended leach times.

Glycine as an additive improved Pd recoveries, even at low dosages. Further exploratory tests to investigate optimised dosages should be investigated.

Other additives, temperature or high NaCN dosages did not further improve recovery.

13.5.9 Gold

Like Pd, gold showed best recoveries in the range of 10.5 pH and NaCN dosage of 5000ppm. Gold recoveries were neutral to extended leaching times with leach curves stabilizing after 24hr. Additives, temperature augmentation and high NaCN dosages did not further improve Au recoveries.

13.5.10 Platinum

Like the initial exploratory tests conducted in 2022/2023, Pt showed both lower and highly variable recovery during leaching test work. Due to low liquor Pt tenors, analytics were less stable compared to Pd and Au.

Best recoveries for Pt were achieved with high dosages of NaCN with shorter leach times (24hr). Glycine additive improved recoveries, even at low dosages and warrant further investigation.

13.5.11 Rhodium

Rhodium showed both lower and highly variable recovery during leaching test work (2 – 95%). Due to low liquor Rh tenors, analytics were less stable compared to Pd and Au, similar to platinum.

In general, best recoveries were achieved at the base line conditions of pH10.5 and 5000ppm NaCN dosage.

13.5.12 PGM Speciation

Over 38 individual platinum group mineral species have been identified at Luanga. Differences in PGM speciation, specifically as it relates to platinum and rhodium recovery may play an important role in understanding metallurgical performance.

This is evidently demonstrated in the stark performance difference between the Phase 1 core composite sample (18 – 61%), Phase 2 bulk sample rhodium recovery performance (2 – 15%), the standardized supplementary tests (2 – 25%), and the Blend tests recovery performance (81 – 95%).

As previously described, the bulk Phase 2 sample consists of excavated soil-oxide material. The standardized supplementary test samples originate from composites within the oxide material below the soil horizon. The blend sample consists of a composite from the lower part of the oxide and the upper part of the fresh rock horizon in the Southwest Sector of the Luanga deposit. The blend sample showed very high levels of alteration (+60% talc).

The differences in Rh recovery could potentially be attributed to varying PGM speciation within the different domains within the oxide horizon. More detailed domaining and complimentary metallurgical within discrete oxide horizons will be required to gain a more complete understanding of metallurgical performance.

13.5.13 Size-by-Size Analysis

A granulo-chemical assessment was done of the oxide bulk sample used for the Phase 2 leaching program to better understand the deportment of metals by size fraction within the soil oxide domain (Table 13-36). A 20kg split sample was deagglomerated in a steel concrete mixer drum for 15min after which the sample was screened to varying size fractions from +1/4” to -38μm

It was found that 77% Pd, 81% Pt, 75% and 51% Au by contained metal is in the +1mm fraction while the +1mm fraction accounts for 41% of the mass. Furthermore, the grade of +1mm fraction is approximately double that of the total sample.

These results demonstrate that there exists potential to optimize the envisaged oxide processing route by incorporating screening into the circuit. This could have a potential positive impact on equipment sizing, plant capital expenditure, feed grade and recovery. A trade-off investigation will be required to consider the benefit of this circuit relative to the potential loss of metal in the finer fraction. The high clay content of the oxide zone will likely be an impediment to screening operations and should be included in future investigation

Table 13-36: Average grades on granulo-chemical of the bulk sample used for the Phase 2 leaching program

Sample	Mass	Mass	Grade Au	Au	Au	Grade Pd	Pd	pd
	(kg)	(%)	(g/t)	(mg)	(%)	(g/t)	(mg)	(%)
BRV01 - 1/4	3.79	21.91%	0.04	0.14	13.42%	6.52	24.70	28.06%
BRV01 - 1 mm	4.00	23.12%	0.04	0.17	16.05%	10.23	40.93	46.50%
BRV01 - 300 µm	1.18	6.82%	0.05	0.05	5.01%	4.78	5.64	6.41%
BRV01 - 150 µm	0.54	3.11%	0.04	0.02	2.03%	5.57	3.00	3.40%
BRV01 - 75 µm	0.57	3.29%	0.03	0.02	1.61%	3.08	1.75	1.99%
BRV01 - 45 µm	0.80	4.60%	0.25	0.20	18.78%	2.19	1.74	1.98%
BRV01 - 38 µm	0.24	1.41%	0.35	0.09	8.07%	2.04	0.50	0.57%
BRV01 - < 38 µm	6.18	35.74%	0.06	0.37	35.03%	1.58	9.77	11.10%
Total	17.3	100.00%	0.06	1.06	100.00%	5.09	88.03	100.00%

Sample	Mass (kg)	Mass (%)	Grade Pt (g/t)	Pt (mg)	Pt (%)	Grade Rh (g/)	Rh (mg)	Rh (%)
BRV01 - 1/4	3.79	21.91%	6.13	23.23	25.45%	1.67	6.35	36.67%
BRV01 - 1 mm	4.00	23.12%	10.79	43.16	47.28%	2.03	8.11	46.83%
BRV01 - 300 µm	1.18	6.82%	4.46	5.26	5.76%	0.38	0.45	2.61%
BRV01 - 150 µm	0.54	3.11%	5.90	3.17	3.48%	0.59	0.32	1.84%
BRV01 - 75 µm	0.57	3.29%	4.24	2.41	2.64%	0.39	0.22	1.27%
BRV01 - 45 µm	0.80	4.60%	0.52	0.42	0.46%	0.37	0.29	1.70%
BRV01 - 38 µm	0.24	1.41%	0.14	0.03	0.04%	0.34	0.08	0.47%
BRV01 - < 38 µm	6.18	35.74%	2.20	13.60	14.90%	0.24	1.49	8.61%
Total	17.30	100.00%	5.28	91.29	100.00%	1.00	17.3	100.00%

Source: Bravo, 2025.

13.6.5 Tailings and Concentrate Thickening and Filtration

13.5.13.1.1Westech – Fresh Rock Tailings and Concentrate

Bravo Mining contracted Westech (Swire Water) to conduct vacuum sedimentation and filtration tests on fresh rock tailings and concentrate material from the Luanga project. Sample material was sourced from the mini plant test work program which provided sufficient material for such test work (Table 13-37). Based on these results vacuum filtration of flotation concentrates is unlikely to achieve acceptable shipping moisture contents. Future work will instead focus on pressure plate and frame filtration.

Table 13-37: Vacuum sedimentation and filtration test material

Description	Tailings Sample	Concentrate Sample
Solids Concentration (%)	35	17
Solids Density (t/m3)	2.50	2.86
Liquid Density (t/m3)	1.00	1.00
Pulp Density (t/m3)	1.26	1.12
P80 (μm)	Ca. 25	Ca. 20

Source: Bravo, 2025.

Tests included dilution optimization, flocculant dosage optimization, sedimentation, and filtration tests. A summary of the results is presented in Table 13-38 and Table 13-39.

Table 13-38: Vacuum sedimentation and filtration test results

Description	Tailings Sample	Concentrate Sample
Optimum Dilution	7.0 % Solids	4.6 % Solids
Best Flocculant	Magnafloc 10 (BASF)	Magnafloc (BASF)
Best Dosage	50 g/t	40 g/t
Concentrate Underflow	46.85 % Solids	45.81 % Solids
Unit Area	0.45 m2/tpd	0.67 m2/tpd

Source: Bravo, 2025.

Table 13-39: Vacuum sedimentation and filtration test results

Description	Tailings Sample	Concentrate Sample
Fabric Selection	7μm aperture	20μm aperture
Cake Moisture	32.0 %	35.0 %
Vacuum Pressure	21 – 22 “Hg	18 – 20 “Hg
Cake Thickness	15.0mm	15.0mm
Filtration Rate	0.440 t/h.m2	0.700 t/h.m2

Source: Bravo, 2025.

13.5.14 Watershed Laboratories – Oxide Tailings

Watershed Laboratories in Brazil conducted thickening, water recovery and density profile evaluation tests on oxide tailings material from the Luanga project. Tailings material was composited from available tailings at TESTWORK Laboratories from Phase 2 test tailings.

Free drainage, compressive drainage and compressive densities were evaluated in three tests and various flocculant dosages (300/500/800g/t) (Nalco 7763, emulsion polymer).

Samples were tested at the treatment pulp density of 29-30%. Total water recovery of 70% was achieved with a thickened product density of 2.80 t/m3 and water turbidity of 316 NTU of suspended solids (or 100mg/l).

The best results were achieved with 500g/t and the 300g/t test. Dosage at 800g/t negatively affected all parameters.

Test parameters and results are summarised in the table below (Table 13-40).

Table 13-40: Watershed in oxide tailings tests parameters

Sample - FEED				
Test	**#**	**1**	**2**	**3**
Original slurry (as received)	solids %	28.6%	28.6%	28.6%
Product	code	7,763	7,763	7,763
	concentration %	1.00	1.00	1.00
Dilution	V/V	40%	40%	40%
Dose	g/t	300	500	800
Free Drainage	solids %	38.8%	41.7%	30.0%
Compressive Drainage	solids %	54.2%	57.3%	43.3%
Compressive Density	g/cm3	2.63	2.8	
Water Recovery based on Water in the Feed Sample				
Free Drainage Water Recovery	%	37.0%	44.1%	6.8%
Compressive Drainage Water Recovery	%	29.2%	26.1%	40.9%
Total Water Recovered	%	66.2%	70.2%	47.7%
Feed Sample	g	640	640	640
Feed Solids	g	182.9	182.9	182.9
Feed Water	g	457.1	457.1	457.1
Free Drainage Water Recovery Free Drainage on screen	g	169.13 470.87	201.64 438.36	31.08 608.92
Compressive Drainage Water Rec Compressive Drainage - Plug	g g	133.51 337.36	119.34 319.01	186.84 422.08
Ballance checking		640	640	640
		0.00	0.00	0.00

Source: Bravo, 2025.

13.5.15 Pyrometallurgy

A 68g/t concentrate sample from Luanga was sent to Arxo Metals in South Africa for roasting and smelting tests. Final report pending while assay results have been received.

The concentrate sample was roasted at 1000°C for 120 min which effectively reduced sulphur and other volatile content to 1.23% (target below 2% for reductive smelting).

Bravo roasted concentrate was bulked with a chemically matched concentrate from Tharisa Minerals to meet the furnace charge requirement.

The smelting test in a 35kVA DC furnace produced a Ni-Fe alloy with 716g/t 4E PGM, while slag PGM concentration was below the detection limit for all precious metals, suggesting +99% recovery. Slag Ni was below the detection limit, while Cu concentration was reported as 1%, suggesting base metal recoveries of +99% and 99%, respectively and no alloy entrapment in slag.

Some results are shown in Table 13-41, Table 13-42, and Figure 13-13.

Table 13-41: PGM summary of results

Summary of Results:										
	4E (g/t)	Fe	Al	Cr	Ca	Cu	Ni	Si	Mg	S
Bravo PGM conc	68.15	11.35%	1.72%	0.21%	2.86%	1.12%	3.47%	22.94%	14.90%	5.11%
Roasted Bravo PGM Conc	70.99	11,37%	1.96%	0.23%	3.00%	1.43%	3.82%	23.29%	16.47%	1.23%
Tharisa PGM Conc	71.84	7,37%	2.33%	2.13%	1.99%	o. 29%	0.38%	27.51%	18.16%	0.73%
Combined PGM Conc	71.66	8,50%	2.59%	1.73%	2.40%	0,47%	0.86%	23.33%	15.25%	0.84%

Source: Bravo, 2025.

Table 13-42: Smelting (35kVA DC R&D Furnace)

Smelting (35kVA DC R&D Furnace)						
	% Alloy fall	Upgrade	Assays			
				Feed	Alloy	Slag
PGM Combined Conc 10kg (Bravo:Tharisa 2.1:7.9)	8.0	9.0	4E (g/t)	82.1	716.8	ND
			% Cu	1.7	2.3	0.5
			% Ni	0.4	9.7	0.1
			% Fe	8.8	77.5	7.5
			% Cr	2.2	0.6	2.1
			Total mass (kg)	**10**	**0.8**	**9.3**

Source: Bravo, 2025.

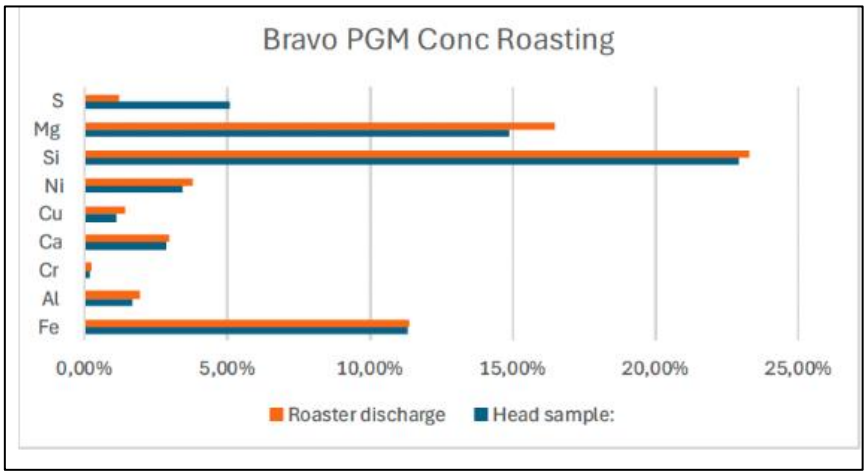

Figure 13-13: Bravo PGM conc roasting

Source: Bravo, 2025.

13.6 MRE Recommendation

The basis of recommendations for metallurgical inputs into the determination of Mineral Resources are from validated, reproduced historical metallurgical test results, newly generated tests results and external comparable results, where deemed “reasonable” for Fresh Material Flotation.

Vale, through external independent laboratories (SGS Lakefield, Mintek) and internal development work, reported their conclusion, that 74% of PGM could reasonably and economically be recovered at a LOM average feed grade of 1.24 g/t PGM+Au with demonstrated concentrate grades of 80 – 150 g/t.

Bravo, through its 2022/2023 metallurgical program has reproduced and validated the nature of the historical results achieved by Vale and elucidated further areas of potential improvement.

For the purposes of Mineral Resource estimation, the recovery numbers were simplistically modelled for tests across the grade profile and achieved concentrates of saleable grades (80 - 90 g/t). Concentrate quality considerations were based on concentrates from one operating and one development project and their qualities and terms for delivery to two separate Southern African smelters.

In the 2023 MRE, recovery estimate values were adjusted to accommodate for improvement demonstrated on Luanga recoveries through exploratory ultrafine hydrodynamic cavitation tests. An improvement of 6.1% was achieved at rougher stage flotation. This result replicated improved recoveries reported from Rustenburg tailings retreatment facilities at materially lower grades (0.69 g/t) of 5% at rougher stage. Global recovery improvement stabilized at 10% under these reported results.

For the 2025 MRE, the Luanga metallurgical model has removed any benefit previously attributed from additional fines flotation technology application assumptions and relied only on unadjusted performance recovery numbers. Bravo was not able to complete additional circuit tests aside from the initial rougher exploratory tests due to equipment availability and may update the metallurgical model at a later stage when such benefit can be demonstrated throughout the circuit, especially into the cleaner cycle. Previous investigation of cleaner tails at Luanga has demonstrated that +50% of fines losses to tails were liberated PGM or PGM attached to liberated base metal sulphides underscoring the potential to further improve flotation performance through the recovery of this fine fraction.

The average concentrate grade of tests under consideration equaled 174 g/t PGM+Au. Maintaining a saleable concentrate grade target of 80-90 g/t PGM+Au, additional recovery benefits may be realized by adjusting flotation times and/or reagent aggressiveness. For the 2023 MRE, an average recovery benefit was attributed to tests that achieved above-target concentrate grades. For the 2025 MRE, a more quantitative approach was taken, with high grade concentrates linearly regressed to target grade and improved recoveries measured accordingly. Concentrates that were near target grade and up to approximately 120 g/t were not adjusted.

The current metallurgical model shows recoveries of ca. 75 – 84% across a feed grade of 0.9 – 7.0 g/t PGM+Au for concentrates above 80 g/t, slightly lower than the 2023 MRE estimate of 76 – 85% (Figure 13-14).

Results from the mini-plant have been appropriately incorporated into the metallurgical assumptions by regressing recoveries generated to target concentrate grade. A qualitative talc abundance map was modelled for the Southwest Sector, which represents a minor portion of the overall MRE (see Section 14 below), and treated as a unique geological domain, to which the regressed recoveries were applied directly and separately from the global recovery assumptions

generated for the rest of the Luanga deposit. The resultant recoveries for the localised high-talc domain are assumed to be Pd 51%, Pt 56%, Rh 27%, Au 27%.

The graph below demonstrates the modelled metallurgical input parameters for the purposes of the 2025 Luanga Mineral Resource Estimate. The logarithmic model trend line has a formula of:

$$y = 4.317\ln(x) + 77.656$$

where, y = (recovery) and x = (material grade)

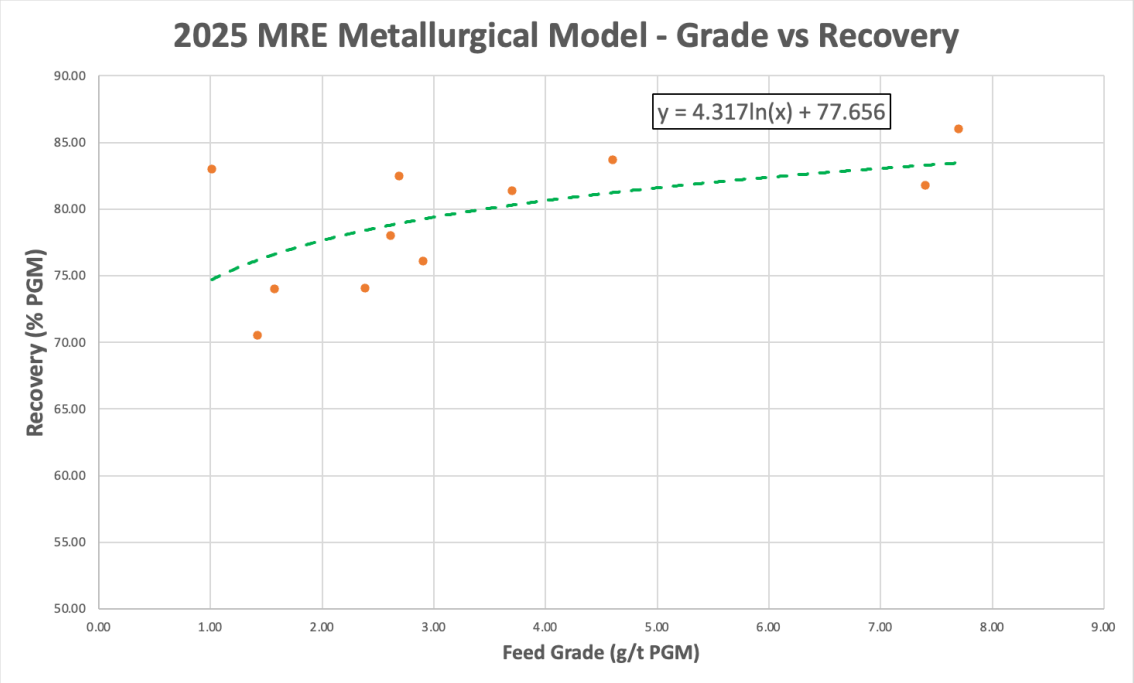

Figure 13-14: MRE metallurgical model – grade vs recovery

Source: Bravo, 2025.

Nickel recoveries have been demonstrated through Vale locked cycle tests to be achievable with between 45 and 47% recoveries at a feed grade of 0.19 %. Recent locked cycle test work performed by Bravo at Base Metal Labs demonstrated 62% Ni recovery in both sets of North Sector tests at feed grades of 0.21% Ni. Locked cycle test 34 on the Central Sector global composite demonstrated a 44% recovery from a 0.3% Ni feed grade while producing the highest Ni grade in concentrate yet seen at Luanga at 16% Ni in concentrate (plus 202 g/t PGM in concentrate). While these results clearly demonstrate the further potential to improve Ni recoveries at Luanga, the Company has maintained the 50% recovery assumption from the 2023 MRE until these results can be demonstrated more conclusively (Table 13-43).

Table 13-43: MRE Recommendation fresh rock global recovery

MRE Recommendation Fresh Rock Material	4E PGM	Pt	Pd	Rh	Au	Ni
Global Recovery (2 g/t PGM feed)	78 %	81 %	77 %	51 %	48 %	50 %
MRE Recommendation High-Talc Domain	**Pt**	**Pd**	**Rh**	**Au**	**Ni**	
Global Recovery (2 g/t PGM feed)	51 %	56 %	27 %	27 %	0 %	

Source: Bravo, 2025.

13.6.1 Oxide Material Leaching

The hydrometallurgical recoveries achieved to date demonstrate relatively high and consistent recoveries for Pd and Au, with lower and more variable recoveries for Pt and Rh. The recoveries have been verified through multiple leaching tests and the conceptual processing flowsheet has been validated with tests including PGM solubility in the presence of cyanide at ambient temperature and pressure, and within reasonable reagent dosage conditions, PGM adsorption onto carbon, and final product generation as saleable, high grade, PGM residue. The current data demonstrates the probability for economic recovery of PGM+Au from oxide material at Luanga through conventional sodium cyanide leaching and carbon-in-leach extraction.

For the purposes of the 2023 MRE, individual best element recoveries based on exploratory tests were used to inform the metallurgical input assumptions.

Input assumptions for the 2025 MRE have relied on data from extensive follow-up parameter investigation test work, which has resulted in improved assumptions for Pd, similar assumptions for Au and more conservative assumptions for Pt and Rh.

Bravo has relied on average recoveries from relevant parameter tests instead of individual best element recoveries as the project can now rely on a larger, more comprehensive data set of results from which to evaluate potential recoveries. (Table 13-44).

Table 13-44: MRE recommendation oxide global recovery

	Au	Pd	Pt	Rh
Global Recovery (1-3 g/t)	90 %	81 %	23 %	54 %

Source: Bravo, 2025.

14 MINERAL RESOURCE ESTIMATES

GE21 carried out the 3D geological modelling, statistical and geostatistical studies, and grade estimate for the Luanga Project, assessing a set of factors, including the amount, and spacing of available data, interpreted mineralization controls, mineralization style, and quality of used data.

Geological modelling and estimation were performed using Leapfrog 2024.1 and Isatis.Neo, respectively. The UTM Projection – Zone 22 South, Datum: SIRGAS 2000 was adopted as a reference for the database of this work.

14.1 Drilling Database

The drilling database supplied by Bravo was visually validated, considering the relationship between tables, gaps, overlaps, and the absence of essential information. Using Leapfrog Geo software, GE21 also validated the Collar, Survey, Assay, and Lithology tables. No relevant inconsistencies were identified in this stage of the work since this was verified in the Data Verification stage.

GE21 used Trench channel (TRC) samples and Diamond drill hole (DDH) core samples from both Vale and Bravo campaigns, available on the Effective Date. Table 14-1 summarizes the drilling database used in this project stage. The map shown in Figure 14-1 shows the spatial distribution of the holes used.

Table 14-1: Luanga Project drill holes summary

Company	Type	Count	Length (m)
Bravo	DDH	295	62,952
	TRC	45	8,714
	TOTAL Bravo	340	71,666
Vale	DDH	191	36,677
OVERALL TOTAL		**531**	**108,343**

Source: GE21, 2025.

The database has geochemical results of the variables: Pd (ppm), Pt (ppm), Rh (ppm), Au (ppm), and Ni (ppm). Apart from these five elements of interest, an additional 35 elements were analyzed (Ag, Al, As, Ba, Be, Bi, Ca, Cd, Co, Cr, Cu, Fe, K, La, Li, Mg, Mn, Mo, Na, P, Pb, S, Sb, Sc, Sr, Sn, Th, Ti, Tl, U, V, W, Y, Zn, and Zr).

The database has analysis from Vale and Bravo campaigns, including Vale assays resampled by Bravo. The Mineral Resource Estimation (MRE) database contains data from the Vale campaign. This data was transformed using the correlation correction presented in Section 11.5.3. The assay results are quantitative for the presented variables, separated by sampling method and campaign, and are quantified in Table 14-2.

Table 14-2: Luanga Project assays summary

Company	Variable	Diamond drill holes		Trenches	
		Number of Samples	Length (m)	Number of Samples	Length (m)
Bravo	Pd	62,606	62,223	9,355	9,070
	Pt	62,606	62,223	9,355	9,070
	Rh	62,606	62,223	9,355	9,070
	Au	62,606	62,223	9,355	9,070
	Ni	62,606	62,223	169	168
Vale	Pd	36,259	36,223	-	-
	Pt	36,259	36,223	-	-
	Rh	36,259	36,223	-	-
	Au	36,259	36,223	-	-
	Ni	36,259	36,223	-	-

	Number of Samples	Length (m)
Total PGM + Au	108,220	107,516
Total Ni	98,644	98,231

Source: GE21, 2025.

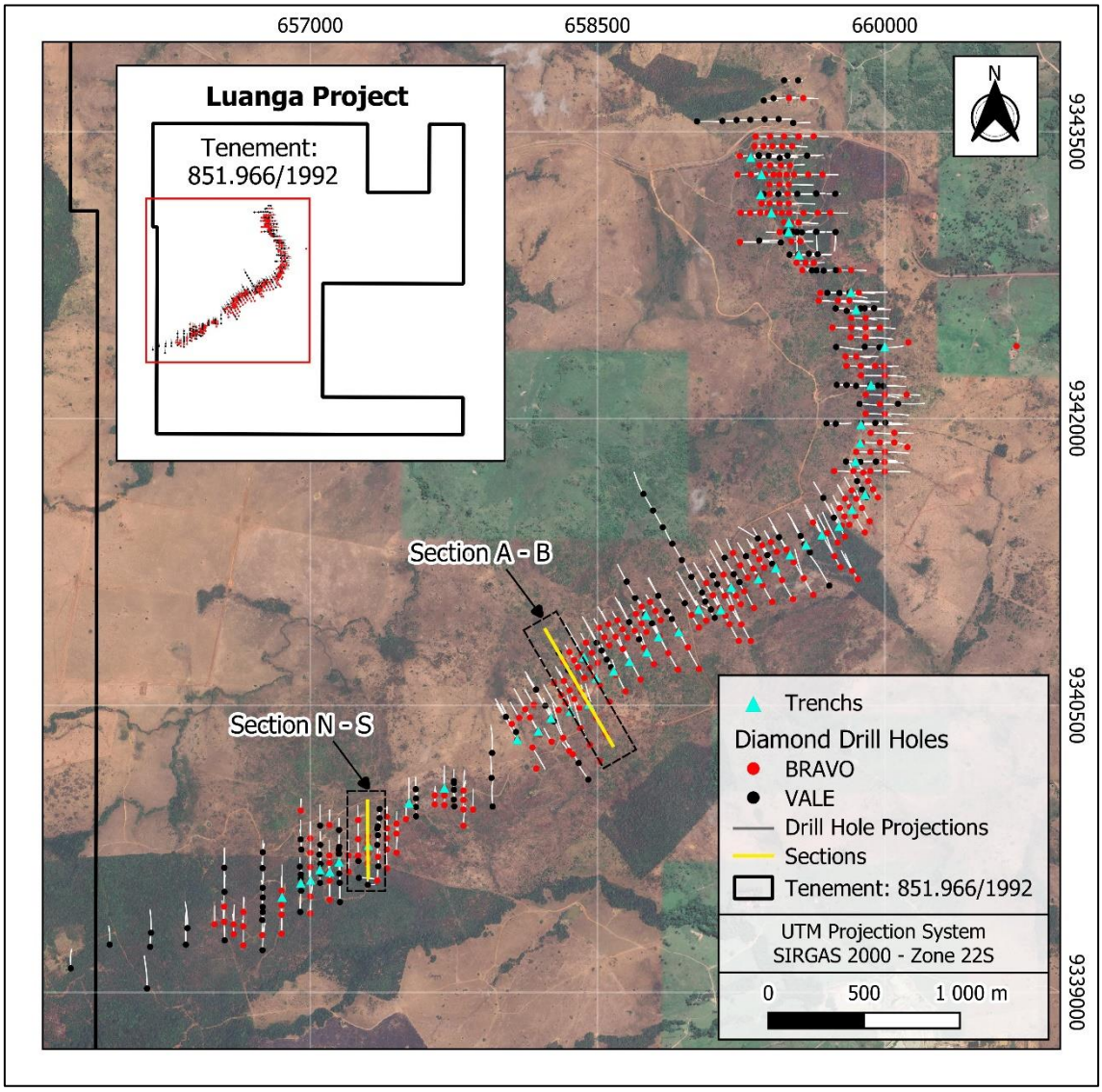

Figure 14-1: Map presenting the MRE database and the location of geologic models' sections

Source: GE21, 2025.

14.2 Geological Modeling

For the Luanga Project, four 3D models were generated. Each model spatializes different information regarding the mineralization and the host rocks. These models are:

- **Grade Shell Model**: defines mineralized grade shells of low grade (≥ 0.3 ppm PGM + Au) and high grade (≥ 1.0 ppm PGM + Au)
- **Regolith Model**: represents the weathering stages of the rock in the project area.
- **Estimation Domains**: combines the Grade Shell and the Regolith Models for a grade estimation.
- **Metallurgical Recovery Model**: defines zones with different metallurgical responses.

14.2.1 Grade Shell Model

Bravo's geologists interpreted the mineralized grade shell and lithology model along the 118 drill sections. The mineralized zone interpretation was modelled using continuity of PGM + Au grade. Two types of iso-grade surfaces were generated for the Luanga Project:

- Low Grade (LG): 3PGMs + Au > 0.3 ppm
- High Grade (HG): 3PGMs + Au > 1.0 ppm

The Mineralization Model was split into nine regions, generating 18 grade shell groups (9 LG + 9 HG). These groups are comprised of a total of 157 individual lenses. Figure 14-2 presents a section view of the Grade Shell Model. The regions of the mineralization are:

- North N
- North S
- Central HW
- Central Main
- Central FW
- Southwest N
- Southwest HW
- Southwest Main
- Southwest FW

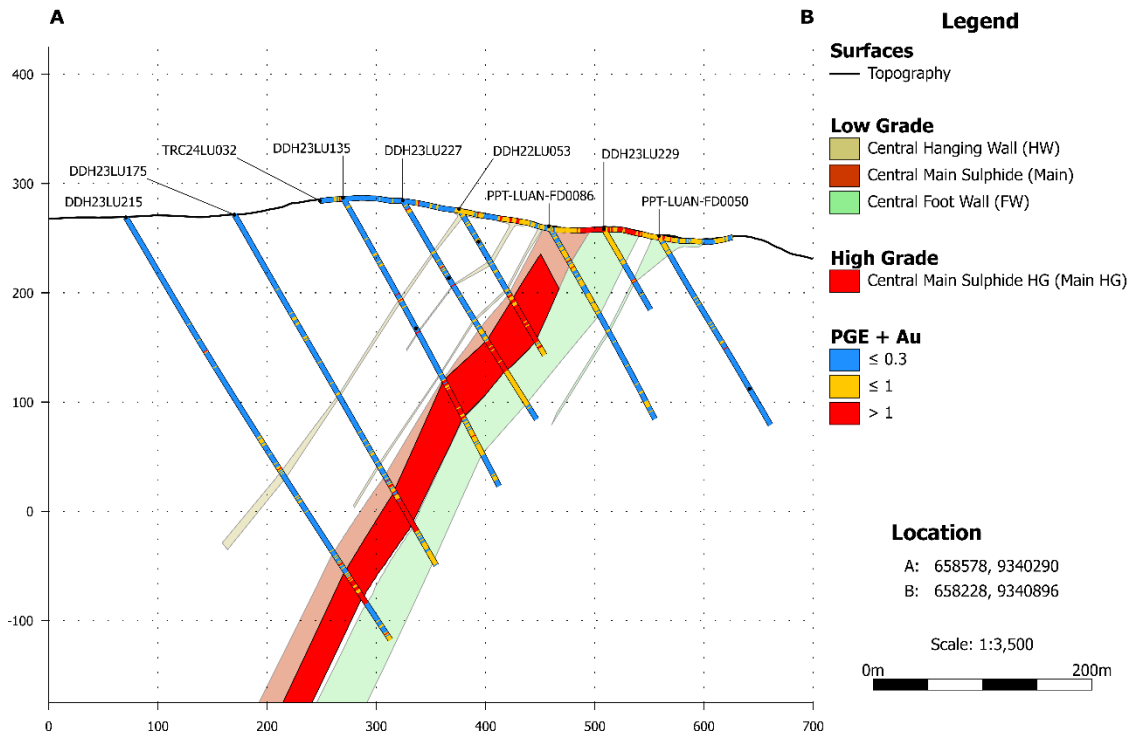

Figure 14-2: Grade shell model – section A-B – view of the central area

Source: GE21, 2025.

14.2.2 Regolith Model

The Regolith Model was built using the information on drill hole logs, RQD, and weathering types defined in the geological description. Given the metallurgical similarities and very small volumes of some, this was distilled to two defined zones (Figure 14-3):

- Oxidized Zone (Soil and saprolite): SO_SAP
- Fresh (Unweathered) Rock: FR

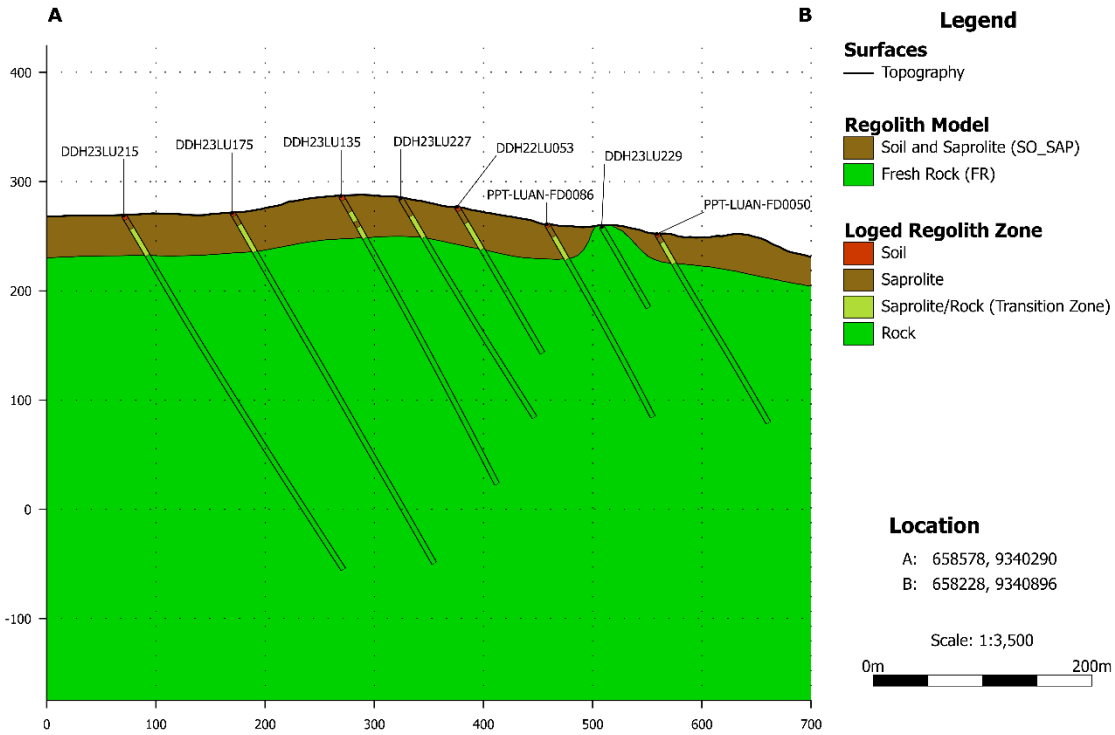

Figure 14-3: Regolith Model – Section A-B – View of the Central area

Source: GE21, 2025.

14.2.3 Estimation Domains

After the construction of all 3D models, the estimation domains were defined. The intersection of the Grade Shells with the Weathering Model generated 157 fresh rock lenses (HG + LG), that were grouped in main zones (Central, Southwest, North N and North S) with respect to the stationary domain (HG and LG). These zones were estimated separately (a total of 8 domains).

The upper zone of the Regolith Model, Soil and Saprolite (SO_SAP), intersection with the Grade Shells generated three additional Estimation Domains (Oxidation zones):

- SO_SAP_North
- SO_SAP_Central
- SO_SAP_Southwest.

Chemical elements are estimated using different estimation methodologies according to the Weathering Model. Ordinary Kriging was applied to the Oxidized domain, while the Turning Bands Simulation was applied to fresh rock. The Stationary Domains (High grade and Low grade), presented in Table 14-3, were estimated individually.

Table 14-3: Summary of estimation domains and relationships between weathering model, stationary domain and estimation methodology

Domain Number	Weathering Model	Position	Stationary Domain	Estimation Method
1	Oxidized	Soil + Sap North	Soil + Sap North	Ordinary Kriging
2		Soil + Sap Central	Soil + Sap Central	
3		Soil + Sap Southwest	Soil + Sap Southwest	
4	Fresh	Central	LG (Low Grade)	Turning bands simulation
5			HG (High Grade)	
6		Southwest	LG (Low Grade)	
7			HG (High Grade)	
8		North S	LG (Low Grade)	
9			HG (High Grade)	
10		North N	LG (Low Grade)	
11			HG (High Grade)	

Source: GE21, 2025.

14.2.4 Metallurgic Recovery Model

The Metallurgic Recovery 3D model was constructed to define different recovery factors for zones with different mineralogical and geochemical setups. A total of three domains were individualized (Figure 14-4):

- High Talc Material (High Talc)
- Oxidized Material (Ox)
- Fresh Material (Fresh)

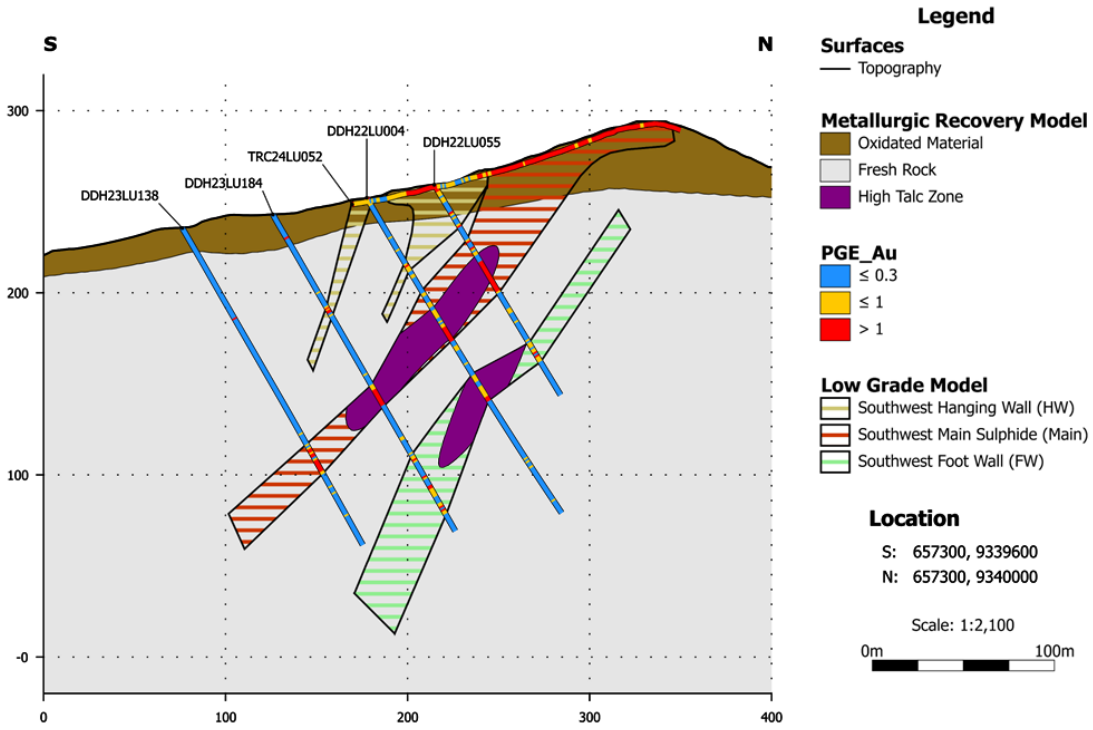

Figure 14-4: Metallurgic Recovery Model and Low-Grade Shells – Section N-S – View of the Southwest area

Source: GE21, 2025.

14.2.5 QP Opinion

The Qualified Person considers the geological interpretations and modelling to be adequate for a Mineral Resource Estimation study. The mineralized 3D bodies honour the mineralized intervals and have adequate continuity. Weathering and Oxidation models are consistent with drill hole logs and assays. QA/QC procedures follow the industry's practices.

The QP recommends, in further geological models, adopting an approach with implicit modelling methods and reducing domain internal dilution.

14.3 Statistical Analysis

14.3.1 Regularization of Samples

The analysis of the sample database showed that more than 97% of the drilling samples have a length of less than or equal to 1 meter. GE21 performed the regularization of samples inside the modelled domains. The chosen composite size is 1 meter. This composite was used for the complementary studies of statistics and geostatistics (Figure 14-5).

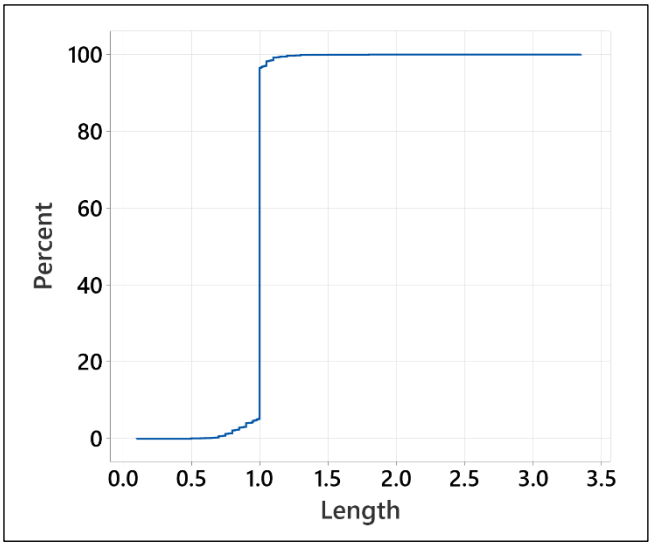

Parameter	Value
Count	107,449
Mean	0.995
SD	0.055
CV	0.056
Variance	0.003
Minimum	0.10
Q1	1.00
Q2	1.00
Q3	1.00
Maximum	3.35

Figure 14-5: Un-composited assay interval length statistics

Source: GE21, 2025.

14.3.2 Support Correction of Trench Dataset

The geostatistical concept of support is associated with average values in volumes, positions, areas and lengths that have the same statistical population. Different analytical and sampling methodologies could represent different support, since present differences in variability due to the precision of these methods. To merge the databases of different sampling methodologies, a support correction was applied to trench data, converting it to the same population as diamond drill holes. Figure 14-6 shows the process for support correction of the trench dataset using the Discrete Gaussian Model. Transformation is performed in Pd, Pt, Au and Rh values. Ni values are not present in trench samples.

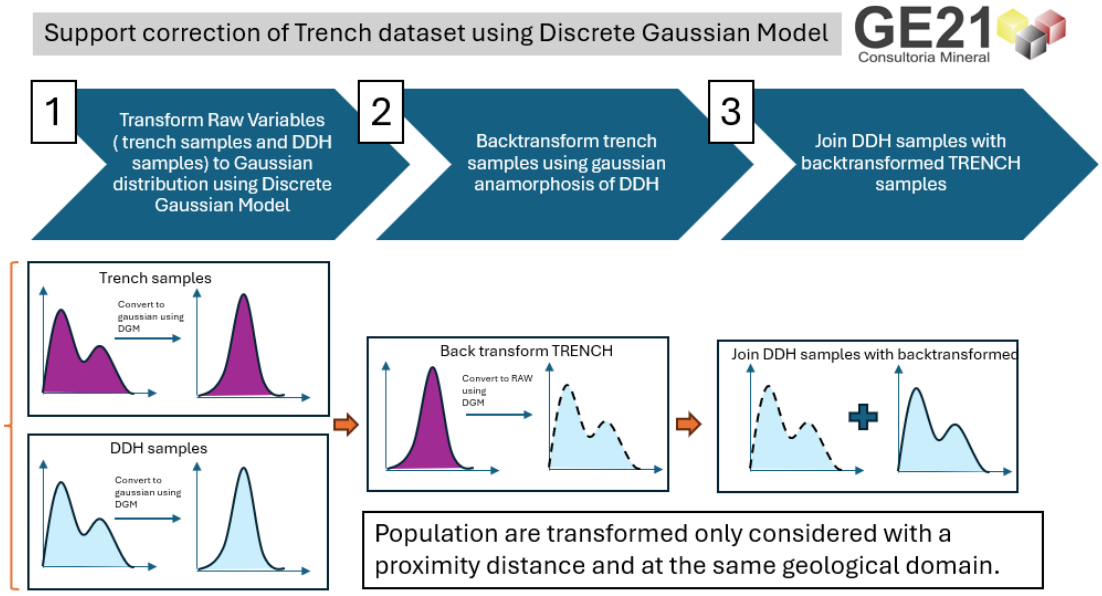

Figure 14-6: Process of support correction of trench dataset using discrete Gaussian model

Source: GE21, 2025.

A boundary of 50m from Trench data and DDH was used to transform the trench variables. Only samples inside soil and saprock (SO_SAP) were considered for this transformation.

The dataset used for support correction of drill holes, and trenches are shown in Figure 14-7.

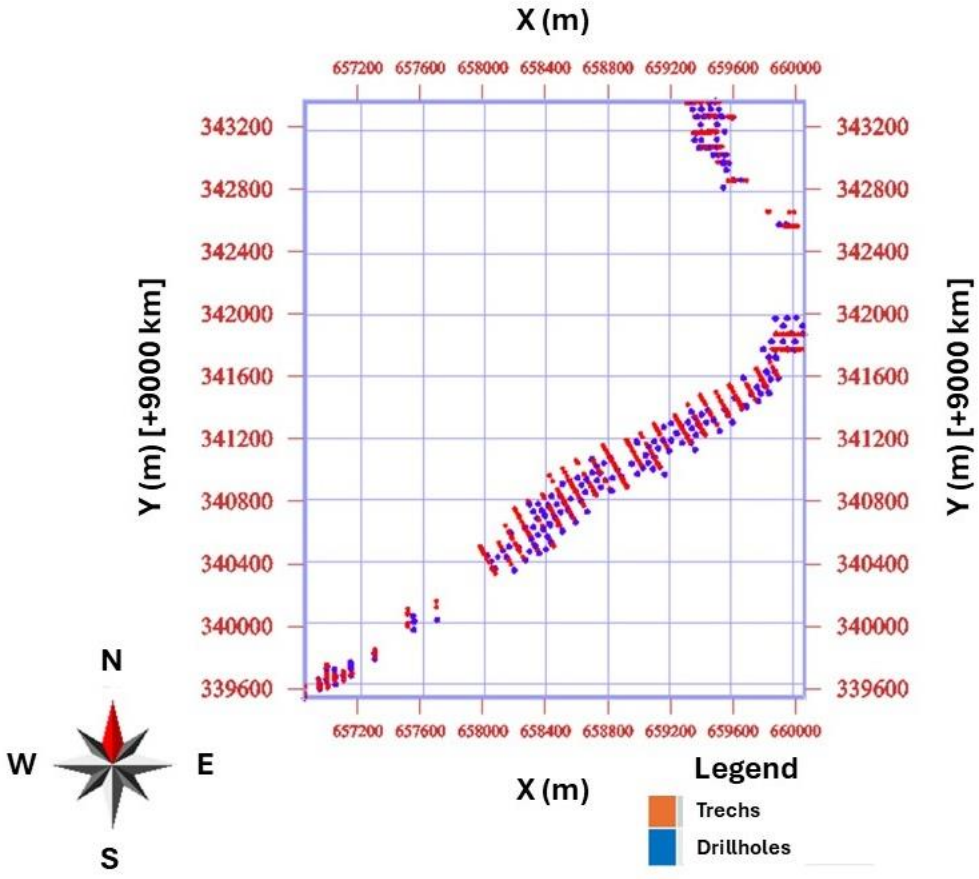

Figure 14-7: Dataset used for transformation of trench data and DDH

Source: GE21, 2025.

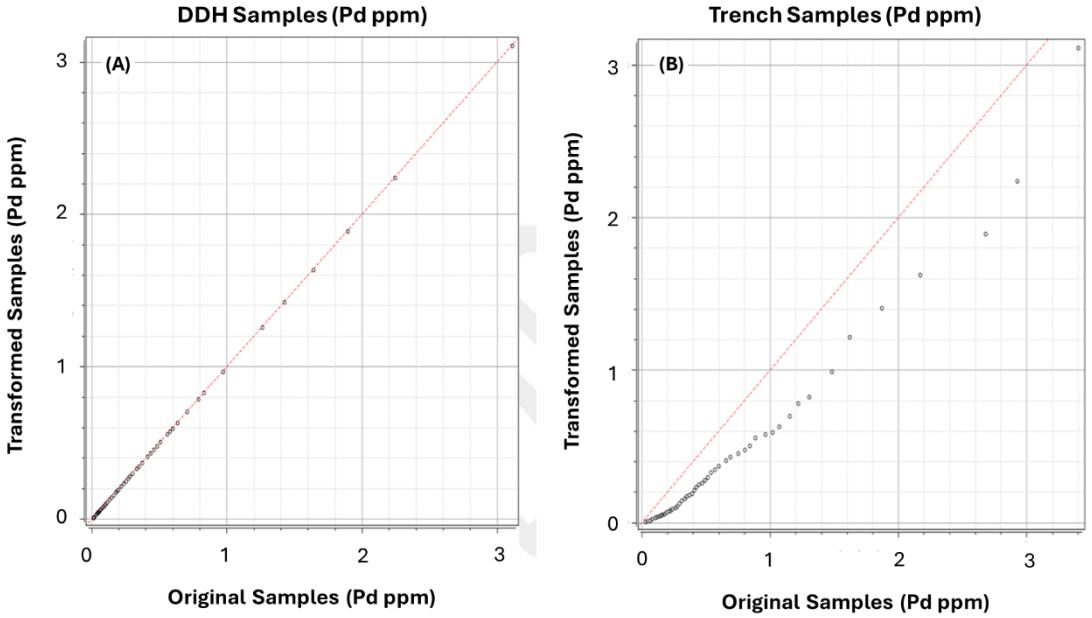

Figure 14-8: QQ plot of transformed and raw Pd values (trench data and DDH data)

Legend: A) QQ-Plot of DDH raw and transformed samples. B) QQ-Plot of TRENCH raw and transformed samples.
Source: GE21, 2025.

Table 14-4 shows the statistics for transformed and original composite data.

Table 14-4: Statistical for transformed and composite dataset

Variable	Unit	Count	Mean	Standard Deviation	Coefficient of variation	Minimum	Maximum	Quantile 25%	Quantile 50%	Quantile 75%
Au	ppm	30,035	0.04	0.09	2.49	0.00	3.91	0.00	0.01	0.03
Au transformed	ppm	30,035	0.04	0.10	2.51	0.00	3.91	0.01	0.01	0.03
Pd	ppm	30,035	0.66	1.70	2.57	0.00	156.29	0.18	0.33	0.69
Pd transformed	ppm	30,035	0.66	1.80	2.75	0.00	156.29	0.18	0.33	0.67
Pt	ppm	30,035	0.47	1.83	3.92	0.00	158.09	0.13	0.24	0.47
Pt transformed	ppm	30,035	0.47	1.95	4.10	0.00	158.09	0.13	0.23	0.46
Rh	ppm	30,035	0.06	0.25	4.21	0.00	17.33	0.00	0.02	0.05
Rh transformed	ppm	30,035	0.06	0.29	4.81	0.00	17.33	0.00	0.02	0.05

Source: GE21, 2025.

14.3.3 Exploratory Data Analysis (EDA)

Drilling samples composite statistical analysis was performed for Pd (ppm), Pt (ppm), Rh (ppm), Au (ppm) and Ni (ppm) variables. The EDA was performed using the sample composites and considering the estimation domains presented in Section 14.2.3. Table 14-5 shows the basic statistics for these variables.

Figure 14-9 to Figure 14-13 show the box plots for the Pd (ppm), Pt(ppm), Rh (ppm), Au (ppm) and Ni (ppm) variables.

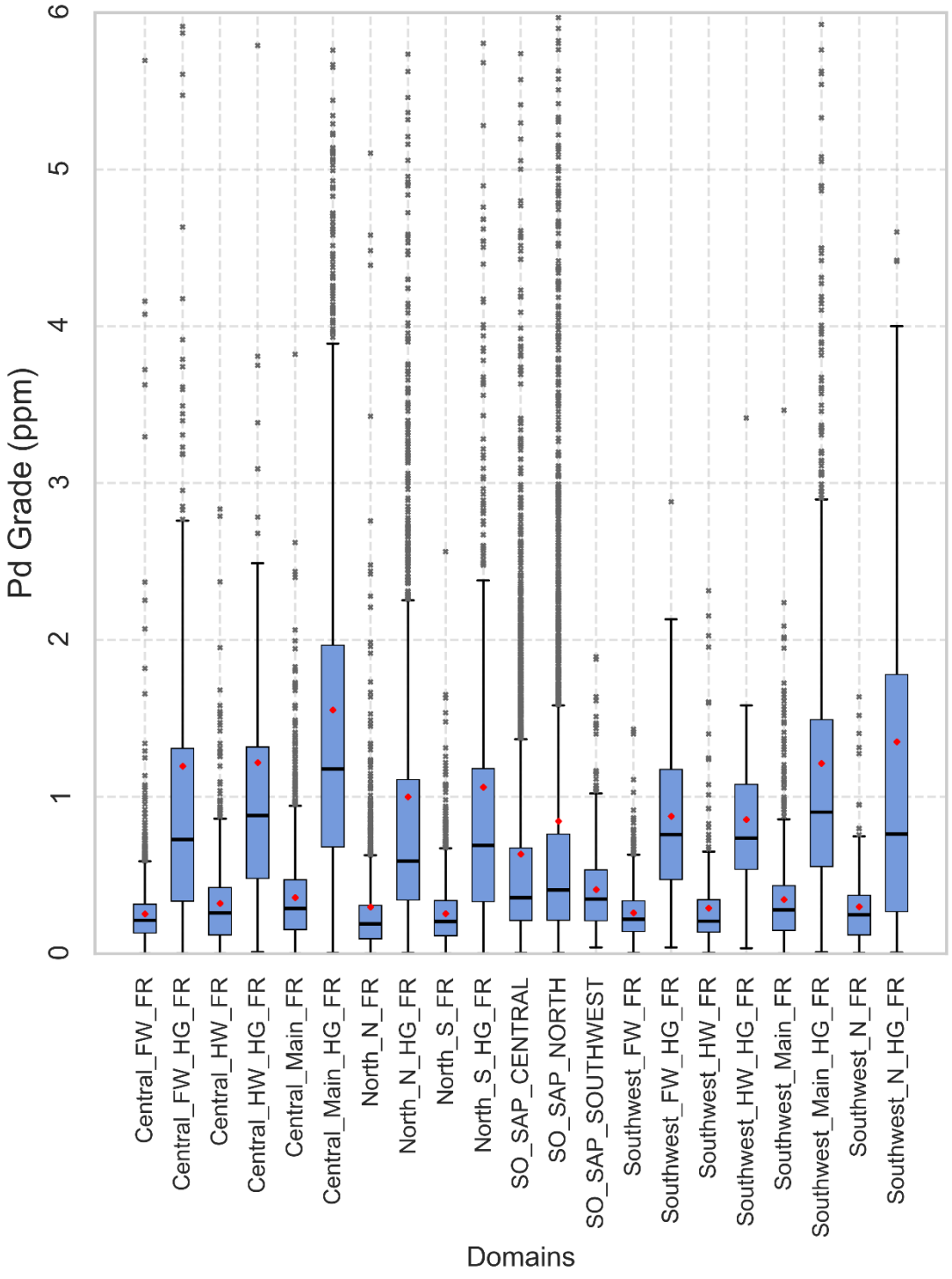

Figure 14-9: Pd ppm box plot chart by domains

Source: GE21, 2025.

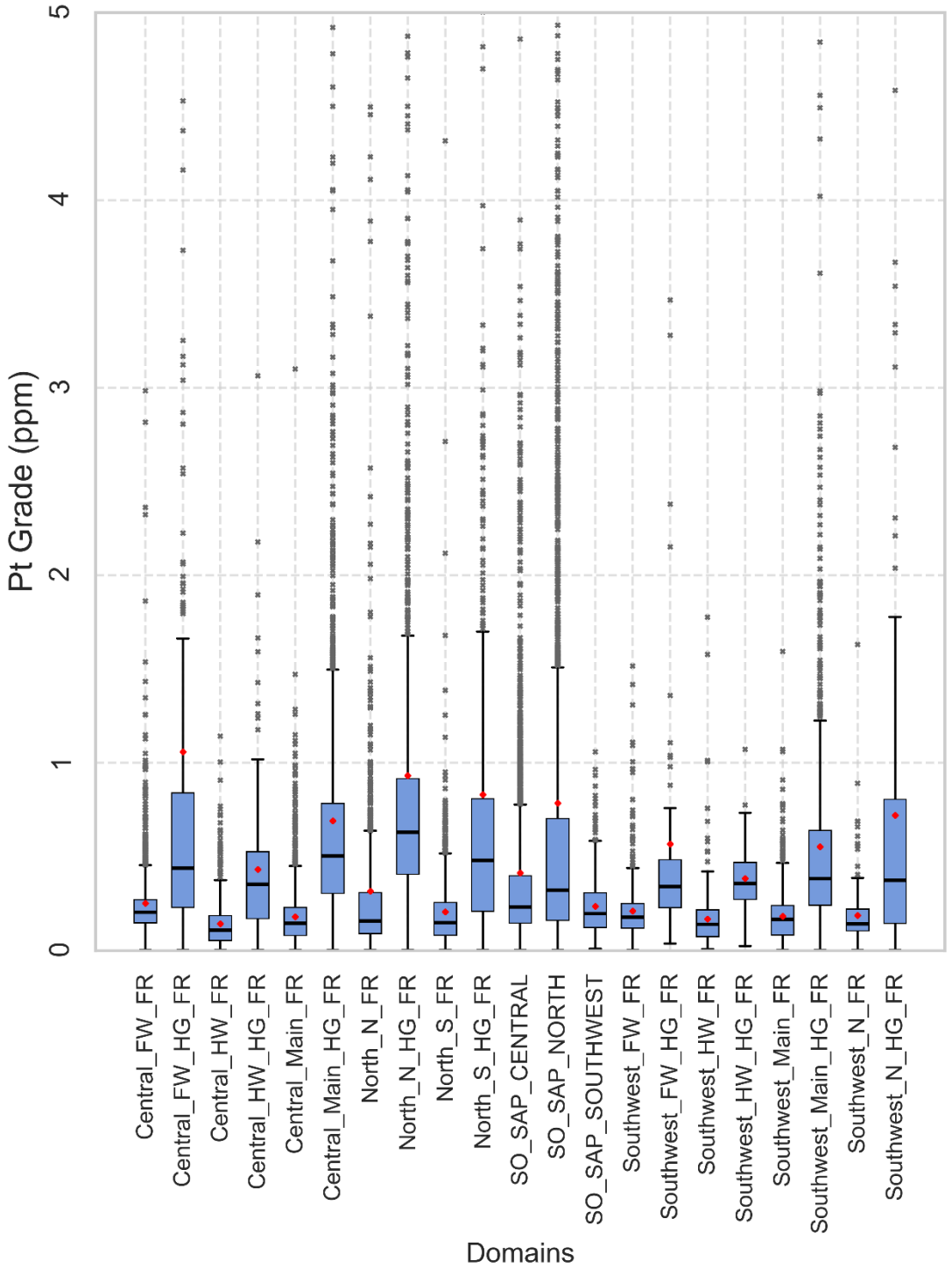

Figure 14-10: Pt ppm box plot chart by domains

Source: GE21, 2025.

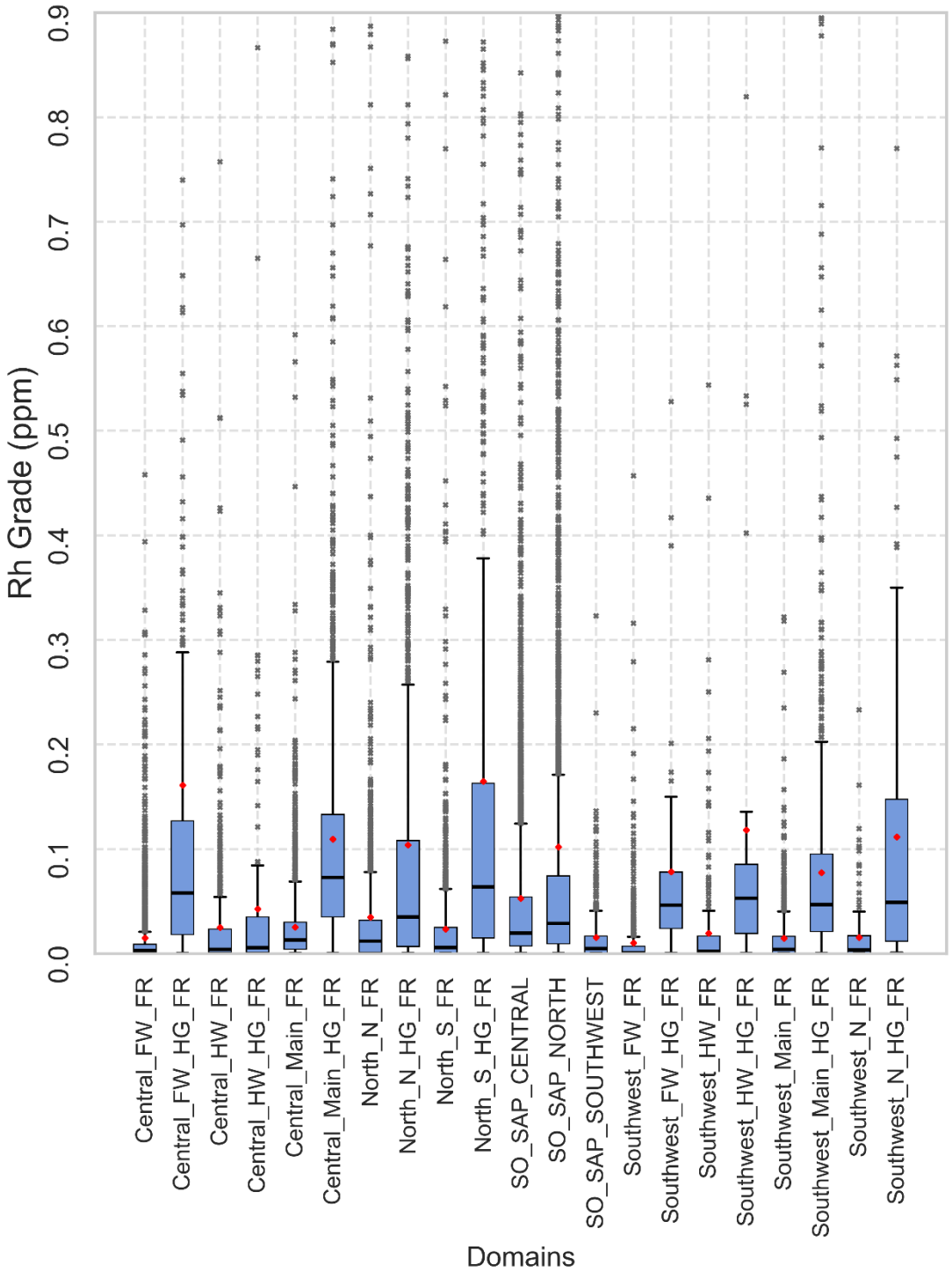

Figure 14-11: Rh ppm box plot chart by domains

Source: GE21, 2025.

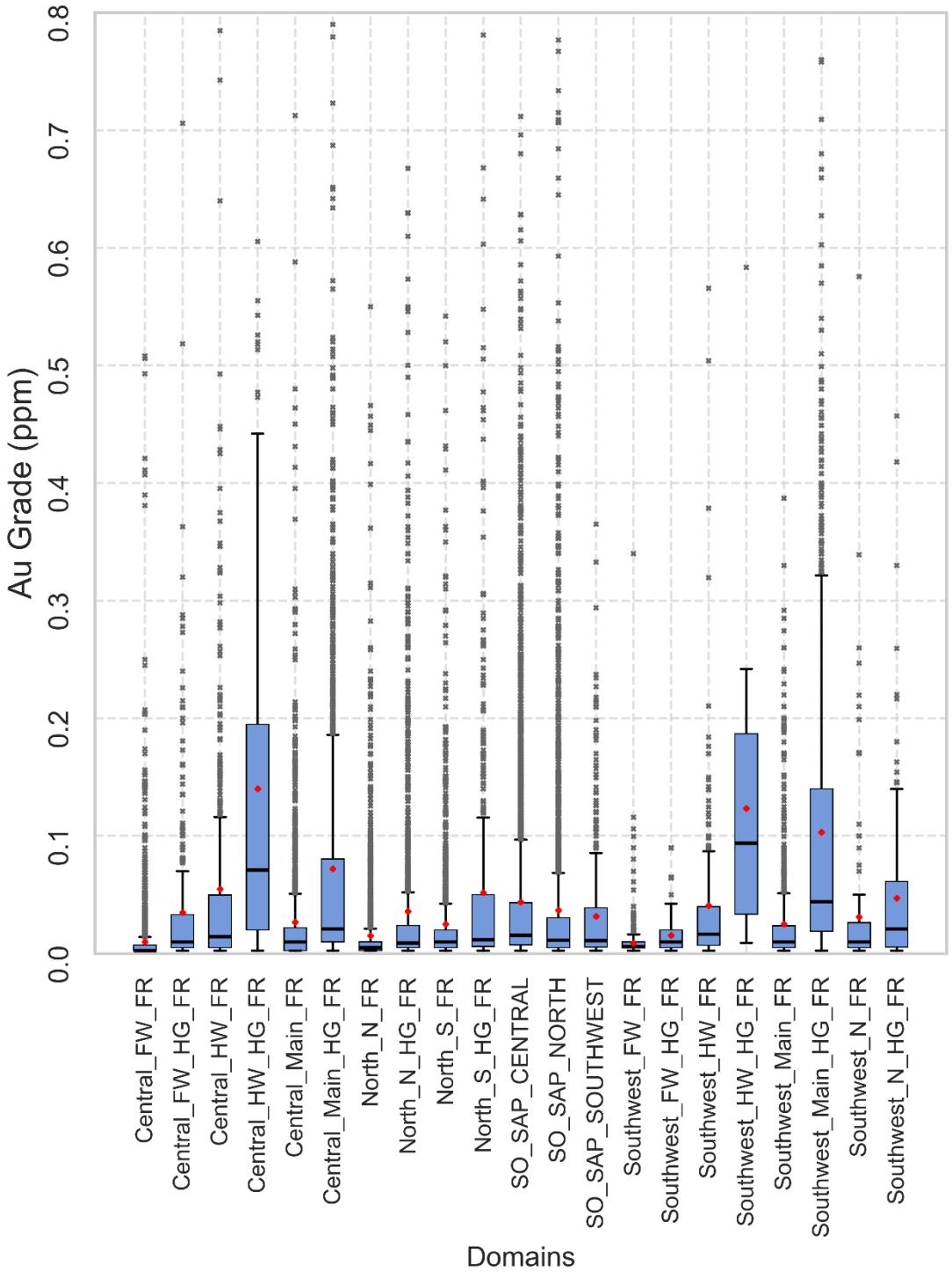

Figure 14-12: Au ppm box plot chart by domains

Source: GE21, 2025.

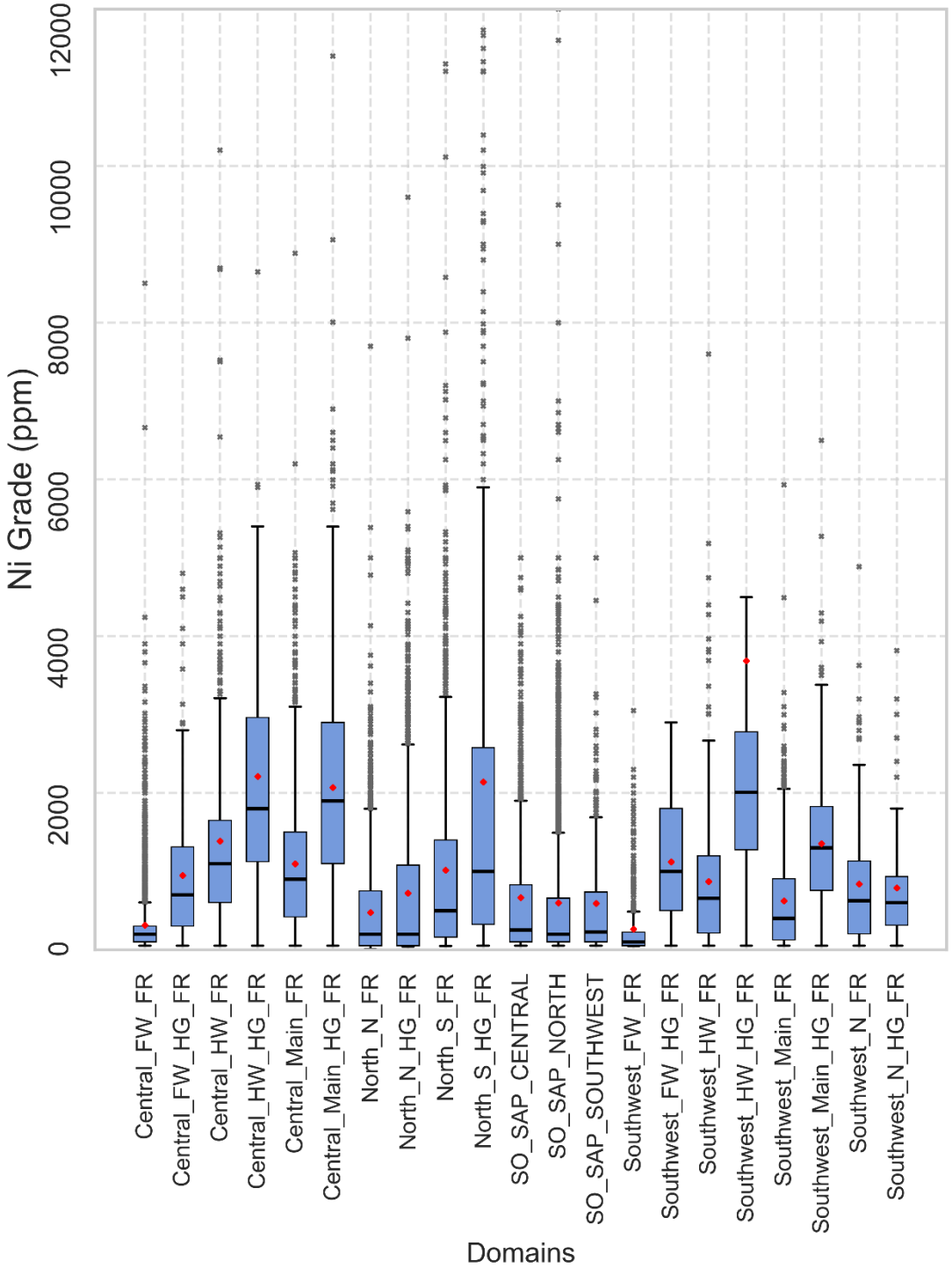

Figure 14-13: Ni ppm box plot chart by domains

Source: GE21, 2025.

Table 14-5: Basic statistics of Pd, Pt, Rh, Au, and Ni in the domains

Variable	Domain	Length (m)	Mean	S.D.	C.V.	Var.	Min.	Q25	Q50	Q75	Max.
Pd (ppm)	Central_FW_FR	2,986.3	0.253	0.328	1.297	0.108	0.0005	0.132	0.213	0.315	12.436
	Central_FW_HG_FR	374.3	1.189	2.864	2.410	8.204	0.0005	0.334	0.727	1.304	50.965
	Central_HW_FR	883.0	0.320	0.305	0.953	0.093	0.0005	0.119	0.260	0.420	2.835
	Central_HW_HG_FR	162.6	1.225	1.446	1.180	2.092	0.0100	0.479	0.882	1.317	8.764
	Central_Main_FR	1,895.0	0.357	0.347	0.972	0.121	0.0005	0.153	0.289	0.469	7.250
	Central_Main_HG_FR	1,915.7	1.553	1.750	1.126	3.061	0.0025	0.679	1.180	1.970	38.374
	North_N_FR	2,990.5	0.296	2.870	9.681	8.239	0.0010	0.093	0.190	0.307	156.291
	North_N_HG_FR	1,779.4	0.998	1.425	1.428	2.031	0.0025	0.341	0.591	1.109	20.233
	North_S_FR	1,776.3	0.255	0.209	0.821	0.044	0.0005	0.113	0.206	0.338	2.563
	North_S_HG_FR	739.7	1.060	1.360	1.283	1.850	0.0005	0.330	0.690	1.175	11.333
	SAP_SO_CENTRAL	5,545.7	0.745	1.367	1.834	1.868	0.0025	0.224	0.405	0.820	36.293
	SAP_SO_NORTH	4,820.5	0.846	2.570	3.037	6.604	0.0025	0.212	0.407	0.762	97.162
	SAP_SO_SOUTHWEST	891.3	0.420	0.317	0.754	0.100	0.0051	0.222	0.350	0.530	3.299
	Southwest_FW_FR	771.6	0.260	0.181	0.698	0.033	0.0025	0.139	0.220	0.337	1.430
	Southwest_FW_HG_FR	116.4	0.878	0.535	0.609	0.286	0.0400	0.472	0.760	1.174	2.880
	Southwest_HW_FR	327.7	0.290	0.306	1.057	0.094	0.0050	0.136	0.208	0.346	2.314
	Southwest_HW_HG_FR	28.5	0.859	0.663	0.771	0.439	0.0344	0.553	0.728	1.047	3.415
	Southwest_Main_FR	938.5	0.345	0.323	0.937	0.104	0.0005	0.145	0.280	0.433	3.465
	Southwest_Main_HG_FR	1,058.8	1.214	1.153	0.949	1.329	0.0079	0.554	0.902	1.499	9.913
	Southwest_N_FR	171.3	0.299	0.275	0.920	0.076	0.0025	0.119	0.248	0.374	1.637
	Southwest_N_HG_FR	135.6	1.358	1.704	1.255	2.903	0.0067	0.260	0.750	1.799	8.614
Pt (ppm)	Central_FW_FR	2,986.3	0.252	1.062	4.215	1.127	0.0025	0.148	0.205	0.271	54.012
	Central_FW_HG_FR	374.3	1.045	3.236	3.096	10.470	0.0028	0.227	0.440	0.840	39.685
	Central_HW_FR	883.0	0.143	0.135	0.947	0.018	0.0025	0.053	0.110	0.188	1.143
	Central_HW_HG_FR	162.6	0.430	0.416	0.969	0.173	0.0025	0.170	0.354	0.528	3.064
	Central_Main_FR	1,895.0	0.181	0.171	0.947	0.029	0.0025	0.080	0.146	0.230	3.100
	Central_Main_HG_FR	1,915.7	0.691	0.921	1.333	0.848	0.0025	0.305	0.505	0.784	18.189
	North_N_FR	2,990.5	0.317	2.937	9.260	8.624	0.0025	0.090	0.158	0.309	158.089
	North_N_HG_FR	1,779.4	0.930	1.697	1.825	2.880	0.0025	0.404	0.631	0.914	42.494
	North_S_FR	1776.3	0.206	0.448	2.173	0.201	0.0043	0.082	0.150	0.257	17.055
	North_S_HG_FR	739.7	0.832	1.782	2.141	3.176	0.0027	0.210	0.482	0.810	33.432
	SAP_SO_CENTRAL	5,545.7	0.446	1.770	3.966	3.134	0.0025	0.154	0.255	0.451	104.310

Variable	Domain	Length (m)	Mean	S.D.	C.V.	Var.	Min.	Q25	Q50	Q75	Max.
	SAP_SO_NORTH	4,820.5	0.788	2.868	3.640	8.228	0.0025	0.162	0.323	0.704	94.405
	SAP_SO_SOUTHWEST	891.3	0.230	0.167	0.727	0.028	0.0050	0.122	0.194	0.292	1.608
	Southwest_FW_FR	771.6	0.211	0.262	1.238	0.068	0.0025	0.120	0.176	0.250	5.960
	Southwest_FW_HG_FR	116.4	0.569	1.294	2.276	1.674	0.0375	0.228	0.342	0.484	13.270
	Southwest_HW_FR	327.7	0.168	0.177	1.054	0.031	0.0081	0.074	0.140	0.217	1.776
	Southwest_HW_HG_FR	28.5	0.386	0.233	0.604	0.054	0.0237	0.277	0.362	0.476	1.073
	Southwest_Main_FR	938.5	0.183	0.144	0.787	0.021	0.0025	0.083	0.168	0.244	1.594
	Southwest_Main_HG_FR	1,058.8	0.554	0.570	1.029	0.325	0.0026	0.241	0.383	0.644	5.334
	Southwest_N_FR	171.3	0.183	0.159	0.868	0.025	0.0025	0.102	0.141	0.221	1.632
	Southwest_N_HG_FR	135.6	0.700	0.930	1.329	0.865	0.0025	0.144	0.371	0.796	7.280
Rh (ppm)	Central_FW_FR	2,986.3	0.015	0.070	4.708	0.005	0.0005	0.001	0.003	0.009	2.607
	Central_FW_HG_FR	374.3	0.159	0.484	3.043	0.234	0.0005	0.018	0.058	0.124	6.062
	Central_HW_FR	883.0	0.025	0.059	2.358	0.003	0.0005	0.001	0.004	0.024	0.757
	Central_HW_HG_FR	162.6	0.043	0.105	2.430	0.011	0.0005	0.001	0.006	0.036	0.866
	Central_Main_FR	1,895.0	0.025	0.042	1.667	0.002	0.0005	0.004	0.013	0.030	0.592
	Central_Main_HG_FR	1,915.7	0.109	0.148	1.353	0.022	0.0005	0.035	0.073	0.133	2.011
	North_N_FR	2,990.5	0.035	0.224	6.458	0.050	0.0005	0.001	0.012	0.032	10.988
	North_N_HG_FR	1,779.4	0.103	0.294	2.843	0.086	0.0005	0.007	0.035	0.108	8.369
	North_S_FR	1,776.3	0.024	0.061	2.566	0.004	0.0005	0.001	0.006	0.025	0.873
	North_S_HG_FR	739.7	0.165	0.345	2.095	0.119	0.0005	0.015	0.064	0.162	4.770
	SAP_SO_CENTRAL	5,545.7	0.057	0.123	2.144	0.015	0.0005	0.008	0.024	0.065	3.202
	SAP_SO_NORTH	4,820.5	0.102	0.496	4.846	0.246	0.0005	0.009	0.029	0.074	17.334
	SAP_SO_SOUTHWEST	891.3	0.017	0.027	1.631	0.001	0.0005	0.001	0.007	0.019	0.323
	Southwest_FW_FR	771.6	0.010	0.031	3.024	0.001	0.0005	0.001	0.001	0.007	0.457
	Southwest_FW_HG_FR	116.4	0.078	0.201	2.569	0.040	0.0005	0.024	0.047	0.078	2.073
	Southwest_HW_FR	327.7	0.019	0.052	2.681	0.003	0.0005	0.001	0.002	0.017	0.544
	Southwest_HW_HG_FR	28.5	0.122	0.203	1.673	0.041	0.0005	0.020	0.053	0.087	0.820
	Southwest_Main_FR	938.5	0.015	0.029	1.961	0.001	0.0005	0.001	0.004	0.016	0.322
	Southwest_Main_HG_FR	1,058.8	0.077	0.111	1.436	0.012	0.0005	0.021	0.047	0.096	1.535
	Southwest_N_FR	171.3	0.015	0.030	1.965	0.001	0.0005	0.001	0.003	0.017	0.233
	Southwest_N_HG_FR	135.6	0.110	0.140	1.278	0.020	0.0010	0.011	0.048	0.145	0.770
Au (ppm)	Central_FW_FR	2,986.3	0.010	0.029	2.931	0.001	0.0025	0.003	0.003	0.007	0.508
	Central_FW_HG_FR	374.3	0.035	0.068	1.950	0.005	0.0025	0.005	0.010	0.033	0.706
	Central_HW_FR	883.0	0.055	0.182	3.293	0.033	0.0025	0.005	0.014	0.050	3.896

Variable	Domain	Length (m)	Mean	S.D.	C.V.	Var.	Min.	Q25	Q50	Q75	Max.
	Central_HW_HG_FR	162.6	0.140	0.173	1.233	0.030	0.0025	0.020	0.071	0.195	1.023
	Central_Main_FR	1,895.0	0.027	0.054	2.015	0.003	0.0025	0.003	0.010	0.022	0.712
	Central_Main_HG_FR	1,915.7	0.072	0.131	1.816	0.017	0.0025	0.010	0.021	0.081	2.354
	North_N_FR	2,990.5	0.015	0.053	3.464	0.003	0.0025	0.003	0.005	0.010	2.158
	North_N_HG_FR	1,779.4	0.036	0.089	2.485	0.008	0.0025	0.005	0.009	0.024	2.058
	North_S_FR	1,776.3	0.025	0.050	2.018	0.003	0.0025	0.005	0.010	0.020	0.542
	North_S_HG_FR	739.7	0.052	0.099	1.891	0.010	0.0025	0.006	0.012	0.050	1.040
	SAP_SO_CENTRAL	5,545.7	0.053	0.107	2.034	0.011	0.0025	0.008	0.018	0.051	2.563
	SAP_SO_NORTH	4,820.5	0.037	0.106	2.874	0.011	0.0025	0.005	0.011	0.030	3.912
	SAP_SO_SOUTHWEST	891.3	0.028	0.040	1.419	0.002	0.0025	0.007	0.012	0.033	0.365
	Southwest_FW_FR	771.6	0.009	0.015	1.700	0.000	0.0025	0.005	0.006	0.010	0.340
	Southwest_FW_HG_FR	116.4	0.016	0.017	1.103	0.000	0.0025	0.005	0.010	0.020	0.090
	Southwest_HW_FR	327.7	0.041	0.094	2.326	0.009	0.0025	0.007	0.016	0.040	1.083
	Southwest_HW_HG_FR	28.5	0.124	0.120	0.969	0.014	0.0091	0.035	0.114	0.194	0.583
	Southwest_Main_FR	938.5	0.025	0.043	1.702	0.002	0.0025	0.005	0.010	0.024	0.387
	Southwest_Main_HG_FR	1,058.8	0.103	0.152	1.476	0.023	0.0025	0.019	0.044	0.140	2.400
	Southwest_N_FR	171.3	0.031	0.067	2.140	0.004	0.0025	0.005	0.010	0.026	0.576
	Southwest_N_HG_FR	135.6	0.047	0.072	1.530	0.005	0.0025	0.005	0.020	0.062	0.457
Ni (ppm)	Central_FW_FR	2,986.3	312	455	1.5	206575	50	100	200	300	8503
	Central_FW_HG_FR	374.3	949	815	0.9	664598	50	300	700	1312	4800
	Central_HW_FR	883.0	1,379	1787	1.3	3194888	50	600	1098	1649	32063
	Central_HW_HG_FR	162.6	2,221	1914	0.9	3663130	50	1124	1800	3000	18767
	Central_Main_FR	1,895.0	1,094	942	0.9	888094	50	417	900	1500	17410
	Central_Main_HG_FR	1,915.7	2,072	1284	0.6	1649055	50	1100	1900	2900	14207
	North_N_FR	2,863.4	476	596	1.3	355278	5	50	200	750	7700
	North_N_HG_FR	1,737.5	722	1030	1.4	1061372	40	50	200	1088	9600
	North_S_FR	1,776.3	1,018	1346	1.3	1811107	48	161	500	1400	17544
	North_S_HG_FR	739.7	2,121	3157	1.5	9966045	50	317	1000	2572	25269
	SAP_SO_CENTRAL	1,777.3	612	886	1.4	785780	50	100	213	725	5000
	SAP_SO_NORTH	2,951.7	597	1069	1.8	1143613	50	100	200	658	20995
	SAP_SO_SOUTHWEST	465.8	686	940	1.4	883853	50	100	250	886	5000
	Southwest_FW_FR	771.6	263	388	1.5	150880	46	50	101	225	3051
	Southwest_FW_HG_FR	116.4	1,127	809	0.7	654313	50	500	999	1800	2900
	Southwest_HW_FR	327.7	869	908	1.0	824057	50	215	663	1200	7600

Variable	Domain	Length (m)	Mean	S.D.	C.V.	Var.	Min.	Q25	Q50	Q75	Max.
	Southwest_HW_HG_FR	28.5	3784	5567	1.5	30989448	52	1302	2020	3402	25018
	Southwest_Main_FR	938.5	624	647	1.0	418231	50	126	399	905	5930
	Southwest_Main_HG_FR	1,058.8	1,355	813	0.6	660621	50	751	1300	1830	6500
	Southwest_N_FR	171.3	839	812	1.0	659308	50	203	649	1108	4886
	Southwest_N_HG_FR	135.6	791	658	0.8	433066	50	315	600	997	3818

Source: GE21, 2025.

14.4 Grade Estimation

14.4.1 Simulation Approach and Kriging Estimation

Geostatistical simulation and kriging are both spatial interpolation methods abroad by Geostatistics, but they have different purposes and methodologies. The kriging estimation produces a smooth Best Linear Unbiased Estimator value at unsampled locations (BLUE), with a single interpolated map. This map represents the expected value (mean value) in block models. Geostatistical simulations generate multiple realizations (possible scenarios) of spatial variability, capturing uncertainty. Figure 14-14 represents the difference between the two methods. The geostatistical simulation is represented by Figure 14-14 (a) which each Selective Mining Unit (SMU) is characterized by a probabilistic distribution of some feature, while Figure 14-14 (b) represent the estimation (kriging) process which a single average value is associated with the SMU. The geostatistical simulations allow quantifying spatial uncertainty, risk assessment, and decision-making in resource estimation.

The E-type post processing consists of given the average of overall simulations in some support and is close to kriging estimation. The importance of simulations in Mineral Resource Estimation is defined by the possibility of measurement of the production uncertainties in the advanced steps in the mining project, the calculation of recoverable resources and dimension definition of sampling strategies. These steps form the foundation of the mining planning and future activities in mining project.

A valid conditional simulation in geostatistics ensures that simulated values honour both spatial continuity and data distribution:

- The **variogram** characterizes the spatial dependence of the data by defining how values at different locations are correlated. A valid conditional simulation reproduces the input modeled variogram.
- The **histogram** (or probability distribution function - PDF) represents the statistical distribution of values in the dataset. A valid conditional simulation preserves the histogram of the data.

If these conditions are satisfied, the simulations ensuring statistical realism and spatial realism of mineral deposit.

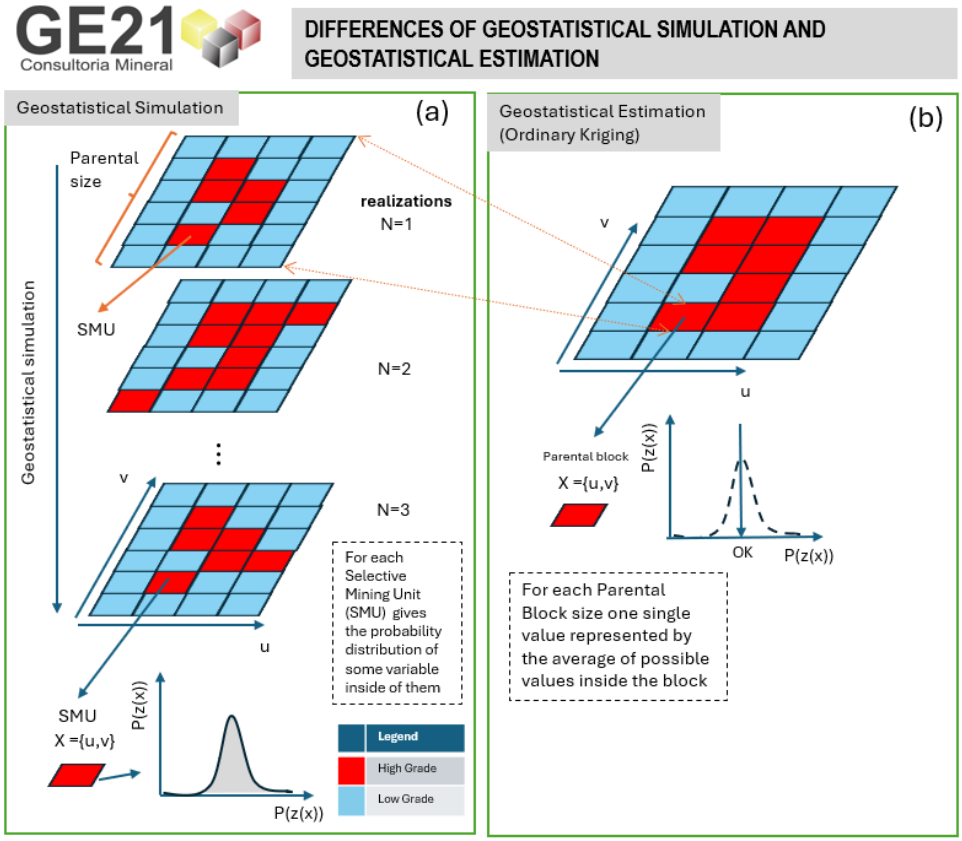

Figure 14-14: Differences between geostatistical simulations and geostatistical estimation

Source: GE21, 2025.

14.4.2 Simulation and Kriging Strategies

A test for defining the number of simulations was conducted in Pd in Central Domain, for High and Low Grade. Figure 14-15 and Figure 14-16 indicate that 50 simulations are sufficient to account for the full range of ergodic variations in the simulations.

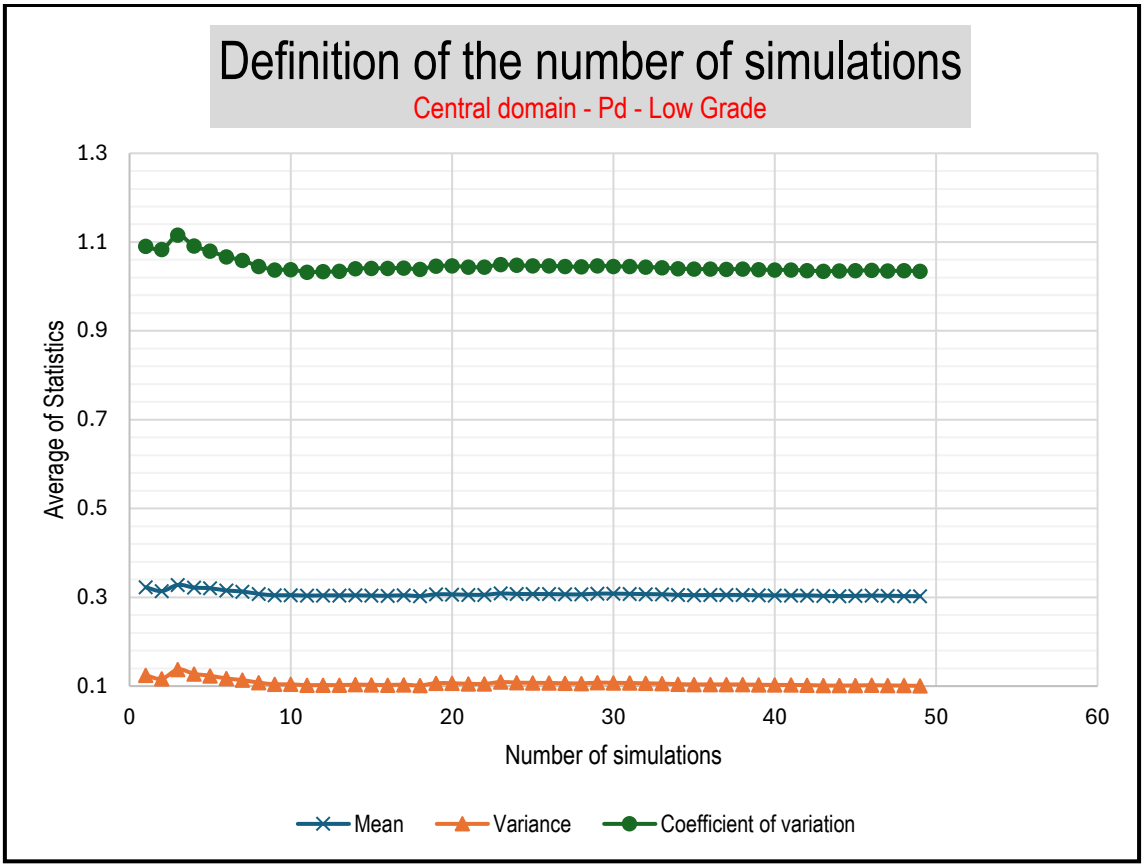

Figure 14-15: Average of Statistics according to the number of simulations (Pd Central Low Grade)

Source: GE21, 2025.

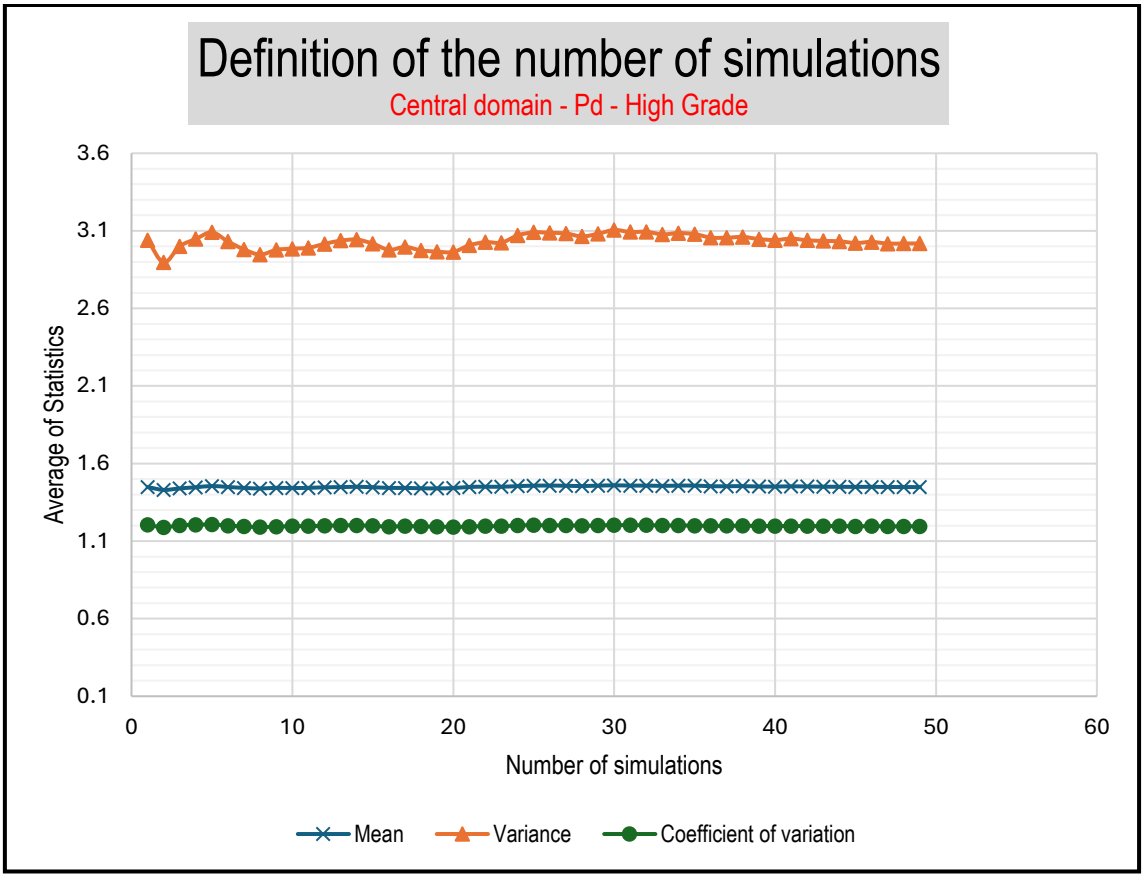

Figure 14-16: Definition of the number of simulations (Pd Central High Grade)

Source: GE21, 2025.

Table 14-6 shows the simulation strategy used for all domains.

Table 14-6: Simulation strategy for all domains and chemical elements

Region	Variable	Orientation			Ranges			Min number of samples	Max number of samples	Nested
		Dip	Azim	Rake	Max	Med	Min			Ellipsoid factor
		Degrees	Degrees	Degrees	m	m	m			
Central	Pd	60	140	90	40	40	10	3	20	2x, 3x and infinite
	Pt	60	140	90	20	20	10	3	20	2x, 3x and infinite
	Au	60	140	90	100	100	10	5	20	2x, 3x and infinite
	Ni	60	140	90	100	100	10	5	20	2x, 3x and infinite
	Rh	60	140	90	100	100	10	5	20	2x, 3x and infinite
	Cu	60	140	90	100	100	10	5	20	2x, 3x and infinite
Southwest	Pd	65	150	90	40	40	10	5	20	2x, 3x and infinite
	Pt	65	150	90	100	100	10	5	20	2x, 3x and infinite
	Au	65	150	90	100	100	10	5	20	2x, 3x and infinite
	Ni	65	150	90	100	100	10	5	20	2x, 3x and infinite
	Rh	65	150	90	100	100	10	5	20	2x, 3x and infinite
	Cu	65	150	90	100	100	10	5	20	2x, 3x and infinite
North N	Pd	80	260	90	40	40	10	5	20	2x, 3x and infinite
	Pt	80	260	90	100	100	10	5	20	2x, 3x and infinite
	Au	80	260	90	40	40	10	5	20	2x, 3x and infinite
	Ni	80	260	90	100	100	10	5	20	2x, 3x and infinite
	Rh	80	260	90	100	100	10	5	20	2x, 3x and infinite

Region	Variable	Orientation			Ranges			Min number of samples	Max number of samples	Nested
		Dip	Azim	Rake	Max	Med	Min			Ellipsoid factor
		Degrees	Degrees	Degrees	m	m	m			
	Cu	80	260	90	100	100	10	5	20	2x, 3x and infinite
North S	Pd	64	260	90	100	100	10	5	20	2x, 3x and infinite
	Pt	64	260	90	100	100	10	5	20	2x, 3x and infinite
	Au	64	260	90	40	40	10	5	20	2x, 3x and infinite
	Ni	64	260	90	100	100	10	5	20	2x, 3x and infinite
	Rh	64	260	90	40	40	10	4	12	2x, 3x and infinite
	Cu	64	260	90	100	100	10	5	20	2x, 3x and infinite

Source: GE21, 2025.

Table 14-7 shows the estimation strategy for oxide domain.

Table 14-7: Search strategy for oxide domain

Region	Orientation			Ranges			Min number of samples	Max number of samples first factor	Max number of samples second factor	Max number of samples third factor	Maximum number per drill hole	Nested factors
	Dip	Azim	Rake	Max	Med	Min						
	Degrees	Degrees	Degrees	m	m	m						
Central	60	140	90	40	40	10	3	8	10	15	2	2x, 3x and infinite
Southwest	65	150	90	40	40	10	3	8	10	15	2	2x, 3x and infinite
North N	80	260	90	40	40	10	3	8	10	15	2	2x, 3x and infinite
North S	64	260	90	40	40	10	3	8	10	15	2	2x, 3x and infinite
Soil	0	0	90	40	40	10	3	8	10	15	2	2x, 3x and infinite

Source: GE21, 2025.

The ordinary kriging strategy shown on Table 14-7 was used for estimation of the variables in fresh domain, which purpose for comparison with E-type simulation values.

14.4.3 Variograms and Simulation Validation

Simulation was calculated using Isatis.Neo Mining (Version 2024.04.2), performing 50 realizations with 800 bands (Seed: 165426). Simulations are compared with raw variogram and histogram values. Table 14-8 shows an example of simulation validation in Central Domain, variable Pd. It can be observed that ergodic fluctuations encompass all raw variograms and histograms, representing valid realizations.

Source: GE21, 2025.

Table 14-9 shows the variogram models used for simulation of all domains and Table 14-10 shows the variogram models for oxide domain.

Table 14-8: Example of simulation validation for Pd in the central area domains

Dom	Histogram	Major Axis	Intermediate Axis	Minimum Axis
Pd Central HG	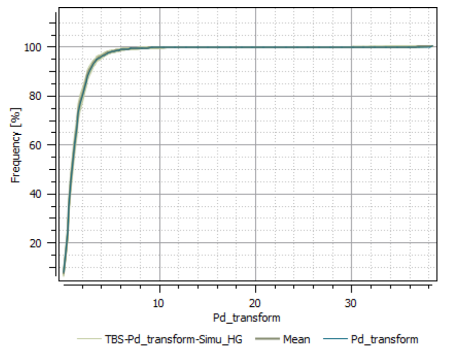	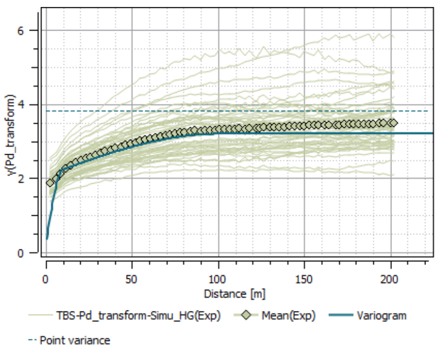	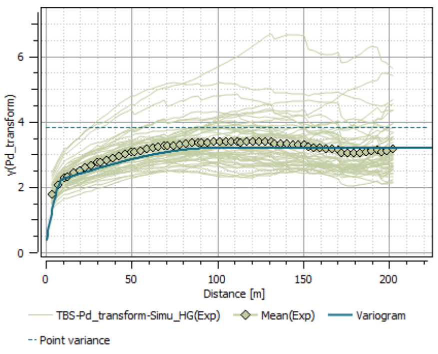	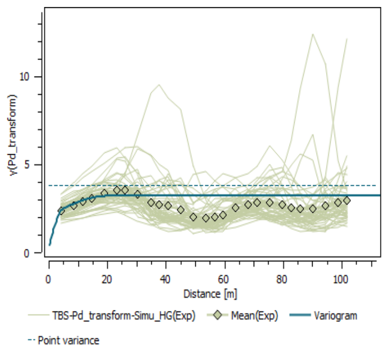
Pd Central LG	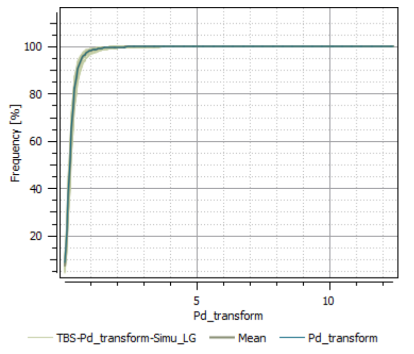	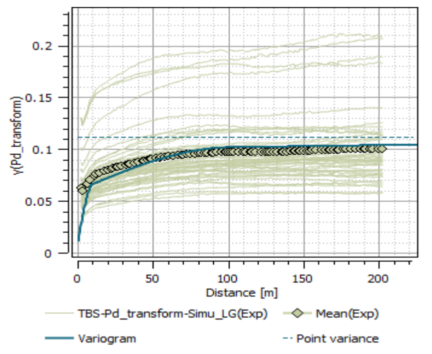	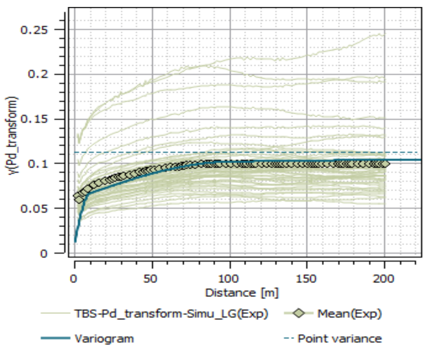	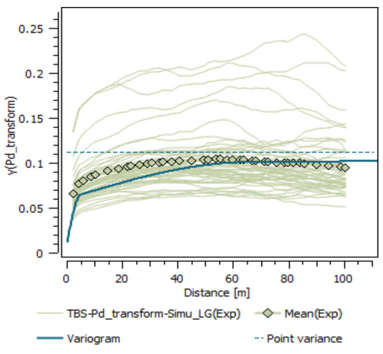

Source: GE21, 2025.

Table 14-9: Variogram models for each element and domain

Geostatistical Set	Variable	Dip (°)	Dip Azimuth (°)	Pitch (°)	Nugget	Structure 1					Structure 2					Structure 3				
						Model	Sill	Range			Model	Sill	Range			Model	Sill	Range		
								Major (m)	Semi (m)	Minor (m)			Major (m)	Semi (m)	Minor (m)			Major (m)	Semi (m)	Minor (m)
Ag_Central_HG	Ag	60	140	90	0.30	Sph	0.15	40	40	10	Sph	0.25	100	100	20	Exp	0.30	∞*	∞*	∞*
Ag_Central_LG	Ag	60	140	90	0.30	Sph	0.70	50	50	10	-	-	-	-	-	-	-	-	-	-
Ag_NN_HG	Ag	80	260	90	0.33	Sph	0.67	50	30	10	-	-	-	-	-	-	-	-	-	-
Ag_NN_LG	Ag	80	260	90	0.33	Sph	0.67	50	30	10	-	-	-	-	-	-	-	-	-	-
Ag_NS_HG	Ag	64	260	90	0.32	Sph	0.12	45	25	5	Sph	0.56	90	45	10	-	-	-	-	-
Ag_Southwest_HG	Ag	65	150	90	0.20	Sph	0.20	40	40	40	Exp	0.10	100	100	80	Exp	0.50	∞*	∞*	∞*
Ag_Southwest_LG	Ag	65	150	90	0.31	Sph	0.69	40	20	10	-	0.00	-	-	-	-	-	-	-	-
Au_Central_HG	Au	60	140	90	0.30	Sph	0.25	40	40	10	Sph	0.45	100	80	20	-	-	-	-	-
Au_Central_LG	Au	60	140	90	0.39	Exp	0.27	20	20	5	Sph	0.34	60	60	25	-	-	-	-	-
Au_NN_HG	Au	80	260	90	0.33	Sph	0.67	50	30	20	-	-	-	-	-	-	-	-	-	-
Au_NN_LG	Au	80	260	90	0.34	Exp	0.56	40	40	20	Sph	0.10	∞*	∞*	∞*	-	-	-	-	-
Au_NS_HG	Au	64	260	90	0.32	Sph	0.12	45	25	5	Sph	0.56	90	45	10	-	-	-	-	-
Au_NS_LG	Au	64	260	90	0.33	Sph	0.05	100	25	5	Sph	0.51	150	45	10	Exp	0.10	∞*	∞*	∞*
Au_Southwest_HG	Au	65	150	90	0.22	Exp	0.73	100	100	40	Sph	0.05	∞*	∞*	∞*	-	-	-	-	-
Au_Southwest_LG	Au	65	150	90	0.32	Exp	0.38	100	50	50	Exp	0.30	∞*	∞*	100	-	-	-	-	-
Ni_Central_HG	Ni	60	140	90	0.30	Sph	0.25	40	40	10	Sph	0.45	90	90	20	-	-	-	-	-
Ni_Central_LG	Ni	60	140	90	0.30	Sph	0.70	40	40	10	-	-	-	-	-	-	-	-	-	-
Ni_NN_HG	Ni	80	260	90	0.20	Sph	0.25	10	10	10	Sph	0.55	50	50	40	-	-	-	-	-
Ni_NN_LG	Ni	80	260	90	0.30	Exp	0.10	20	20	15	Exp	0.60	60	60	50	-	-	-	-	-
Ni_NS_HG	Ni	64	260	90	0.25	Sph	0.20	80	25	5	Sph	0.55	90	45	10	-	-	-	-	-
Ni_NS_LG	Ni	64	260	90	0.20	Sph	0.20	80	25	5	Sph	0.60	100	45	15	-	-	-	-	-
Ni_Southwest_HG	Ni	65	150	90	0.28	Sph	0.11	50	50	50	Exp	0.33	200	200	100	Sph	0.28	∞*	∞*	∞*
Ni_Southwest_LG	Ni	65	150	90	0.25	Sph	0.25	80	80	50	Exp	0.50	250	250	150	-	-	-	-	-

Geostatistical Set	Variable	Dip (°)	Dip Azimuth (°)	Pitch (°)	Nugget	Structure 1					Structure 2					Structure 3				
						Model	Sill	Range			Model	Sill	Range			Model	Sill	Range		
								Major (m)	Semi (m)	Minor (m)			Major (m)	Semi (m)	Minor (m)			Major (m)	Semi (m)	Minor (m)
Pd_Central_HG	Pd	60	140	90	0.07	Sph	0.57	10	10	5	Sph	0.35	100	100	20	-	-	-	-	-
Pd_Central_LG	Pd	60	140	90	0.07	Sph	0.47	10	10	5	Sph	0.35	100	100	65	Exp	0.10	∞*	∞*	∞*
Pd_NN_HG	Pd	80	260	90	0.20	Sph	0.45	8	8	8	Sph	0.35	80	30	15	-	-	-	-	-
Pd_NN_LG	Pd	80	260	90	0.30	Sph	0.50	10	10	10	Sph	0.20	inf	inf	inf	-	-	-	-	-
Pd_NS_HG	Pd	64	260	90	0.31	Sph	0.33	10	10	5	Sph	0.36	55	40	25	-	-	-	-	-
Pd_NS_LG	Pd	64	260	90	0.31	Sph	0.33	10	10	8	Sph	0.36	55	55	25	-	-	-	-	-
Pd_Southwest_HG	Pd	65	150	90	0.31	Sph	0.38	8	8	8	Sph	0.31	50	30	30	-	-	-	-	-
Pd_Southwest_LG	Pd	65	150	90	0.31	Sph	0.40	5	5	5	Sph	0.29	45	35	35	-	-	-	-	-
Pt_Central_HG	Pt	60	140	90	0.27	Sph	0.49	10	10	3	Sph	0.24	70	70	30	-	-	-	-	-
Pt_Central_LG	Pt	60	140	90	0.27	Sph	0.48	10	10	3	Sph	0.13	70	70	30	Exp	0.13	∞*	∞*	∞*
Pt_ddh	Pt	0	90	90	0.82	Sph	0.09	66	66	66	Sph	0.09	367	367	367	-	-	-	-	-
Pt_NN_HG	Pt	80	260	90	0.18	Exp	0.60	4	4	4	Sph	0.17	20	10	10	Sph	0.05	∞*	∞*	∞*
Pt_NN_LG	Pt	80	260	90	0.18	Sph	0.53	3	3	3	Sph	0.10	22	10	10	Exp	0.19	∞*	∞*	∞*
Pt_NS_HG	Pt	64	260	90	0.33	Sph	0.50	5	5	5	Sph	0.10	10	10	10	Sph	0.07	∞*	∞*	∞*
Pt_NS_LG	Pt	64	260	90	0.33	Sph	0.40	5	5	5	Exp	0.15	10	10	10	Exp	0.11	∞*	∞*	∞*
Pt_Southwest_HG	Pt	65	150	90	0.19	Exp	0.66	5	3	3	Sph	0.15	20	10	10	-	-	-	-	-
Pt_Southwest_LG	Pt	65	150	90	0.22	Sph	0.62	5	5	3	Sph	0.11	40	10	10	Exp	0.04	∞*	∞*	∞*
Rh_Central_HG	Rh	60	140	90	0.24	Sph	0.33	10	10	3	Sph	0.34	100	50	16	Exp	0.09	∞*	∞*	∞*
Rh_Central_LG	Rh	60	140	90	0.36	Sph	0.47	50	10	3	Sph	0.17	134	55	16	-	-	-	-	-
Rh_NN_HG	Rh	80	260	90	0.32	Sph	0.37	10	10	5	Sph	0.21	100	50	30	Exp	0.11	∞*	∞*	∞*
Rh_NN_LG	Rh	64	260	90	0.50	Exp	0.25	20	10	5	Sph	0.10	60	30	30	Sph	0.15	∞*	∞*	∞*
Rh_NS_HG	Rh	60	260	90	0.10	Sph	0.35	15	5	2	Sph	0.55	55	20	20	-	-	-	-	-
Rh_NS_LG	Rh	60	260	90	0.15	Exp	0.79	20	20	3	Sph	0.06	100	100	15	-	-	-	-	-
Rh_Southwest_HG	Rh	65	150	90	0.30	Exp	0.55	10	10	5	Sph	0.15	80	30	30	-	-	-	-	-

Geostatistical Set	Variable	Dip (°)	Dip Azimuth (°)	Pitch (°)	Nugget	Structure 1					Structure 2					Structure 3					
						Model	Sill	Range			Model	Sill	Range			Model	Sill	Range			
								Major (m)	Semi (m)	Minor (m)			Major (m)	Semi (m)	Minor (m)			Major (m)	Semi (m)	Minor (m)	
Rh_Southwest_LG	Rh	65	150	90	0.25	Exp	0.65	8	8	5	Sph	0.10	50	30	30	-	-	-	-	-	
* Infinite (Range greater than 1000m)																					

Source: GE21, 2025.

Table 14-10: Variogram models for oxide domain

Geostatistical Set	Variable	Dip (°)	Dip Azimuth (°)	Pitch (°)	Nugget	Structure 1					Structure 2				
						Model	Sill	Range			Model	Sill	Range		
								Major (m)	Semi (m)	Minor (m)			Major (m)	Semi (m)	Minor (m)
Au_Solo	Au	0	90	90	0.16	Sph	0.33	5	5	5	Sph	0.51	20	20	20
Ni_Solo	Ni	0	90	90	0.08	Sph	0.00	22	22	22	Sph	0.92	37	37	37
Pd_Solo	Pd	0	90	90	0.50	Sph	0.18	5	5	5	Sph	0.32	20	20	20
Pt_Solo	Pt	0	90	90	0.65	Sph	0.17	6	6	6	Sph	0.18	27	27	27
Rh_Solo	Rh	0	90	90	0.61	Sph	0.16	2	2	2	Sph	0.23	16	16	16

Source: GE21, 2025.

14.4.4 Block Model

The simulation approach is commonly performed in point support. The QP consider that a block 10 times discretized is sufficient for represent the point variability of the data. The simulation block has the support of 2.5m x 2.5m x 2.5m. The parameters of simulation block model are related to Table 14-11.

Table 14-11: Grid geometry of simulation block size

	X	Y	Z
Number of nodes	1920	2240	320
Mesh size	2.5 m	2.5 m	2.5 m
Grid origin (center)	655775.00 m	9338780.00 m	-241.49 m
Grid origin (corner)	655773.75 m	9338778.75 m	-242.74 m

Source: GE21, 2025.

After simulation the realizations are upscaled for a parental block model with the dimensions of 25mx25mx5 according to Table 14-12. The value of the block is considered by the average mean of all upscaled realizations.

Table 14-12: Grid geometry of parental block size 25x25x5

	X	Y	Z
Number of nodes	192	224	160
Mesh size	25 m	25 m	5 m
Grid origin (center)	655,786.25 m	9,338,791.25 m	-240.24 m
Grid origin (corner)	655,773.75 m	9,338,778.75 m	-242.74 m

Source: GE21, 2025.

The parental block model data was migrated to a subblock with 8m x 8m x 4m divisions, for reporting the feature average values with a valid reproduction of geological models and volumes. The final block model attributes are present in Table 14-13.

Table 14-13: Block model attributes

Attribute Name	Type	Decimals	Background	Description
Au	Float	2	-99	Au ppm E-type estimated grade
Pd	Float	2	-99	Pd ppm E-type estimated grade
Pt	Float	2	-99	Pt ppm E-type estimated grade
Ni	Float	2	-99	Ni ppm E-type estimated grade
Rh	Float	2	-99	Rh ppm E-type estimated grade
Pd_Eq	Float	2	-99	Pd equivalent – grade calculation
Density	Float	2	-99	Density g/cm3
ANM	Character	-	-	Mineral Right (ANM Process)
Mineralization	Character	-	0	Mineralization Grade Shell
Rec_class	Integer	-	0	1 = measured, 2 = indicated, 3 = inferred, 4 = exploratory potential, 0 = not classified
Weathering	Float	2	-99	Weathered zones

Source: GE21, 2025.

14.4.5 Density

GE21 has applied an Inverse of Quadradic Distance (IQD) to estimate density samples in the fresh domain, using an 80m x 80m x 50m ellipsoid aligned to the main directions of the mineral lens. A fixed value of 1.46 g/cm^3 was defined for the oxide domain according to the analysis of the *in-situ* sampling dataset. The averages of types for the block model attribution are shown in Table 14-14.

Table 14-14: Bravo's density values by all domains

Density (g/cm3)										
Name	Block Count	Mean	Standard Deviation	Coefficient of Variation	Variance	Minimum	Lower quartile	Median	Upper quartile	Maximum
Oxide Domain	1253506	1.46	0.01	0.01	0.00	1.46	1.46	1.46	1.46	2.96
Central FW HG	424558	2.85	0.14	0.05	0.02	2.47	2.74	2.81	2.95	3.25
Central FW LG	820882	2.89	0.13	0.05	0.02	2.46	2.82	2.88	2.97	3.43
Central HW HG	188528	2.83	0.18	0.06	0.03	2.58	2.71	2.81	3.02	3.43
Central HW LG	267722	2.82	0.13	0.05	0.02	2.47	2.73	2.80	2.88	3.44
Central Main HG	1970980	2.86	0.13	0.05	0.02	2.52	2.78	2.85	2.93	3.54
Central Main LG	293494	2.94	0.17	0.06	0.03	2.58	2.80	2.90	3.10	3.42
North N HG	1015581	2.75	0.11	0.04	0.01	2.19	2.67	2.73	2.82	3.36
North N LG	370692	2.77	0.10	0.04	0.01	2.56	2.69	2.74	2.88	2.97
North S HG	507543	2.85	0.18	0.06	0.03	2.50	2.74	2.81	2.91	3.53
North S LG	303666	2.92	0.13	0.04	0.02	2.59	2.81	2.92	3.04	3.23
Southwest FW HG	178859	2.78	0.05	0.02	0.00	2.46	2.74	2.81	2.81	2.96
Southwest FW LG	312514	2.84	0.12	0.04	0.02	2.56	2.71	2.93	2.94	2.99
Southwest HW HG	12454	3.00	0.30	0.10	0.09	2.64	2.79	2.83	3.46	3.47
Southwest HW LG	102013	2.80	0.12	0.04	0.01	2.58	2.72	2.78	2.90	3.20
Southwest Main HG	647558	2.81	0.09	0.03	0.01	2.61	2.74	2.80	2.91	3.01
Southwest Main LG	127113	2.79	0.12	0.04	0.01	2.53	2.69	2.76	2.90	3.13
Southwest N HG	49404	2.74	0.05	0.02	0.00	2.67	2.71	2.72	2.76	2.86
Southwest N LG	40546	2.71	0.11	0.04	0.01	2.58	2.59	2.71	2.78	3.00

Source: GE21, 2025.

14.5 Estimates Validation

The QP carried out the validation of the estimate through visual verification and by the Global and Local bias verification. The global and local bias checks used the Nearest Neighbour (NN) and Ordinary Kriging (OK) as the comparison with the Simulation (E-type) estimate.

NN-Checks plots, (Figure 14-17 and Figure 14-20) show the results for global bias analysis of the estimated Pd ppm, which allowed verifying the occurrence of expected smoothing of the estimation by E-type within the acceptance limits. The comparison showed that E-type globally respected the average grades, and the global bias in the estimated grades is within the limits of acceptance.

The local bias assessment by the swath plot method aims to analyze the occurrence of local bias by comparing the average grades for the model through E-type, Ordinary Kriging, and

the Nearest Neighbour method in swath coordinate intervals graphs along the X, Y, and Z axes. Figure 14-23 shows the swath plot validation results of the estimated Pd ppm.

Figure 14-21 and Figure 14-22 show the swath plot comparison of ordinary kriging, simulation E-type and Nearest Neighbour values. The E-type post-processing shows smoother estimations than ordinary kriging since it accounts for the average of the possibility of high and low values since kriging is too much affected by the presence of local sample values. Because simulation is conditional, the effect of conditioning bias is much more expressed in ordinary kriging results. The QP considered the result obtained from the estimation by the E-type of simulations to be acceptable, noting that there was no local or global bias outside the acceptance limits.

Nearest Neighbour

Variable	Pd Grades (ppm)
Domain	HG
N. of Samples	5084775
Minimum	0.001
Maximum	50.965
Average	1.224
Variance	2.634
Std Deviation	1.623

NN Quantiles

Quantile	Value
2.5%	0.116
5%	0.198
25%	0.625
Median	0.889
75%	1.39
95%	3.051
97.5%	4.117

Ordinary Kriging

Variable	Pd Grades (ppm)
Domain	HG
N. of Samples	5084775
Minimum	0.021
Maximum	18.129
Average	1.258
Variance	0.74
Std Deviation	0.86

OK Quantiles

Quantile	Value
2.5%	0.293
5%	0.374
25%	0.787
Median	1.061
75%	1.552
95%	2.607
97.5%	3.123

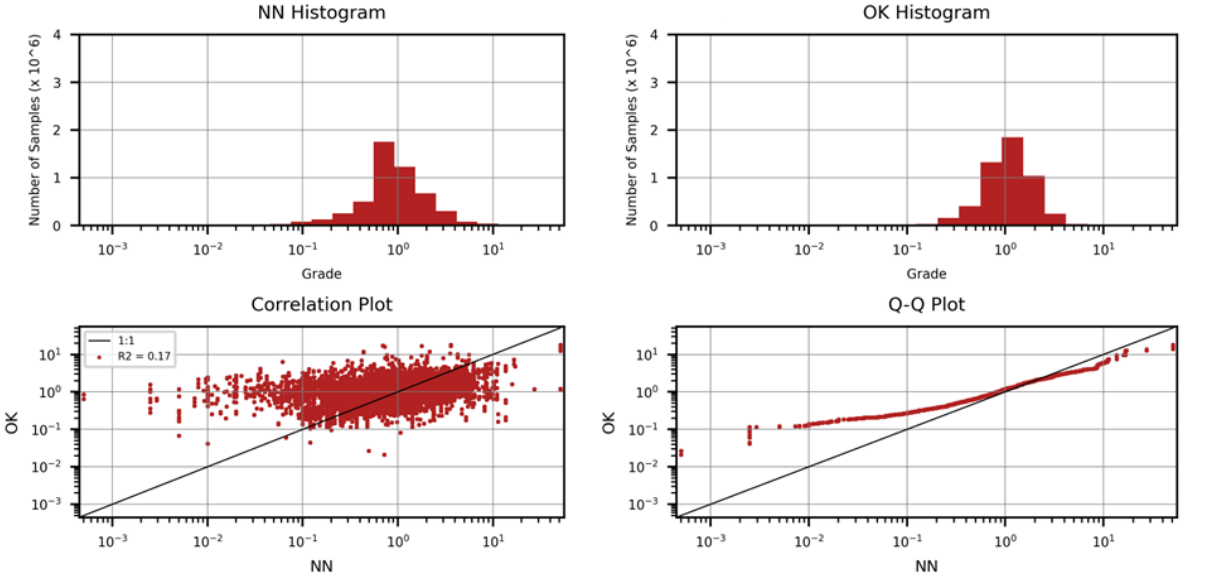

Figure 14-17: NN vs OK (HG)

Source: GE21, 2025.

Nearest Neighbour

Variable	Pd Grades (ppm)
Domain	LG
N. of Samples	2577592
Minimum	0.001
Maximum	156.291
Average	0.319
Variance	3.885
Std Deviation	1.971

NN Quantiles

Quantile	Value
2.5%	0.039
5%	0.061
25%	0.158
Median	0.248
75%	0.36
95%	0.68
97.5%	0.914

Ordinary Kriging

Variable	Pd Grades (ppm)
Domain	LG
N. of Samples	2577592
Minimum	0.005
Maximum	67.891
Average	0.318
Variance	1.17
Std Deviation	1.082

OK Quantiles

Quantile	Value
2.5%	0.107
5%	0.126
25%	0.198
Median	0.27
75%	0.357
95%	0.529
97.5%	0.602

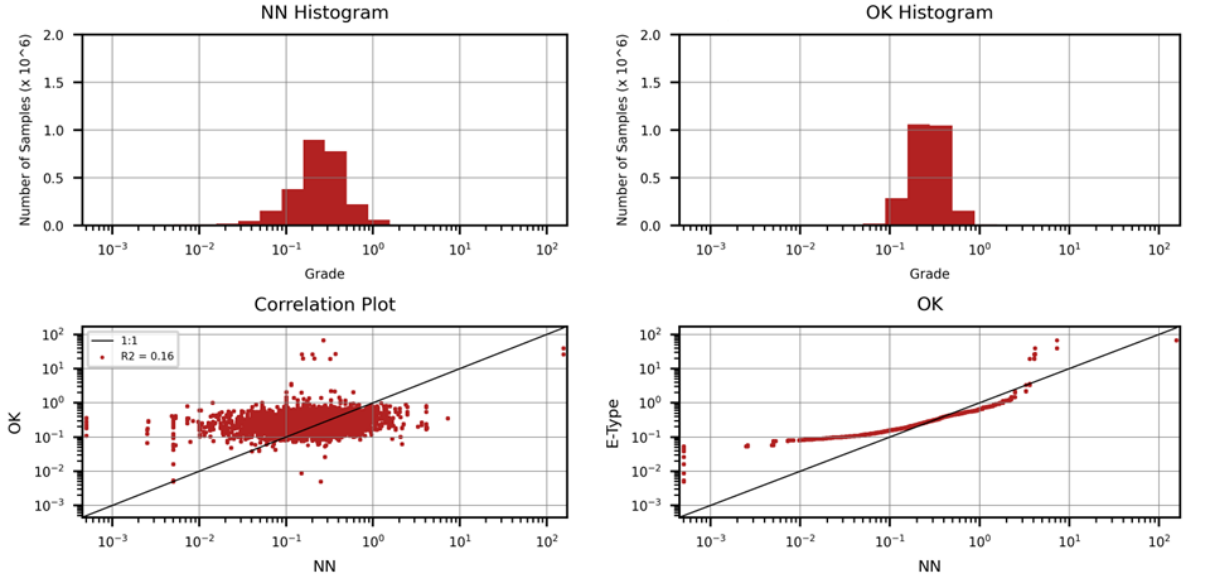

Figure 14-18: NN vs OK (LG)

Source: GE21, 2025.

Nearest Neighbour

Variable	Pd Grades (ppm)
Domain	HG
N. of Samples	5084775
Minimum	0.001
Maximum	50.965
Average	1.224
Variance	2.634
Std Deviation	1.623

NN Quantiles

Quantile	Value
2.5%	0.116
5%	0.198
25%	0.625
Median	0.889
75%	1.39
95%	3.051
97.5%	4.117

Simulation E-Type

Variable	Pd Grades (ppm)
Domain	HG
N. of Samples	5084775
Minimum	0.386
Maximum	3.834
Average	1.244
Variance	0.097
Std Deviation	0.311

E-Type Quantiles

Quantile	Value
2.5%	0.796
5%	0.858
25%	1.025
Median	1.187
75%	1.414
95%	1.809
97.5%	2.004

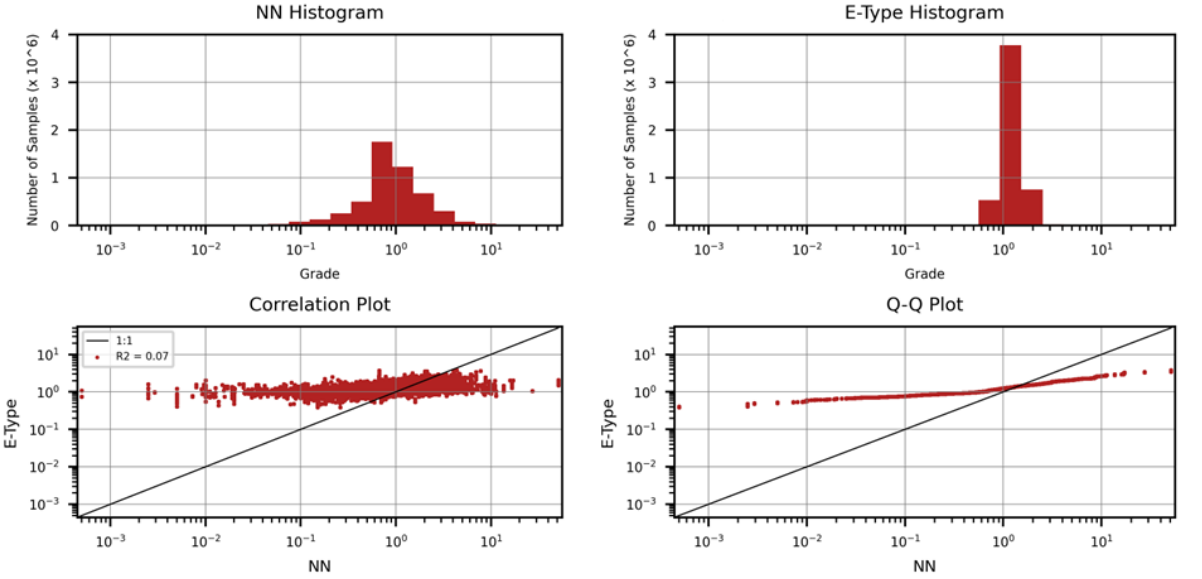

Figure 14-19: NN check vs E-type (HG)

Source: GE21, 2025.

Nearest Neighbour

Variable	Pd Grades (ppm)
Domain	LG
N. of Samples	2577592
Minimum	0.001
Maximum	156.291
Average	0.319
Variance	3.885
Std Deviation	1.971

NN Quantiles

Quantile	Value
2.5%	0.039
5%	0.061
25%	0.158
Median	0.248
75%	0.36
95%	0.68
97.5%	0.914

Simulation E-Type

Variable	Pd Grades (ppm)
Domain	LG
N. of Samples	2577592
Minimum	0.124
Maximum	0.592
Average	0.294
Variance	0.002
Std Deviation	0.041

E-Type Quantiles

Quantile	Value
2.5%	0.204
5%	0.22
25%	0.271
Median	0.298
75%	0.317
95%	0.356
97.5%	0.374

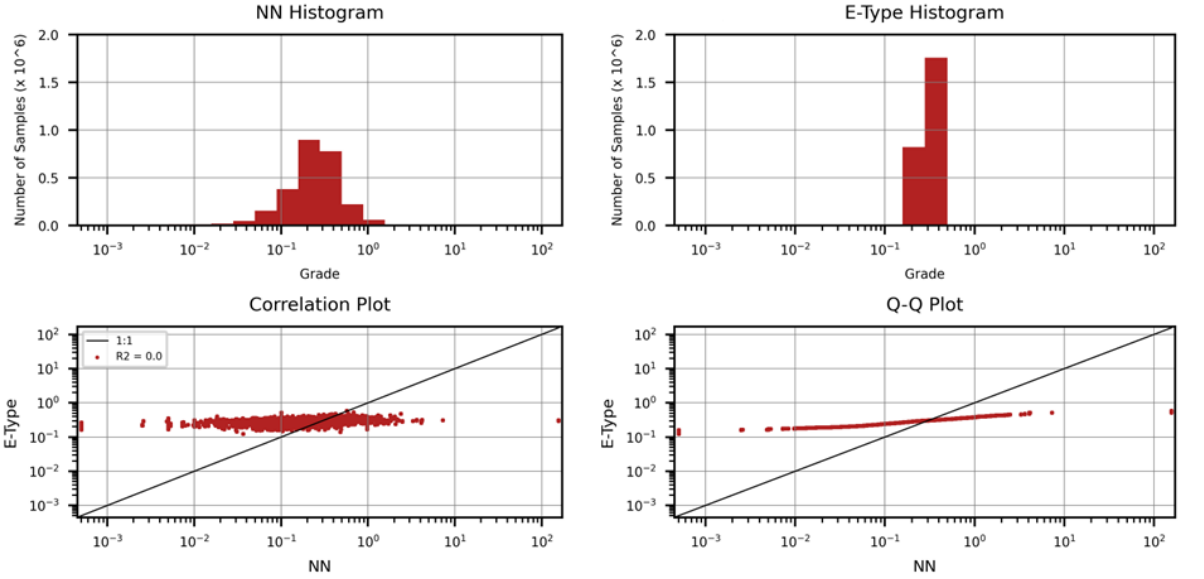

Figure 14-20: NN vs E-type (LG)

Source: GE21, 2025.

Ordinary Kriging

Variable	Pd Grades (ppm)
Domain	HG
N. of Samples	5084775
Minimum	0.021
Maximum	18.129
Average	1.258
Variance	0.74
Std Deviation	0.86

OK Quantiles

Quantile	Value
2.5%	0.293
5%	0.374
25%	0.787
Median	1.061
75%	1.552
95%	2.607
97.5%	3.123

Simulation E-Type

Variable	Pd Grades (ppm)
Domain	HG
N. of Samples	5084775
Minimum	0.386
Maximum	3.834
Average	1.244
Variance	0.097
Std Deviation	0.311

E-Type Quantiles

Quantile	Value
2.5%	0.796
5%	0.858
25%	1.025
Median	1.187
75%	1.414
95%	1.809
97.5%	2.004

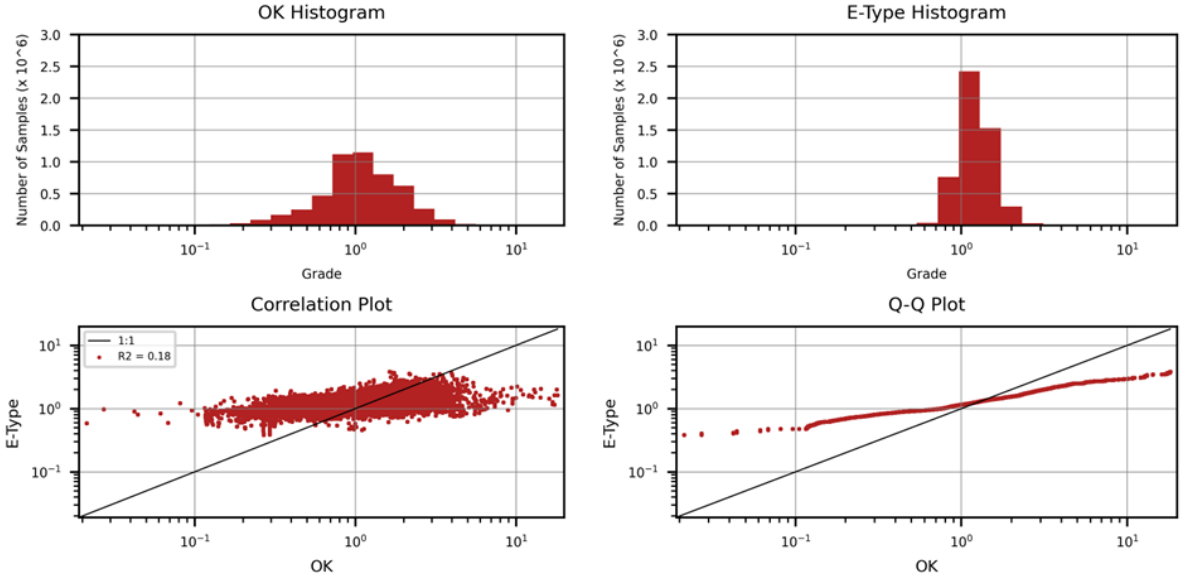

Figure 14-21: OK vs E-type (HG)

Source: GE21, 2025.

Ordinary Kriging

Variable	Pd Grades (ppm)
Domain	LG
N. of Samples	2577592
Minimum	0.005
Maximum	67.891
Average	0.318
Variance	1.17
Std Deviation	1.082

OK Quantiles

Quantile	Value
2.5%	0.107
5%	0.126
25%	0.198
Median	0.27
75%	0.357
95%	0.529
97.5%	0.602

Simulation E-Type

Variable	Pd Grades (ppm)
Domain	LG
N. of Samples	2577592
Minimum	0.124
Maximum	0.592
Average	0.294
Variance	0.002
Std Deviation	0.041

E-Type Quantiles

Quantile	Value
2.5%	0.204
5%	0.22
25%	0.271
Median	0.298
75%	0.317
95%	0.356
97.5%	0.374

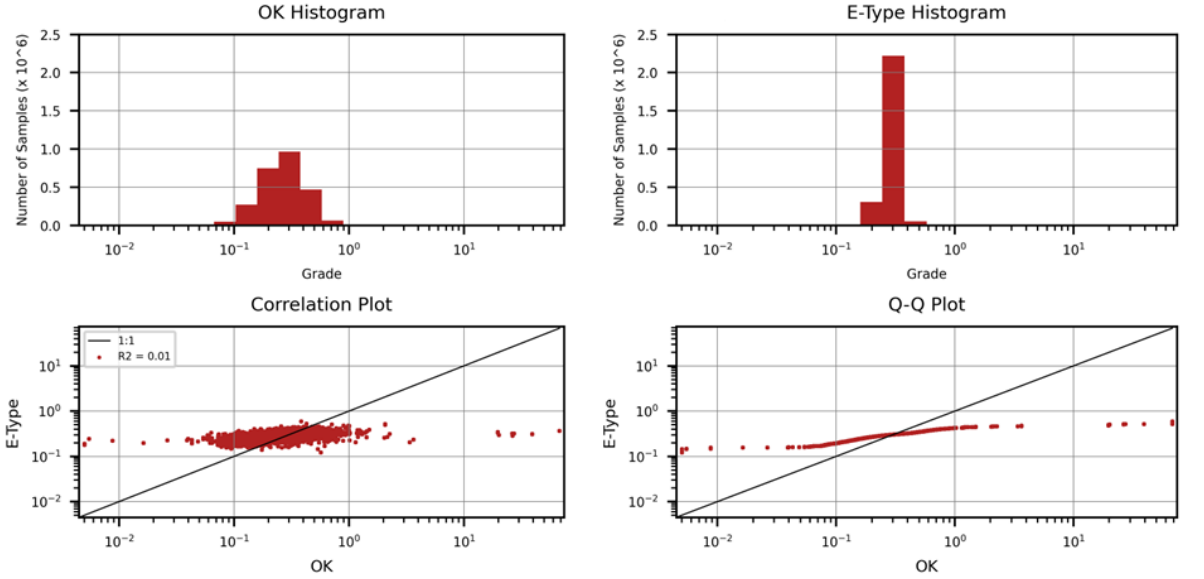

Figure 14-22: OK vs E-type (LG)

Source: GE21, 2025.

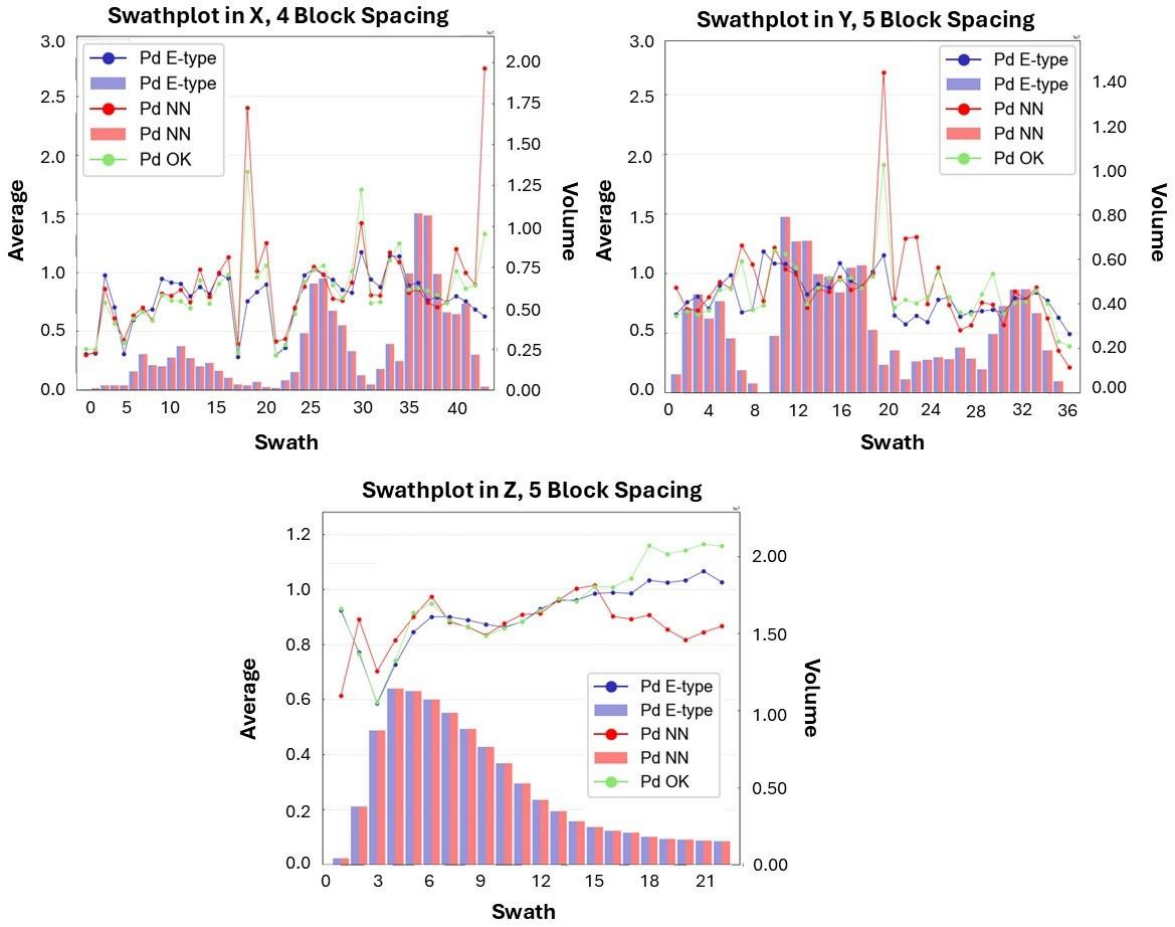

Figure 14-23: Swath plot E-type vs NN vs OK grades Pd (ppm)

Source: GE21, 2025.

14.6 Classification of Mineral Resources

The Mineral Resource was classified per CIM Standards (2014) and CIM Best Practices Guidelines (2019), utilizing geostatistical and classical methods, along with economically- and mining-appropriate parameters relevant to the deposit type.

The Mineral Resource definitions by CIM are transcribed below:

- A Mineral Resource is a concentration or occurrence of diamonds, a natural solid inorganic material or natural fossilized solid organic material, including base and precious metals, coal and industrial minerals in the earth's crust or in the earth's crust in such form and quantity and of such grade or quality that allows reasonable prospects of economic extraction. The location, quantity, level, geological characteristics, and continuity of a Mineral Resource are known, estimated, or interpreted from specific geological evidence and knowledge.
- An "Inferred Mineral Resource" is that part of a Mineral Resource for which the quantity and level or quality can be estimated on the basis of geological evidence and limited sampling and reasonably presumed but not verified geological and grade continuity. The estimation is based on limited information and sampling collected using appropriate techniques from locations such as outcrops, trenches, wells, and drill holes.
- An "Indicated Mineral Resource" is that part of a Mineral Resource for which quantity, grade or quality, densities, shape and physical characteristics can be estimated with a level of confidence sufficient to allow the appropriate application of technical and economic parameters, to support mine planning and assessment of the deposit's economic viability. The estimation is based on thorough and reliable exploration and testing information gathered using appropriate techniques from locations such as outcrops, trenches, wells, works, and drill holes spaced far enough apart for geological and level continuity to be reasonably assumed.
- A "Measured Mineral Resource" is that part of a Mineral Resource for which quantity, level or quality, densities, shape, and physical characteristics are so well established that they can be estimated with sufficient confidence to allow the appropriate application of technical and economic parameters, to support production planning and assessment of the deposit's economic viability. The estimation is based on thorough and reliable exploration, sampling, and analysis of information gathered using appropriate techniques from locations such as outcrops, trenches, wells, works, and drill holes spaced far enough apart to confirm geological and level continuity.

The classification boundaries made by GE21 for the Measured, Indicated, and Inferred categories were established through an approach that considered a comprehensive set of factors. These factors included the sampling procedure analysis, the sample grid spacing, the survey methodology, and the quality of assay data. Additionally, drilling spacing and the progressive expansion of the search radius during grade estimation stages were also considered, as well as the average anisotropic distance of the samples and the continuity of pegmatite mineralization. This multi-faceted approach ensured the robustness and accuracy of the classification process.

To classify Mineral Resources, a study of spatial continuity for Pd Equivalent was conducted using variography followed by ordinary kriging interpolation. This study established a continuity zone suitable for considering:

- The Measured Mineral Resource was classified according to a reference grid of approximately 45m x 45m, with a minimum number of 3 holes in the section along the strike and dip directions, surrounded by the pit shell.
- The Indicated Mineral Resource classification had as a reference a drilling grid of approximately 75m x 75m, extending both along the strike and dip directions, and requiring a minimum of two drill holes.
- Manual post-processing was undertaken to construct wireframes representing the volumes categorized as Measured and Indicated, while considering the blocks within the resource pit shell.
- The Inferred Mineral Resource classification is all remaining estimated blocks within the resource pit shell.

The total Mineral Resources all lie within the Mining Rights boundaries.

According to CIM Guidelines, the Mineral Resource classification should be supported by Reasonable Prospect for Eventual Economic Extraction (RPEEE), which GE21 usually performs through a mathematical model pit shell which limits the blocks classified as a resource generated from an economic and geometric function.

GE21 performed a pit optimization study to classify the project's Mineral Resources to ensure the RPEEE was met. Parameters in the benefit function are presented in Table 14-15.

Luanga Project's updated, pit-constrained MRE has an effective date of February 18, 2025. It comprises 36 Mt at 2.00 g/t Pd Eq for a total of 2.3 Moz Pd Eq in the Measured category, 122 Mt at 2.06 g/t Pd Eq for 8.0 Moz Pd Eq in the Indicated category, 158 Mt at 2.04 g/t Pd Eq for a total of 10.4 Moz Pd Eq in the Measured + Indicated categories, and 78 Mt at 2.01 g/t Pd Eq for a total of 5.0 Moz Pd Eq in the Inferred category (Table 14-16).

Figure 14-24 shows a perspective view of the Luanga Project's MRE classification.

Table 14-15: Pit parameters generated by RPEEE

Optimization Parameters - RPEEE				
Item				Unit
Lithotype	Fresh & Weathered & High Talc			-
Slope Angle	Weathered		40	°
	Fresh / High Talc		50	°
Mining	Density	Block Model		
	Mining Recovery		100	%
	Mining Dilution		0	%
	MCAF		ANM Mineral Rights	
	Cut-off grade (Whittle)	Fresh	-	-
		Weathered	-	-
Processing	Metallurgic Recovery - Weathered	Pd	81.0%	Mill
		Pt	23.0%	Mill
		Rh	54.0%	Mill
		Au	90.0%	Mill
		Ni	0.0%	Mill

Optimization Parameters - RPEEE				
Item				Unit
	Metallurgic Recovery - Fresh	Pd	77.0%	Mill
		Pt	81.0%	Mill
		Rh	51.0%	Mill
		Au	48.0%	Mill
		Ni	50.0%	Mill
	Metallurgic Recovery - High Talc	Pd	51.0%	Mill
		Pt	55.5%	Mill
		Rh	27.3%	Mill
		Au	27.0%	Mill
		Ni	0.0%	Mill
Costs	Weathered	Mining Cost	2.00	USD/t mined
		Processing Cost	7.50	USD/t ROM
		Grade Control	1.00	
		Logistics	0.50	
		Rehabilitation	1.00	
		G&A	1.50	
	Fresh / High Talc	Mining Cost	3.00	USD/t mined
		Processing Cost	9.00	USD/t ROM
		Grade Control	1.00	
		Logistics	0.50	
		Rehabilitation	1.00	
		G&A	1.50	
Selling	Price	Pd	1,380	USD/oz
		Pt	1,100	USD/oz
		Rh	6,200	USD/oz
		Au	1,500	USD/oz
		Ni	7.10	USD/lb
	Royalties	All	2.0	%

Source: GE21, 2025.

Table 14-16: MRE statement at a cut-off of 0.5g/t Pd Eq*

Resource	Classification	Domain	*Average Value*							*Material Content*					
			Mass	Pd eq	Pd	Pt	Au	Rh	Ni	Pd eq	Pd	Pt	Au	Rh	Ni
			Mt	ppm	g/t	g/t	g/t	g/t	%	koz	koz	koz	koz	koz	klb
Open Pit	Measured	Ox	4	1.51	0.90	0.88	0.05	0.12	0.00	197	117	115	7	15	—
		High Talc	—	—	—	—	—	—	—	—	—	—	—	—	—
		Fresh	32	2.06	0.97	0.67	0.04	0.08	0.11	2,144	1,009	694	46	88	77,621
		Total	**36**	**2.00**	**0.96**	**0.69**	**0.04**	**0.09**	**0.10**	**2,340**	**1,126**	**809**	**53**	**104**	**77,621**
	Indicated	Ox	6	1.51	0.97	0.73	0.04	0.11	0.00	314	200	151	9	23	0
		High Talc	2	1.83	1.12	0.54	0.11	0.08	0.13	146	89	43	9	6	6,952
		Fresh	113	2.09	0.99	0.59	0.05	0.09	0.14	7,599	3,583	2,133	193	318	344,092
		Total	**122**	**2.06**	**0.99**	**0.59**	**0.05**	**0.09**	**0.13**	**8,058**	**3,872**	**2,326**	**210**	**348**	**351,044**
	Measured + Indicated	**Ox**	**10**	**1.51**	**0.94**	**0.79**	**0.04**	**0.11**	**0.00**	**510**	**317**	**266**	**15**	**38**	—
		High Talc	**2**	**1.83**	**1.12**	**0.54**	**0.11**	**0.08**	**0.13**	**146**	**89**	**43**	**9**	**6**	**6,952**
		Fresh	**145**	**2.08**	**0.98**	**0.60**	**0.05**	**0.09**	**0.13**	**9,743**	**4,592**	**2,827**	**239**	**407**	**421,713**
		Total	**158**	**2.04**	**0.98**	**0.62**	**0.05**	**0.09**	**0.12**	**10,399**	**4,998**	**3,135**	**262**	**451**	**428,665**
	Inferred	Ox	3	1.57	0.88	1.04	0.05	0.13	—	130	73	86	4	11	—
		High Talc	0	1.76	1.08	0.53	0.10	0.07	0.14	5	3	2	0	0	292
		Fresh	75	2.02	0.97	0.58	0.05	0.08	0.13	4,878	2,344	1,389	123	191	214,690
		Total	**78**	**2.01**	**0.97**	**0.59**	**0.05**	**0.08**	**0.13**	**5,013**	**2,421**	**1,476**	**128**	**202**	**214,981**

Notes:

1. The MRE has been prepared by Porfirio Cabaleiro Rodriguez, Mining Engineer, BSc (Mine Eng), MAIG, director of GE21 Consultoria Mineral Ltda., an independent Qualified Persons (QP) under NI43-101. The effective date of the MRE is February 18, 2025.
2. Mineral resources are reported using the 2014 CIM Definition Standards and were estimated in accordance with the CIM 2019 Best Practices Guidelines, as required by National Instrument 43-101 Standards of Disclosure for Mineral Projects (NI 43-101).
3. Mineral resources that are not Mineral Reserves do not have demonstrated economic viability. There is no certainty that all Mineral Resources will be converted into Mineral Reserves.
4. Chemical elements are estimated using different estimation methodologies according to the Weathering Model. Ordinary Kriging was applied to the Oxidized domain, while the Turning Bands Simulation was applied to fresh rock.
5. This MRE includes Inferred Mineral Resources, which have had insufficient work to classify them as Indicated Mineral Resources. It is uncertain but reasonably expected that inferred Mineral Resources could be upgraded to indicated Mineral Resources with continued exploration.
   - The Mineral Resource Estimate is reported/confined within an economic pit shell generated by Dassault Geovia Whittle software, using the following assumptions (Generated from work completed for Bravo and historical test work):
     - Metallurgical recovery in sulphide material of 77% Pd, 81% Pt, 51% Rh, 48% Au, 50% Ni to a saleable Ni-PGM concentrate.
     - Metallurgical recovery in oxide material of 81% Pd, 23% Pt, 54% Rh, 90% Au to a saleable PGM ash residue (Ni not applicable).
     - Metallurgical recovery in high-talc sulphide material of 51% Pd, 55% Pt, 27% Rh, 27% Au, 0% Ni to a saleable Ni-PGM concentrate.
     - Independent Geotechnical Testwork – Overall pit slopes of 40 degrees in oxide and 50 degrees in Fresh Rock.
     - Densities are based on 27,170 drill hole cores and 112 in situ sample density measurements. The Mineral Resources are reported on a dry density basis.
     - External downstream payability has not been included, as the base case MRE assumption considers internal downstream processing.

   a. Payable royalties of 2%, (only considering CFEM, for reserves, a complete set of royalties must be considered)
6. Metal Pricing

a. Metal price assumptions are based on 10-year trailing averages (2014-2023): Pd price of US$1,380/oz, Pt price of US$1,100/oz, Rh price of US$6,200/oz, Au price of US$1,500/oz, Ni price of US$7,10/lb.
b. Palladium Equivalent (PdEq) Calculation
c. The PdEq equation is: PdEq = Pd g/t + F1 + F2 + F3 + F4

Where: $\boldsymbol{F1} = \frac{(Pt_p * Pt_R)}{(Pd_p * Pd_R)} \boldsymbol{Pt_t}$ $\boldsymbol{F2} = \frac{(Rh_p * Rh_R)}{(Pd_p * Pd_R)} \boldsymbol{Rh_t}$ $\boldsymbol{F3} = \frac{(Au_p * Au_R)}{(Pd_p * Pd_R)} \boldsymbol{Au_t}$ $\boldsymbol{F4} = \frac{(Ni_p * Ni_R)}{(Pd_p * Pd_R)} \boldsymbol{Ni_t}$

$_P$ = Metal Price
$_R$ = Metallurgical Recovery

7. Costs are taken from comparable projects in GE21's extensive database of mining operations in Brazil, which includes not only operating mines, but recent actual costs from what could potentially be similarly sized operating mines in the Carajás. Costs considered a throughput rate of ca. 10Mtpa:
   a. Mining costs: US$2.00/t oxide, US$3.00/t Fresh Rock. Processing costs: US$9.00/t fresh rock, US$7.50/t oxide. US$1.50/t processed, for General & Administration. US$1.00/t processed for grade control. US$0.50/t processed for rehabilitation.
   b. Several of these considerations (metallurgical recovery, metal price projections, for example) should be regarded as preliminary in nature, and therefore, PdEq calculations should be regarded as preliminary in nature.
8. The current MRE supersedes and replaces the Previous Estimate (2023), which should no longer be relied upon.
9. The QP is not aware of political, environmental, or other risks that could materially affect the potential development of the Mineral Resources other than those typical for mining projects at this stage of development and as identified in this report.
10. Totals may not sum due to rounding.

Source: GE21, 2025.

Table 14-17: MRE statement based on mineralization style

Resource	Classification	Weathering	Min Styles	Mass	Average Value						Material Content					
					Pd eq	Pd	Pt	Au	Rh	Ni	Pd eq	Pd	Pt	Au	Rh	Ni
				Mt	g/t	g/t	g/t	g/t	g/t	%	kOz	kOz	kOz	kOz	kOz	klb
Open Pit	Measured	Ox	CENTRAL_LSZ	0.2	0.80	0.59	0.38	0.03	0.03	—	6	4	3	0	0	—
			CENTRAL_MSZ	0.4	1.34	0.95	0.43	0.09	0.06	—	19	14	6	1	1	—
			CENTRAL_NR	0.1	0.70	0.41	0.18	0.14	0.03	—	2	1	0	0	0	—
			NORTH_LSZ	0.2	2.02	1.38	0.98	0.02	0.13	—	14	10	7	0	1	—
			NORTH_LSZ+CHR	1.4	1.50	0.88	1.47	0.02	0.09	—	65	38	64	1	4	—
			NORTH_MSZ	1.5	1.71	0.95	0.67	0.07	0.18	—	83	46	33	3	8	—
			NORTH_SZ	0.2	1.03	0.56	0.30	0.02	0.13	—	7	4	2	0	1	—
			Total	**4.1**	**1.51**	**0.90**	**0.88**	**0.05**	**0.12**	—	**197**	**117**	**115**	**7**	**15**	—
		Fresh	CENTRAL_LSZ	9.2	1.42	0.70	0.44	0.03	0.05	0.08	421	208	129	8	14	16,652.92
			CENTRAL_MSZ	6.1	3.06	1.59	0.68	0.08	0.10	0.24	597	310	133	16	20	31,905.83
			CENTRAL_NR	1.4	1.63	0.71	0.35	0.07	0.06	0.18	74	32	16	3	3	5,583.34
			NORTH_LSZ	1.1	2.12	0.98	0.73	0.05	0.09	0.10	75	35	26	2	3	2,455.10
			NORTH_LSZ+CHR	6.5	2.15	0.97	0.89	0.03	0.09	0.06	450	202	187	6	20	8,319.56
			NORTH_MSZ	6.9	2.05	0.86	0.78	0.04	0.12	0.07	452	190	172	9	26	10,545.82
			NORTH_SZ	1.3	1.83	0.77	0.76	0.03	0.07	0.08	75	32	31	1	3	2,158.09
			Total	**32.4**	**2.06**	**0.97**	**0.67**	**0.04**	**0.08**	**0.11**	**2 144**	**1 009**	**694**	**46**	**88**	**77,620.66**
		Total	**CENTRAL_LSZ**	**9.4**	**1.41**	**0.70**	**0.44**	**0.03**	**0.05**	**0.08**	**427**	**213**	**132**	**9**	**15**	**16,652.92**
			CENTRAL_MSZ	**6.5**	**2.95**	**1.55**	**0.66**	**0.08**	**0.10**	**0.22**	**616**	**323**	**139**	**18**	**21**	**31,905.83**
			CENTRAL_NR	**1.5**	**1.58**	**0.69**	**0.34**	**0.08**	**0.06**	**0.17**	**76**	**33**	**16**	**4**	**3**	**5,583.34**
			NORTH_LSZ	**1.3**	**2.11**	**1.04**	**0.77**	**0.05**	**0.10**	**0.08**	**89**	**44**	**33**	**2**	**4**	**2,455.10**
			NORTH_LSZ+CHR	**7.9**	**2.04**	**0.95**	**0.99**	**0.03**	**0.09**	**0.05**	**515**	**241**	**251**	**7**	**24**	**8,319.56**
			NORTH_MSZ	**8.4**	**1.99**	**0.88**	**0.76**	**0.05**	**0.13**	**0.06**	**535**	**236**	**205**	**12**	**34**	**10,545.82**
			NORTH_SZ	**1.5**	**1.71**	**0.74**	**0.70**	**0.03**	**0.08**	**0.07**	**82**	**36**	**33**	**1**	**4**	**2,158.09**
			Total	**36.5**	**2.00**	**0.96**	**0.69**	**0.04**	**0.09**	**0.10**	**2 340**	**1 126**	**809**	**53**	**104**	**77,620.66**
	Indicated	Ox	CENTRAL_LSZ	1.3	1.52	1.02	0.78	0.04	0.09	—	64	43	33	2	4	—
			CENTRAL_MSZ	1.4	1.37	0.94	0.52	0.05	0.09	—	64	44	24	2	4	—
			CENTRAL_NR	0.1	0.75	0.49	0.21	0.08	0.03	—	2	1	0	0	0	—
			NORTH_LSZ	0.5	4.31	2.31	1.61	0.03	0.53	—	70	37	26	1	9	—
			NORTH_LSZ+CHR	0.7	1.26	0.67	1.49	0.01	0.08	—	28	15	33	0	2	—
			NORTH_MSU	0.1	0.78	0.44	0.43	0.04	0.06	—	2	1	1	0	0	—
			NORTH_MSZ	0.7	1.15	0.70	0.61	0.05	0.08	—	26	16	14	1	2	—
			NORTH_SZ	0.2	0.74	0.47	0.25	0.03	0.06	—	5	3	2	0	0	—
			SW_LSZ	0.4	1.36	1.05	0.43	0.03	0.06	—	15	12	5	0	1	—
			SW_MSZ	1.1	1.11	0.82	0.37	0.06	0.05	—	38	28	12	2	2	—
			SW_NR	0.0	0.72	0.45	0.21	0.07	0.04	—	1	0	0	0	0	—
			Total	**6.4**	**1.51**	**0.97**	**0.73**	**0.04**	**0.11**	—	**314**	**200**	**151**	**9**	**23**	—
		High Talc	SW_LSZ	0.2	1.45	0.84	0.48	0.02	0.08	0.02	11	6	4	0	1	106.43
			SW_MSZ	2.2	1.87	1.14	0.55	0.12	0.08	0.14	134	82	39	8	5	6,767.92
			SW_NR	0.0	1.82	1.12	0.56	0.08	0.07	0.16	1	1	0	0	0	77.48
			Total	**2.5**	**1.83**	**1.12**	**0.54**	**0.11**	**0.08**	**0.13**	**146**	**89**	**43**	**9**	**6**	**6,951.83**
		Fresh	CENTRAL_LSZ	23.3	1.67	0.81	0.47	0.04	0.06	0.11	1,247	603	348	31	48	55,944.03

Resource	Classification	Weathering	Min Styles	Mass	Average Value						Material Content					
					Pd eq	Pd	Pt	Au	Rh	Ni	Pd eq	Pd	Pt	Au	Rh	Ni
				Mt	g/t	g/t	g/t	g/t	g/t	%	kOz	kOz	kOz	kOz	kOz	klb
			CENTRAL_MSZ	33.3	2.64	1.32	0.67	0.07	0.10	0.18	2,823	1,414	713	72	112	129,117.13
			CENTRAL_NR	3.6	1.68	0.76	0.39	0.06	0.06	0.17	192	87	44	7	6	13,171.62
			NORTH_LSZ	4.0	1.73	0.68	0.59	0.04	0.11	0.10	225	88	77	5	14	8,717.12
			NORTH_LSZ+CHR	5.7	1.95	0.86	0.86	0.03	0.07	0.06	356	156	157	5	13	7,397.52
			NORTH_MSU	3.3	2.52	0.91	0.66	0.05	0.13	0.28	269	97	71	5	13	20,809.50
			NORTH_MSZ	13.9	2.32	0.90	0.72	0.04	0.13	0.17	1,035	399	323	20	60	52,036.89
			NORTH_MSZ+MSU	0.2	2.78	1.05	0.81	0.04	0.15	0.25	16	6	5	0	1	983.01
			NORTH_SZ	2.4	1.94	0.85	0.77	0.04	0.08	0.07	148	65	59	3	6	3,934.26
			SW_LSZ	4.1	0.84	0.44	0.26	0.02	0.03	0.03	111	58	35	3	4	3,117.92
			SW_MSZ	18.7	1.89	0.98	0.49	0.07	0.07	0.11	1,138	592	293	39	40	46,394.12
			SW_NR	0.6	2.02	0.93	0.47	0.08	0.07	0.19	38	17	9	1	1	2,469.17
			Total	**113.0**	**2.09**	**0.99**	**0.59**	**0.05**	**0.09**	**0.14**	**7,599**	**3,583**	**2,133**	**193**	**318**	**344,092.29**
		Total	**CENTRAL_LSZ**	**24.6**	**1.66**	**0.82**	**0.48**	**0.04**	**0.07**	**0.10**	**1,311**	**646**	**381**	**32**	**52**	**55,944.03**
			CENTRAL_MSZ	**34.7**	**2.58**	**1.30**	**0.66**	**0.07**	**0.10**	**0.17**	**2,887**	**1,457**	**737**	**74**	**116**	**129,117.13**
			CENTRAL_NR	**3.6**	**1.66**	**0.76**	**0.39**	**0.06**	**0.05**	**0.16**	**194**	**88**	**45**	**7**	**6**	**13,171.62**
			NORTH_LSZ	**4.6**	**2.02**	**0.86**	**0.70**	**0.04**	**0.15**	**0.09**	**295**	**125**	**103**	**6**	**22**	**8,717.12**
			NORTH_LSZ+CHR	**6.4**	**1.88**	**0.84**	**0.93**	**0.03**	**0.07**	**0.05**	**384**	**171**	**190**	**6**	**15**	**7,397.52**
			NORTH_MSU	**3.4**	**2.49**	**0.90**	**0.66**	**0.05**	**0.12**	**0.28**	**271**	**98**	**72**	**5**	**14**	**20,809.50**
			NORTH_MSZ	**14.6**	**2.26**	**0.89**	**0.72**	**0.04**	**0.13**	**0.16**	**1,062**	**416**	**337**	**21**	**62**	**52,036.89**
			NORTH_MSZ+MSU	**0.2**	**2.78**	**1.05**	**0.81**	**0.04**	**0.15**	**0.25**	**16**	**6**	**5**	**0**	**1**	**983.01**
			NORTH_SZ	**2.6**	**1.85**	**0.82**	**0.73**	**0.04**	**0.08**	**0.07**	**153**	**68**	**60**	**4**	**7**	**3,934.26**
			SW_LSZ	**4.7**	**0.91**	**0.51**	**0.29**	**0.02**	**0.03**	**0.03**	**137**	**76**	**43**	**3**	**5**	**3,224.35**
			SW_MSZ	**22.0**	**1.85**	**0.99**	**0.49**	**0.07**	**0.07**	**0.11**	**1,310**	**702**	**345**	**50**	**47**	**53,162.05**
			SW_NR	**0.6**	**1.96**	**0.92**	**0.47**	**0.08**	**0.07**	**0.18**	**40**	**19**	**9**	**2**	**1**	**2,546.65**
			Total	**121.9**	**2.06**	**0.99**	**0.59**	**0.05**	**0.09**	**0.13**	**8,058**	**3,872**	**2,326**	**210**	**348**	**351,044.13**
	Measured + Indicated	**Ox**	**CENTRAL_LSZ**	**1.5**	**1.41**	**0.95**	**0.72**	**0.04**	**0.08**	—	**70**	**47**	**36**	**2**	**4**	—
			CENTRAL_MSZ	**1.9**	**1.36**	**0.94**	**0.50**	**0.06**	**0.08**	—	**83**	**57**	**30**	**3**	**5**	—
			CENTRAL_NR	**0.2**	**0.72**	**0.44**	**0.19**	**0.12**	**0.03**	—	**4**	**2**	**1**	**1**	**0**	—
			NORTH_LSZ	**0.7**	**3.62**	**2.03**	**1.42**	**0.03**	**0.41**	—	**84**	**47**	**33**	**1**	**9**	—
			NORTH_LSZ+CHR	**2.0**	**1.42**	**0.81**	**1.48**	**0.02**	**0.09**	—	**94**	**53**	**97**	**1**	**6**	—
			NORTH_MSU	**0.1**	**0.78**	**0.44**	**0.43**	**0.04**	**0.06**	—	**2**	**1**	**1**	**0**	**0**	—
			NORTH_MSZ	**2.2**	**1.53**	**0.87**	**0.65**	**0.07**	**0.14**	—	**109**	**62**	**47**	**5**	**10**	—
			NORTH_SZ	**0.4**	**0.89**	**0.52**	**0.28**	**0.02**	**0.09**	—	**12**	**7**	**4**	**0**	**1**	—
			SW_LSZ	**0.4**	**1.36**	**1.05**	**0.43**	**0.03**	**0.06**	—	**15**	**12**	**5**	**0**	**1**	—
			SW_MSZ	**1.1**	**1.11**	**0.82**	**0.37**	**0.06**	**0.05**	—	**38**	**28**	**12**	**2**	**2**	—
			SW_NR	**0.0**	**0.72**	**0.45**	**0.21**	**0.07**	**0.04**	—	**1**	**0**	**0**	**0**	**0**	—
			Total	**10.5**	**1.51**	**0.94**	**0.79**	**0.04**	**0.11**	—	**510**	**317**	**266**	**15**	**38**	—
		High Talc	**SW_LSZ**	**0.2**	**1.45**	**0.84**	**0.48**	**0.02**	**0.08**	**0.02**	**11**	**6**	**4**	**0**	**1**	**106.43**
			SW_MSZ	**2.2**	**1.87**	**1.14**	**0.55**	**0.12**	**0.08**	**0.14**	**134**	**82**	**39**	**8**	**5**	**6,767.92**
			SW_NR	**0.0**	**1.82**	**1.12**	**0.56**	**0.08**	**0.07**	**0.16**	**1**	**1**	**0**	**0**	**0**	**77.48**
			Total	**2.5**	**1.83**	**1.12**	**0.54**	**0.11**	**0.08**	**0.13**	**146**	**89**	**43**	**9**	**6**	**6,951.83**
		Fresh	**CENTRAL_LSZ**	**32.5**	**1.60**	**0.78**	**0.46**	**0.04**	**0.06**	**0.10**	**1,668**	**811**	**477**	**39**	**63**	**72,596.95**
			CENTRAL_MSZ	**39.4**	**2.70**	**1.36**	**0.67**	**0.07**	**0.10**	**0.19**	**3,420**	**1,724**	**845**	**88**	**131**	**161,022.96**

Resource	Classification	Weathering	Min Styles	Mass	Average Value						Material Content					
					Pd eq	Pd	Pt	Au	Rh	Ni	Pd eq	Pd	Pt	Au	Rh	Ni
				Mt	g/t	g/t	g/t	g/t	g/t	%	kOz	kOz	kOz	kOz	kOz	klb
			CENTRAL_NR	**5.0**	**1.67**	**0.75**	**0.38**	**0.07**	**0.06**	**0.17**	**266**	**119**	**60**	**11**	**9**	**18,754.97**
			NORTH_LSZ	**5.2**	**1.82**	**0.74**	**0.62**	**0.04**	**0.10**	**0.10**	**301**	**123**	**103**	**7**	**17**	**11,172.21**
			NORTH_LSZ+CHR	**12.2**	**2.06**	**0.92**	**0.88**	**0.03**	**0.08**	**0.06**	**805**	**358**	**344**	**11**	**33**	**15,717.08**
			NORTH_MSU	**3.3**	**2.52**	**0.91**	**0.66**	**0.05**	**0.13**	**0.28**	**269**	**97**	**71**	**5**	**13**	**20,809.50**
			NORTH_MSZ	**20.7**	**2.23**	**0.89**	**0.74**	**0.04**	**0.13**	**0.14**	**1,487**	**590**	**495**	**29**	**85**	**62,582.71**
			NORTH_MSZ+MSU	**0.2**	**2.78**	**1.05**	**0.81**	**0.04**	**0.15**	**0.25**	**16**	**6**	**5**	**0**	**1**	**983.01**
			NORTH_SZ	**3.7**	**1.90**	**0.82**	**0.77**	**0.04**	**0.08**	**0.08**	**224**	**97**	**90**	**5**	**9**	**6,092.35**
			SW_LSZ	**4.1**	**0.84**	**0.44**	**0.26**	**0.02**	**0.03**	**0.03**	**111**	**58**	**35**	**3**	**4**	**3,117.92**
			SW_MSZ	**18.7**	**1.89**	**0.98**	**0.49**	**0.07**	**0.07**	**0.11**	**1,138**	**592**	**293**	**39**	**40**	**46,394.12**
			SW_NR	**0.6**	**2.02**	**0.93**	**0.47**	**0.08**	**0.07**	**0.19**	**38**	**17**	**9**	**1**	**1**	**2,469.17**
			Total	**145.4**	**2.08**	**0.98**	**0.60**	**0.05**	**0.09**	**0.13**	**9,743**	**4,592**	**2,827**	**239**	**407**	**421,712.96**
		Total	**CENTRAL_LSZ**	**34.0**	**1.59**	**0.79**	**0.47**	**0.04**	**0.06**	**0.10**	**1,737**	**858**	**513**	**41**	**67**	**72,596.95**
			CENTRAL_MSZ	**41.3**	**2.64**	**1.34**	**0.66**	**0.07**	**0.10**	**0.18**	**3,503**	**1,781**	**876**	**92**	**136**	**161,022.96**
			CENTRAL_NR	**5.1**	**1.64**	**0.74**	**0.37**	**0.07**	**0.05**	**0.17**	**269**	**121**	**61**	**11**	**9**	**18,754.97**
			NORTH_LSZ	**5.9**	**2.04**	**0.90**	**0.72**	**0.04**	**0.14**	**0.09**	**384**	**169**	**135**	**8**	**26**	**11,172.21**
			NORTH_LSZ+CHR	**14.2**	**1.97**	**0.90**	**0.96**	**0.03**	**0.08**	**0.05**	**899**	**412**	**441**	**13**	**39**	**15,717.08**
			NORTH_MSU	**3.4**	**2.49**	**0.90**	**0.66**	**0.05**	**0.12**	**0.28**	**271**	**98**	**72**	**5**	**14**	**20,809.50**
			NORTH_MSZ	**23.0**	**2.16**	**0.88**	**0.73**	**0.05**	**0.13**	**0.12**	**1,597**	**652**	**542**	**33**	**96**	**62,582.71**
			NORTH_MSZ+MSU	**0.2**	**2.78**	**1.05**	**0.81**	**0.04**	**0.15**	**0.25**	**16**	**6**	**5**	**0**	**1**	**983.01**
			NORTH_SZ	**4.1**	**1.80**	**0.79**	**0.72**	**0.04**	**0.08**	**0.07**	**236**	**104**	**94**	**5**	**11**	**6,092.35**
			SW_LSZ	**4.7**	**0.91**	**0.51**	**0.29**	**0.02**	**0.03**	**0.03**	**137**	**76**	**43**	**3**	**5**	**3,224.35**
			SW_MSZ	**22.0**	**1.85**	**0.99**	**0.49**	**0.07**	**0.07**	**0.11**	**1,310**	**702**	**345**	**50**	**47**	**53,162.05**
			SW_NR	**0.6**	**1.96**	**0.92**	**0.47**	**0.08**	**0.07**	**0.18**	**40**	**19**	**9**	**2**	**1**	**2,546.65**
			Total	**158.4**	**2.04**	**0.98**	**0.62**	**0.05**	**0.09**	**0.12**	**10,399**	**4,998**	**3,135**	**262**	**451**	**428,664.79**
	Inferred	Ox	CENTRAL_LSZ	0.2	0.81	0.52	0.40	0.03	0.06	—	5	3	2	0	0	—
			CENTRAL_MSZ	0.0	0.88	0.60	0.31	0.03	0.06	—	0	0	0	0	0	—
			CENTRAL_NR	0.0	0.62	0.42	0.17	0.09	0.02	—	0	0	0	0	0	—
			NORTH_LSZ	0.7	2.38	1.25	0.96	0.06	0.28	—	51	27	20	1	6	—
			NORTH_LSZ+CHR	0.5	1.34	0.52	2.33	0.01	0.09	—	23	9	40	0	2	—
			NORTH_MSU	0.1	1.04	0.62	0.54	0.04	0.08	—	2	1	1	0	0	—
			NORTH_MSZ	0.3	1.05	0.56	0.79	0.02	0.10	—	10	5	8	0	1	—
			NORTH_SZ	0.1	0.86	0.46	0.62	0.02	0.08	—	2	1	1	0	0	—
			SW_LSZ	0.5	1.76	1.26	0.62	0.09	0.08	—	26	18	9	1	1	—
			SW_MSZ	0.3	1.24	0.88	0.44	0.09	0.05	—	11	8	4	1	0	—
			SW_NR	0.0	0.60	0.46	0.16	0.06	0.01	—	0	0	0	0	0	—
			Total	**2.6**	**1.57**	**0.88**	**1.04**	**0.05**	**0.13**	—	**130**	**73**	**86**	**4**	**11**	—
		High Talc	SW_LSZ	0.0	0.57	0.32	0.22	0.01	0.02	0.01	0	0	0	0	0	0.67
			SW_MSZ	0.1	1.81	1.11	0.54	0.11	0.07	0.14	5	3	2	0	0	291.09
			Total	**0.1**	**1.76**	**1.08**	**0.53**	**0.10**	**0.07**	**0.14**	**5**	**3**	**2**	**0**	**0**	**291.76**
		Fresh	CENTRAL_LSZ	13.5	1.61	0.78	0.45	0.04	0.06	0.11	697	336	196	18	26	32,097.18
			CENTRAL_MSZ	25.5	2.60	1.32	0.65	0.07	0.10	0.18	2,132	1,080	534	55	79	99,268.68
			CENTRAL_NR	5.1	1.79	0.85	0.43	0.06	0.06	0.16	291	138	70	10	10	17,389.35
			NORTH_LSZ	8.3	1.34	0.56	0.53	0.03	0.06	0.07	358	148	140	7	16	12,100.96

Resource	Classification	Weathering	Min Styles	Mass	Average Value						Material Content					
					Pd eq	Pd	Pt	Au	Rh	Ni	Pd eq	Pd	Pt	Au	Rh	Ni
				Mt	g/t	g/t	g/t	g/t	g/t	%	kOz	kOz	kOz	kOz	kOz	klb
			NORTH_LSZ+CHR	5.9	2.07	0.92	0.86	0.03	0.09	0.07	390	174	162	6	16	8,435.83
			NORTH_MSU	0.8	2.25	0.84	0.64	0.04	0.13	0.20	57	21	16	1	3	3,487.55
			NORTH_MSZ	5.1	1.88	0.72	0.61	0.04	0.11	0.14	311	119	100	6	18	15,354.68
			NORTH_MSZ+MSU	0.1	2.43	0.93	0.71	0.04	0.14	0.20	5	2	1	0	0	254.20
			NORTH_ND	0.3	3.14	1.13	0.76	0.09	0.19	0.33	31	11	8	1	2	2,262.27
			NORTH_SZ	0.3	1.86	0.78	0.77	0.03	0.09	0.06	19	8	8	0	1	453.99
			SW_LSZ	4.9	1.66	0.88	0.44	0.04	0.06	0.09	261	138	69	7	9	10,020.39
			SW_MSZ	5.0	1.97	1.02	0.50	0.07	0.07	0.12	317	164	81	11	11	13,244.47
			SW_NR	0.2	1.26	0.66	0.33	0.05	0.04	0.07	9	5	2	0	0	320.05
			Total	**74.9**	**2.02**	**0.97**	**0.58**	**0.05**	**0.08**	**0.13**	**4,878**	**2,344**	**1,389**	**123**	**191**	**214,689.59**
		Total	**CENTRAL_LSZ**	13.6	1.60	0.77	0.45	0.04	0.06	0.11	701	339	199	18	26	32,097.18
			CENTRAL_MSZ	25.5	2.60	1.32	0.65	0.07	0.10	0.18	2,132	1,080	534	55	79	99,268.68
			CENTRAL_NR	5.1	1.78	0.85	0.43	0.06	0.06	0.16	291	138	70	11	10	17,389.35
			NORTH_LSZ	9.0	1.42	0.61	0.56	0.03	0.08	0.06	409	175	161	8	22	12,100.96
			NORTH_LSZ+CHR	6.4	2.01	0.89	0.98	0.03	0.09	0.06	413	183	202	7	18	8,435.83
			NORTH_MSU	0.8	2.17	0.82	0.64	0.04	0.13	0.19	59	22	17	1	3	3,487.55
			NORTH_MSZ	5.4	1.84	0.71	0.62	0.04	0.11	0.13	321	124	108	6	19	15,354.68
			NORTH_MSZ+MSU	0.1	2.43	0.93	0.71	0.04	0.14	0.20	5	2	1	0	0	254.20
			NORTH_ND	0.3	3.14	1.13	0.76	0.09	0.19	0.33	31	11	8	1	2	2,262.27
			NORTH_SZ	0.4	1.70	0.73	0.74	0.03	0.09	0.05	21	9	9	0	1	453.99
			SW_LSZ	5.4	1.66	0.91	0.45	0.05	0.06	0.08	287	157	78	8	10	10,021.06
			SW_MSZ	5.4	1.93	1.02	0.50	0.07	0.07	0.11	333	175	86	12	12	13,535.55
			SW_NR	0.2	1.21	0.64	0.32	0.05	0.04	0.06	9	5	2	0	0	320.05
			Total	**77.6**	**2.01**	**0.97**	**0.59**	**0.05**	**0.08**	**0.13**	**5,013**	**2,421**	**1,476**	**128**	**202**	**214,981.35**

Notes:

1. The MRE has been prepared Porfirio Cabaleiro Rodriguez, Mining Engineer, BSc (Mine Eng), MAIG, director of GE21 Consultoria Mineral Ltda., an independent Qualified Persons (QP) under NI43-101. The effective date of the MRE is February 18, 2025.
2. Mineral resources are reported using the 2014 CIM Definition Standards and were estimated in accordance with the CIM 2019 Best Practices Guidelines, as required by National Instrument 43-101 Standards of Disclosure for Mineral Projects (NI 43-101).
3. Mineral resources that are not Mineral Reserves do not have demonstrated economic viability. There is no certainty that all Mineral Resources will be converted into Mineral Reserves.
4. Chemical elements are estimated using different estimation methodologies according to the Weathering Model. Ordinary Kriging was applied to Oxidized domain while the Turning Bands Simulation was applied for fresh rock.
5. This MRE includes Inferred Mineral Resources which have had insufficient work to classify them as Indicated Mineral Resources. It is uncertain but reasonably expected that inferred Mineral Resources could be upgraded to indicated Mineral Resources with continued exploration.
6. The Mineral Resource Estimate is reported/confined within an economic pit shell generated by Dassault Geovia Whittle software, using the following assumptions (generated from work completed for Bravo and historical test work):
   - Metallurgical recovery in sulphide material of 77% Pd, 81% Pt, 51% Rh, 48% Au, 50% Ni to a saleable Ni-PGM concentrate.
   - Metallurgical recovery in oxide material of 81% Pd, 23% Pt, 54% Rh, 90% Au to a saleable PGM ash residue (Ni not applicable).
   - Metallurgical recovery in high-talc sulphide material of 51% Pd, 55% Pt, 27% Rh, 27% Au, 0% Ni to a saleable Ni-PGM concentrate.
   - Independent Geotechnical Testwork – Overall pit slopes of 40 degrees in oxide and 50 degrees in Fresh Rock.
   - Densities are based on 27,170 drill hole core and 112 in situ samples density measurements. The Mineral Resources are reported on a dry density basis.
   - External downstream payability has not been included, as the base case MRE assumption considers internal downstream processing.
     a. Payable royalties of 2%, (only considering CFEM, for reserves, a complete set of royalties must be considered)

- Metal Pricing
  - Metal price assumptions are based on 10-year trailing averages (2014-2023): Pd price of US$1,380/oz, Pt price of US$1,100/oz, Rh price of US$6,200/oz, Au price of US$1,500/oz, Ni price of US$7,10/lb.
  - Palladium Equivalent (PdEq) Calculation
  - The PdEq equation is: PdEq = Pd g/t + F1 + F2 + F3 + F4

    Where: $\boldsymbol{F1} = \frac{(Pt_p * Pt_R)}{(Pd_p * Pd_R)} \boldsymbol{Pt_t}\ \boldsymbol{F2} = \frac{(Rh_p * Rh_R)}{(Pd_p * Pd_R)} \boldsymbol{Rh_t}\ \boldsymbol{F3} = \frac{(Au_p * Au_R)}{(Pd_p * Pd_R)} \boldsymbol{Au_t}\ \boldsymbol{F4} = \frac{(Ni_p * Ni_R)}{(Pd_p * Pd_R)} \boldsymbol{Ni_t}$

    $_P$ = Metal Price

    $_R$ = Metallurgical Recovery
- Costs are taken from comparable projects in GE21's extensive database of mining operations in Brazil, which includes not only operating mines, but recent actual costs from what could potentially be similarly sized operating mines in the Carajás. Costs considered a throughput rate of ca. 10Mtpa:
  - Mining costs: US$2.00/t oxide, US$3.00/t Fresh Rock. Processing costs: US$9.00/t fresh rock, US$7.50/t oxide. US$1.50/t processed, for General & Administration. US$1.00/t processed for grade control. US$0.50/t processed for rehabilitation.
  - Several of these considerations (metallurgical recovery, metal price projections for example) should be regarded as preliminary in nature, and therefore PdEq calculations should be regarded as preliminary in nature.

7. The current MRE supersedes and replaces the Previous Estimate (2023), which should be no longer relied upon.
8. The QP is not aware of political, environmental, or other risks that could materially affect the potential development of the Mineral Resources other than those typical for mining projects at this stage of development and as identified in this report.
9. Totals may not sum due to rounding.

Source: GE21, 2025.

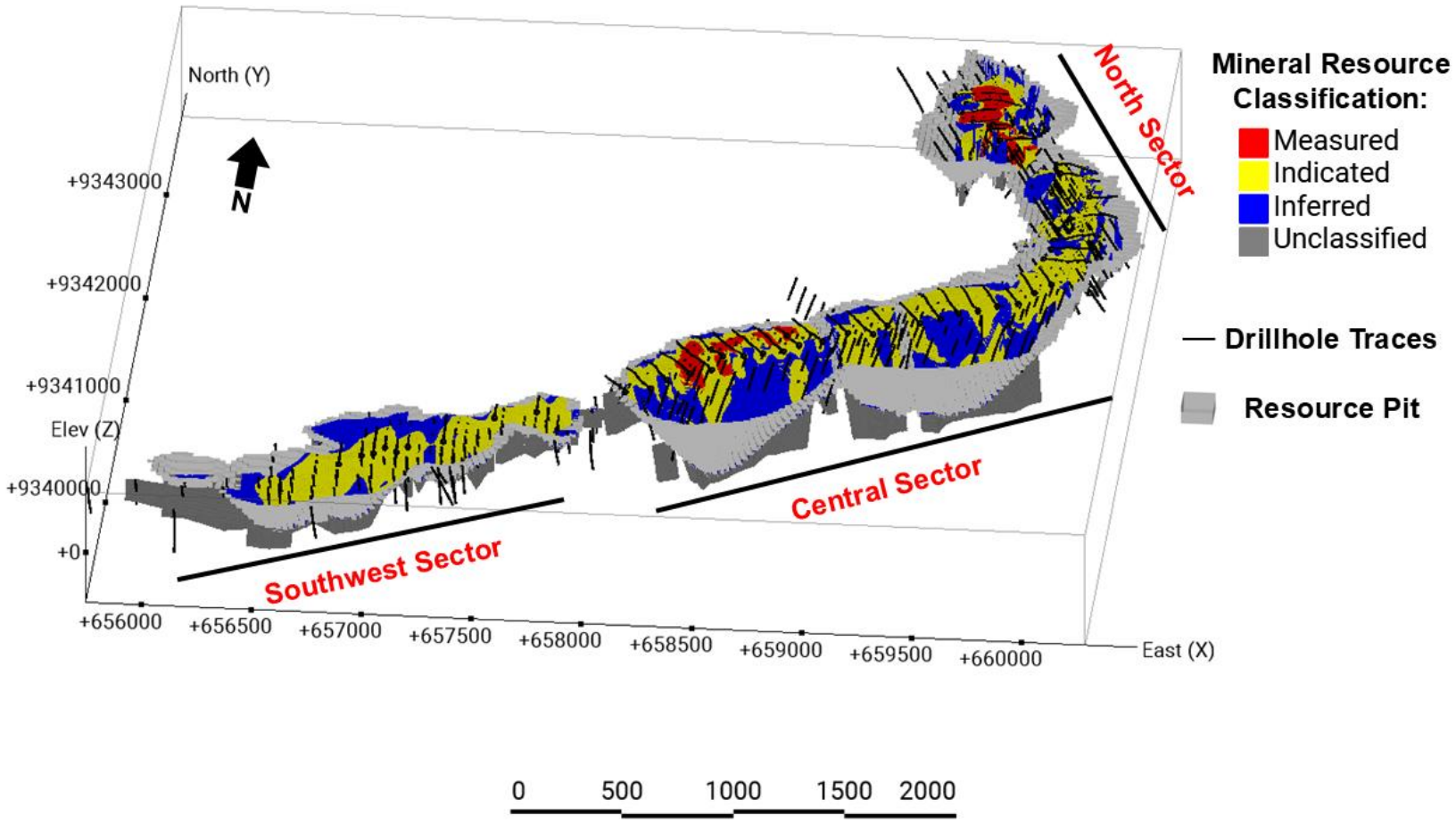

Figure 14-24: Mineral Resource classification 3D view

Source: GE21, 2024.

14.7 QP Opinion

Based on the validation methods employed, GE21 considers the results obtained for the estimate via Conditional Simulation acceptable and notes that no observable overall or local bias, as demonstrated by the NN and Swath Plot check analysis. GE21 also considers the quality of the data used for the estimate acceptable for classifying the Mineral Resources estimate.

If a further MRE upgrade is deemed desirable, GE21 recommends future work targets:

- Drilling at depth in areas where the constraining pit that encapsulates the reported Luanga MRE is limited due to the absence of drill data at depth.
- Further refinement of the geological and mineralogical models, which may result in unlocking a modest gain in MRE metal grades. An update of the mineralization geological model adopting an approach with implicit modelling methods and reducing domain internal dilution.
- Completion of the outstanding 2024 metallurgical test work, and 2025 metallurgical test work program.
- Resource estimation by the conditional simulation method defining the SMU to define the recoverable resource.

15 MINERAL RESERVES ESTIMATES

These sections are not applicable to Luanga given it is an exploration stage project.

16 MINING METHODS

These sections are not applicable to Luanga given it is an exploration stage project.

17 RECOVERY METHODS

These sections are not applicable to Luanga given it is an exploration stage project.

18 PROJECT INFRASTRUCTURE

These sections are not applicable to Luanga given it is an exploration stage project.

19 MARKET STUDIES AND CONTRACTS

These sections are not applicable to Luanga given it is an exploration stage project.

20 ENVIRONMENTAL STUDIES, PERMITTING, AND SOCIAL OR COMMUNITY IMPACTS

20.1 Permitting

The Pará State Environmental Agency (Secretaria de Estado de Meio Ambiente e Sustentabilidade – SEMAS) has granted Bravo a preliminary license (LP) for the Luanga deposit.

The Brazilian mine permitting process consists of three key stages: the preliminary license (LP), which has now been granted, followed by the installation license (LI) and, finally, the license to operate (LO). The LP is the most critical, time-consuming and challenging to secure, as it defines the project's fundamental parameters and requires both environmental feasibility and social acceptance – both of which were affirmed during the successful public hearing in December 2024.

This LP provides for the extraction and processing of metallic minerals, including platinum group metals as well as for nickel, copper and gold. The subsequent LI is applied for as a prerequisite for the commencement of construction activities, while the final license (LO) is granted upon completion of construction and the start of operations.

20.2 Independent Legal Opinion

Bravo retained Linneu de Albuquerque Mello, whose lawyers are qualified to practice law in the Federative Republic of Brazil. According to a title opinion by Linneu de Albuquerque Mello dated January 31, 2025, the Luanga Mineral Rights were valid and in good standing at that time.

The letter from Linneu de Alburquerque Mello is reproduced below.

Rio de Janeiro, January 31, 2025.

To

BRAVO MINERAÇÃO LTDA.
Avenida Jornalista Ricardo Marinho,
No. 360, Suite 111
22.631-350 - Rio de Janeiro, RJ, Brazil

BRAVO MINING CORP.
c/o Suite 1008, Bentall 5 550 Burrard Street
Vancouver, BC V6C 2B5, Canada

GE21 CONSULTORIA MINERAL LTDA.
Afonso Pena, nº 3130, 9th,12th and 13th floor
30.130-910, Belo Horizonte, MG, Brazil

COZEN O'CONNOR LLP
Bentall 5, 550 Burrard Street, Suite 1008
Vancouver, BC. V6C 2B5, Canada

Ref.: Legal Opinion on the Title of Mineral Rights for Luanga Project – Update 2025

Dear Sirs/Mesdames,

In 2023, you requested our opinion with respect to the legal aspects of the mineral rights owned by Bravo Mineração Ltda., formerly known as BPGM Mineração Ltda. (BRAVO), in connection with the Title Rights ANM No. 851.966/1992, located in the cities of Curionópolis and Marabá, in the State of Pará, Brazil ("Mineral Rights" or "Luanga Project"), which was subsequently updated in 2024.

In light of that, at the time we were expressly requested to confirm

the following:

(i) title rights in respect of the Mineral Rights;

(ii) the status of the application for the mining concession (*concessão de lavra*); and

(iii) the good standing of the company.

Additionally, we were also requested, based on additional documentation provided by BRAVO, to (i) summarize the royalty payment structure provided for in the contracts entered into by BRAVO in connection with the Mineral Rights, including the obligation to pay the CFEM (as defined below), and (ii) summarize the rights of the landowners where the Mineral Rights will be explored (*superficiários*).

Now, we are requested to update once more our legal opinion as to the points and issues above, considering the situation of Bravo as of January 31, 2025.

Rua Araújo Porto Alegre 70 11º Andar Centro Rio de Janeiro 20030-015
+55 (21) 3942-7292 +55 (21) 98847-2027 linneu@albuquerquemello.com.br
www.albuquerquemello.com.br

20.3 Documents Reviewed

To provide our opinion, we have reviewed originals, copies or conformed copies of the following documents:

1. "*Contrato para Realização de Pesquisa Mineral e Opção de Aquisição de Direito Minerário e outras Avenças*", entered into between Vale S.A., BRAVO and Atlantica do Brasil Mineração Ltda., dated as of October 13, 2020, providing for the purchase option of the Mineral Rights, among other things (Main Agreement).
2. "*Instrumento Particular de Cessão e Transferência de Direito Minerário*", entered into between Vale S.A., as assignor, and BRAVO, as assignee, dated as of November 3, 2020, providing for the transfer of the Mineral Rights (Mineral Rights Transfer Agreement).
3. "*Instrumento Particular de Acordo de Cooperação Técnica*", entered into between Vale S.A. and BRAVO, dated as of October 13, 2020, providing for technical cooperation between the two companies (Technical Cooperation Agreement).
4. "*Contrato de NSR Royalties*", entered into between Vale S.A. and BRAVO, dated as of October 13, 2020, providing for and detailing the payment
5. of royalties by BRAVO to Vale S.A. as a consequence of the mineral exploration in connection with the Mineral Rights Transfer Agreement (Vale Royalty Agreement).
6. "*Contrato No. 21.2.0295.1*", entered into between BRAVO and the Banco Nacional de Desenvolvimento Econômico – BNDES (the Brazilian Development and ExIm bank), dated as of November 1, 2021, providing for royalty payments to be made to BNDES in connection with the exploration of the Mineral Rights and as provided for in the Main Agreement (BNDES Royalty Agreement).
7. Several surface access agreements entered into with landowners within the area of the Mineral Rights, providing for the right to access the landowners' property to conduct exploration activities, among other things ("Landowners Agreements" and, together with the Main Agreement, the Mineral Rights Transfer Agreement, the Technical Cooperation Agreement, the Vale Royalty Agreement, and the BNDES Royalty Agreement, the "Transactional Documents".
8. A certain "*Relatório de Reavaliação de Recursos e Reservas*", dated of January 12, 2024, presented to the local mining authorities in the State of Pará, and a communication to ANM of the finding of copper, as a new mineral to be explored, dated of May 29, 2024; and
9. Several updated good standing certificates issued by certain courthouses in Rio de Janeiro and the State of Pará, and certain tax authorities all related to BRAVO and its branch.

20.4 Assumptions

The following opinions are given only as to, and based on, circumstances and matters of fact existing and known to us on the date of this opinion letter. These opinions only relate to the laws of Brazil which are in force on the date of this opinion letter. In giving the following opinions, we have relied (without further verification) upon completeness and accuracy, as at the date of this opinion letter, of certificates of good standing, without further investigation. We have also relied upon the following assumptions, which we have not independently verified:

1. All documents submitted to us as originals are authentic and all documents submitted to us as copies conform to authentic original documents.

2. All facts set forth in official public records, certificates and other documents supplied by public officials or otherwise conveyed to us by public officials are complete, true and accurate.
3. The information contained on the mining processes that we have had access through copies provided by the titleholders is accurate and up to date.
4. All signatures, initials and seals are genuine.
5. The capacity, power, authority and legal rights of all parties under all relevant laws and regulations to execute, unconditionally deliver and perform their respective obligations under the Transaction Documents.
6. There is no contractual or other prohibition or restriction (other than as arising under Brazilian law) prohibiting or restricting it from entering into and performing its obligations under the Transaction Documents.
7. The information contained on the electronic records of the *Agência Nacional of Mineração* (the Brazilian mining agency – ANM) website as being accurate and up to date; and
8. There has been no modification on the Transaction Documents and the debt clearance certificates have all been clear also on this date.

20.5 Opinion

Based upon, and subject to, the foregoing assumptions and the qualifications set out below, and having regard to such legal considerations as we deem relevant, we remain of the opinion that:

The Title Rights No. ANM 851.966/1992 is currently held by BRAVO and includes the right to conduct exploration activities for any minerals in the designated area, as provided for in Attachment I of this opinion letter. BRAVO presented to ANM for registration the Mineral Rights Transfer Agreement on November 10, 2021. ANM approved the transfer of the Mineral Rights on November 29, 2021. There is an indication of an archeological site in the area. The Mineral Rights are valid, regular and belong to BRAVO, and are waiting for the analysis of the mining concession application dated June 20, 2014, submitted by Vale S.A. (*concessão de lavra* – "Mining Concession"). ANM concluded the analysis of the Mining Concession application in May of 2018 and requested additional documents which were presented by Vale S.A. in September 2018. The analysis of the Mining Concession does not affect the validity of the Mineral Rights nor the ownership of the Mineral Rights by BRAVO, as its purpose is to confirm that all legal and technical requirements for the Mining Concession have been accomplished by the titleholder. Such analysis has already been done by ANM. On April 24, 2022, BRAVO filed a petition before the ANM informing it has requested Terms of Reference for the environmental licensing of the Luanga Project before the Environmental Agency in the State of Pará – SEMAS/PA, which has issued Technical Note No.32995/DLA/SAGRA/2022, stating it has not identified any "exclusion area" to be taken into consideration. Also, on June 16, 2024, BRAVO presented to this same environmental agency its request for the preliminary license, the first stage of the environmental licensing process to start mining the region. Furthermore, on May 29, 2024, BRAVO communicated to the ANM the finding of copper in the area, in addition to other minerals already

informed. On November 7, 2024, BRAVO requested to ANM a Trial Mining License (*Guia de Utilização*), for the experimental mining of 1,000,000 tpa of minerals.

20.6 Bravo Good Standing

BRAVO is a legal entity duly incorporated under Brazilian law and in good standing.

20.6.1 Summary of the Royalty Payment Structure

To transfer the Mineral Rights to BRAVO, the Main Agreement provides for payment of a purchase price and royalties by BRAVO to both Vale S.A. and BNDES. In addition, as a condition precedent to entering into the Main Agreement, both Vale S.A. and BRAVO had to obtain approval from BNDES. BNDES authorized the transfer of the Mineral Rights from Vale S.A. to BRAVO on September 16, 2021, through Dec. Dir. No. 0295/2021, as well as BRAVO entering into the BNDES Royalty Agreement. No modification was made to this agreement since our legal opinion dated June 8, 2023. BRAVO has finished paying the purchase price agreed upon in the Main Agreement.

On July 16, 2024, Vale S.A. novated and assigned the Main Agreement and the Vale Royalty Agreement to its wholly owned subsidiary, Mineração Onça Puma S.A., effective on July 1, 2023.

The novation and assignment of both the Main Agreement and the Vale Royalty Agreement to Mineração Onça Puma S.A. and the fact that the CFEM legislation remains unchanged, does not alter our opinion expressed in our letter of June 8, 2023, and subsequent updates.

20.7 Summary of the Rights of the Landowners

BRAVO has increased the number of agreements with the main landowners within the total area of the Mineral Rights, providing for, among other things, the right of BRAVO to conduct exploration activities within their property. Our opinions issued in our letter of June 8, 2023, and subsequent updates remain.

20.8 Conclusion

After the analysis of the legal requirements involving the Mineral Rights in the aspects that we consider necessary for this purpose, we consider that:

(a) The title of the Mineral Rights remains valid, has been properly instructed, and is ready for the mining concession to be granted.

(b) The existence of archeological site on the area does not impact on the capacity of the titleholder to explore and produce in the area.

(c) BRAVO is duly incorporated and existing under Brazilian law and is in good standing.

(d) After starting production, BRAVO will be required to pay royalty to Mineração Onça Puma S.A., BNDES, and the CFEM.

(e) BRAVO has increased its permission from landowners to access their property in most of the areas of the Mineral Rights. Nonetheless, the law grants a mineral title holder the right to demand access in case a landowner may oppose.

Yours faithfully,

Linneu de Albuquerque Mello

ATTACHMENT I:

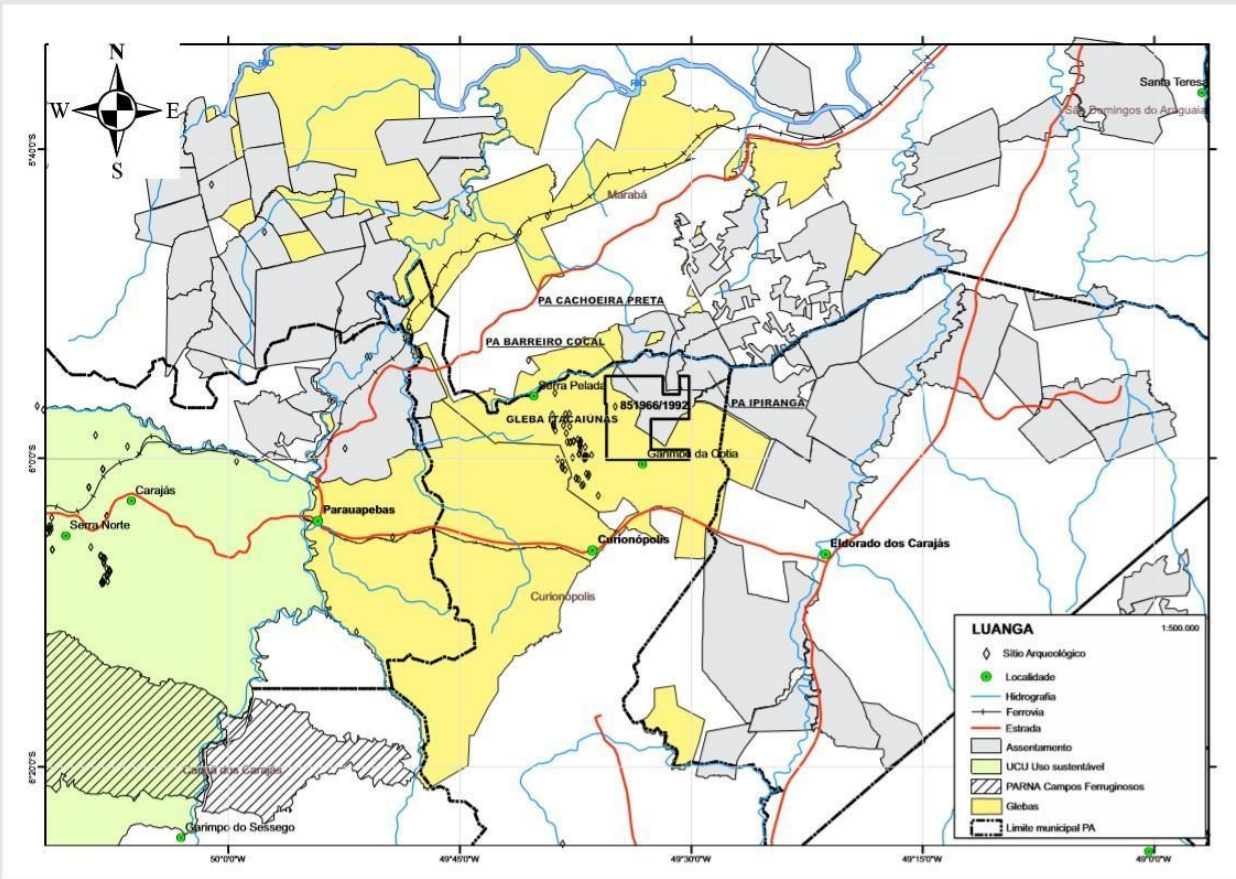

20.9 Environmental Liabilities

No environmental liabilities have been identified within the Luanga Exploration License. The current land use at the Luanga Project is solely agricultural cattle grazing. There are no significant rivers within the property. There are also no existing forests on the property, thus no deforestation is required.

The most significant activity to be completed by the company is relatively low impact drilling. Bravo will concurrently rehabilitate drill sites.

Social or community impact is expected to be negligible since the nearest community is the village of Serra Pelada, which is approximately 8km away. However, Bravo through its ESG program actively support the Serra Pelada community.

There are no indigenous communities within 25km of Luanga.

20.10 Social

Bravo has implemented several initiatives related to Environmental, Social, and Governance (ESG) performance during the implementation and development of Luanga. One of the ESG initiatives is related to environmental management. Bravo has implemented measures to minimize the impact of its operations on the environment. For example, it has developed a water management plan that includes monitoring water quality and quantity and implementing measures to reduce water consumption. Additionally, Bravo has implemented a waste management plan that provides recycling and proper disposal of waste material. In order to enhance the natural environment, Bravo created an internal procedure to plant ten new trees for each drill hole carried out on the Project area and, to the Effective Date, has planted 11,630 trees (or approximately 50 trees per hole drilled). Currently, the Company has over 20,000 trees in its local nursery, awaiting planting (Figure 5-9 and Figure 5-10).

21 CAPITAL AND OPERATING COSTS

These sections are not applicable to Luanga given it is an exploration stage project.

22 ECONOMIC ANALYSIS

These sections are not applicable to Luanga given it is an exploration stage project.

23 ADJACENT PROPERTIES

Within 10km of the Project, there are two main mineral deposits of relevance to Luanga: the Serra Pelada PGM + Au deposit and the Serra Leste iron ore deposit (Figure 23-1), neither of which have similar geology to Luanga, and are unrelated to mafic-ultramafic intrusions. In addition, there are several minor gold occurrences, mostly operated by artisanal miners, in the area. These projects are located to the west of the Luanga Project.

The Serra Pelada PGM + Au deposit occurs 8km west of Luanga in a tenement with a Mining License held by Serra Pelada Companhia de Desenvolvimento Mineral. During the 1980s, there were tens of thousands of illegal miners active in the Serra Pelada open pit, the largest gold mine in Brazil in its day. The pit reached 400m in length by 300m wide, to a depth over 120m below surface, all dug by hand. History records that 1.04Moz Au was extracted (Source: Meireles & Silva, 1988).

The Serra Leste high-grade hematite open pit iron ore mine occurs approximately 8.5km southwest of the Luanga Project, in a tenement held by Vale. Serra Leste includes active open pit mining and a beneficiation process comprising screening, hydrocycloning, crushing and filtration (Source: Vale public records)

There is no open ground for new exploration claims surrounding the Luanga License, and Vale is the major holder of exploration claims in the region.

The QP has not been able to verify the information on the adjacent properties and observes that the information in Section 23 is not indicative of the mineralization on the property that is the subject of this technical report.

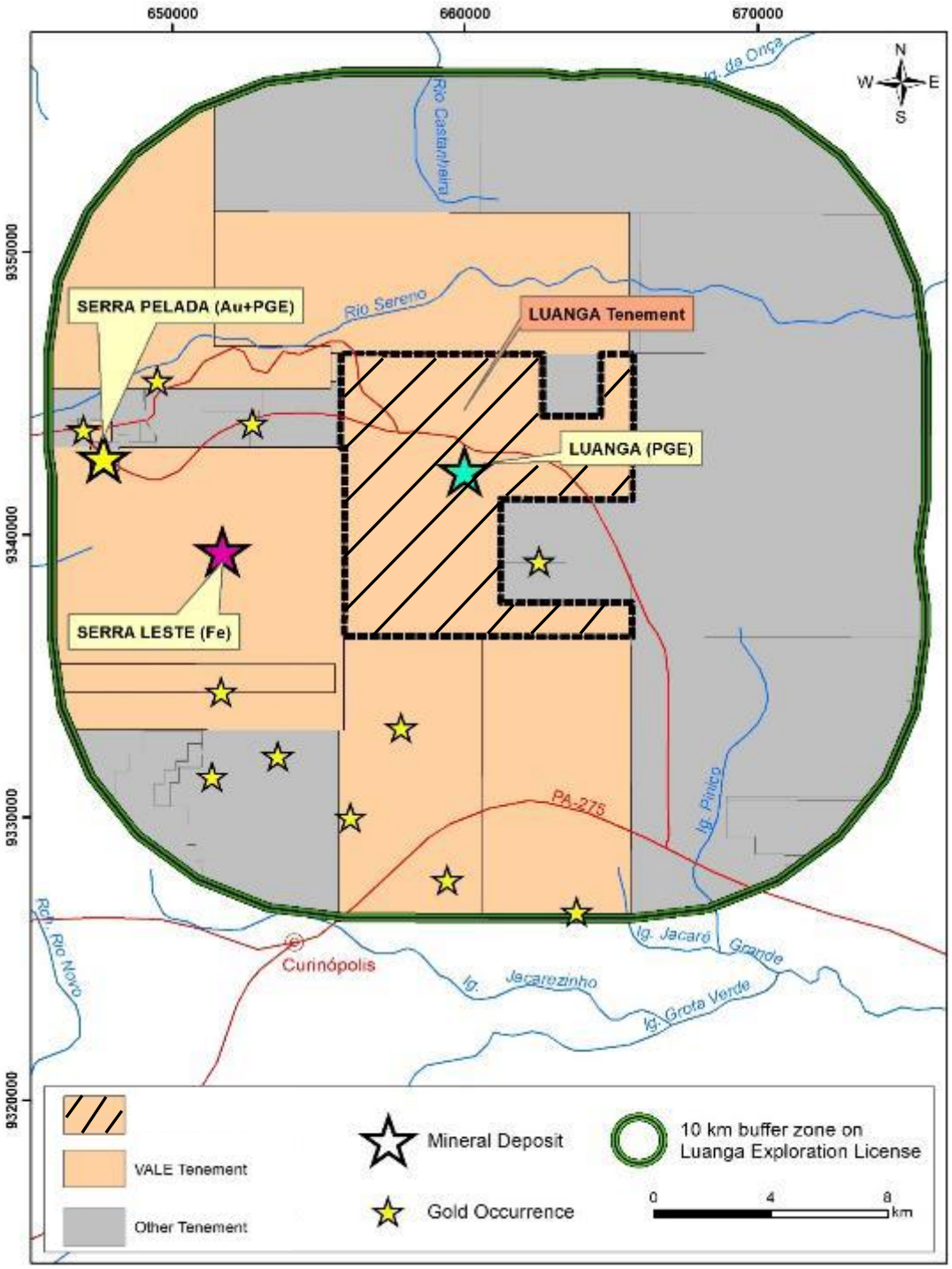

Figure 23-1: Mineral deposits adjacent to Luanga Project

Source: Bravo, 2023.

24 OTHER RELEVANT DATA AND INFORMATION

Apart from the Luanga PGM + Au + Ni deposit, Bravo is also conducting exploration works over an EM target, named as T5 Target (T5) or T5 Cu-Au Prospect. This target is located outside the Luanga Complex (~1.1km to east) and is currently an exploration stage prospect where Cu-Au mineralization was intercepted is several drill holes carried out to test EM conductors.

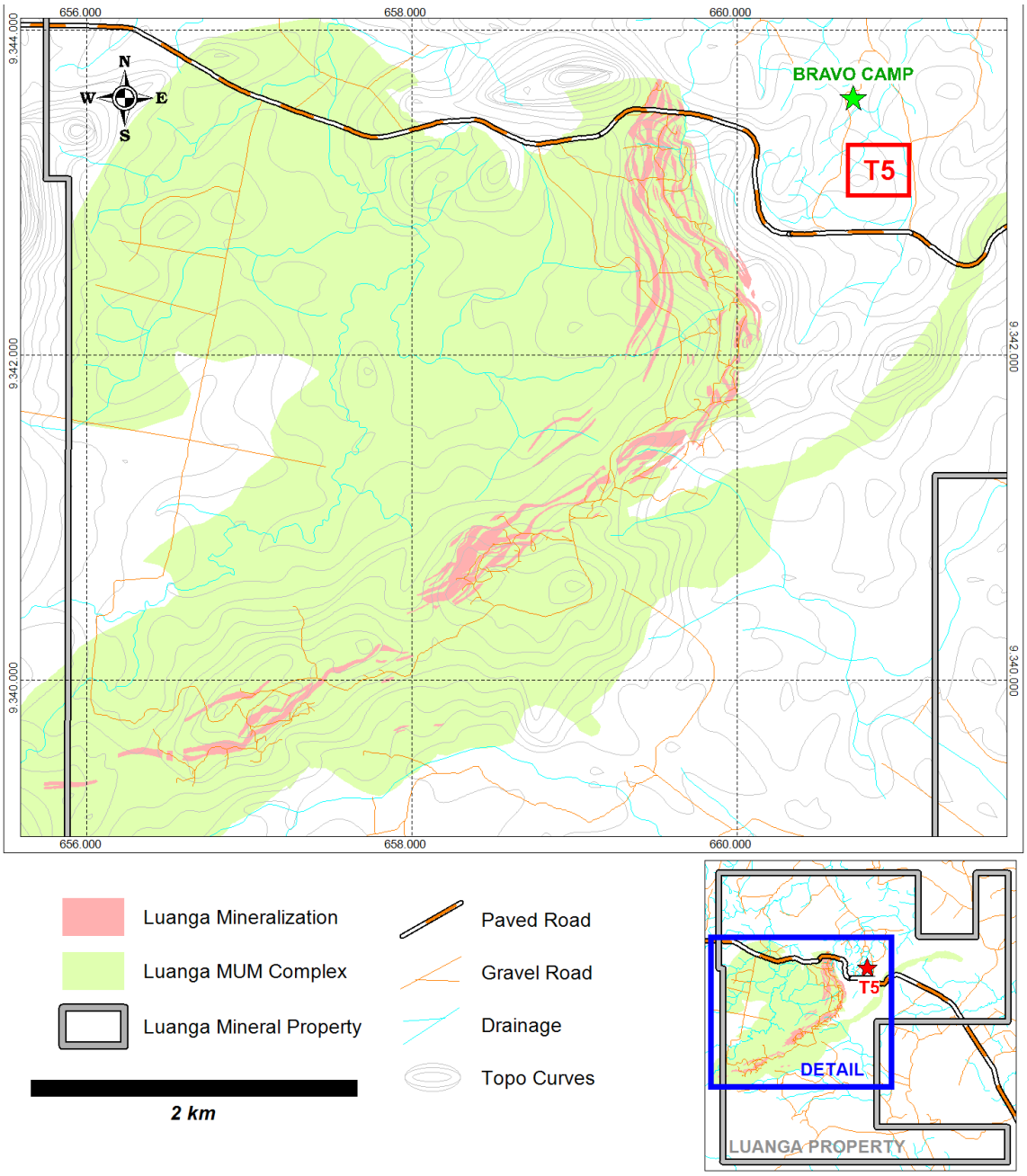

Figure 24-1: Location of T5 target in respect to Luanga MUM Complex.

Source: Bravo, 2025

Cu-Au sulphide mineralization at T5 occurs primarily as chalcopyrite with subordinate pyrrhotite plus pyrite and can be grouped into four main styles: i) massive to semi-massive sulphide, ii) disseminated, iii) brecciated and iv) vein. The sulphide mineralization is enveloped

by a hydrothermal zone associated with the development of biotite, actinolite, scapolite, chlorite, apatite, tourmaline, carbonate and silica (Figure 24-2). The whole system is controlled by a WNW-ESE fault structure steeply dipping to NNE that was generated under a brittle regime (brecciation with incipient foliation). The country host rock is a tonalite intrusion supported by petrographic studies and with a Th + U radiometric signature on the airborne survey. The hydrothermal assemblage together with the structural control suggest the T5 Cu-Au mineralization can be postulated as a IOCG type, which is a typical style of mineralization in the Carajás Mineral Province. The best result was from DDH2405T002, returning 11.5m @ 14.3% Cu, 3.3g/t from 165.6m downhole.

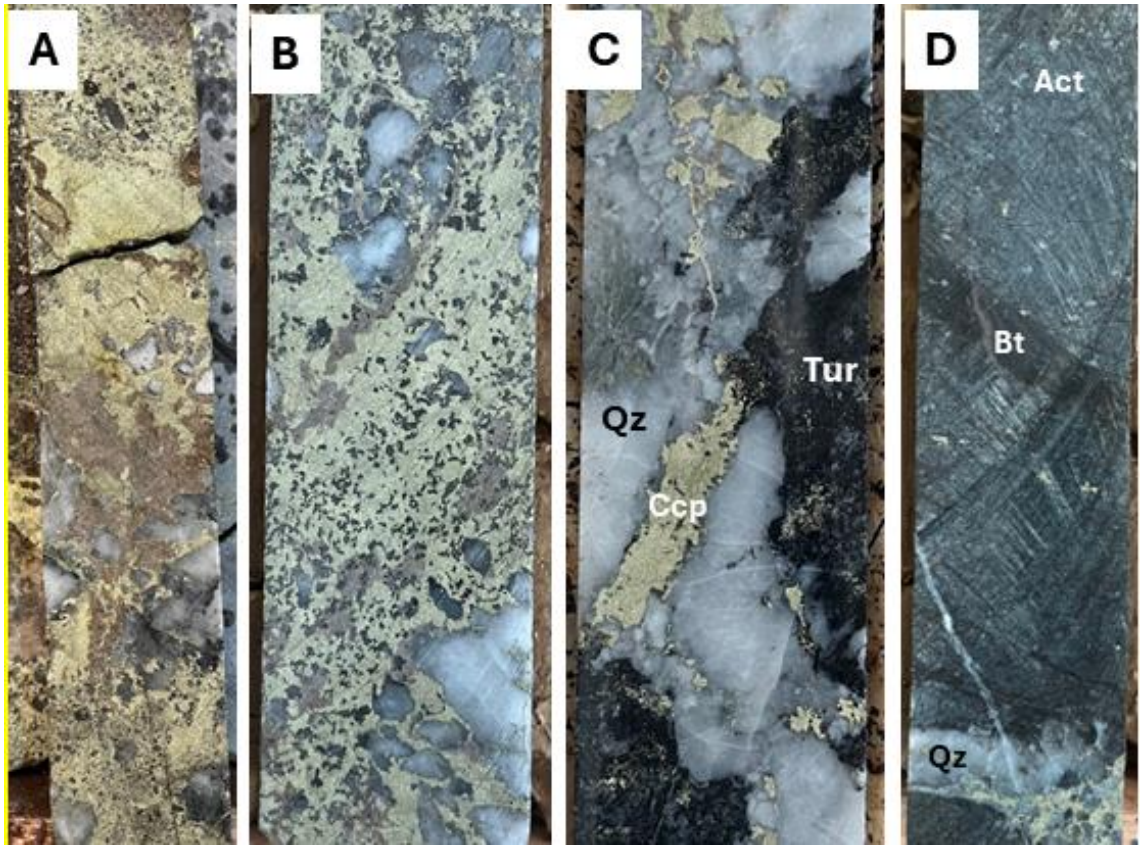

Figure 24-2: Core samples from T5 mineralization and hydrothermal alteration

Legend: A & B) Sulphide breccia (chalcopyrite+pyhrrotite) with quartz clasts [DDH2405T002]. C) Breccia crosscutting quartz (Qz) and tourmaline clusters (Tur) with chalcopyrite (Ccp) [DDH2405T010]. D) Actinolite (Act) crosscut by biotite (Bt) and quartz+chalcopyrite veinlets [DDH2405T012].
Source: Bravo, 2025.

Bravo continues the exploration activities on T5 Cu-Au prospect, where more drilling is planned for 2025 program. To date, no Mineral Resources has been estimated to this area.

25 INTERPRETATION AND CONCLUSIONS

25.1 Mineral Exploration and Geology

In general terms, the geological descriptions, sampling procedures and density tests that were evaluated were found to be of acceptable quality and in accordance with industry best practices.

It was noted that the data collection process was executed with the aim of maintaining data security. Data was stored in a standardized database, which was found to be secure and auditable.

GE21 supervised the process through which density was determined and concluded that it was in conformity with industry best practices.

25.2 QA/QC

GE21 performed the evaluation of the QA/QC data, which includes Blanks, CRMs, Field Duplicates, Check Assays, and Umpire Check Assays.

The AMIS standards data used by Bravo were revised for QA/QC programs. The recommendations state that new Reference Grades and Standard Deviations should be obtained from the data acquired during the Project (after outlier treatment). After this procedure, new reference values were generated. No significant biases were found after the correction of Reference Values. Control Charts using the new calculated reference value were done.

Although the Vale database was historical in nature, the validation and correlation procedures applied, and the results obtained, enable the QP of this report to consider this database to be valid for Mineral Resource estimation work.

QA/QC procedures, sampling methodology, and analytical methods applied by Bravo are within the industry's best practices standard. The QP responsible for this report, considering the data presented in Section 11, is of the opinion that the Luanga Project's Database is suited for a Mineral Resource Estimation work.

25.3 Geological Model

The procedure that was adopted to produce the 3D geological models (wireframes), consisting of generating triangulations between interpreted geological cross sections, was executed properly and aligns with the opinions of GE21 staff.

25.4 Grade Estimation

The heterogeneity of the geological model lead GE21 to select the Turning Bands Simulation method to estimate the grades for Luanga Project.

The variograms that were used in the estimation method are satisfactory and consistent with respect to the grade estimation that was calculated via Simulation (E-Type), making use of search anisotropy determined in the variography study. A valid conditional simulation in geostatistics ensured that simulated values honor both spatial continuity and the data distribution

To classify Mineral Resources, a study of spatial continuity for Pd Equivalent was conducted using variography followed by ordinary kriging interpolation. This study established a continuity zone suitable for considering:

- The Measured Mineral Resource was classified according to a reference grid of approximately 45mx45m, with a minimum number of 3 holes in section along the strike and dip directions, surrounded by the pit shell.
- The Indicated Mineral Resource classification had as a reference a drilling grid of approximately 75m x 75m, extending both along the strike and dip directions, and requiring a minimum of two drill holes.
- Manual post-processing was undertaken to construct wireframes representing the volumes categorized as Measured and Indicated, while considering the blocks within the resource pit shell.
- The Inferred Mineral Resource classification is all remaining estimated blocks within the resource pit shell.

GE21 considers the Mineral Resource classification model and the analysis of criteria for the classification of those Mineral Resources, to be satisfactory although some items could be improved.

25.5 Reasonable Prospects for Eventual Economic Extraction (RPEEE)

GE21 has not identified any mining, metallurgical, infrastructure, permitting, legal, political, environmental, technical, or other relevant factors that could materially affect the potential development of the Mineral Resources, other than those typical for a mineral deposit at this stage of development and as identified in this report.

GE21 performed a pit optimization study to classify the project's Mineral Resources to ensure the requirement for RPEEE was met. Parameters in the benefit function are presented in Table 25-1.

Table 25-1: Pit parameters generated by RPEEE

Optimization Parameters - RPEEE				
Item				Unit
Lithotype	Fresh & Weathered & High Talc			-
Slope Angle	Weathered		40	°
	Fresh / High Talc		50	°
Mining	Density	Block Model		
	Mining Recovery		100	%
	Mining Dilution		0	%
	MCAF		ANM Mineral Rights	
	Cut-off grade (Whittle)	Fresh	-	-
		Weathered	-	-
Processing		Pd	81.0%	Mill

Optimization Parameters - RPEEE				
Item				Unit
	Metallurgic Recovery - Weathered	Pt	23.0%	Mill
		Rh	54.0%	Mill
		Au	90.0%	Mill
		Ni	0.0%	Mill
	Metallurgic Recovery - Fresh	Pd	77.0%	Mill
		Pt	81.0%	Mill
		Rh	51.0%	Mill
		Au	48.0%	Mill
		Ni	50.0%	Mill
	Metallurgic Recovery - High Talc	Pd	51.0%	Mill
		Pt	55.5%	Mill
		Rh	27.3%	Mill
		Au	27.0%	Mill
		Ni	0.0%	Mill
Costs	Weathered	Mining Cost	2.00	USD/t mined
		Processing Cost	7.50	USD/t ROM
		Grade Control	1.00	
		Logistics	0.50	
		Rehabilitation	1.00	
		G&A	1.50	
	Fresh / High Talc	Mining Cost	3.00	USD/t mined
		Processing Cost	9.00	USD/t ROM
		Grade Control	1.00	
		Logistics	0.50	
		Rehabilitation	1.00	
		G&A	1.50	
Selling	Price	Pd	1 380	USD/Oz
		Pt	1 100	USD/Oz
		Rh	6 200	USD/Oz
		Au	1 500	USD/Oz
		Ni	7.10	USD/lb
	Royalties	All	2.0	%

Source: GE21, 2025.

25.6 Mineral Resources

Luanga Project's maiden, pit-constrained MRE has an effective date of February 18, 2025. In summary, It comprises 36 Mt at 2.00 g/t Pd Eq for a total of 2.3 Moz Pd Eq in the Measured category, 122 Mt at 2.06 g/t Pd Eq for 8.0 Moz Pd Eq in the Indicated category, 158 Mt at 2.04 g/t Pd Eq for a total of 10.4 Moz Pd Eq in the Measured + Indicated categories, and 78 Mt at 2.01 g/t Pd Eq for a total of 5.0 Moz Pd Eq in the Inferred category (a detailed breakdown by sector and metal can be found in Table 25-2).

Table 25-2: MRE statement at a cut-off of 0.5g/t Pd Eq*

Resource	Classification	Domain	Mass	Average Value						Material Content					
			Mt	Pd eq ppm	Pd g/t	Pt g/t	Au g/t	Rh g/t	Ni %	Pd eq koz	Pd koz	Pt koz	Au koz	Rh koz	Ni klb
Open Pit	Measured	Ox	4	1.51	0.90	0.88	0.05	0.12	0.00	197	117	115	7	15	—
		High Talc	—	—	—	—	—	—	—	—	—	—	—	—	—
		Fresh	32	2.06	0.97	0.67	0.04	0.08	0.11	2,144	1,009	694	46	88	77,621
		Total	**36**	**2.00**	**0.96**	**0.69**	**0.04**	**0.09**	**0.10**	**2,340**	**1,126**	**809**	**53**	**104**	**77,621**
	Indicated	Ox	6	1.51	0.97	0.73	0.04	0.11	0.00	314	200	151	9	23	0
		High Talc	2	1.83	1.12	0.54	0.11	0.08	0.13	146	89	43	9	6	6,952
		Fresh	113	2.09	0.99	0.59	0.05	0.09	0.14	7,599	3,583	2,133	193	318	344,092
		Total	**122**	**2.06**	**0.99**	**0.59**	**0.05**	**0.09**	**0.13**	**8,058**	**3,872**	**2,326**	**210**	**348**	**351,044**
	Measured + Indicated	**Ox**	**10**	**1.51**	**0.94**	**0.79**	**0.04**	**0.11**	**0.00**	**510**	**317**	**266**	**15**	**38**	—
		High Talc	**2**	**1.83**	**1.12**	**0.54**	**0.11**	**0.08**	**0.13**	**146**	**89**	**43**	**9**	**6**	**6,952**
		Fresh	**145**	**2.08**	**0.98**	**0.60**	**0.05**	**0.09**	**0.13**	**9,743**	**4,592**	**2,827**	**239**	**407**	**421,713**
		Total	**158**	**2.04**	**0.98**	**0.62**	**0.05**	**0.09**	**0.12**	**10,399**	**4,998**	**3,135**	**262**	**451**	**428,665**
	Inferred	Ox	3	1.57	0.88	1.04	0.05	0.13	—	130	73	86	4	11	—
		High Talc	0	1.76	1.08	0.53	0.10	0.07	0.14	5	3	2	0	0	292
		Fresh	75	2.02	0.97	0.58	0.05	0.08	0.13	4,878	2,344	1,389	123	191	214,690
		Total	**78**	**2.01**	**0.97**	**0.59**	**0.05**	**0.08**	**0.13**	**5,013**	**2,421**	**1,476**	**128**	**202**	**214,981**

Notes:

1. The MRE has been prepared by Porfirio Cabaleiro Rodriguez, Mining Engineer, BSc (Mine Eng), MAIG, director of GE21 Consultoria Mineral Ltda., an independent Qualified Persons (QP) under NI43-101. The effective date of the MRE is February 18, 2025.
2. Mineral resources are reported using the 2014 CIM Definition Standards and were estimated in accordance with the CIM 2019 Best Practices Guidelines, as required by National Instrument 43-101 Standards of Disclosure for Mineral Projects (NI 43-101).
3. Mineral resources that are not Mineral Reserves do not have demonstrated economic viability. There is no certainty that all Mineral Resources will be converted into Mineral Reserves.
4. Chemical elements are estimated using different estimation methodologies according to the Weathering Model. Ordinary Kriging was applied to Oxidized domain while the Turning Bands Simulation was applied for fresh rock.
5. This MRE includes Inferred Mineral Resources which have had insufficient work to classify them as Indicated Mineral Resources. It is uncertain but reasonably expected that inferred Mineral Resources could be upgraded to indicated Mineral Resources with continued exploration.
   - The Mineral Resource Estimate is reported/confined within an economic pit shell generated by Dassault Geovia Whittle software, using the following assumptions (Generated from work completed for Bravo and historical test work):
     - Metallurgical recovery in sulphide material of 77% Pd, 81% Pt, 51% Rh, 48% Au, 50% Ni to a saleable Ni-PGM concentrate.
     - Metallurgical recovery in oxide material of 81% Pd, 23% Pt, 54% Rh, 90% Au to a saleable PGM ash residue (Ni not applicable).
     - Metallurgical recovery in high-talc sulphide material of 51% Pd, 55% Pt, 27% Rh, 27% Au, 0% Ni to a saleable Ni-PGM concentrate.
     - Independent Geotechnical Testwork – Overall pit slopes of 40 degrees in oxide and 50 degrees in Fresh Rock.
     - Densities are based on 27,170 drill hole core and 112 in situ samples density measurements. The Mineral Resources are reported on a dry density basis.
     - External downstream payability has not been included, as the base case MRE assumption considers internal downstream processing.

a. Payable royalties of 2%, (only considering CFEM, for reserves, a complete set of royalties must be considered)

6. Metal Pricing
   a. Metal price assumptions are based on 10-year trailing averages (2014-2023): Pd price of US$1,380/oz, Pt price of US$1,100/oz, Rh price of US$6,200/oz, Au price of US$1,500/oz, Ni price of US$7,10/lb.
   b. Palladium Equivalent (PdEq) Calculation
   c. The PdEq equation is: PdEq = Pd g/t + F1 + F2 + F3 + F4

      Where: $\boldsymbol{F1} = \frac{(Pt_p * Pt_R)}{(Pd_p * Pd_R)} \boldsymbol{Pt_t}$ $\boldsymbol{F2} = \frac{(Rh_p * Rh_R)}{(Pd_p * Pd_R)} \boldsymbol{Rh_t}$ $\boldsymbol{F3} = \frac{(Au_p * Au_R)}{(Pd_p * Pd_R)} \boldsymbol{Au_t}$ $\boldsymbol{F4} = \frac{(Ni_p * Ni_R)}{(Pd_p * Pd_R)} \boldsymbol{Ni_t}$

      $_P$ = Metal Price

      $_R$ = Metallurgical Recovery

7. Costs are taken from comparable projects in GE21's extensive database of mining operations in Brazil, which includes not only operating mines, but recent actual costs from what could potentially be similarly sized operating mines in the Carajás. Costs considered a throughput rate of ca. 10Mtpa:
   a. Mining costs: US$2.00/t oxide, US$3.00/t Fresh Rock. Processing costs: US$9.00/t fresh rock, US$7.50/t oxide. US$1.50/t processed, for General & Administration. US$1.00/t processed for grade control. US$0.50/t processed for rehabilitation.
   b. Several of these considerations (metallurgical recovery, metal price projections for example) should be regarded as preliminary in nature, and therefore PdEq calculations should be regarded as preliminary in nature.

8. The current MRE supersedes and replaces the Previous Estimate (2023), which should be no longer relied upon.
9. The QP is not aware of political, environmental, or other risks that could materially affect the potential development of the Mineral Resources other than those typical for mining projects at this stage of development and as identified in this report.
10. Totals may not sum due to rounding.

Source: GE21, 2025.

26 RECOMMENDATIONS

26.1 Luanga PGM + Au + Ni Deposit

GE21 recommends completion of the outstanding metallurgical work that was not completed in 2024, including final assays, review, interpretation and reporting. This may unlock modest gains in metallurgical recoveries, which could be applied to subsequent updates to the current 2025 MRE.

If a further MRE upgrade is deemed desirable, GE21 recommends future work targets:

- Drilling at depth in areas where the constraining pit that encapsulates the reported Luanga MRE is limited due to the absence of drill data at depth.
- Further refinement of the geological and mineralogical models, which may result in unlocking a modest gain in MRE metal grades. An update of the mineralization geological model adopting an approach with implicit modelling methods and reducing domain internal dilution.
- Completion of the outstanding metallurgical testwork noted above.

Resource estimation by the conditional simulation method defining the SMU to define the recoverable resource.

Collectively, the above work could deliver a further upgrade to the Luanga MRE, both in overall tonnage and, potentially, the average grade of the MRE.

Further, additional metallurgical programs are recommended, building off the 2024 test work results, to further optimize metallurgical recoveries and concentrate grades in various types of mineralization with a view to increasing potential payabilities at third part facilities.

Following on from the successful and significant upgrade to the Luanga MRE in the 2025 MRE (as compared to the maiden 2023 MRE), the next significant stage for the Company would be the completion of a Preliminary Economic Assessment (PEA) and/or a Pre-Feasibility Study (PFS) to define mineral reserves (given that most of the MRE is now classified in the Measured and Indicated categories).

26.2 Luanga Area Exploration Potential

The results of Bravo's 2024 exploration, based on the previously completed HeliTEM Electromagnetic (EM) survey covering the entire Luanga property, has generated intersections of massive sulphide mineralization, including:

- Ni/Cu/PGM and Ni/Cu massive sulphides, probably related to the emplacement of the Luanga PGM+Au+Ni deposit.

- More interestingly, compelling evidence of Carajás style Iron Oxide Copper Gold mineralization, particularly in work reported from the T5 target.

GE21 recommends that exploration work in 2025 should focus on continuing the exploration for mineralization outside of the Luanga PGM+Au+Ni deposit, and particularly the potential for IOCG deposits given the results from early exploration works in 2024.

26.3 Luanga Carbon Capture Potential

The Luanga deposit is hosted almost entirely in ultramafic rocks which early works indicate the potential for permanent carbon sequestration in tailings and/or waste rock. This is an opportunity that can be investigated further, subject to test results and economic assessment, could be incorporated into future study phases with the potential to create a carbon negative operation in combination with other mitigation efforts such as use of hydroelectric power, mine electrification and reforestation.

The recommended work program comprises:

PHASE 5A – Metallurgical testwork at Luanga

Completion of outstanding 2024 metallurgical testwork:

Estimate	US$0.20M

Continuation of carbon sequestration study:

Estimate	US$0.05M

Continued Metallurgical testwork and optimization

Estimate	US$0.20M

Updated MRE and technical report in accordance with NI 43-101:

Estimate	US$0.10M
Sub-total – Phase 5A	***US$0.55M***

PHASE 5B – PEA

MRE Update implicit model:

Estimate	US$0.3M

Completion of a PEA, including market studies:

Estimate	US$0.3M
Sub-total – Phase 5B	***US$0.6M***

PHASE 5C – Deep Drilling below the Luanga PGM+Au+Ni deposit

Deep drilling at the Luanga PGM+Au+Ni deposit.

8 holes @ ~500m = 4,000m @ US$450/m

Estimate	US$1.8M
Sub-total – Phase 5C	***US$1.8M***

Phase 5D – Regional Exploration

Exploration of new (IOCG and/or massive sulphide Ni/Cu/ PGM targets):

Geological, geophysical and drilling programs to evaluate the potential for the discovery of additional zones of mineralization:

Geophysics	US$0.1M
Drilling: 35 holes x 200m for 7,000m @ US$400m (all inclusive)	US$2.8M
Sub-total – Phase 5D	***US$2.9M***
TOTAL – PHASE 5	***US$5.85M***

PHASE 6 – PFS following favorable results from a PEA

Completion of a PFS:

Estimate	US$1.0M
Sub-total – Phase 6	***US$1.0M***

These work programs and cost estimates are preliminary in nature and will be refined, adjusted and modified as additional information is compiled, contracts for the various aspects of the work program entered, and results from new work are received. This could result in some movement in funds between different categories.

27 REFERENCES

ARAÚJO, O. J. B.; MAIA, R. G. N. Projeto especial mapas de recursos minerais, de solos e de vegetação para a área do Programa Grande Carajás; Subprojeto Recursos Minerais; Folha SB.22-Z-A Serra dos Carajás - Estado do Pará: DNPM/CPRM, 1991.

ARAÚJO, O. J. B.; MAIA, R. G. N.; JOÃO, X.S.J.; COSTA, J. B. S. A megaestruturação arqueana da Folha Serra dos Carajás. Congresso Latino-Americano de Geologia, Belém Brazil, Anais, p. 324-338, 1988.

BARNES, S. J. et al. Sulfide-silicate textures in magmatic Ni-Cu-PGE sulfide ore deposits: Massive, semi-massive and sulfide-matrix breccia ores. Ore Geology Reviews, v. 101, p. 629-651, 2018.

BARNES, S. J. et al. The mineral system approach applied to magmatic Ni–Cu–PGE sulfide deposits. Ore geology reviews, v. 76, p. 296-316, 2016.

BARNES, S. J.; DAVID, A. H. Margaux Le Vaillant; Depósitos de minério de sulfeto magnético. Elementos 2017; 13 (2): 89–95.

CABRI, L. J. A Mineralogical Study of Samples from the Luanga Layered PGE Deposit, Carajás, Brazil. Parte 5: Samples from the Luanga Orebody. Confidential Report 2003-07. 74p, 2003.

DALL'AGNOL, R.; OLIVEIRA, M. A.; ALMEIDA, J. A. C.; ALTHOFF, F. J.; LEITE, A. A. S.; OLIVEIRA, D. C.; BARROS, C. E. M. Archean and Paleoproterozoic granitoids of the Carajás metallogenetic province, eastern Amazonian craton. Symposium on Magmatism, Crustal Evolution, and Metallogenesis of the Amazonian Craton, Abstracts Volume and Field Trips Guide, 150 pp, 2006.

DARDENNE, M. A; FERREIRA FILHO, C. F.; MEIRELLES, M. R. The role of shoshonitic and calc-alkaline suites in the tectonic evolution of the Carajás District, Brazil. Journal of South American Earth Sciences 1, 363–372, 1988.

DIELLA, V.; FERRARIO, A.; GIRARDI, V. A. V. PGE and PGM in the Luanga Mafic-Ultramafic Intrusion in Serra dos Carajás (Pará State, Brazil). 9p, 1995.

DOCEGEO - Rio Doce Geologia e Mineração. Revisão Litoestratigráfica da Província Mineral de Carajás, in, SBG-NNO, ed., 35º Congresso Brasileiro Geologia, Belém, Anais: p. 11-59, 1988.

FEIO, G. R. L.; DALL'AGNOL, R.; DANTAS, E. L.; MACAMBIRA, M. J. B.; SANTOS, J. O. S.; ALTHOFF, F. J.; SOARES, J. E. B. Archean granitoid magmatism in the Canaã dos Carajás area: Implications for crustal evolution of the Carajás province, Amazonian craton, Brazil. Precambrian Research 227, 157-185, 2013.

FERREIRA FILHO, C. F.; CANÇADO, F.; CORREA, C.; MACAMBIRA, E. M. B.; SIEPIERSKI, L.; BROD, T. C. J. Mineralizações estratiformes de EGP-Ni associadas a complexos 91 acamadados em Carajás: os exemplos de Luanga e Serra da Onça. In: Publitec Gráfica & Editora, Contribuições à Geologia da Amazônia, vol. 5, pp. 01-14. 2007.

FERREIRA FILHO, C.F. Petrography. Report on Luanga. 2022 to 2024.

GE21 Consultoria Mineral. Independent Technical Report for the Luanga PGM+Au+Ni Project, Pará State, Brazil. Report on Luanga, 2023.

GIBBS, A. K.; WIRTH, K. R.; HIRATA, W. K.; OLSZEWSKI Jr, W. J. Age and composition of the Grão Pará Group volcanics, Serra dos Carajás. Revista Brasileira de Geociências 16, 201-211, 1986.

HDK Engenharia. Caracterização de Amostras e Dimensionamento Preliminar de Circuito de Moagem – Depósito Luanga. 28p, 2003.

HOATSON, D. M.; JAIRETH, S.; JAQUES, A. L. Nickel sulphide deposits in Australia: Characteristics, resources, and potential: Ore Geology Reviews, v. 29, p. 177–241, 2006.

HOLDSWORTH, R. E.; PINHEIRO, R. V. L. The anatomy of shallow-crustal transpressional structures: insights from the Archean Carajás fault zone, Amazon, Brazil. Journal of Structural Geology 61, 1105-1123, 2000.

HUHN, S. R. B., SANTOS, A. B. S.; AMARAL, A. F.; LEDSHAM, E. J.; GOUVEIA, J. L.; MARTINS, L. P. B.; MONTALVÃO, R. M. G.; COSTA, V. C. O terreno granito-greenstone da região de Rio Maria-Sul do Pará. 35º Congresso Brasileiro de Geologia, Belém, Brasil, Anais, Sociedade Brasileira de Geologia, pp. 1438-1452, 1986.

LIGHTFOOT, P. C.; LAMSWOOD, D. E. Structural controls on the primary distribution of mafic–ultramafic intrusions containing Ni–Cu–Co–(PGE) sulfide mineralization in the roots of large igneous provinces. Ore Geology Reviews - Elsevier, v. 64, p. 354-386, 2015.

MACHADO, N.; LINDENMAYER, Z. G.; KROGH, T. E.; LINDENMAYER, D. U-Pb geochronology of Archean magmatism and basement reactivation in the Carajás area, Amazon shield, Brazil. Precambrian Research 49, 329-354, 1991.

MANSUR, E. T. Caracterização e Metalogênese do Depósito de Elementos do Grupo da Platina do Complexo Luanga, Província Mineral do Carajás. 158p, 2017.

MANSUR, E. T.; FERREIRA FILHO, C. F. Magmatic structure and geochemistry of the Luanga Mafic–Ultramafic Complex: Further constraints for the PGE-mineralized magmatism in Carajás, Brazil. Lithos, v. 266, p. 28-43, 2016.

MANSUR, E.T.; FERREIRA FILHO, C. F.; OLIVEIRA, D. P. L. The Luanga deposit, Carajás Mineral Province, Brazil: Different styles of PGE mineralization hosted in a medium-size layered intrusion. Ore Geology Reviews. 18p, 2020.

MEIRELES, E. M.; SILVA, A. R. B. Depósito de ouro de Serra Pelada, Marabá, Pará, in Schobbenhaus, C., and Coelho, C.E.S., eds., Principais depósitos minerais do Brasil – volume III: Brasília, Departamento Nacional da Produção Mineral, Companhia Vale do Rio Doce, p. 547–557, 1988.

MULLER, P. H. Technical Report on Luanga PGE+Au Project, State of Para, Brazil, 2020.

MUNGALL, J. E.; NALDRETT, A. J. Ore deposits of the platinum-group elements. Elements, v. 4, n. 4, p. 253-258, 2008.

NALDRETT, A. J. Depósitos de elementos do grupo da platina (PGE). Depósitos de sulfeto magmático: Geologia, Geoquímica e exploração, p. 481-612, 2004.

NALDRETT, A. J. Secular variation of magmatic sulphide deposits and their source magmas: Economic Geology, v. 105, p. 669–688, 2010a.

PIDGEON, R. T.; MACAMBIRA, M. J. B.; LAFON, J. M. Th-U-Pb isotopic systems and internal structures of complex zircons from enderbite from the Pium Complex, Carajás Province, Brazil: evidence for the ages of granulite facies metamorphism and the protolith of the enderbite. Chemical Geology 166, 159-171, 2000.

PRINSLOO, C. F. Investigation into the Recovery of PGM Values from a Brazilian Ore Type for Companhia Vale do Rio Doce (CVRD). Mintek. 98p, 2002.

RIBEIRO, V. E. Gênese e Controle das Mineralizações de Pt-Pd nos Alvos Luanga e Fênix – Complexo Máfico-Ultramáfico Luanga, Província Mineral de Carajás, Pará. 210p, 2020.

ROLIM, V. K. Geotectonic environment and Structural control of Luanga Complex. Report on Luanga, 2023.

ROSA, W. D. Complexos acamadados da Serra da Onça e Serra do Puma: Geologia e petrologia de duas intrusões Máfico-Ultramáficas com sequência de 94 cristalização distinta na Província Arqueana de Carajás, Brasil. Unpublished M.Sc. Thesis, Universidade de Brasília, Brazil, 65 p, 2014.

SANTOS, J. O. S. et al. Age and autochthonous evolution of the Sunsás Orogen in West Amazon Craton based on mapping and U–Pb geochronology. Precambrian Research, v. 165, n. 3-4, p. 120-152, 2008.

SGS Lakefield Research Limited. Applicability of the PLATSOL® Process to Five Samples from the Luanga Deposit. 64p, 2005.

SGS Lakefield Research Limited. Locked Cycle Flotation Products, Luanga Deposit, Brazil. 131p, 2004.

SIEPIERSKI, L.; FERREIRA FILHO, C.F. Spinifex-textured komatiites in the south border of the Carajas ridge, Selva Greenstone belt, Carajás Province, Brazil. Journal of South American Earth Sciences 66, 41-55, 2016.

SOUZA, Z. S.; DALL'AGNOL, R. Caracterização geoquímica e tectônica de rochas meta vulcânicas de "greenstone belts" arqueanos da região de Rio Maria, SE do Pará. Boletim. IG-USP, special publication, online, vol.18, pp. 97-101. ISSN 0102-6275, 1996.

SOUZA, Z. S.; POTREL, A.; LAFON, J. M.; ALTHOFF, F.J.; PIMENTEL, M. M., DALL'AGNOL, R.; OLIVEIRA, C. G. Nd, Pb and Sr isotopes in the Identidade Belt, an Archean greenstone belt of Rio Maria region (Carajás Province, Brazil): implications for the geodynamic evolution of the Amazonian Craton. Precambrian Research 109, 293-315, 2001.

TALLARICO, J. B. C. Caracterização de Amostras de Cromitito. Projeto Platina – Luanga. 14p, 2002.

TALLARICO, J. B. C. Projeto Platina, Carajás – Caracterização Mineralógica de Amostra de Minério tipo "Sulfeto Oxidado" (SO-1). 32p, 2003.

TALLARICO, J. B. C. Projeto Platina, Carajás – Caracterização Mineralógica de Quatro Amostras Iniciais (S1 a S4) de Minério Sulfetado de Luanga. 46p, 2003.

TALLARICO, J. B. C. Projeto Platina, Carajás: Petrografia de Amostras Testadas para WI do Minério. 13p, 2003.

TALLARICO, J. B. C.; SÁ, L. R. B. M. Projeto Platina, Carajás – Caracterização Mineralógica de Amostra Inicial (SB) de Minério Sulfetado. 43p, 2004.

TAVARES, F. M. Evolução geotectônica do nordeste da Província Carajás. Unpublish, Ph.D. Thesis, Universidade Federal do Rio de Janeiro, p. 115 p, 2015.

TEIXEIRA, A. S. Geologia, Petrologia e Geocronologia do Complexo Acamadado Lago Grande: Evidência para uma Suíte Magmática Mineralizada a EGP na Província Mineral de Carajás, Brasil. 216p, 2013.

TEIXEIRA, A. S.; FERREIRA FILHO, C. F.; GIUSTINA, M. E. S. D.; ARAUJO, S. M.; SILVA, H. H. A. B. Geology, petrology and geochronology of the Lago Grande layered complex: Evidence

for a PGE-mineralized magmatic suite in the Carajás Mineral Province, Brazil. J. South Am. Earth Sci. 64, 116-138, 2015.

TEIXEIRA, J. B. G.; EGGLER, D. H. Petrology, Geochemistry, and Tectonic Setting of Archaean Basaltic and Dioritic Rocks from the N4 Iron Deposit, Serra dos Carajás, Pará, Brazil. Acta Geologica Leopoldensia 17, 71-114, 1994.

TEIXEIRA, N. A. et al. Carajás Mineral Province-Example of metallogeny of a rift above a cratonic lithospheric keel. Journal of South American Earth Sciences, v. 108, p. 103091, 2021.

TRUNFULL, E. F. et al. Critical assessment of geochronological data from the Carajás Mineral Province, Brazil: implications for metallogeny and tectonic evolution. Ore Geology Reviews, v. 121, p. 103556, 2020.

VALE. (Unknown date). Report Luanga. 159p.

VASQUEZ, M. L.; CARVALHO, J. M. A.; SOUSA, C. S.; RICCI, P. S. F.; MACAMBIRA, E. M. B.; COSTA, L. T. R. Geological map of the Pará state in GIS, Geological Survey of Brazil-CPRM, 2008.

VILLAS BOAS, J. M.; ARAÚJO, C. C. de. Projeto Especial. Mapas de Recursos Minerais, de Solos e de Vegetação para Área do Programa Grande Carajás. Subprojeto de Recursos Minerais. Açailândia. CPRM, 1999.

VILLAS, R. N., SANTOS, M. D. Gold deposits of the Carajás Mineral Province: deposit types and metallogenesis. Mineralium Deposita 36, 300–331, 2001.

XCALIBUR MULTIPHYSICS. Time Domain Electromagnetic and Magnetic Survey. Report on Luanga, 2023.

ZACHARIAS, O. Estudos de Flotação com Amostras de PGM Luanga – Relatório de Progresso 1. 24p, 2007.

ZACHARIAS, O.; TALLARICO, J. B. C. Caracterização de Amostras de Cromititos de Luanga – Estudo em Escala de Bancada. Relatório Final. 33p, 2002.

ZIENTEK, M. L. Magmatic ore deposits in layered intrusions-Descriptive model for reef-type PGE and contact-type Cu-Ni-PGE deposits. US Geological Survey, 2012.

APPENDIX A – QUALIFIED PERSON CERTIFICATE

QP CERTIFICATE OF BERNARDO HORTA DE CERQUEIRA VIANA

I, **Bernardo Horta de Cerqueira Viana**, FAIG (#3709), as an author of the independent technical report titled "NI 43-101 Independent Technical Report, Luanga PGM + Au + Ni Project Pará State, Brazil" dated April 2, 2025, with an effective date of February 18, 2025 (Technical Report), prepared for Bravo Mining Corp. (Issuer), do hereby certify that:

1. I am a Geologist and Director for GE21 Consultoria Mineral Ltda., which is located on Avenida Afonso Pena, 3130, 9th floor, Savassi, Belo Horizonte, MG, Brazil - CEP 30130-910.
2. I am a graduate of the Federal University of Minas Gerais, located in Belo Horizonte, Brazil, and hold a Bachelor of Science Degree in Geology (2002). I have practised my profession continuously since 2002.
3. I am a professional enrolled with the Australian Institute of Geoscientists (AIG) Fellow (FAIG #3709).
4. I am a professional Mining Engineer, with over 20 years of relevant experience in Mineral Resource and Mineral Reserves estimation, including QA/QC, geological exploration and economic geology, which includes numerous mineral properties in Brazil, including iron ore and manganese properties.
5. I have read the definition of "qualified person" set out in National Instrument 43-101 – *Standards of Disclosure for Mineral Projects* (NI 43-101) – and certify that, by reason of my education, affiliation with a professional association and past relevant work experience, I fulfill the requirements to be a qualified person for the purposes of NI 43-101.
6. I am responsible for Sections 7, 8, 9, 10 and 20, and co-responsible for Sections1, 11, 12, 24, 25, 26 and 27.
7. I supervised the preparation of the Technical Report, being responsible for reviewing the database information presented by the Issuer and the definitions of the study strategy that underpinned it.
8. I personally inspected the property that is the subject of the Technical Report from 3rd October to 6th October 2023 and from January 27th to January 31st, 2025.
9. I have no prior involvement with the property that is the subject of the Technical Report other than as an author of the Technical Report and the technical report titled "Independent Technical Report on Resources estimate for Luanga PGM + Au + Ni Project Pará State, Brazil" dated October 22, 2023 with an effective date of December 1, 2023 (which technical report is superseded by the Technical Report).
10. As of the effective date of the Technical Report, to the best of my knowledge, information, and belief, the sections in the Technical Report I have authored and am responsible for contain all scientific and technical information that is required to be disclosed to make the Technical Report not misleading.
11. I have no personal knowledge of any material fact or material change which is not reflected in this Technical Report as of the date of this certificate.
12. I am independent of the Issuer, applying all tests in section 1.5 of NI 43-101.
13. I have read NI 43-101 and Form 43-101F1 – Technical Report, and the Technical Report has been prepared in compliance that instrument and form.

Belo Horizonte, Brazil, April 2, 2025.

<Signed and sealed in the original>

_____

Bernardo Horta de Cerqueira Viana

QP CERTIFICATE OF PORFIRIO CABALEIRO RODRIGUEZ

I, **Porfirio Cabaleiro Rodriguez**, FAIG (#3708), as an author of the independent technical report titled "NI 43-101 Independent Technical Report, Luanga PGM + Au + Ni Project Pará State, Brazil" dated April 2, 2025, with an effective date of February 18, 2025 (Technical Report), prepared for Bravo Mining Corp. (Issuer), do hereby certify that:

1. I am a Mining Engineer and Director for GE21 Consultoria Mineral Ltda., which is located on Avenida Afonso Pena, 3130, 9th floor, Savassi, Belo Horizonte, MG, Brazil - CEP 30130-910.
2. I am a graduate of the Federal University of Minas Gerais, located in Belo Horizonte, Brazil, and hold a Bachelor of Science Degree in Mining Engineering (1978). I have practised my profession continuously since 1979.
3. I am a professional enrolled with the Australian Institute of Geoscientists (AIG) Fellow (FAIG #3708).
4. I am a professional Mining Engineer, with over 40 years of relevant experience in Mineral Resource and Mineral Reserves estimation, including numerous mineral properties in Brazil, including iron ore and manganese properties.
5. I have read the definition of "qualified person" set out in National Instrument 43-101 – *Standards of Disclosure for Mineral Projects* (NI 43-101) – and certify that, by reason of my education, affiliation with a professional association and past relevant work experience, I fulfill the requirements to be a qualified person for the purposes of NI 43-101.
6. I personally inspected the property that is the subject of the Technical Report from July 4th to July 7th, 2023, 3rd October to 6th October 2023, and January 27th to January 31st, 2025.
7. I have no prior involvement with the property that is the subject of the Technical Report other than as an author of the Technical Report and the technical report titled "Independent Technical Report on Resources estimate for Luanga PGM + Au + Ni Project Pará State, Brazil" dated October 22, 2023 with an effective date of December 1, 2023 (which technical report is superseded by the Technical Report).
8. I am responsible for Sections 2, 3, 4, 5, 6, 13, 14, and 23, with co-responsibility for Sections 1, 11, 12, 24, 25, 26 and 27 of the Technical Report.
9. I visited the Project site from July 4 to 7, 2023; October 3 to 6, 2023; and January 27 to 31, 2025.
10. As for the effective date of the Technical Report, to the best of my knowledge, information, and belief, the sections in the Technical Report that I have authored and am responsible for contain all scientific and technical information that is required to be disclosed to make the Technical Report not misleading.
11. I am independent of the Issuer, applying all tests in section 1.5 of NI 43-101.
12. I have read NI 43-101 and Form 43-101F1, and this Technical Report has been prepared in compliance with that instrument form documents.

Belo Horizonte, Brazil, April 2, 2025.

<Signed and sealed in the original>

_____

Porfirio Cabaleiro Rodriguez